

Dottorato di Ricerca in Scienze Cardio-Nefro-Toraciche

Ciclo XXXV

Settore Concorsuale: 06/D1

Settore Scientifico Disciplinare: MED/11

**Correlations between Cardiac Magnetic Resonance
and Histologic Findings in Anderson Fabry disease**

Presentata da

Dr. Raffaello Ditaranto

Coordinatore Dottorato: Prof. Gaetano Domenico Gargiulo

Supervisore: Prof. Nazzareno Galie`

Co-supervisori: Dr.ssa Elena Biagini; Dr.ssa Ornella Leone

Esame finale anno 2023

ABSTRACT

Background

Cardiac magnetic resonance (CMR) has been shown as promising diagnostic tool in Anderson-Fabry disease (AFD) cardiomyopathy due to its ability to detect fat deposits through lower native T1 values. However no histological validation has been provided to date.

Objectives

To correlate CMR and histologic findings in different cardiac stages of AFD focusing on T1 mapping.

Methods

Fifteen AFD patients (49 years [IQR 39-63], 60% females) undergoing CMR (cines, native T1 and T2 mapping, LGE and post-contrast T1 imaging) and endomyocardial biopsy (EMB, n=11) or septal myectomy (n=4), were retrospectively evaluated. Tissue specimens were analyzed with light/electron microscopy and vacuolization amount calculated as percentages of vacuolated myocytes and vacuolated myocyte area (%VMA) through a quantitative histomorphometric color-based analysis.

Results

In patients without increased indexed left ventricular mass (LVMI) at CMR (67%), T1 fell as %VMA increased ($r = -0.883$; $p < 0.001$), whereas no clear relationship was evident once increased LVMI occurred ($r = -0.501$; $p = 0.389$). At least 45% of vacuolized myocytes and 10% of VMA were needed for low T1 to occur. %VMA positively correlate with maximal wall thickness (MWT, $r = 0.860$, $p < 0.0001$) and LVMI ($r = 0.762$; $p < 0.001$). Increased MWT and LVMI were present with at least 45% and 80% of vacuolated myocytes, respectively, and 18% and 22% of VMA.

Conclusions

This study demonstrated an inverse correlation between native T1 and the vacuolization amount in patients without increased LVMI at CMR, providing a histological validation of low native T1 in AFD. Importantly, a significant vacuolization burden was needed before low T1 and left ventricle hypertrophy occurred.

BACKGROUND

Anderson Fabry disease (AFD) is an X-linked metabolic disorder due to mutations in the gene coding for α -galactosidase A (*GLA*) involved in glycosphingolipid catabolism. Enzyme deficiency causes a progressive lysosomal accumulation of ceramides (mainly globotriaosylceramide [Gb3]), with cytotoxic, proinflammatory, and profibrotic effects leading to progressive multiorgan dysfunction.(1) Heart involvement represents the main prognostic determinant and the leading cause of mortality. Cardiac manifestations include left ventricle hypertrophy (LVH), angina pectoris, conduction abnormalities and tachyarrhythmias. Pathology represents the gold standard for tissue characterization and diagnosis, typically showing myocytes engulfed by storage vacuoles at light microscopy (LM) and zebra or myelin bodies at ultrastructure analysis (in the absence of medication [eg. chloroquine, amiodarone] that may induce similar storage). However, due to the risk of procedural complications of the endomyocardial biopsy (EMB) and its limited availability, non-invasive techniques have emerged as possible alternatives, being cardiac magnetic resonance (CMR) the key diagnostic tool.(2) Particularly, low non-contrast myocardial T1 values, due to increased glycosphingolipid (i.e. fat) content in the myocardium, have proved to be an useful instrument for both differential diagnosis among LVH aetiologies and early diagnosis in AFD patients without LVH (3) with subsequent normalization - once LVH is present - as mass increases. Despite widespread diffusion of this technique in clinical practice, a correlation between CMR findings and pathology has never been done. Therefore, the aim of our study was to correlate CMR and pathology findings in different stages of AFD cardiomyopathy, focusing on T1 mapping.

METHODS

We performed a retrospective study of 15 AFD patients (60% females; median age 49 years, IQR 39-63) who underwent - according to clinical standard of care - EMB (n=11) or septal myectomy (n=4) and CMR (within 1 month) at St. Orsola University Hospital in Bologna, Italy (IRCCS Azienda

Ospedaliero-Universitaria), from February 2018 to March 2022. AFD diagnosis was based on current international guidelines.(4) Clinical, instrumental (electrocardiogram, echocardiogram), and laboratory data were also systematically collected. Written informed consent for anonymous scientific use of personal data had been obtained in each case, after ethical local committee approval.

CMR

CMR was carried out on a 1.5 Tesla scanner (Philips; Ingenia) using a standardized protocol. Steady-state free precession (SSFP) techniques for cine movies of left and right ventricle were acquired during breath holds for evaluation of cardiac volumes and systolic function. Ventricular volumes and mass were calculated using dedicated software and indexed to BSA. LVH was defined as a maximum wall thickness (MWT) ≥ 12 mm and/or an increased indexed LV mass (LVMI) on CMR as previously reported (>92 g/m² for males; >79 g/m² for females).(3) Native T1 mapping was performed before contrast bolus administration on basal, mid, and apical left ventricular short-axis slices using a modified Look-Locker inversion recovery sequence (MOLLI). Native T2 mapping was acquired on the same slices using a gradient spin echo (GraSe) sequence. Late gadolinium-enhanced (LGE) imaging was performed 15 minutes after bolus injection of 0.1 mmol/kg of body weight of gadobutrol (Gadovist). LGE positivity was considered when visible in 2 phase-encoding directions and 2 orthogonal planes. Post-contrast T1 mapping was performed 15 minutes after contrast administration for extracellular volume (ECV) fraction quantification, on the same location as native T1. All images were analyzed using CVI42 software (Circle Cardiovascular Imaging, Inc, Calgary, Canada). A region of interest (ROI) avoiding the blood-myocardial boundary was manually drawn in the basal/medium interventricular septum for T1 and T2 maps. Normal native T1 and T2 reference ranges (mean \pm 2SD) were defined using healthy volunteers, free of any history or symptoms of cardiovascular disease or other comorbidities, and not taking any medications. The normal native septal T1 ranges (mean \pm 2SD, lower limit of normal) were: 983 \pm 26ms, 931ms in males; 1015 \pm 27ms, 961ms in females. The normal native septal T2 ranges (mean \pm 2SD, upper limit of normal)

were: 48 ± 3 ms, 54 ms in males; 50 ± 3 ms, 56ms in females. Global longitudinal 2-dimensional strain (GLS) values were obtained using feature tracking analysis of 4, 2, and 3-chamber and short-axis cine stack.(5)

All AFD patients had blood collected just before CMR scan and analyzed for hematocrit, high-sensitivity troponin I (hsTnI, chemiluminescence-immunoassay [Access hsTnI assay, Beckman Coulter, Inc. Brea, CA, USA]; limit of detection 2,3 ng/L; upper limit values (99th percentile) 19,8 and 11,6 ng/L for males and females) and brain natriuretic peptide (BNP, chemiluminescence immunoassay, normal < 100 pgl/mL).

Light and electronic microscopy

Patients underwent EMB or septal myectomy within 1 month after CMR. Bioptic samples (at least five) were taken from the right side of the interventricular septum, through right jugular vein, with a fluoroscopically directed bioptome. Transaortic surgical myectomy was performed in symptomatic LV outflow tract obstruction patients by longitudinal incisions in the basal septum below the aortic valve. Endomyocardial fragments and surgical samples were treated according to standard protocols: formalin-fixed and paraffin embedded (FFPE) samples were used for histology examination with LM; one/two samples were fixed in 2.5% buffered glutaraldehyde solution and embedded in epoxy resin (Araldite) for ultrastructural analysis.(6)

An expert cardiovascular pathologist, blind to clinical data, performed histology analysis on serial (n. 30) Haematoxylin-Eosin (H&E) and Azan Mallory trichrome (AMT) stained sections using a microscope AXIO Imager M2. In H&E the vacuoles appeared as clear spaces, in the majority optically empty and more focally with fine eosinophilic granules. The percentage of vacuolated myocyte area ($\%VMA = \frac{\text{vacuolated area}}{\text{not vacuolated myocyte area} + \text{vacuolated area}} \times 100$) was evaluated with semi-automated histomorphometric quantitative analysis on digitally acquired AMT stained images (myocytes in red Bordeaux, fibrosis in blue) at high power (200 \times) magnification using ZEISS ZEN Blue software. Colored images were split into bright red (for myocytes) and green (for

vacuoles) by a color-based calculation analysis. Imprecisions were corrected using a freehand selection tool, excluding vessels and interstitium. The average of all images, taken as much as possible from each section, was considered the final result for each patient (Figure 1). Additionally, the number of affected myocytes was counted on the whole section and reported as a percentage of vacuolated myocytes (%VM), average of all images.

Two morphological types of myocyte vacuolization were qualitatively recognized: *micro-vacuolization* (tiny small vacuoles scattered in the cytoplasm) and *macro-vacuolization type* (single vacuoles, that might occupy almost the entire sarcoplasm and displace the nuclei peripherally). Accordingly, four vacuolization patterns were defined: microvacuolization, mixed with prevalent microvacuoles, mixed with prevalent macrovacuoles and macrovacuolization (supplemental figure 1). Myocyte diameter was measured on cross section with the nucleus centrally located: it was considered increased when $>15 \mu\text{m}$.⁽⁷⁾ For each case five fields at $400\times$ high power were examined, and the diameter of the 5 largest hypertrophic vacuolated cells and of the 5 largest hypertrophic non-vacuolated was measured. When non-vacuolated cells were less than 5 per field, due to the preponderance of vacuolated cells in the examined field, data were not collected.

Subendocardial and myocardial fibrosis was recorded on AMT stained sections and myocardial type classified as replacement (scar-like) or interstitial. ⁽⁸⁾

Presence of myocardial disarray was registered and small intramural coronary artery alterations analyzed in terms of parietal wall thickening (presence/absence), tunica media involvement (hypertrophy/fibrosis/vacuolization/mixed changes) and endothelial cell vacuolation/enlargement.

Inflammation was defined as ≥ 14 leukocytes/ mm^2 in the myocardium, including up to 4 monocytes/ mm^2 , with CD3 positive T lymphocytes > 7 cells/ mm^2 .⁽⁹⁾ Myocyte damage and fibrosis within inflammatory infiltrates were also noticed. Distribution of inflammatory infiltrates was classified as focal ($<30\%$ of the specimen), multifocal (30% to 60%), and diffuse ($>60\%$).

Immunohistochemical staining included CD68 and CD3 antibodies for inflammatory cell typing.

Transmission electron microscopy analysis was performed on thin sections to demonstrate autophagolysosomes containing diagnostic lamellar electron-dense lipid deposits as finger-print or zebra bodies. Twenty random micrographs per subject were taken with Philips CM100 transmission electron microscope at 13500 \times , with a Megaview digital camera (Olympus Soft Imaging Solutions, Münster, Germany) using iTEM Megaview (Olympus Soft Imaging Solutions). Digital images were manually analyzed using Image J software (National Institute of Health Image; Bethesda, MD, USA) to calculate averaged area of autophagolysosomal lipid accumulation (grid with squares of 0.05 μm^2). (10)

Statistical analysis

Discrete data were expressed as counts and percentages (i.e. events/total number of patients \times 100) and continuous data as median and IQR, according to sample distribution. χ^2 test was used for comparison of categorical data. Pearson correlation coefficients or Spearman's rho (r_s) were used to report the relationship between CMR and histological findings. Statistical significance was considered for p value $<$ 0.05. Accordingly to what previously found, for correlation of T1 values with %VMA, MWT and LVMI, patients were divided based on the presence or not of increased LVMI. (3).

RESULTS

Baseline clinical, instrumental and laboratory characteristics are shown in Table 1. hsTnI values were increased in 7 patients (50%) and BNP in 9 (60%). TnI and BNP were strongly correlated ($r=0.732$; $p=0.002$).

Light microscopy

All patients' samples showed vacuolated myocytes. %VM was \leq 30% in 4 patients, 45% and 50% in 2 and \geq 80% in 9. Similarly, %VMA was $<$ 10% in 4 patients, between 10 and 20% in 2 and $>$ 20% in 9, with the highest value 38% (median 22%, IQR 8-30%) (Table 2): these two parameters were strongly correlated ($r=0.938$; $p<0.00001$). Microvacuolization patterns was present in all cases with no LVH at CMR, whereas

macrovacuolization in those with LVH except one. Both vacuolated and non-vacuolated myocytes were hypertrophic, with the former significantly greater in diameter ($35\mu\text{m}$ [27-43] vs μm 18 [17 -20] $p<0.001$; supplemental figure 2). Vacuolated myocytes' diameter correlated with %VMA ($r=0.618$; $p=0.014$) and with %VM ($r=0.688$; $p=0.004$). Disarray was identified in 13 patients (87%; 6 focal, 7 multifocal). All patients but one had fibrosis, in different combinations: 11 (73%) subendocardial fibrosis (mild 5, moderate 6), 12 (80%) interstitial myocardial fibrosis (mild 8, moderate 4) and 2 (16%) replacement myocardial fibrosis (mild 1, severe 1) (Table 2). Seven patients (47%) had inflammatory infiltrates (mild in all cases) with focal ($n=3$) or multifocal ($n=4$) distribution. All were composed of T lymphocytes and macrophages in various proportions, except one presenting exclusively macrophages. Inflammatory foci were isolated ($n=2$), or adjacent to myocytes degeneration and/or subepi/subendocardial fibrosis ($n=5$). Prevalence of increased TnI did not differ between patients with and without inflammatory infiltrates (57% vs 37%; $p=0.619$). Myocardial edema was absent in all samples. Eleven patients (73%) had thickened vessel walls with tunica media hypertrophy, associated with smooth muscle cell vacuolation in 4 cases, fibrosis in 1 and vacuolization plus fibrosis in 2. Endothelial cells were prominent and swollen in all cases but one.

Transmission electronic microscopy

All samples showed autophagolysosomal accumulations of glycosphingolipid occupying a variable part of the sarcoplasm, consisting of enlarged secondary lysosomes filled with osmiophilic lamellar inclusions with finger-print or zebra bodies appearance due to concentric lamellation of dark layers of lipid inclusions. In the milder cases they were mainly scattered in the sarcoplasm, extending progressively causing myofibrillar displacement and loss in the advanced cases (supplemental Figure 3). Mitochondrial hyperplasia and lipofuscins were also detected. Mean autophagolysosome area increased with %VMA ($r=0.622$; $p=0.023$) (Table 2, supplemental Figure 4).

Cardiac Magnetic Resonance

Median indexed end diastolic LV volume was 83 ml/m² (69-92), with 2 patients presenting a dilated LV. Median LV ejection fraction was 64% (58-67), reduced in 3 patients. Five patients (33%) had no LVH and no LGE: 1 of them had low T1 and 1 high/border line T2 (with normal T1). Among the 10

patients with LVH, 6 had low T1 with a female having high T2 (associated to high troponin levels) and 4 had (pseudo)normal T1 with high/border-line T2 in 1 female. Among LVH patients, 7 showed LGE: all shared basal postero-lateral involvement; 2 had septal LGE at apical level and 1 at basal septal/inferior and apical segments. In the whole population T1 values did not correlate with the MWT ($r=-0.153$; $p=0.587$) and LVMI ($r=-0.057$; $p=0.842$). However, when considering only the patients without increased LVMI ($n=10$), T1 values showed a significant inverse correlation with LVMI ($r=-0.793$; $p=0.006$) and MWT ($r=-0.680$; $p=0.03$).

Comparison between histology and MRI – tissue characterization

For what concern native T1 values and myocytes vacuolization, in patients without increased LVMI T1 values fell as %VMA increased ($r=-0.883$; $p<0.001$), whereas in the other cases T1 tended toward normalization with no clear relationship ($r=-0.501$; $p=0.389$) (Figure 2; Central Illustration). For low T1 to occur $\geq 45\%$ of VM and $\geq 10\%$ of VMA were needed (Table 2).

With regard to histologic inflammation and T2 mapping (available in 14 cases), out of 7 patients with mild inflammatory foci only 1 female had elevated T2 values (59 ms) with hsTnI and BNP. Two females had border-line T2: one had moderate aortic stenosis (bicuspid valve), normal hsTnI and increased BNP, whereas the other one had both biomarkers increased (Figure 3).

Septum ECV (available in 13) did not correlate with T1 values ($r=0.452$; $p=0.140$), %VM ($r=-0.105$; $p=0.745$), %VMA ($r=-0.140$; $p=0.664$), MWT ($r=0.161$; $p=0.616$), and LVMI ($r=0.033$; $p=0.918$).

The extent of fibrosis at histology was related to LVH at CMR, with at least moderate fibrosis more frequent in patient with LVH (78% vs 17%; $p=0.041$). Moreover, although at histology all but one had fibrosis only 3 patients had septal LGE at CMR.

Comparison between histology and MRI – ventricular hypertrophy

Maximal cellular diameter and %VMA positively correlated with MWT ($r=0.645$; $p=0.009$ and $r=0.859$; $p<0.0001$, respectively) and with LVMI ($r=0.579$; $p=0.024$ and $r=0.762$; $p<0.001$, respectively). Furthermore, the relationship between LVMI and %VM/%VMA was exponential

(Figure 4). In particular the curves that best fitted the data points had a two and single term exponential growth, respectively. Accordingly, in the first case the curve was flatter in the first part (i.e, significant increase in %VM despite small changing in LVMi) and grew more quickly in the second part. As a consequence, patients of the first part of the curves, had normal LVMi despite a wide spectrum of vacuolization. Patients of the second part of the curves had significant differences in terms of LVMi despite slight differences of vacuolization (Figure 5). Diversity in the curves reflects the different way they look at storage: number of myocytes affected vs myocyte area affected. It can be hypothesized that the disease causes a rapid involvement of most of the myocyte population, while a slow and progressive engulfment of each cell goes on over time. Increased MWT and LVMi were present with at least 45% and 80% of VM, respectively, and 18% and 22% of VMA.

DISCUSSION

This study compared for the first time CMR assessment with histology in a series of AFD patients at different stages of cardiac involvement focusing on the relationship between native T1 values and histological findings. Main results of the present study were:

1. Septal native T1 values inversely correlated with storage (%VMA) in patients without increased LVMi, and a not negligible myocytes' vacuolization was needed before achieving low T1 (45% of MV and 10% of VMA);
2. A significant vacuolization burden was needed before LVH developed at CMR;
3. LVMi increased exponentially with %VMA and %VM: in the early phase of disease a normal LVMi concealed a wide spectrum of vacuolization amount and – *vice versa* – in the late phase relevant differences in LVMi might be present despite not significant differences in the vacuolization burden.
4. Despite the high frequency of mild inflammatory infiltrates at LM (almost half of cases) only one patient had high T2 septal values.

Glycosphingolipid storage and T1 mapping

Historical autoptic studies of AFD patients with cardiac involvement reported a myocardial concentration of Gb3 100-350 times higher than controls.(11) Consequently, based on the assumption that fat has a very low T1 (~250 ms at 1.5T) and that native T1 may measure lipid myocardial storage in AFD, two different groups independently showed that native myocardial T1 is substantially lower in AFD compared to other LVH aetiologies.(12,13) It was not clear if low T1 was due to the glycosphingolipid deposit *per se*, or to the repetitive architecture of stored lipids, causing water constrain and reduction of longitudinal relaxation. Thereafter, lower T1 values were reported in half of AFD patients without LVH when compared to healthy volunteers.(14). However, no histological validation has been reported to date to demonstrate what theoretically supposed. In this case series, for the first time a relationship between native T1 values and myocytes storage was found. Indeed, in patients without increased LVMi, T1 falling paralleled the increase of vacuolization. On the contrary, in patients with increased LVMi, T1 was mainly (pseudo)normal despite abundant vacuolization, and no clear trend was found with storage. Although T1 behavior in AFD cardiomyopathy was reported previously, our study showed the underlying histologic abnormalities characterizing the different stages of the disease.(3) Even if cerebroside deposits starts *in utero*, cardiac T1 values were found to remain in normal range during childhood, while a subclinical myocyte infiltration occurs.(3,15) This period, called *accumulation phase*, is characterized by T1 falling and normal LV mass. Accordingly, in our series, 4 patients without LVH and normal T1, TnI and ECG, showed initial signs of disease at microscopy (i.e., vacuolated myocytes), confirming pathology as the most sensitive tool for precocious disease detection. During this early stage, before low T1, other non-invasive parameters - GLS, stress myocardial blood flow and ECG abnormalities – have been proposed for non-invasive early disease detection.(16) Notably, in our cohort a significant myocytes' vacuolization was needed before achieving low T1 values, both in terms of %VM (45%) and %VMA (10%).

Glycosphingolipid storage and LVH

Regardless of the presence of LVH at CMR, all patients had cellular hypertrophy, even with normal wall thickness and LVMI. As previously reported, apart from vacuolated cells (all hypertrophic) also unaffected cardiomyocytes presented increased diameter, although smaller than the formers.(17) Several hypotheses may be advanced: paracrine secretion of pro-hypertrophic mediators from neighboring affected cells, circulating stimulating factors, or even initial lipid storage undetectable at light microscopy. In addition, concomitant hemodynamic factors, such as systemic arterial hypertension or valve diseases, must be taken into consideration.

In this study LVMI at CMR exponentially increased with %VM and %VMA: hence, patients with higher amount of vacuolization at histology showed a wide range of LVMI, with 4 patients with diffuse storage and low T1 presenting only mild LVH. Similarly, *Ogawa et al.* reported in one postmortem case a discrepancy between mild LVH and massive Gb3 storage.(18) This highlights the ability of histology to estimate disease burden, more closely than wall thickening, myocardial mass at imaging and T1 values. Therefore, it might play a central role in preclinical phase to define the timing for specific therapy starting, when macroscopic imaging misses microscopic hypertrophy. The explanation of this discordance remains an open question. Previously, parietal hypertrophy was supposed as not simply caused by storage but also by sarcomeric protein synthesis.(3) This, together with sex dimorphism (due to Lyonization phenomenon and sex-specific myocyte response to a definite trigger) would justify T1 trend - once LVH develops - flattening in women and rising in men, due to different degrees of hypertrophy. However, in our cohort, the comparison of light and electronic microscopy showed that the optical free spaces at histology do not correspond entirely to the endolysosomal glycosphingolipid accumulation at ultrastructure (i.e. lamellar and myelin bodies) in the affected myocytes, but also to myofibrinolysis, hyperplastic and degenerate mitochondria, lipofuscines etc. The dramatic disruption of the myocytes in the advanced stages and the break-up of the contractile apparatus we reported, suggest that other factors may account for T1 behavior. In this

regard, the profound changes of the myocell may contribute to the T1 pseudonormalization together with the offset provided by fibrosis.

Interstitial: fibrosis and inflammation

Mild to moderate fibrosis, interstitial and/or subendocardial, was common in our population, especially in patients with LVH, whereas replacement fibrosis was quite rare. Accordingly septal LGE was reported only in three cases: our data are consistent with previous CMR series and autoptic findings, showing limited replacement fibrosis in the septum.(19,20)

Recent findings have suggested a central role for myocardial inflammation in AFD and, in this regard, T2 mapping is faced to as promising surrogate for histology.(21,22) In fact, the increased tissue water content (edema) prolongs T2 values (and T1 at a lesser extent) in the myocardium and T2 mapping allows for the direct measurement of water-induced prolongation of T2 relaxation time.(23) Furthermore a previous PET/CMR study showed that among AFD patients with focal LGE only those with positive short tau inversion recovery (STIR) MR sequences had focal FDG uptake; conversely, patients with LGE and negative STIR MR images did not.(24) In our study mild infiltrates of macrophages and/or lymphocytes were detected in half the population, associated with fibrosis and/or myocytes injury that may represent a chronic stage of inflammation. However, only one of them had septal high T2 and increased TnI. Accordingly, *Frustaci et al.* found signs of inflammation at histology in 56% of EMB from AFD patients, with evidence of edema at CMR (T2w-STIR images) only in one third.(25) Although increased T2 is considered representative of increased water content, no one had edema at histology in our cohort. Reasons for our results remain speculative: edema might be confined intracellularly and not detected at histology (intracellular edema) or increased T2 might reflect something different than tissue water content, similarly to what reported in cardiomyopathies without signs of inflammation at EMB. (26,27) It should be noted that the presence of high T2 is shared with hypertrophic cardiomyopathy, where it seems caused by ischemia resulting from microvascular dysfunction, impaired diastolic relaxation, mismatched capillary density and,

myocardial interstitial fibrosis: all factors in common with AFD.(28,29) Therefore a double mechanism, at least, should be supposed for explanation of T2 in AFD. In this regard in our cohort TnI values were closely related to BNP, which is released in response to high ventricular filling pressure as in diastolic dysfunction.

Finally, a not significant relationship was observed between septal ECV and LVH or vacuolization. Myocardial ECV is known to provide limited added value in AFD, being similar to healthy subjects. Furthermore, as previously reported, if increased lipid content is the source of the reduced non contrast T1 values in AFD, then ECV equation might not be accurate.(30)

LIMITATIONS

This study was limited by the number of patients enrolled: however this is a single center cohort of a rare disease and the first study to compare CMR and histology, focusing on native T1. With regard to EMB, only small myocardial specimens are retrieved thus, the distribution and extent of cell vacuolization did not necessarily reflect the entire myocardium.

CONCLUSION

This study provided for the first time a histological validation of the relationship between glycosphingolipid storage and low native T1 in AFD, showing an inverse correlation between the amount of vacuolization and T1 in patients without increased LVMI. Importantly, significant %VM and %VMA were needed for low T1 to occur, as well as for LVH at CMR. Additionally, patients with high vacuolization amount, might present significant difference in MWT/LVMI despite similar %VM and %VMA, suggesting adjunctive mechanism as causative of ventricular hypertrophy.

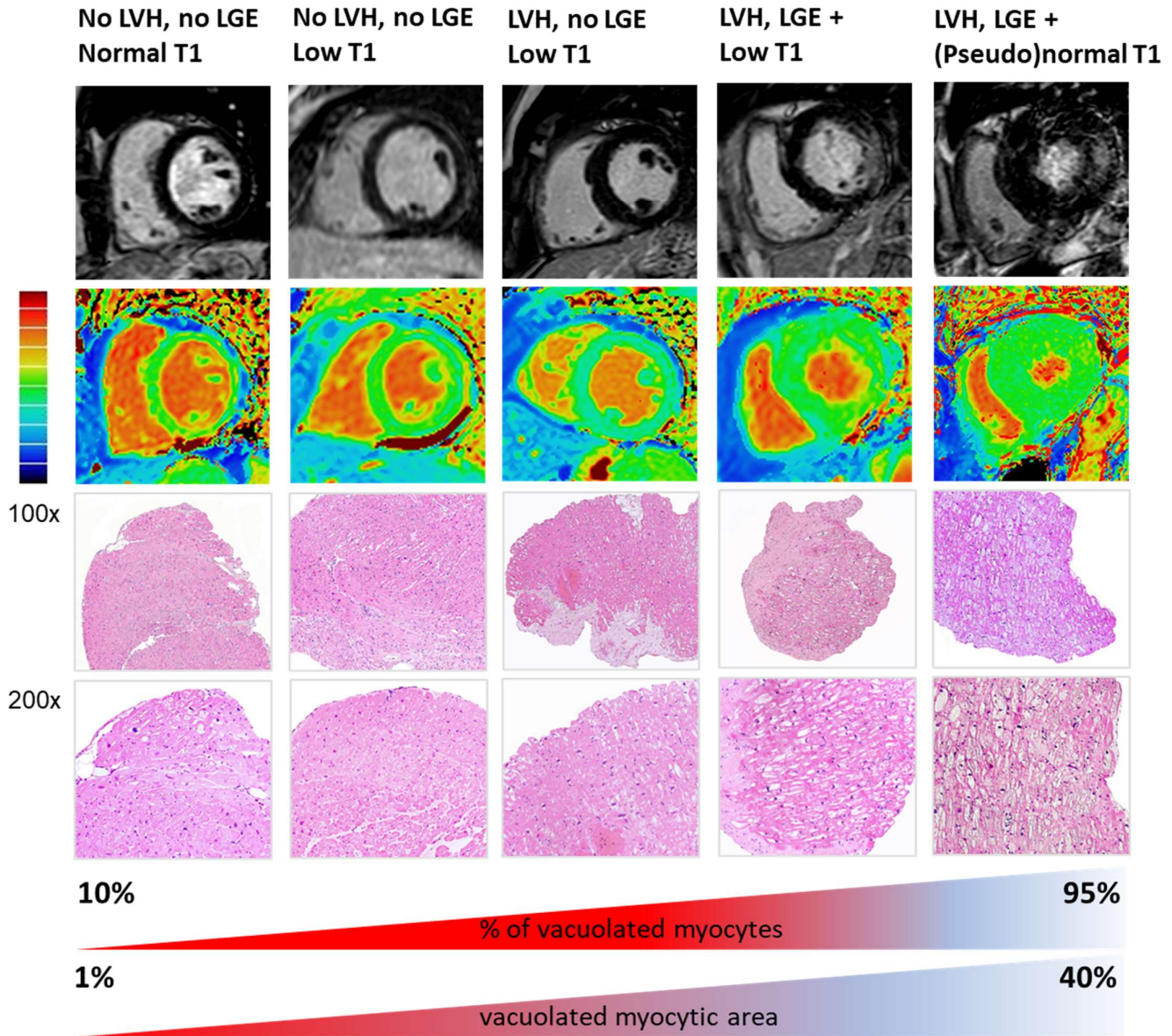
REFERENCES

1. Pieroni M, Moon JC, Arbustini E et al. Cardiac Involvement in Fabry Disease: JACC Review Topic of the Week. *Journal of the American College of Cardiology* 2021;77:922-936.
2. Perry R, Shah R, Saiedi M et al. The Role of Cardiac Imaging in the Diagnosis and Management of Anderson-Fabry Disease. *JACC Cardiovascular imaging* 2019;12:1230-1242.
3. Nordin S, Kozor R, Medina-Menacho K et al. Proposed Stages of Myocardial Phenotype Development in Fabry Disease. *JACC Cardiovascular imaging* 2019;12:1673-1683.
4. Smid BE, van der Tol L, Cecchi F et al. Uncertain diagnosis of Fabry disease: consensus recommendation on diagnosis in adults with left ventricular hypertrophy and genetic variants of unknown significance. *International journal of cardiology* 2014;177:400-8.
5. Augusto JB, Nordin S, Vijapurapu R et al. Myocardial Edema, Myocyte Injury, and Disease Severity in Fabry Disease. *Circulation Cardiovascular imaging* 2020;13:e010171.
6. Leone O, Veinot JP, Angelini A et al. 2011 consensus statement on endomyocardial biopsy from the Association for European Cardiovascular Pathology and the Society for Cardiovascular Pathology. *Cardiovascular pathology : the official journal of the Society for Cardiovascular Pathology* 2012;21:245-74.
7. Basso C, Michaud K, d'Amati G et al. Cardiac hypertrophy at autopsy. *Virchows Archiv : an international journal of pathology* 2021;479:79-94.
8. Galati G, Leone O, Pasquale F et al. Histological and Histometric Characterization of Myocardial Fibrosis in End-Stage Hypertrophic Cardiomyopathy: A Clinical-Pathological Study of 30 Explanted Hearts. *Circulation Heart failure* 2016;9.
9. Caforio AL, Pankuweit S, Arbustini E et al. Current state of knowledge on aetiology, diagnosis, management, and therapy of myocarditis: a position statement of the European Society of Cardiology Working Group on Myocardial and Pericardial Diseases. *European heart journal* 2013;34:2636-48, 2648a-2648d.
10. Broskey NT, Daraspe J, Humbel BM, Amati F. Skeletal muscle mitochondrial and lipid droplet content assessed with standardized grid sizes for stereology. *Journal of applied physiology* 2013;115:765-70.
11. von Scheidt W, Eng CM, Fitzmaurice TF et al. An atypical variant of Fabry's disease with manifestations confined to the myocardium. *The New England journal of medicine* 1991;324:395-9.
12. Thompson RB, Chow K, Khan A et al. T(1) mapping with cardiovascular MRI is highly sensitive for Fabry disease independent of hypertrophy and sex. *Circulation Cardiovascular imaging* 2013;6:637-45.
13. Sado DM, White SK, Piechnik SK et al. Identification and assessment of Anderson-Fabry disease by cardiovascular magnetic resonance noncontrast myocardial T1 mapping. *Circulation Cardiovascular imaging* 2013;6:392-8.
14. Pica S, Sado DM, Maestrini V et al. Reproducibility of native myocardial T1 mapping in the assessment of Fabry disease and its role in early detection of cardiac involvement by cardiovascular magnetic resonance. *Journal of cardiovascular magnetic resonance : official journal of the Society for Cardiovascular Magnetic Resonance* 2014;16:99.
15. Vedder AC, Strijland A, vd Bergh Weerman MA, Florquin S, Aerts JM, Hollak CE. Manifestations of Fabry disease in placental tissue. *Journal of inherited metabolic disease* 2006;29:106-11.

16. Augusto JB, Johner N, Shah D et al. The myocardial phenotype of Fabry disease pre-hypertrophy and pre-detectable storage. *European heart journal cardiovascular Imaging* 2020.
17. Frustaci A, Chimenti C, Doheny D, Desnick RJ. Evolution of cardiac pathology in classic Fabry disease: Progressive cardiomyocyte enlargement leads to increased cell death and fibrosis, and correlates with severity of ventricular hypertrophy. *International journal of cardiology* 2017;248:257-262.
18. Ogawa K AT, Yoshimura K, Nagashima K, Nagashima T. Cardiac accumulation of trihexosyl ceramide in a case with amyotrophic lateral sclerosis. *Jpn J Exp Med* 1985;55:123-127.
19. Sheppard MN, Cane P, Florio R et al. A detailed pathologic examination of heart tissue from three older patients with Anderson-Fabry disease on enzyme replacement therapy. *Cardiovascular pathology : the official journal of the Society for Cardiovascular Pathology* 2010;19:293-301.
20. Deva DP, Hanneman K, Li Q et al. Cardiovascular magnetic resonance demonstration of the spectrum of morphological phenotypes and patterns of myocardial scarring in Anderson-Fabry disease. *Journal of cardiovascular magnetic resonance : official journal of the Society for Cardiovascular Magnetic Resonance* 2016;18:14.
21. Nordin S, Kozor R, Bulluck H et al. Cardiac Fabry Disease With Late Gadolinium Enhancement Is a Chronic Inflammatory Cardiomyopathy. *Journal of the American College of Cardiology* 2016;68:1707-1708.
22. Nordin S, Kozor R, Vijapurapu R et al. Myocardial Storage, Inflammation, and Cardiac Phenotype in Fabry Disease After One Year of Enzyme Replacement Therapy. *Circulation Cardiovascular imaging* 2019;12:e009430.
23. Higgins CB, Herfkens R, Lipton MJ et al. Nuclear magnetic resonance imaging of acute myocardial infarction in dogs: alterations in magnetic relaxation times. *The American journal of cardiology* 1983;52:184-8.
24. Nappi C, Altiero M, Imbriaco M et al. First experience of simultaneous PET/MRI for the early detection of cardiac involvement in patients with Anderson-Fabry disease. *European journal of nuclear medicine and molecular imaging* 2015;42:1025-31.
25. Frustaci A, Verardo R, Grande C et al. Immune-Mediated Myocarditis in Fabry Disease Cardiomyopathy. *Journal of the American Heart Association* 2018;7:e009052.
26. Friedrich MG. Myocardial edema--a new clinical entity? *Nature reviews Cardiology* 2010;7:292-6.
27. Bohnen S, Radunski UK, Lund GK et al. Performance of t1 and t2 mapping cardiovascular magnetic resonance to detect active myocarditis in patients with recent-onset heart failure. *Circulation Cardiovascular imaging* 2015;8.
28. Amano Y, Yanagisawa F, Tachi M, Hashimoto H, Imai S, Kumita S. Myocardial T2 Mapping in Patients With Hypertrophic Cardiomyopathy. *Journal of computer assisted tomography* 2017;41:344-348.
29. Todiere G, Piscicella L, Barison A et al. Abnormal T2-STIR magnetic resonance in hypertrophic cardiomyopathy: a marker of advanced disease and electrical myocardial instability. *PloS one* 2014;9:e111366.
30. Sado DM, Flett AS, Banypersad SM et al. Cardiovascular magnetic resonance measurement of myocardial extracellular volume in health and disease. *Heart* 2012;98:1436-41.

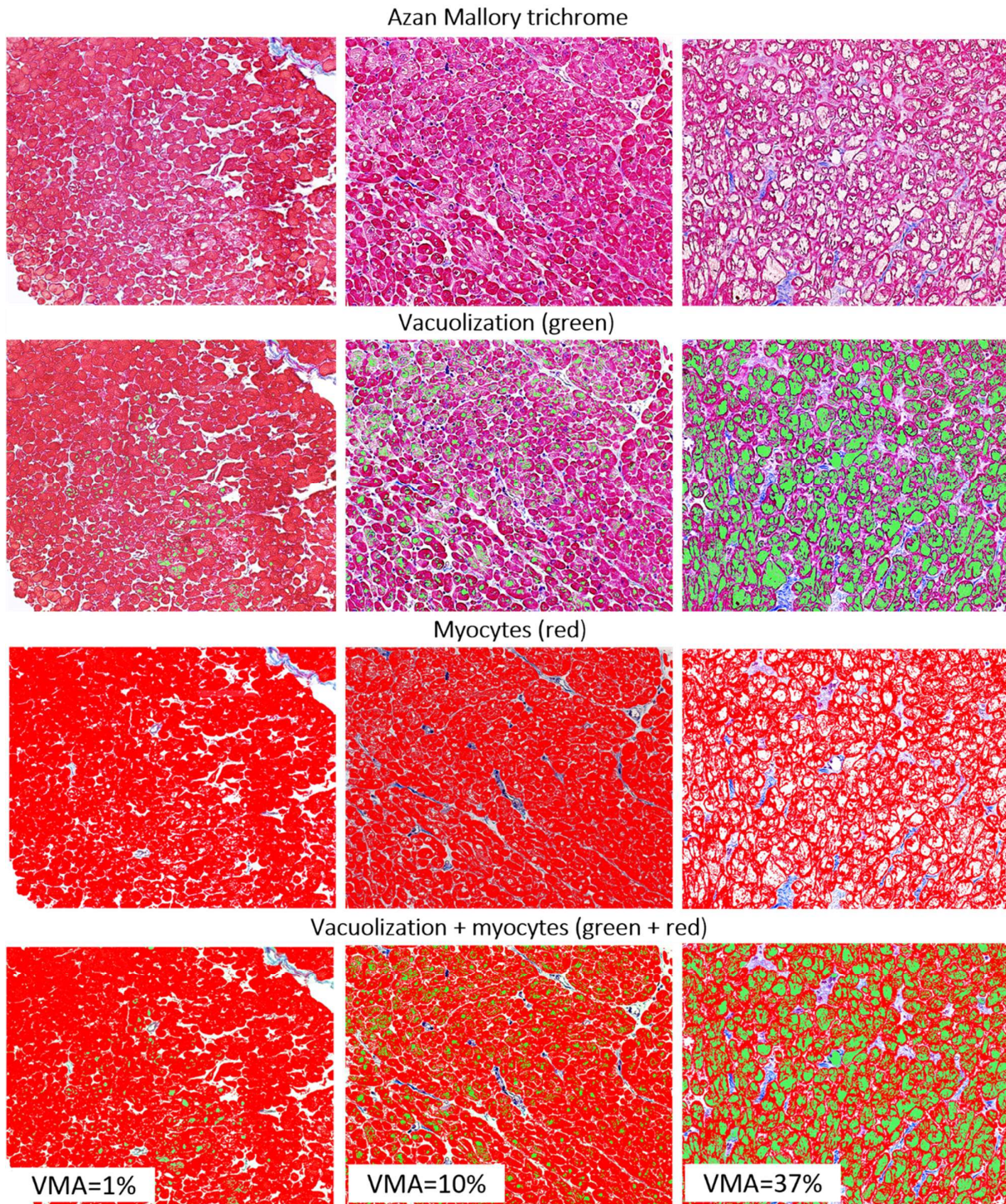
FIGURES

Central illustration



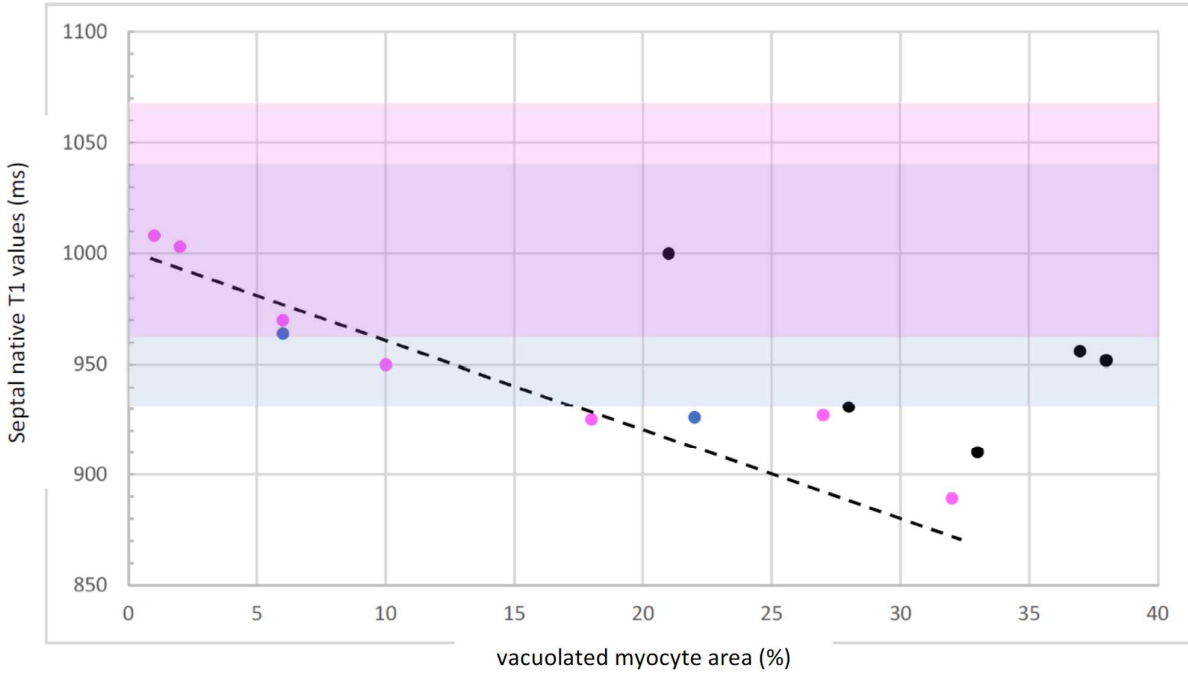
Correlation among post-contrast cardiac magnetic resonance images (first row), native T1 maps (second row) and histology (third [x100 magnification] and fourth [x200 magnification] row) of Anderson-Fabry disease patients, from early (left) to late (right) stages of cardiac disease. In T1 color maps normal myocardium is green, increasing native T1 red, and decreasing native T1 blue. LGE: late gadolinium enhancement.

Figure 1



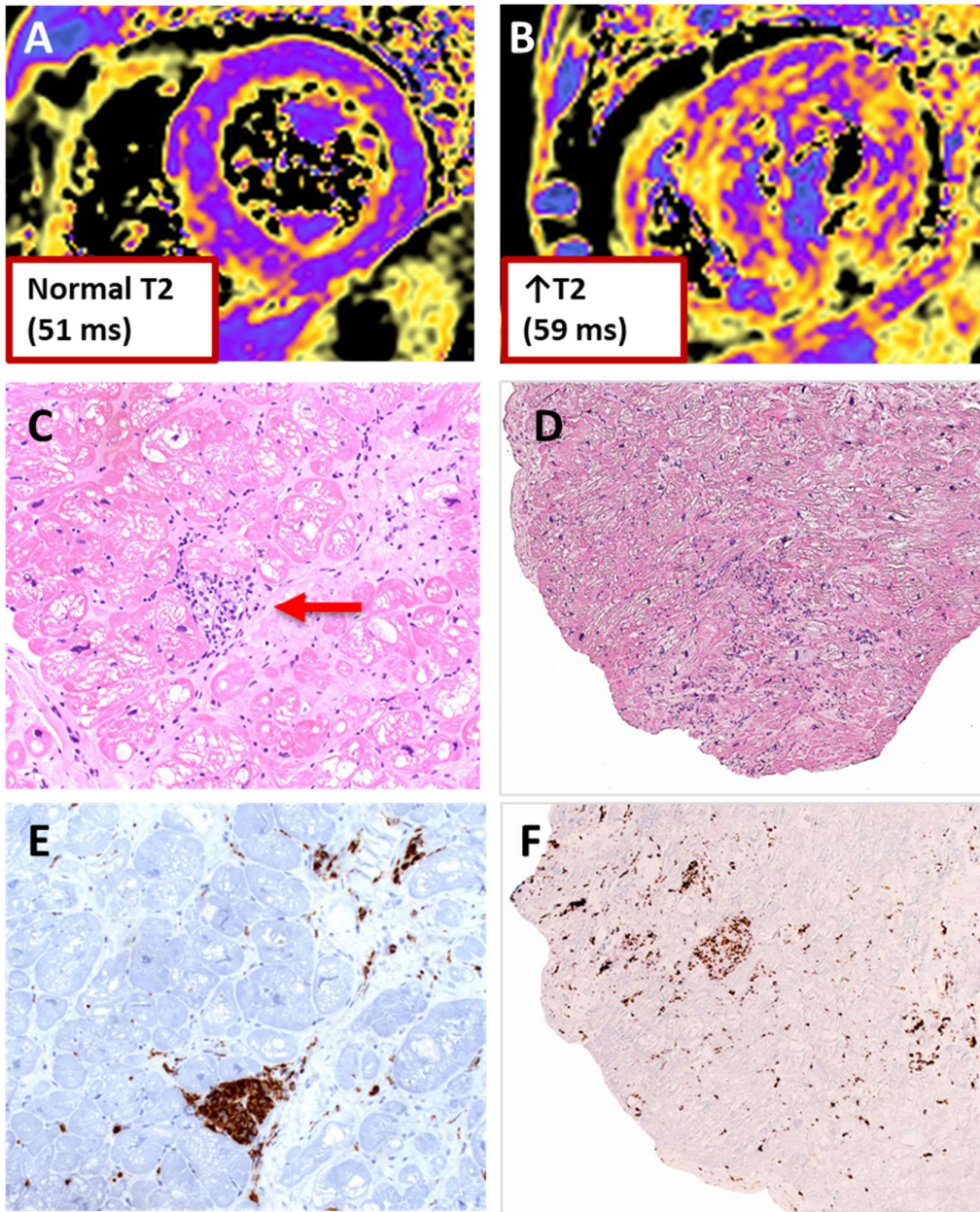
Histomorphometric color-based analysis of vacuolization representative of increasing vacuolated myocyte area (left [1%], center [10%], and right [37%] columns). Azan-Mallory trichrome staining (first row) are split into green (for vacuoles [second row]), red (for not vacuolated myocyte area [third row]) and combined [fourth row], excluding vessels and interstitium.

Figure 2



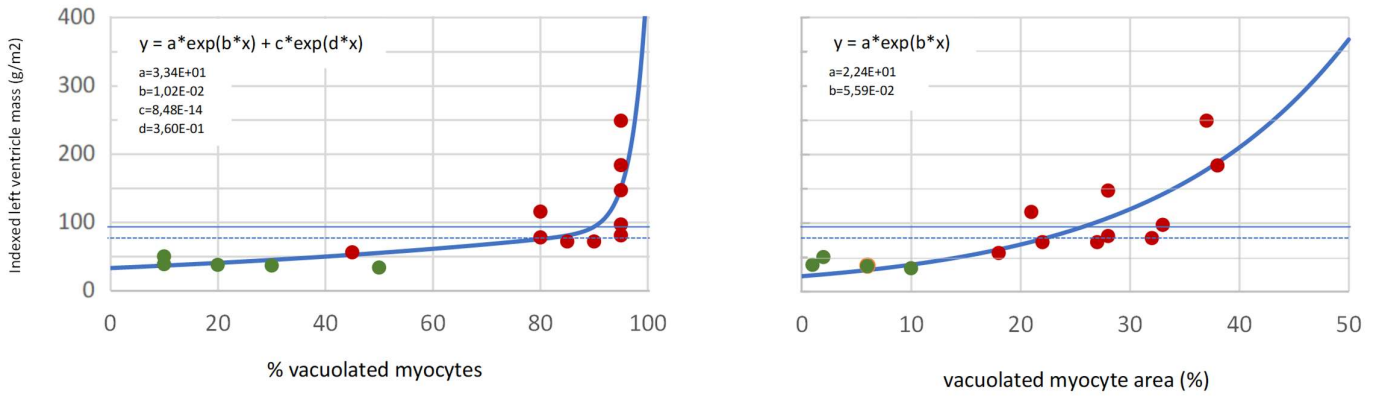
The dashed trend-line indicates the negative correlation ($r = -0.883$; $p < 0.001$) between native septal T1 values (ms) and vacuolated myocyte area in patients without increased LVMI (females: pink points; males: blue points). Black points indicate patients with increased LVMI ($>92 \text{ g/m}^2$ for males; $>79 \text{ g/m}^2$ for females) excluded from correlation. LVMI: indexed left ventricle mass. Pink and blue band indicates normal native T1 ranges for females (961-1069 ms) and males (931-1035 ms).

Figure 3



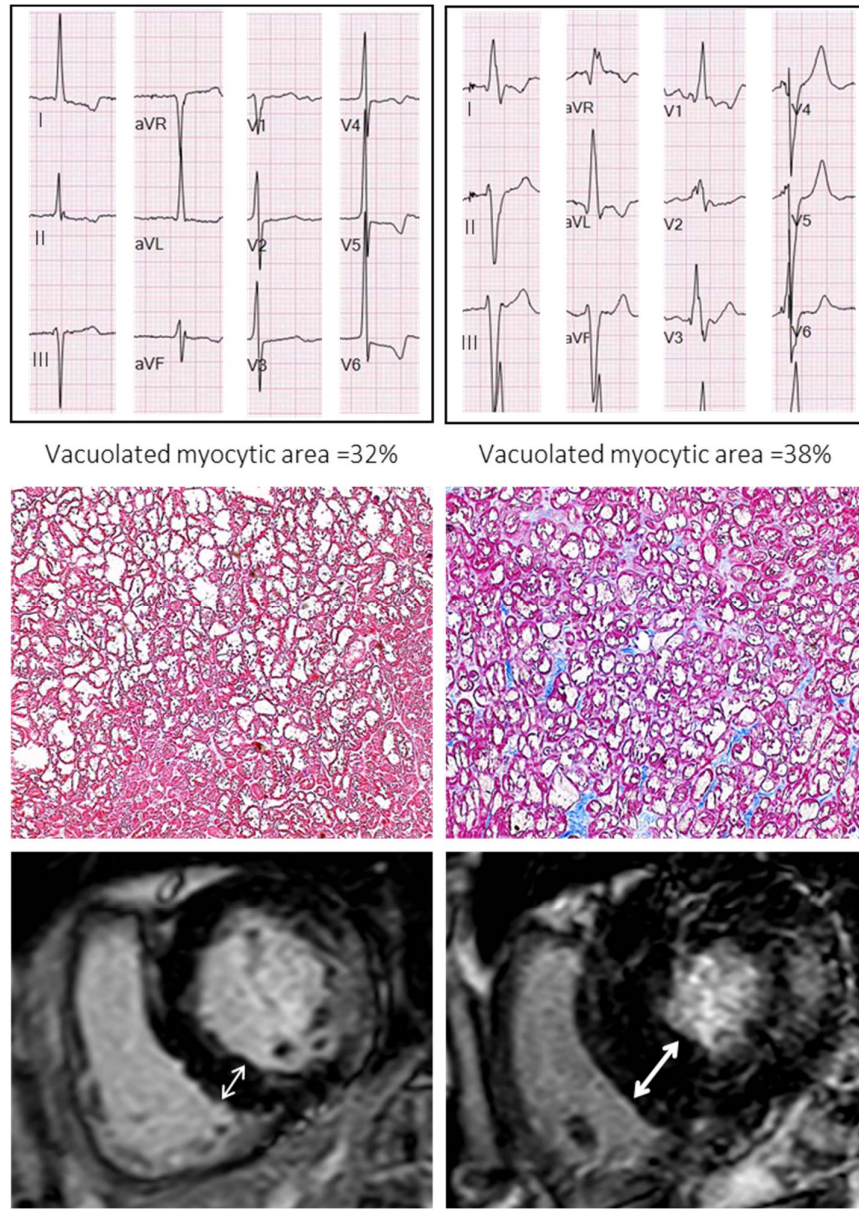
T2 maps (A, B) in 2 patients with inflammatory infiltrates at histology. C-E. focal inflammatory infiltrate made up mainly of macrophages with a small micro-granuloma (C, arrow), as confirmed by CD68-immunostaining (E). D-F. In the myocardial interstitium an inflammatory infiltrate is visible with both macrophages and lymphocytes, with double CD68-CD3 immunostaining positivity (F).

Figure 4



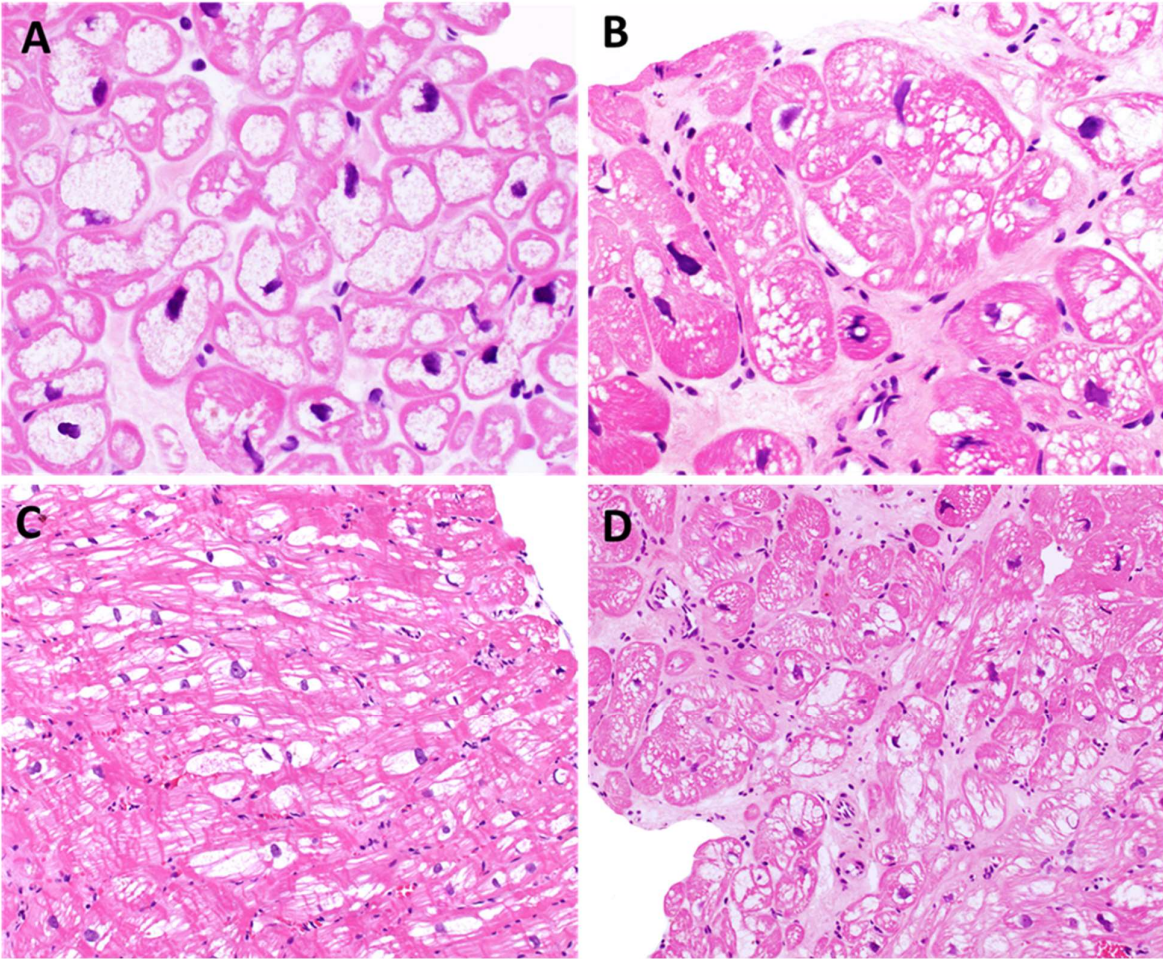
Trend line summarizing the exponential relationship between LVMi at CMR and the percentages of vacuolated myocytes (two-term model; on the left) and myocyte vacuolated area (single-term model; on the right). Green points= patients without LVH. Red points= patients with LVH (either increased left ventricular walls or LVMi). The solid and dashed straight lines indicate the cut-off values for increased LVMi for males (>92 g/m²) and female (>79 g/m² for females), respectively. LVMi: indexed left ventricular mass. LVH: left ventricle hypertrophy.

Figure 5



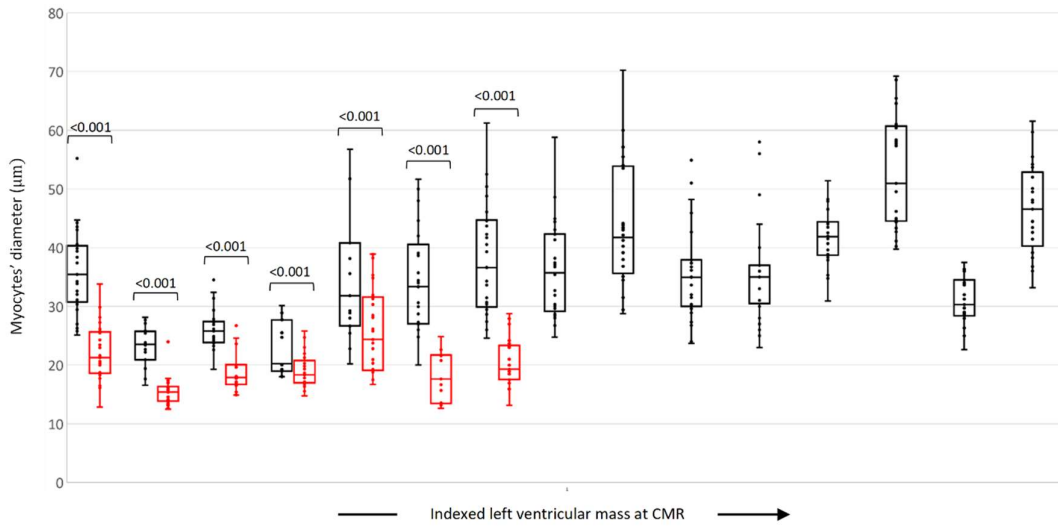
Comparison between 2 relatives, brother (62 yo on the right) and sister (73 yo on the left). Despite similar vacuolated myocyte areas, significant differences in terms of left ventricle hypertrophy at CMR and ECG abnormalities are noticed.

Supplemental figure 1



Pattern of myocyte vacuolization: macrovacuolization only (A), microvacuolization only (B), mixed but mainly macrovacuoles (C), , mixed but mainly microvacuoles (D).

Supplemental figure 2



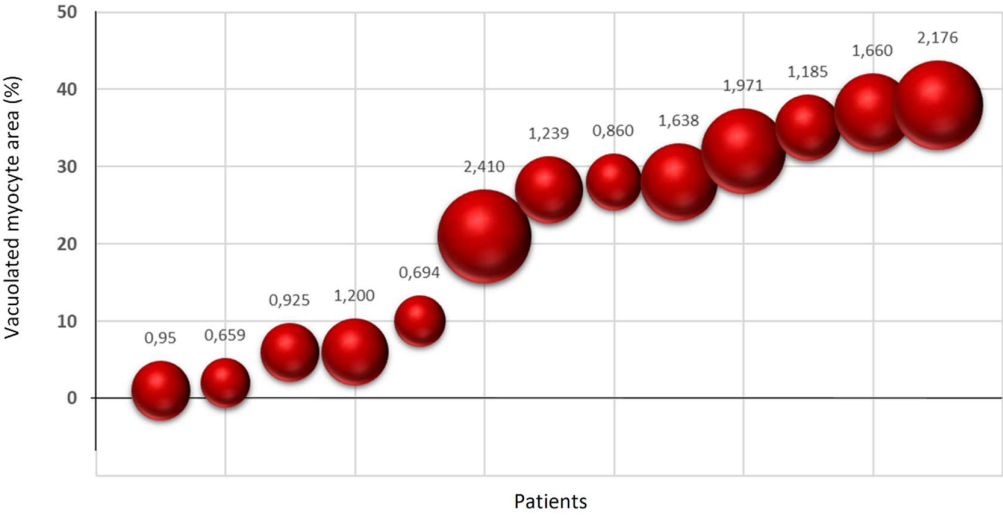
Box and whiskers plot showing distribution of hypertrophic vacuolated (black) and not vacuolated (red) cell diameter according to increasing indexed left ventricle mass at CMR. When non-vacuolated cells were less than 5 per field, due to the preponderance of vacuolated cells in the examined field, data was not collected. Middle horizontal line inside box indicates median. Bottom and top of the box are 25th/75th percentiles, the whiskers the lowest and highest value. CMR: cardiac magnetic resonance.

Supplemental figure 3



Electron microscopy photographs of endomyocardial biopsies comparing 3 cases at different cardiac stages, showing in early stage (A) few and scattered glycosphingolipid accumulations (arrows), while in intermediate (B) and mostly in advanced (C) stage extended with myofibrillar displacement and loss.

Supplemental figure 4



Correlation between mean endolysosome area (µm²) at electron microscope (proportional to the area of spheres in the graph) and vacuolated myocyte area.

TABLES

Table 1 Clinical, instrumental and laboratory characteristics of patients.

PATIENT	1	2	3	4	5	6	7	8	9	10	11	12	13	14	15
Age	49	39	43	22	22	71	39	73	66	39	60	64	49	62	54
Sex	f	f	f	m	f	f	m	f	f	m	f	f	m	m	m
Mutation	c.644A>G p.Asn215Ser	c.644A>G p.Asn215Ser	c.644A>G p.Asn215Ser	c.644A>G p.Asn215Ser	c.486G>T p.(Trp162Cys)	c.644A>G p.Asn215Ser	Leu414 CysfsTer4	c.1025G>A p.(Arg342Gln)	c.950T>C p.(Ile317Thr)	c.950T>C p.(Ile317Thr)	c.818T>C p.Phe273Ser	c.1078G>A p.Gly360Ser	c.644A>G p.Asn215Ser	c.1025G>A p.(Arg342Gln)	c.801+1G>T IVS5+1G>T
AFD type	Late onset	Late onset	Late onset	Late onset	Late onset	Late onset	Classic	Classic	Classic	Classic	Classic	Late onset	Late onset	Classic	classic
Diagnostic pathway	screening	screening	screening	screening	screening	cardiologic	screening	screening	nephrologic	screening	cardiologic	screening	Lower limb acute ischemia	nephrologic	dermatologic
Symptoms	None	none	None	none	none	palpitation, asthenia	acroparesthesias ; hypohydrosis	dyspnea (NYHA III)	dyspnea (NYHA II)	acroparesthesias; migraine ; hyperhidrosis	dyspnea (NYHA III); chest pain	palpitations; dispnea (NYHA II-III)	dyspnea (NYHA II)	dispnea (NYHA III)	effort angina; dyspnea (NYHA III)
CV Drugs	β-blocker, ARB	none	none	None	none	β-blocker; Ca-antagonist; warfarin	ACE-i	β-blocker; ARB, diuretics, warfarin	β-blocker	β-blocker	β-blocker; diltiazem. ARB, furosemide, warfarin	ACE-i ezetimibe, atorvastatin	ACE-i; b-blocker; edoxaban	β-blocker, warfarin, furosemide, canrenone	β-blocker, amiodarone, acetylsalicylic acid, furosemide, canrenone, atorvastatin
Specific therapy (duration)	-	-	-	-	-	-	-	algasidase alpha (2 years)	-	-	algasidase alpha (5 years)	algasidase alpha (8 years)	-	algasidase alpha (14 years)	algasidase alpha (5 years)
Extracardiac manifestations	absent	absent	tortuosity of conjunctival vessels	Renal impairment	absent	ESKD with emodyalisis; ischaemic stroke	Chronic kidney disease; proteinuria,	Cornea verticillate; peripheral neuropathy, pulmonary renal	ischaemic stroke neuro-sensorial hypoacusia	proteinuria, hypoacusia	ESKD Cornea verticillata	peripheral neuropathy	absent	ESKD with renal transplantation; TIA; basilar artery ectasia	ESKD with renal transplantation; angiokeratomas; peripheral neuropathy
CV risk factors	HBP; cigarette smoke	dyslipidemia		none	none	HBP; cigarette smoke	Previous cigarette smoking	HBP	Previous cigarette smoking	none	HBP, dyslipidemia	HBP; dyslipidemia	Previous cigarette smoking	cigarette smoke	HBP
Heart valve disease at echo	Bicuspid aortic valve with moderate stenosis	none	none	none	none	Moderate aortic regurgitation	none	Severe mitral and tricuspidal regurgitation	none	none	Moderate-severe mitral regurgitation	LVOTO	none	Moderate aortic stenosis; moderate mitral regurgitation	LVOTO
LysoGb3 (ng/mL)	0,8	1,1	0,9	3,2	2,8	1,3	Not available	5,3	4,8	36	10,7	1,7	5,2	33,3	24,3
Tnl hs (ng/L)	<2,3	<2,3	< 2,3	4,3	2,7	49	17,5	28,6	59	13	55	33,5	151	18	425
BNP (pg/mL)	174	9	18	12	25	108	26	369	113	22	1446	158	372	1332	1951

Creatinine (mg/dL)	0,68	0,74	0,57	1,3	0,76	4,09	2,08	1,37	0,64	0,91	3,25	0,96	0,93	2,6	1,3
eGFR (ml/mi/1,73 m2; CKD-EPI)	101	101	114	78	111	11	36	38	94	106	15	62	96	24	65
ECG	Normal	Normal	Normal	Normal (rSr' V1)	Normal	SR, LVH, strain	SR, picked precordial T wave	AF; LVH, strain	SR, Diffuse TWI	SR; peaked T waves	AF; LVH + strain	SR; I AVB; RBBB	SR; RBBB; LAFB; LVH	AF; RBBB; LAFB; LVH	SR; RBBB; LAFB; LVH
Cardiac Magnetic Resonance															
LVEDD, mm	5,1	5,0	4,5	4,3	4,3	5,7	5,2	5,5	4,5	5,3	5,1	4,5	6,1	5,4	5,2
LVEDV, mL/m2	82	84	76	68	66	100	92	70	47	98	86	65	177	91	89
LVEF, %	65	58	61	58	71	69	66	70	64	64	54	68	60	51	58
GLS (FT)	-14	-14	-17	-15	-17	na	-11	-16	-15	-12	-11	-13	-7	-4	na
LV mass, g/m2	50	39	38	37	34	56	72	78	72	81	97	116	147	184	249
IVS mm	0,9	0,8	0,7	0,6	0,6	0,8	0,9	1,2	1,2	1,3	1,5	1,9	1,6	2,2	2,2
PW mm	0,8	0,6	0,5	0,6	0,6	0,6	0,8	0,9	0,7	1,2	1,7	1,5	0,9	1,6	2,2
Maximum LVWT, mm	0,9	0,8	0,7	0,6	0,6	1,2 (basal IVS)	1,2 (basal IVS)	1,3 (medium IVS)	1,4 (IVS)	1,4 (IVS)	1,7	1,9 (basal)	1,6 (IVS)	2,2	2,2
Basal perfusion defect	No	No	No	no	No	no	No	no	No	No	No	no	No	no	no
LGE	No	No	No	no	no	No	No	Infero-lateral basal	Infero-lateral, medio-basal	No	Apical septum, infero-lateral	Postero-lateral	Basal IVS, basal inferior, infero-lateral, apical	Infero-lateral mediobasal; apical septum	Medio-apical inferior

Table 2 Comparison between cardiac magnetic resonance parameters at septal level and histological findings.

Patient	Magnetic Resonance					Light microscopy							Ultrastructure
	IVS (mm)	IVS T1 values (msec)	IVS T2 values (msec)	Septal LGE	Septal ECV (%)	Vacuolization		Inflammation	Fibrosis				
						Vacuolated myocyte area (%)	% vacuolated cells	Type of vacuolisation	Presence; distribution	subendo	interstitial	replacement	Mean endolysosome area (µm ²)
1	9	1003	54	no	32	2	10	Micro	Mild; focal	mild	mild	absent	0,659
2	8	1008	52	no	31	1	10	Micro	absent	mild	absent	absent	0,950
3	7	970	51	no	28	6	20	Mixed (micro)	Absent	absent	moderate	absent	0,925
4	6	946	45	no	26	6	30	Micro	absent	absent	absent	absent	1,200
5	6	950	50	no	30	10	50	Micro	Mild; multifocal	absent	mild	absent	0,694
6	8	925	50	no	na	18	45	Mixed (micro)	Absent	mild	mild	absent	na
7	12	926		no	29	22	90	Mixed (macro)	mild; multifocal	absent	mild	absent	na
8	12	889	47	no	36	32	80	Mixed (macro)	Absent	moderate	Moderate	absent	1,971
9	14	927	59	no	29	27	85	Mixed (macro)	Mild; multifocal	mild	absent	mild	1,239
10	13	830	46	no	23	28	95	Macro	Absent	moderate	mild	absent	1,638
11	15	910	ua	apical	25	33	95	Mixed (macro)	Absent	moderate	mild	absent	1,185
12	19	1000	55	no	na	21	80	Mixed (macro)	mild; multifocal	moderate	moderate	severe	0,860
13	16	931	52	basal	na	28	95	Mixed (micro)	Mild ; focal	mild	moderate	absent	2,410
14	22	952	45	apical	24	38	95	Macro	absent	moderate	mild	absent	2,176
15	22	956	46	no	na	37	95	Mixed (macro)	Mild	moderate	mild	absent	1,660

RELAZIONE SULLE ATTIVITÀ SVOLTE NEL CORSO DEL DOTTORATO

ATTIVITÀ DI RICERCA

Gli anni di dottorato hanno avuto come oggetto di ricerca quello delle cardiomiopatie, con particolare interesse per la cardiomiopatia ipertrofica sarcomerica, la malattia di Anderson Fabry, la cardiomiopatia aritmogena, la cardiomiopatia da accumulo di amiloide e la cardiomiopatia associata alla mutazione del gene LMNA. L'attività di studio ha portato alla mia collaborazione con diversi gruppi di lavoro, riguardanti la parte clinico-strumentale (Dr.ssa Biagini, Dr.ssa Graziosi), di anatomia patologica (Dr.ssa Leone), di Radiologia (Dr. L. Lovato/Dr. F. Niro) e di Patologia Generale (Prof.ssa Ferracin). In modo particolare ho preso parte nei seguenti lavori di ricerca:

- Ruolo dell'elettrocardiogramma nella diagnosi differenziale tra cardiomiopatia ipertrofica e malattia di Anderson Fabry. Lavoro multicentrico, che ha visto coinvolti oltre al Policlinico di S.Orsola, il Policlinico Umberto I di Roma, l'AUO Careggi di Firenze e il Policlinico S.Donato di Milano.
- Caratterizzazione elettrocardiografica della cardiomiopatia di Anderson-Fabry nelle sue diverse fasi, attraverso la correlazione dei dati ECG con lo spessore di parete del ventricolo sinistro.
- Caratterizzazione dell'eterogeneità delle vie diagnostiche della cardiomiopatia aritmogena del ventricolo sinistro.
- Studio di correlazione tra le caratteristiche istopatologiche e di microscopia elettronica delle biopsie nei pazienti affetti da malattia di Anderson Fabry e dati di risonanza magnetica. Lo studio si è concentrato in modo particolare sulla valutazione dei tempi di T1 mapping alla risonanza magnetica e il grado di accumulo di glicosfingolipidi a livello dei cardiomiociti.
- Ruolo dell'anatomia patologica nella revisione diagnostica dei pazienti con diagnosi iniziale di cardiomiopatia dilatativa primitiva o post-miocardica sottoposti a trapianto di cuore.
- Studio volto a ricercare le variazioni dei mi-RNA sierici e tissutali su biopsia endomiocardica nei pazienti con malattia di Anderson Fabry e coinvolgimento cardiaco, definendo il profilo di espressione trascrittomica attraverso l'impiego della tecnologia single-cell.

ATTIVITÀ CLINICA

- Ambulatorio di ecocardiografia PAD.21 e PAD 23 (U.O. Cardiologia Prof. Galiè; Responsabile Dr.ssa Biagini)
- Ambulatorio dedicato alle Cardiomiopatie (U.O. Cardiologia Prof. Galiè; Responsabile Dr.ssa Biagini)

PARTECIPAZIONE A TRIAL CLINICI

- Sub-investigator nello studio 'TTRACK - Prevalence and characteristics of transthyretin amyloidosis in patients with left ventricular hypertrophy of unknown etiology'. Sponsor – Pfizer. Lo studio cross-sectional si prefigge come outcome primario quello di stabilire la prevalenza della positività della fissazione cardiaca alla scintigrafia ossea totale body con 99mTc-DPD o 99mTc-PYP o 99mTc-HMDP nei pazienti con età > 50 anni con ipertrofia ventricolare sinistra inspiegata (in assenza di stenosi valvolare aortica severa).

ARTICOLI INDICIZZATI SU PUBMED E CAPITOLI DI LIBRO:

- Phospholamban Cardiomyopathy: Unveiling a Distinct Phenotype Through Heart Failure Stages Progression.
Vanda Parisi, Chiara Chiti, Maddalena Graziosi, Ferdinando Pasquale, **Raffaello Ditaranto**, Matteo Minnucci, Mauro Biffi, Luciano Potena, Francesca Girolami, Chiara Baldovini, Ornella Leone, Nazzareno Galiè, Elena Biagini.
Circ Cardiovasc Imaging. 2022 Sep 2:101161CIRCIMAGING122014232.
- Myocardial infarction with non-obstructive coronary arteries in hypertrophic cardiomyopathy vs Fabry disease.
Graziani F, Lillo R, Biagini E, Limongelli G, Autore C, Pieroni M, Lanzillo C, Calò L, Musumeci MB, Ingrasciotta G, Minnucci M, **Ditaranto R**, Milazzo A, Zocchi C, Rubino M, Lanza GA, Olivotto I, Crea F.
Int J Cardiol. 2022 Aug 2:S0167-5273(22)01116-0. doi: 10.1016/j.ijcard.2022.07.046.
- Clinical presentations leading to arrhythmogenic left ventricular cardiomyopathy.
Graziosi M, **Ditaranto R (first co-Author)**, Rapezzi C, Pasquale F, Lovato L, Leone O, Parisi V, Potena L, Ferrara V, Minnucci M, Caponetti AG, Chiti C, Ferlini A, Gualandi F, Rossi C, Berardini A, Tini G, Bertini M, Ziacchi M, Biffi M, Galie N, Olivotto I, Biagini E.
Open Heart. 2022 Apr;9(1):e001914. doi: 10.1136/openhrt-2021-001914.
- Mitral valve prolapse and mitral annulus disjunction: be aware of a potential arrhythmogenic substrate.
Chiti C, Parisi V, Tonet E, Cocco M, Pasquale F, Ferrara V, Minnucci M, Baldassarre R, **Ditaranto R**, Caponetti AG, Saturi G, Galiè N, Campo G, Biagini E.
G Ital Cardiol (Rome). 2022 Mar;23(3):181-189. doi: 10.1714/3751.37337.
- Pediatric Restrictive Cardiomyopathies.
Ditaranto R, Caponetti AG, Ferrara V, Parisi V, Minnucci M, Chiti C, Baldassarre R, Di Nicola F, Bonetti S, Hasan T, Potena L, Galiè N, Ragni L, Biagini E.
Front Pediatr. 2022 Jan 25;9:745365. doi: 10.3389/fped.2021.745365.
- Circulating miR-184 is a potential predictive biomarker of cardiac damage in Anderson-Fabry disease.
Salamon I, Biagini E, Kunderfranco P, Roncarati R, Ferracin M, Taglieri N, Nardi E, Laprovitera N, Tomasi L, Santostefano M, **Ditaranto R**, Vitale G, Cavarretta E, Pisani A, Riccio E, Aiello V, Capelli I, La Manna G, Galiè N, Spinelli L, Condorelli G.
Cell Death Dis. 2021 Dec 11;12(12):1150. doi: 10.1038/s41419-021-04438-5.
- Cum Grano Salis: Cardiac Sarcoidosis as a Perfect Mimic of Arrhythmogenic Right Ventricular Cardiomyopathy.
Giulia Saturi, Angelo Giuseppe Caponetti, Ornella Leone, Luigi Lovato, Simone Longhi, Maddalena Graziosi, **Raffaello Ditaranto**, Mauro Biffi, Nazzareno Galiè, Elena Biagini.
Circ Cardiovasc Imaging. 2021 Jul;14(7):e012355. doi: 10.1161/CIRCIMAGING.120.012355.
- Arrhythmic syncope in a patient with left ventricular dysfunction.
Ditaranto R, Graziosi M, Parisi V.G
Ital Cardiol (Rome). 2021 Nov;22(11):900. doi: 10.1714/3689.36748

- Standard electrocardiogram for differential diagnosis between Anderson-Fabry disease and hypertrophic cardiomyopathy.
 Giovanni Vitale, **Raffaello Ditaranto (first co-authorship)**, Francesca Graziani, Ilaria Tanini, Antonia Camporeale, Rosa Lillo, Marta Rubino, Elena Panaioli, Federico Di Nicola, Valentina Ferrara, Rossana Zanoni, Angelo Giuseppe Caponetti, Ferdinando Pasquale, Maddalena Graziosi, Alessandra Berardini, Matteo Ziacchi, Mauro Biffi, Marisa Santostefano, Rocco Liguori, Nevio Taglieri, Ales Linhart, Iacopo Olivotto, Claudio Rapezzi, Elena Biagini.
 Heart 2021 Feb 9;heartjnl-2020-318271. doi: 10.1136/heartjnl-2020-318271.
- A Pathogenic Galactosidase A Mutation Coexisting With an MYBPC3 Mutation in a Female Patient With Hypertrophic Cardiomyopathy.
 Giovanni Vitale, Ferdinando Pasquale, Ornella Leone, Giovanna Cenacchi, Fabio Niro, Mario Torrado, Emilia Maneiro, Maddalena Graziosi, **Raffaello Ditaranto**, Irene Capelli, Lorenzo Monserrat, Claudio Rapezzi, and Elena Biagini. Canadian Journal of Cardiology 36 (2020) 1554e1-e3
- Postmortem diagnosis of left dominant arrhythmogenic cardiomyopathy: the importance of a multidisciplinary network for sudden death victims. "Hic mors gaudet succurrere vitae".
 Maddalena Graziosi, Ornella Leone, Alberto Foà, Valentina Agostini, **Raffaello Ditaranto**, Marco Foroni, Cesare Rossi, Luigi Lovato, Marco Seri, Claudio Rapezzi.
 Cardiovascular Pathology 44 (2020) 107157.
- Clinical profile of cardiac involvement in Danon disease: a multicenter european registry. Dor Lotan, Joel Salazar-Mendiguchía, Jens Mogensen, Faizan Rathore, Aris Anastasakis, Juan Kaski, Pablo Garcia-Pavia, Iacopo Olivotto, Philippe Charron, Elena Biagini, Anwar Baban, Giuseppe Limongelli, Waddah Ashram, Yishay Wasserstrum, Joe Galvin, Esther Zorio, Attilio Iacovoni, Lorenzo Monserrat, Paolo Spirito, Maria lascone and Michael Arad. (**Raffaello Ditaranto** among Cooperating Investigators) Circ Genom Precis Med. 2020 Dec;13(6):e003117. doi: 10.1161/CIRCGEN.120.003117. Epub 2020 Nov 5. PMID: 33151750
- Differences in cardiac phenotype and natural history of laminopathies with and without neuromuscular onset.
Raffaello Ditaranto, Giuseppe Boriani, Mauro Biffi, Massimiliano Lorenzini, Maddalena Graziosi, Matteo Ziacchi, Ferdinando Pasquale, Giovanni Vitale, Alessandra Berardini, Rita Rinaldi, Giovanna Lattanzi, Luciano Potena, Sofia Martin Suarez, Maria Letizia Bacchi Reggiani, Claudio Rapezzi and Elena Biagini. Orphanet Journal of Rare Diseases (2019) 14:263
- The complex interplay between fitness, genetics, lifestyle, and inflammation in the pathogenesis of coronary atherosclerosis: lessons from the Amazon rainforest.
Ditaranto R, Vitale G, Lorenzini M, Rapezzi C.
 Eur Heart J Suppl. 2019 Mar;21(Suppl B):B76-B79. doi: 10.1093/eurheartj/suz030. Epub 2019 Mar 29.
- Chapter Title: Electrocardiography. Author: Claudio Rapezzi, Alberto Foà and, **Raffaello Ditaranto**. extbook: Myocarditis (A.Caforio; Springer) (2020).

CARDIOVASCULAR IMAGES

Phospholamban Cardiomyopathy: Unveiling a Distinct Phenotype Through Heart Failure Stages Progression

Vanda Parisi¹, MD; Chiara Chiti, MD; Maddalena Graziosi, MD, PhD; Ferdinando Pasquale, MD, PhD; Raffaello Ditaranto, MD; Matteo Minnucci², MD; Mauro Biffi³, MD; Luciano Potena⁴, MD; Francesca Girolami⁵, BSc; Chiara Baldovini, MD, PhD; Ornella Leone, MD; Nazzareno Galiè, MD; Elena Biagini⁶, MD, PhD

A 37-year-old male received a diagnosis of nonobstructive hypertrophic cardiomyopathy (HCM) following atypical chest pain and detection of inferior, anterior, and apical T wave inversions with subtle ST depression laterally at ECG (Figure 1A). His mother, affected by nonischemic dilated cardiomyopathy (DCM), died suddenly at 39 years.

Cardiac magnetic resonance confirmed a mild asymmetrical left ventricular (LV) hypertrophy with normal volume and systolic function (13 mm at basal interventricular septum, end-diastolic volume index 55.2 mL/m², ejection fraction 70%). Late gadolinium enhancement (LGE) was detected at apical anterior wall with mid-wall distribution and basal inferolateral wall with subepicardial distribution. Total LGE amount was 3 g, corresponding to 3.5% of myocardial mass by Full-Width at Half Maximum and 5-Standard Deviations methods (Figure 1B, 1C, and 1D). The right ventricle (RV) was normal.

Frequent isolated premature ventricular beats (N=9500, 11% of total beats) were detected at 24-hour ECG monitoring; bisoprolol was prescribed and uptitrated to 7.5 mg daily with reduction of ventricular arrhythmia burden (4% of total beats in the following ECG monitoring).

Eight years later the patient had an episode of acute heart failure. LV end-diastolic volume index was 85 mL/m² by echocardiography, with 40% LV ejection fraction; coronary angiography excluded significant coronary

artery disease. A subcutaneous implantable cardioverter defibrillator was implanted as primary prevention for sudden cardiac death in end-stage HCM. One year later, repeated ventricular tachycardia requiring appropriate shocks occurred (5 episodes within 10 months, Figure S1), and the patient developed progressive exercise intolerance. He was then referred to our tertiary University Hospital.

The admission ECG revealed significant changes compared to the first one, with widespread loss of QRS potential, extreme QRS prolongation, and fragmentation (Figure 2A). Echocardiography showed severe biventricular dilatation (LV end-diastolic volume index 98 mL/m²; RV end-diastolic area 30 m²) and systolic dysfunction (LV ejection fraction 18%, RV fractional area change 16%), with akinetic and thinned interventricular septum, LV inferoposterior and apical wall, akinesia of the inferior RV wall with aneurism and dyskinesia of the RV outflow tract. Severe functional mitral and tricuspid regurgitation were also present (Video S1 and S2).

During hospitalization, the patient had incessant episodes of sustained ventricular tachycardia with hemodynamic instability requiring inotropes, intraaortic balloon pump, and antiarrhythmic drugs. Cardiac magnetic resonance was repeated despite the limitations posed by the magnetic field distortion due to the subcutaneous implantable cardioverter defibrillator: multiple LGE areas were detected in the LV, with a ring-like

Key Words: cardiomyopathy ■ coronary artery disease ■ death, sudden, cardiac ■ gadolinium ■ hypertrophy

Correspondence to: Elena Biagini, MD, PhD, Cardiology Unit, IRCCS Azienda Ospedaliero-Universitaria di Bologna, European Reference Network for Rare and Low Prevalence Complex Diseases of the Heart (ERN-GUARDHEART), via G. Massarenti N9, 40138, Bologna, Italy. Email elena.biagini73@gmail.com
Supplemental Material is available at <https://www.ahajournals.org/doi/suppl/10.1161/CIRCIMAGING.122.014232>.

For Sources of Funding and Disclosures, see page xxx.

© 2022 American Heart Association, Inc.

Circulation: Cardiovascular Imaging is available at www.ahajournals.org/journal/circimaging

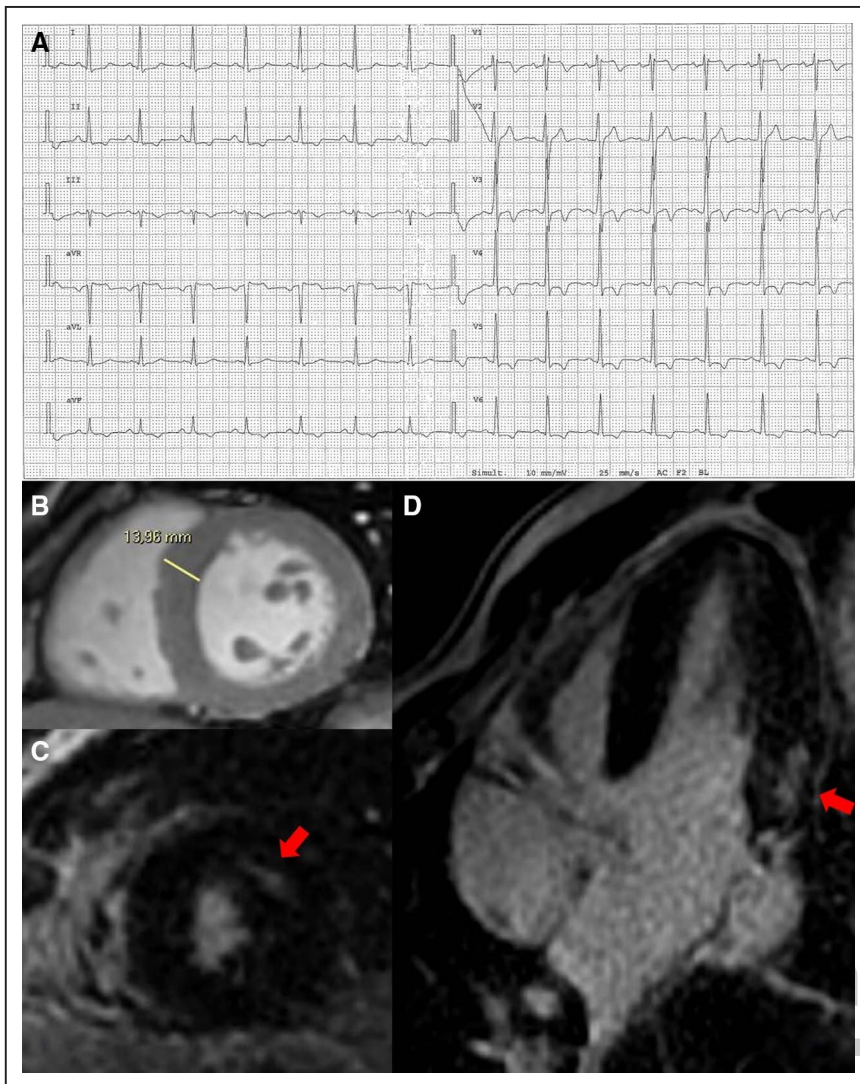


Figure 1. ECG and cardiac magnetic resonance (CMR) at first contact.

A, First ECG: sinus rhythm with inferior, anterior, and apical T wave inversions with subtle ST depression laterally. **B–D**, First CMR: maximum left ventricular (LV) thickness of 13 mm measured at basal interventricular septum; late gadolinium enhancement with intramyocardial distribution at LV anterior apical wall and with subepicardial distribution at LV inferolateral basal segments (red arrows).



aging

distribution pattern (Figure 2B and 2C). Transcatheter radiofrequency ablation at interventricular septum and RV outflow tract was attempted to treat the ventricular arrhythmias, without complete suppression of the arrhythmic burden.

Due to the severity of his medical conditions, the patient was evaluated for orthotopic cardiac transplantation and was transplanted 6 months later.

Gross pathological examination of the explanted heart revealed an enlarged globose organ with RV outflow tract dilation. Transverse sections showed both on macroscopic and microscopic examination an extensive replacement fibrosis of the LV involving: the midmural/subendocardial areas of the anterolateral wall, the midmural areas of both inferolateral wall, and the entire interventricular septum (Figure 3). This pathology pattern was superimposable on the ring-like distribution seen at cardiac magnetic resonance. Hypertrophy and cytoplasmic vacuolization as well as multiple myocardial disarray were observed. In addition, diffuse fibro-fatty replacement of the myocardium, prevalently midmural in the anterolateral

wall and transmural in the inferolateral was present in the RV.

Genetic sequencing revealed a heterozygous stop-loss variant in the phospholamban (PLN) gene, c.157_158del p(*53Lysex*6) with a deletion of 2 nucleotides (thymidine and guanosine) in exon 2 (Gene Bank accession: NM_002667.5) that generates an extension in the reading frame of 6 codons. This variant is not annotated in large controls populations database (Genome Aggregation Database), is reported in Human Gene Mutation Database as Damaging Mutation (ID accession: CD1516318), and is interpretable as likely pathogenic according to 2015 American College of Medical Genetics and Genomics classification guidelines, associated with HCM and DCM phenotypes.^{1,2} In addition, a variant of unknown significance in the ankyrin-2 (*ANK2*) gene (Gene Bank accession: NM_001148.6) c.3623A>C p.(Lys1208Thr) in heterozygous status was identified.

Familial screening was performed, and patient's sister and son revealed no cardiac abnormalities with a negative genetic test.

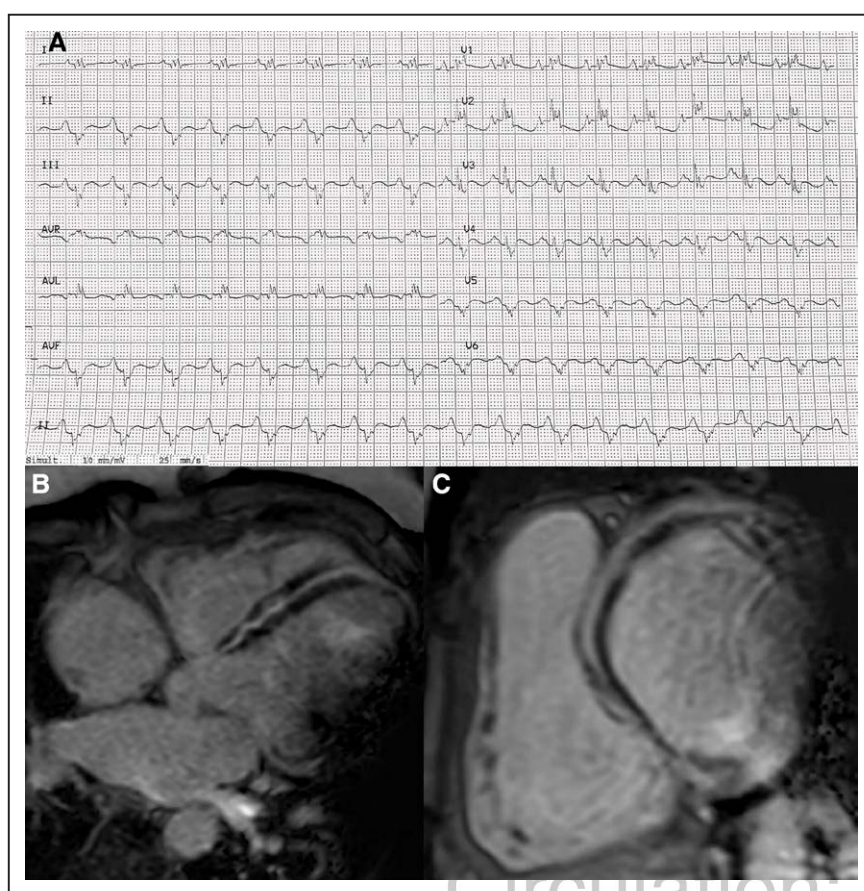


Figure 2. ECG and cardiac magnetic resonance (CMR) before cardiac transplantation.

A, ECG before heart transplantation: note the widespread low QRS voltages with marked QRS prolongation and extreme potential fragmentation coupled to repolarization abnormalities. **B** and **C**, CMR: though affected by magnetic field distortion due to the subcutaneous implantable cardioverter defibrillator presence, multiple late gadolinium enhancement areas were detected in the left ventricle, with a ring-like distribution pattern.



PLN is a key regulator of cardiac contractility and relaxation, influencing the affinity of SERCA2 (Sarco-Endoplasmic Reticulum Calcium ATPase) protein for intracellular calcium. In its dephosphorylated state PLN inhibits SERCA2 activity, whereas after beta-adrenergic stimulation the inhibitory effect is relieved leading to improvement in cardiomyocyte contractility. Mutated PLN aggregates could also result in desmosomal disassembly, explaining the arrhythmogenic profile of these patients.

PLN cardiomyopathy is characterized by early phenotypic expression (II-III decade) usually as DCM or arrhythmogenic cardiomyopathy with biventricular involvement, family history of premature sudden cardiac death, high incidence of ventricular arrhythmias, or cardiac transplantation.³ HCM phenotype at onset is extremely rare but described.² Compared to other genetic cardiomyopathies (ie, lamin A/C, sarcomeric), PLN-associated cardiomyopathy shows a distinctive pattern of fibro-fatty changes, involving the LV inferolateral subepicardium and the RV, even with normal LV ejection fraction, similarly to desmosomal mutations.⁴ These structural alterations correspond to low-voltage QRS and T waves inversion at ECG and portend severe ventricular arrhythmias and heart failure.³

In our patient, some red flags hinted a nonsarcomeric HCM at the early stage: mild hypertrophy of the interventricular septum with basal subepicardial inferolateral LGE and first-degree family history of DCM and sudden cardiac death. The later evolution from a mild HCM phenotype to a severe DCM with highly specific clues to a biventricular arrhythmogenic cardiomyopathy such as the ring-like LV LGE distribution (corresponding to fibro-fatty infiltration at the histological examination) and the bizarre ECG were the main signs for the etiological diagnosis.

A pathogenic PLN mutation detection denotes an important diagnostic information unveiling etiology in borderline/overlapping phenotypes and represents a key point in decision-making for timely implantable cardioverter defibrillator implantation or heart transplantation referral, irrespective of the conventional clinical and instrumental markers of disease progression.

By uncovering distinctive genotype-phenotype correlations and applying a red flags method to the diagnostic pathway, tailored management strategies and therapeutic approaches may be made available for patients with hereditary cardiomyopathies.

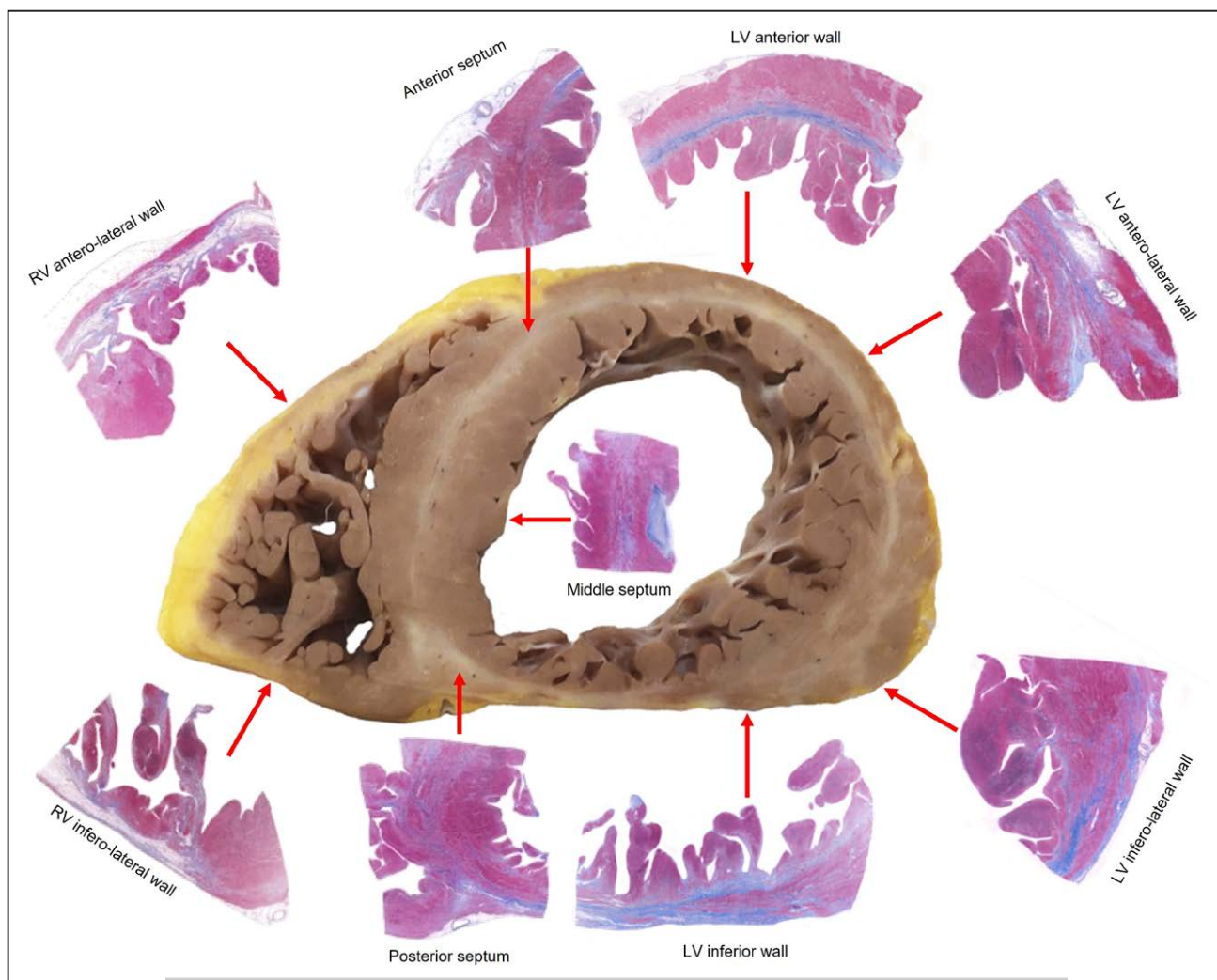


Figure 3. Anatomopathological examination of explanted heart. Macroscopic transverse section of heart and histology slides indicating distribution of myocardial replacement fibrosis (highlighted in blue with Mallory trichrome stain) in various areas of left ventricular (LV) wall and in the septum. In right ventricle (RV) the histology shows predominant fibro-fatty replacement of the myocardium.

ARTICLE INFORMATION

Affiliations

Cardiology Unit, IRCCS Azienda Ospedaliero-Universitaria di Bologna, Italy (V.P., C.C., M.G., F.P., R.D., M.M., M.B., L.P., N.G., E.B.). Department of Experimental, Diagnostic and Specialty Medicine (DIMES), University of Bologna, Italy (V.P., C.C., R.D., M.M., N.G.). European Reference Network for Rare, Low Prevalence, and Complex Diseases of the Heart (ERN GUARD-Heart), Italy (M.G., F.P., M.B., L.P., E.B.). Cardiology Unit, Meyer Children’s Hospital, Florence, Italy (F.G.). Cardiovascular Pathology Unit, IRCCS Azienda Ospedaliero-Universitaria di Bologna, Italy (C.B., O.L.).

Sources of Funding

The work reported in this publication was funded by the Italian Ministry of Health, RC-2022-2773270 project.

Disclosures

None.

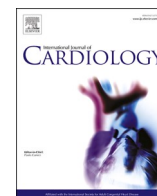
Supplemental Material

Figure S1
Video S1–S2

REFERENCES

1. Haas J, Frese KS, Peil B, Kloos W, Keller A, Nietsch R, Feng Z, Müller S, Kayvanpour E, Vogel B, et al. Atlas of the clinical genetics of human dilated cardiomyopathy. *Eur Heart J*. 2015;36:1123–135a. doi: 10.1093/eurheartj/ehu301
2. Mazzarotto F, Girolami F, Boschi B, Barlocco F, Tomberli A, Baldini K, Coppini R, Tanini I, Bardi S, Contini E, et al. Defining the diagnostic effectiveness of genes for inclusion in panels: the experience of two decades of genetic testing for hypertrophic cardiomyopathy at a single center. *Genet Med*. 2019;21:284–292. doi: 10.1038/s41436-018-0046-0
3. Te Rijdt WP, Ten Sande JN, Gorter TM, van der Zwaag PA, van Rijsingen IA, Boekholdt SM, van Tintelen JP, van Haelst PL, Planken RN, de Boer RA, et al. Myocardial fibrosis as an early feature in phospholamban p.Arg14del mutation carriers: phenotypic insights from cardiovascular magnetic resonance imaging. *Eur Heart J Cardiovasc Imaging*. 2019;20:92–100. doi: 10.1093/ehjci/jeu047
4. Sepehrkhoy S, Gho JM, van Es R, Harakalova M, de Jonge N, Dooijes D, van der Smagt JJ, Buijsrogge MP, Hauer RNW, Goldschmeding R, et al. Distinct fibrosis pattern in desmosomal and phospholamban mutation carriers in hereditary cardiomyopathies. *Heart Rhythm*. 2017;14:1024–1032. doi: 10.1016/j.hrthm.2017.03.034

Downloaded from <http://ahajournals.org> by kerrimuse@heart.org on September 2, 2022



Short communication

Myocardial infarction with non-obstructive coronary arteries in hypertrophic cardiomyopathy vs Fabry disease

Francesca Graziani^{a,*}, Rosa Lillo^{a,b}, Elena Biagini^c, Giuseppe Limongelli^d, Camillo Autore^e, Maurizio Pieroni^f, Chiara Lanzillo^g, Leonardo Calò^g, Maria Beatrice Musumeci^e, Gessica Ingrassiotta^b, Matteo Minnucci^c, Raffaello Ditaranto^c, Alessandra Milazzo^h, Chiara Zocchi^h, Marta Rubino^d, Gaetano Antonio Lanza^{a,b}, Iacopo Olivotto^h, Filippo Crea^{a,b}

^a Department of Cardiovascular Medicine, Fondazione Policlinico Universitario A. Gemelli IRCCS, Rome, Italy

^b Catholic University of the Sacred Heart, Rome, Italy

^c Cardiology Unit, St. Orsola Hospital, IRCCS Azienda Ospedaliero-Universitaria di Bologna, Italy

^d Inherited and Rare Cardiovascular Diseases, Department of Translational Medical Sciences, University of Campania "Luigi Vanvitelli", Monaldi Hospital, Naples, Italy

^e Cardiology Unit, Department of Clinical and Molecular Medicine, Sapienza University of Rome - Sant'Andrea University Hospital, Rome, Italy

^f Cardiovascular Department, San Donato Hospital, Arezzo, Italy

^g Cardiology Department Policlinico Casilino, Rome, Italy

^h Cardiomyopathy Unit, Careggi University Hospital, Florence, Italy



ARTICLE INFO

Keywords:

Fabry disease

Hypertrophic cardiomyopathy

Myocardial infarction

MINOCA

Coronary microvascular dysfunction

ABSTRACT

Background: Little is known about prevalence and predictors of myocardial infarction with non-obstructive coronary arteries (MINOCA) in Fabry disease (FD) and hypertrophic cardiomyopathy (HCM). We assessed and compared the prevalence and predictors of MINOCA in a large cohort of HCM and FD patients.

Methods: In this multicenter, retrospective study we enrolled 2870 adult patients with HCM and 267 with FD. The only exclusion criterion was documented obstructive coronary artery disease. MINOCA was defined according to guidelines. For each patient we collected clinical, ECG and echocardiographic data recorded at initial evaluation. **Results:** Overall, 36 patients had MINOCA during a follow-up period of 4.5 ± 11.2 years. MINOCA occurred in 16 patients with HCM (0.5%) and 20 patients with FD (7.5%; $p < 0.001$). The difference between the 2 groups was highly significant, also after adjustment for the main clinical, ECG and echocardiographic variables (OR 6.12; 95%CI 2.80–13.3; $p < 0.001$). In the FD population MINOCA occurred in 17 out of 96 patients with left ventricle hypertrophy (LVH, 17.7%) and in 3 out of 171 patients without LVH (1.7%; OR 12.0; 95%CI 3.43–42.3; $p < 0.001$). At multivariable analysis, voltage criteria for LVH at ECG (OR 7.3; 95%CI 1.93–27.7; $p = 0.003$) and maximal LV wall thickness at echocardiography (OR 1.15; 95%CI 1.05–1.27; $p = 0.002$) maintained an independent association with MINOCA. No major significant differences were found in clinical, ECG and echocardiographic findings between HCM patients with or without MINOCA.

Conclusions: MINOCA was rare in HCM patients, and 6-fold more frequent in FD patients. MINOCA may be considered a red flag for FD and aid in the differential diagnosis from HCM.

1. Background

Myocardial infarction with non-obstructive coronary arteries (MINOCA) is an increasingly recognized clinical entity [1–4], with significant prognostic implications [5,6]. MINOCA patients represent a

conundrum, given the underlying multiple possible etiologies and pathogenic mechanisms, which, among others, include coronary microvascular dysfunction (CMD) [2]. CMD has been described in patients with hypertrophic cardiomyopathy (HCM) as well as one of its phenocopies, Fabry disease (FD) [7–10]. In both these conditions, CMD was found to

Abbreviations: CMD, coronary microvascular dysfunction; FD, Fabry disease; HCM, Hypertrophic Cardiomyopathy; LVEF, left ventricular ejection fraction; LVH, left ventricle hypertrophy; LVWT, left ventricular wall thickness; MINOCA, Myocardial infarction with non-obstructive coronary arteries.

* Corresponding author at: Department of Cardiovascular Medicine, Fondazione Policlinico Universitario A. Gemelli IRCCS, Largo A. Gemelli 8, 00168 Rome, Italy.

E-mail address: francesca.graziani@policlinicogemelli.it (F. Graziani).

<https://doi.org/10.1016/j.ijcard.2022.07.046>

Received 20 July 2022; Accepted 29 July 2022

Available online 2 August 2022

0167-5273/© 2022 Elsevier B.V. All rights reserved.

Table 1
Baseline characteristics of patients with FD and HCM.

	FD n = 267	HCM n = 2870	P
Sex (M)	112 (41.9)	1846 (64.3)	<0.001
Age at diagnosis (yrs)	41.6 ± 17.1	45.2 ± 18.9	0.03
Hypertension	74 (27.7)	724 (25.2)	0.572
Body mass index (Kg/m ²)	24.3 ± 4.5	25.7 ± 4.2	<0.001
NYHA class III-IV	19 (7.1)	304 (10.5)	0.060
<i>Electrocardiographic findings</i>			
PR interval (ms)	148.2 ± 27.7	169.2 ± 60.7	<0.001
QRS duration (ms)	98.3 ± 26.3	104.8 ± 39.1	0.011
Right bundle branch block	27 (10.1)	42 (1.4)	<0.001
Left bundle branch block	9 (3.3)	46 (1.6)	0.090
<i>Echocardiographic findings</i>			
Maximal wall thickness (mm)	12.4 ± 5.1	19.1 ± 5.5	<0.001
LV ejection fraction (%)	62.5 ± 6.9	66.4 ± 8.0	<0.001
E/e' ratio	8.5 ± 3.8	10.0 ± 5.8	0.001
LAVi (ml/m ²)	34.2 ± 15.4	44.0 ± 20.1	<0.001
LV outflow tract obstruction	9 (3.3)	754 (26)	<0.001
Gmax LV outflow tract (mmHg)	14.1 ± 20.5	28.5 ± 46.5	0.031
PASP (mmHg)	26.9 ± 7.9	23.3 ± 17.1	0.056
LVH (%)	36.7	100	<0.001
<i>Medical therapy</i>			
Beta-blockers (%)	21.8	26.6	0.09
Calcium channel blockers (%)	7.1	4.5	0.07
ACE-i/ARBs (%)	25.1	7.1	<0.001
Diuretics (%)	10.2	5.1	0.002
Amiodarone (%)	13.5	3.3	<0.001
Anti-platelet (%)	17.5	14.2	0.2
Anticoagulant (%)	9.5	4.4	<0.001

ACE-i/ARBs = angiotensin converting enzyme inhibitors/angiotensin receptor blockers; Gmax = maximum gradient; LAVi = left atrial volume index; LV = left ventricle; LVH = left ventricle hypertrophy; NYHA = New York Heart Association; PASP = pulmonary artery systolic pressure;

cause myocardial ischemia and have relevant clinical implications [9,10]. Yet, there are no data about the prevalence and predictors of MINOCA in these patients. In this study, therefore, we aimed to assess: 1) the prevalence of MINOCA in patients with FD and HCM, and 2) identify clinical, electrocardiographic (ECG) and echocardiographic predictors of MINOCA in the 2 conditions.

2. Methods

In this multicenter, observational, retrospective study, we included adult patients with either HCM or FD followed at 6 Italian Centers, and initially evaluated between 1997 and 2020. The only exclusion criterion was documented obstructive coronary artery disease (≥50% stenosis in any epicardial vessel at invasive or computed tomography coronary angiography) [2]. For each patient we collected clinical, ECG and echocardiographic data recorded at the initial evaluation at each participating Centre after a conclusive diagnosis. The diagnosis of HCM was based on echocardiographic documentation of left ventricle hypertrophy (LVH) with LV wall thickness (LVWT) ≥15 mm (or ≥ 13 mm in patients with a first-degree relative with confirmed HCM), in absence of any other cardiac or systemic disease capable of producing a similar magnitude of LVH [11]. The diagnosis of FD was based on plasma and leucocyte α-galactosidase A enzyme activity and sequencing of the GLA gene [12]. In the FD population, LVH was defined as LVWT ≥13 mm [12]. The ECG diagnosis of LVH was done according to Sokolow-Lyon criteria (S wave depth in V1 + tallest R wave height in V5-V6 > 35 mm) [13].

The occurrence of MINOCA was ascertained by reviewing the medical records of each patient, where clinical events are regularly described in detail. We identified all patients admitted with a suspicion of acute coronary syndrome at any time during follow-up. MINOCA was defined according to guidelines by the concomitance of: a) acute myocardial infarction according to the Fourth Universal Definition of Myocardial Infarction [1], i.e., documentation of a rise and fall of troponin levels, with at least 1 value above the 99th percentile upper reference limit, in

Table 2
Comparison between patients with and without MINOCA.

	MINOCA n = 36	No MINOCA n = 3101	p
Fabry disease	20 (55)	247 (7.9)	<0.001
Sex (M)	24 (66.7)	1934 (62.4)	0.730
CM family history	14 (38.9)	1116 (36)	0.920
Age at diagnosis (yrs)	52.7 ± 12.5	44.8 ± 18.8	0.014
Diabetes	3 (8.3)	66 (5.2)	0.435
Hypertension	20 (55.6)	778 (29.1)	0.001
Body mass index (Kg/m ²)	27.4 ± 5.0	25.3 ± 4.0	0.076
NYHA class III-IV	4 (11)	319 (10.2)	0.853
<i>Electrocardiographic findings</i>			
PR interval (ms)	163.8 ± 39.9	164.7 ± 66.8	0.876
QRS duration (ms)	111.3 ± 24.3	104.2 ± 44.7	0.351
Right bundle branch block	5 (13.8)	64 (2.2)	< 0.001
Left bundle branch block	2 (5.5)	53 (1.8)	0.313
<i>Echocardiographic findings</i>			
Maximal wall thickness (mm)	19.2 ± 4.7	18.6 ± 5.8	0.497
LVEF (%)	62.6 ± 9.5	66.1 ± 7.9	0.010
E/e' ratio	12.8 ± 5.1	8.5 ± 5.1	0.001
LAVi (ml/m ²)	41.1 ± 10.9	27.0 ± 20.2	0.008
LV outflow tract obstruction	8 (22)	755 (24)	0.848
Gmax LV outflow tract (mmHg)	20.2 ± 34.9	28.2 ± 46.1	0.453
PASP (mmHg)	30.7 ± 15.9	23.6 ± 16.1	0.052
LVH (%)	91.6	87.4	0.639
<i>Medical therapy</i>			
Beta-blockers (%)	75	25.5	<0.001
Calcium channel blockers (%)	8.3	4.7	0.533
ACE-i/ARBs (%)	44.4	8.2	<0.001
Diuretics (%)	22.2	5.2	<0.001
Amiodarone (%)	36.1	3.8	<0.001
Anti-platelet (%)	30.5	14.4	0.014
Anticoagulant (%)	25	4.6	<0.001

ACE-i/ARBs = angiotensin converting enzyme inhibitors/angiotensin receptor blockers; CM = Cardiomyopathy; Gmax = maximum gradient; LAVi = left atrial volume index; LV = left ventricle; LVH = left ventricle hypertrophy; NYHA = New York Heart Association; PASP = pulmonary artery systolic pressure.

Table 3
Multivariate analysis of predictors of MINOCA in the whole population.

	OR	95% CI	p
FD diagnosis	6.12	2.80–13.3	<0.001
LVH at ECG	18.8	7.71–46.2	<0.001
NYHA	1.43	0.84–2.42	0.181
Hypertension	1.48	0.66–3.30	0.338
Age at diagnosis	1.02	0.99–1.04	0.089
LVEF (%)	0.97	0.93–1.02	0.97

patients admitted to an Emergency Department because of acute chest pain, with or without ST-segment/T wave changes on the ECG; b) absence of obstructive coronary artery disease, i.e. no coronary artery stenosis ≥50% in any epicardial vessel at invasive or computed tomography coronary angiography; c) no alternative diagnosis for the clinical presentation.

The study was approved by the Ethics Committee and was conducted in accordance with the principles of the most recent revision of the Declaration of Helsinki. An informed consent was obtained whenever possible, according to the retrospective nature of the study.

3. Statistics

Continuous variables are presented as mean ± standard deviation and were compared by analysis of variance (ANOVA), whereas chi-square test was used to compare discrete variables, that are reported as raw numbers and percentages. The difference in the rate of MINOCA between patients with HCM and FD was adjusted by multivariable logistic regression for the main clinical variables that showed differences

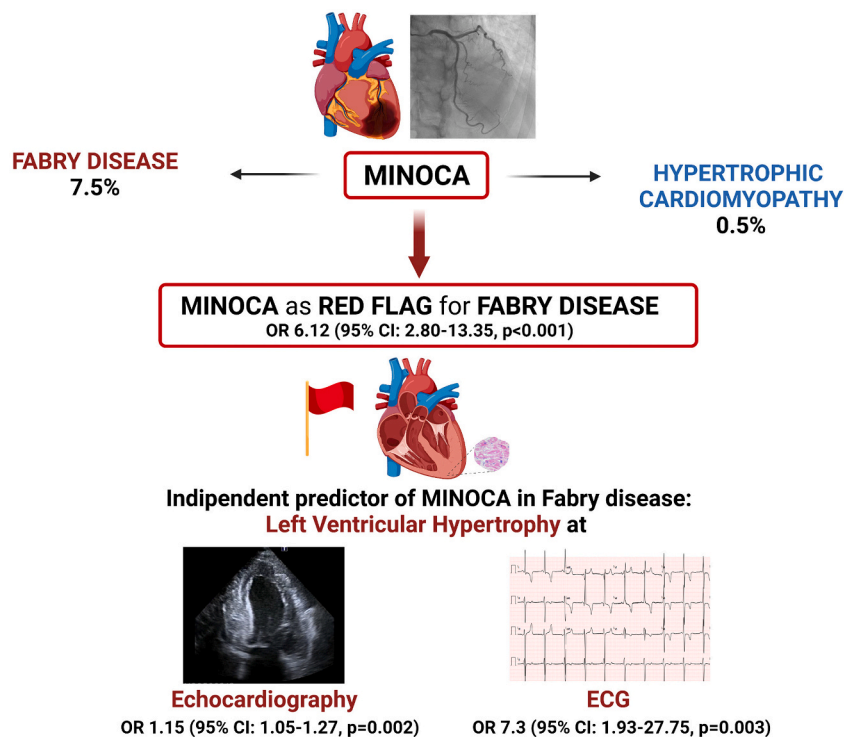


Fig. 1. Main results of the study (created with BioRender).

($p \leq 0.1$) between the 2 groups. A stepwise backward multivariable logistic regression was applied to identify clinical, ECG and echocardiographic variables independently associated with the occurrence of MINOCA. To this aim, only variables with p value ≤ 0.1 at univariate analysis were included in the initial models; non-significant variables were then progressively removed, leaving in the final model only variables with a p value < 0.05 . Statistical tests were done using SPSS statistical software, version 21.0 (SPSS Italia, Inc., Florence, Italy). Statistical significance was considered when $p < 0.05$.

4. Results

A total of 2870 HCM and 267 FD patients were included in the study. The main clinical, ECG and echocardiographic characteristics of the 2 groups are shown in Table 1.

Overall, 36 patients had MINOCA during a follow-up period of 4.5 ± 11.2 years (6.7 ± 6.7 vs. 7 ± 6.5 years in HCM and FD, respectively; $p = 0.889$). Table 2 shows the main clinical and echocardiographic characteristics of patients with MINOCA compared to those without MINOCA in the whole population. MINOCA occurred in 16 patients with HCM (0.5%) and in 20 patients with FD (7.5%). The odds ratio of the rate of MINOCA in FD vs HCM patients was 14.4 (95% CI 7.39–28.2; $p < 0.001$). Importantly, at multivariable analysis the diagnosis of FD was the only independent variable associated with MINOCA (OR 6.12; 95% CI 2.80–13.3; $p < 0.001$), together with the presence of voltage criteria for LVH at the ECG (Table 3).

In FD patients MINOCA occurred in 17/96 patients with LVH (17.7%) and in 3/171 patients without LVH (1.7%; OR 12.05; 95% CI 3.43–42.32; $p < 0.001$). When adjusted for the most important clinical, ECG and echocardiographic variables in multivariable analysis, voltage criteria for LVH at ECG (OR, 7.3; 95% CI 1.93–27.75; $p = 0.003$) and maximal LV wall thickness (OR, 1.15; 95% CI 1.05–1.27; $p = 0.002$) maintained an independent association with the occurrence of MINOCA in FD patients (See Fig. 1).

On the other hand, among HCM patients no differences were found in clinical, ECG and echocardiographic findings between those with and

those without MINOCA.

5. Discussion

To the best of our knowledge, this is the first study that assessed the prevalence of MINOCA and its predictors in a large cohort of HCM and FD patients. The main finding of our work is that MINOCA is a rare event in HCM, while it occurs in a sizeable proportion of FD patients, in whom its adjusted prevalence is about 6-fold greater in the whole population, and even higher when considering only FD patients with overt cardiomyopathy. Such a difference suggests that, among patients with LVH of unknown origin, the occurrence of MINOCA might represent a clinical red flag for FD, thus aiding in the differential diagnosis with HCM (Fig. 1).

The higher rate of MINOCA in FD may be explained by the different pathophysiology of these two phenotypically similar diseases. In HCM, CMD is a prominent feature, which has been associated with adverse prognosis [7] and reflects the interplay of several mechanisms, comprising remodelling of vessel media and intima and extravascular compressive forces [14]. FD, on the other hand, can somehow be considered an “endothelial disease” [15] with a complex interplay between storage, inflammation and endothelial damage/dysfunction associated with Gb3 deposits [16]. Each of these mechanisms might contribute to the higher rate of MINOCA observed in FD patients as compared to HCM, despite a comparable severity of CMD. Given the relevant endothelial involvement, FD is plausibly more unstable and therefore prone to acute vascular events. Endothelial dysfunction, indeed, may favour acute microvascular spasm and/or platelet plugging [17] as well as epicardial spasm. The different type of microvascular involvement in the 2 diseases might also help explain why LVH is a risk factor for MINOCA in FD, but not in HCM patients. Indeed, maximal LVWT and criteria for LVH at the ECG were the only independent predictors of MINOCA in FD patients. These data, along with a younger age at diagnosis, a broader QRS and worse echo findings suggest that MINOCA is associated with a more advanced form of cardiomyopathy in FD patients. These hypotheses, however, require assessment in further

studies.

Notably, although most MINOCA in the FD group occurred in patients with overt cardiomyopathy, three events occurred in patients without LVH. This agrees with previous studies showing that CMD is an early phenomenon in FD that can be present irrespective of LVH and can represent the only sign of cardiac involvement [8].

6. Limitations of the study

Some limitations of our study should be acknowledged. First, this is a retrospective study with the occurrence of MINOCA established from medical records of patients regularly followed at 6 specialized Italian Centers. Thus, we cannot exclude that some events could have been undetected. Second, while we could ascertain the occurrence of MINOCA, we could not establish the underlying mechanisms. Third, our data were acquired over a long time period, during which the diagnosis of acute myocardial infarction underwent some changes; however, we could establish from medical records whether the clinical event of acute coronary syndrome met the criteria of MINOCA according to the 4th Universal definition of acute myocardial infarction. Finally, due to the low rate of events, we were unable to define whether the occurrence of MINOCA had any prognostic role in FD and/or HCM patients.

7. Conclusions

MINOCA is 6-fold more frequent in patients with FD compared with HCM, irrespective of LVH severity and other confounding variables. In FD, MINOCA may affect 1/20 patients, is associated with a more advanced stage of cardiomyopathy but can also occur in individuals without LVH. Among patients with undefined LVH, MINOCA might be considered a red flag for FD, aiding in the differential diagnosis from HCM.

Financial support and conflict of interest disclosure

None.

Acknowledgment

None.

References

- [1] K. Thygesen, J.S. Alpert, A.S. Jaffe, et al., Fourth universal definition of myocardial infarction (2018), *Eur. Heart J.* 40 (3) (2019) 237–269.

- [2] S. Agewall, J.F. Beltrame, H.R. Reynolds, et al., ESC working group position paper on myocardial infarction with non-obstructive coronary arteries, *Eur. Heart J.* 38 (3) (2017) 143–153.
- [3] R.A. Montone, I.K. Jang, J.F. Beltrame, et al., The evolving role of cardiac imaging in patients with myocardial infarction and non-obstructive coronary arteries, *Prog. Cardiovasc. Dis.* 68 (2021 Sep-Oct) 78–87.
- [4] J.E. Tamis-Holland, H. Jneid, H.R. Reynolds, et al., American Heart Association interventional cardiovascular Care Committee of the Council on clinical cardiology; council on cardiovascular and stroke nursing; council on epidemiology and prevention; and council on quality of care and outcomes research. Contemporary diagnosis and management of patients with myocardial infarction in the absence of obstructive coronary artery disease: a scientific statement from the American Heart Association, *Circulation.* 139 (18) (2019 Apr 30) e891–e908.
- [5] A.M. Nordenskjöld, T. Baron, K.M. Eggers, et al., Predictors of adverse outcome in patients with myocardial infarction with non-obstructive coronary artery (MINOCA) disease, *Int. J. Cardiol.* 261 (2018 Jun 15) 18–23.
- [6] T. Rakowski, G. De Luca, Z. Siudak, et al., Characteristics of patients presenting with myocardial infarction with non-obstructive coronary arteries (MINOCA) in Poland: data from the ORPKI national registry, *J. Thromb. Thrombolysis* 47 (3) (2019 Apr) 462–466.
- [7] P.G. Camici, Coronary microvascular dysfunction in patients with cardiomyopathies, *Circ. Heart Fail.* 1 (3) (2008) 150–152.
- [8] B. Tomberli, F. Cecchi, R. Sciagrà, et al., Coronary microvascular dysfunction is an early feature of cardiac involvement in patients with Anderson-Fabry disease, *Eur. J. Heart Fail.* 15 (12) (2013 Dec) 1363–1373.
- [9] F. Cecchi, I. Olivetto, R. Gistri, R. Lorenzoni, G. Chiriatti, P.G. Camici, Coronary microvascular dysfunction and prognosis in hypertrophic cardiomyopathy, *N. Engl. J. Med.* 349 (11) (2003) 1027–1035.
- [10] F. Graziani, R. Lillo, E. Panaioli, et al., Massive coronary microvascular dysfunction in severe Anderson-Fabry disease cardiomyopathy, *Circ. Cardiovasc. Imaging* 12 (6) (2019 Jun), e009104.
- [11] S.R. Ommen, S. Mital, M.A. Burke, et al., 2020 AHA/ACC guideline for the diagnosis and treatment of patients with hypertrophic cardiomyopathy: a report of the American College of Cardiology/American Heart Association joint committee on clinical practice guidelines, *Circulation.* 142 (25) (2020 Dec 22) e558–e631.
- [12] M. Biegstraaten, R. Arngrímsson, F. Barbey, et al., Recommendations for initiation and cessation of enzyme replacement therapy in patients with Fabry disease: the European Fabry Working Group consensus document, *Orphanet J. Rare Dis.* 10 (2015 Mar 27) 36.
- [13] G. Vitale, R. Ditaranto, F. Graziani, et al., Standard ECG for differential diagnosis between Anderson-Fabry disease and hypertrophic cardiomyopathy, *Heart.* 108 (1) (2022 Jan) 54–60.
- [14] P.G. Camici, I. Olivetto, O.E. Rimoldi, The coronary circulation and blood flow in left ventricular hypertrophy, *J. Mol. Cell. Cardiol.* 52 (4) (2012 Apr) 857–864, <https://doi.org/10.1016/j.yjmcc.2011.08.028> (Epub 2011 Sep 5).
- [15] C. Chimenti, E. Morgante, G. Tanzilli, et al., Angina in Fabry disease reflects coronary small vessel disease, *Circ. Heart Fail.* 1 (3) (2008 Sep) 161–169.
- [16] A. Frustaci, M.A. Russo, M. Francone, C. Chimenti, Microvascular angina as prehypertrophic presentation of Fabry disease cardiomyopathy, *Circulation.* 130 (17) (2014 Oct 21) 1530–1531.
- [17] K. Utsumi, N. Yamamoto, R. Kase, et al., High incidence of thrombosis in Fabry's disease, *Intern. Med.* 36 (5) (1997 May) 327–329, <https://doi.org/10.2169/internalmedicine.36.327>.

RESEARCH

Open Access



Differences in cardiac phenotype and natural history of laminopathies with and without neuromuscular onset

Raffaello Ditaranto¹, Giuseppe Boriani², Mauro Biffi¹, Massimiliano Lorenzini^{1,3}, Maddalena Graziosi¹, Matteo Ziacchi¹, Ferdinando Pasquale¹, Giovanni Vitale¹, Alessandra Berardini¹, Rita Rinaldi⁴, Giovanna Lattanzi⁵, Luciano Potena¹, Sofia Martin Suarez¹, Maria Letizia Bacchi Reggiani¹, Claudio Rapezzi¹ and Elena Biagini^{1*}

Abstract

Objective: To investigate differences in cardiac manifestations of patients affected by laminopathy, according to the presence or absence of neuromuscular involvement at presentation.

Methods: We prospectively analyzed 40 consecutive patients with a diagnosis of laminopathy followed at a single centre between 1998 and 2017. Additionally, reports of clinical evaluations and tests prior to referral at our centre were retrospectively evaluated.

Results: Clinical onset was cardiac in 26 cases and neuromuscular in 14. Patients with neuromuscular presentation experienced first symptoms earlier in life (11 vs 39 years; $p < 0.0001$) and developed atrial fibrillation/flutter (AF) and required pacemaker implantation at a younger age (28 vs 41 years [$p = 0.013$] and 30 vs 44 years [$p = 0.086$] respectively), despite a similar overall prevalence of AF (57% vs 65%; $p = 0.735$) and atrio-ventricular (A-V) block (50% vs 65%; $p = 0.500$). Those with a neuromuscular presentation developed a cardiomyopathy less frequently (43% vs 73%; $p = 0.089$) and had a lower rate of sustained ventricular tachyarrhythmias (7% vs 23%; $p = 0.387$). In patients with neuromuscular onset rhythm disturbances occurred usually before evidence of cardiomyopathy. Despite these differences, the need for heart transplantation and median age at intervention were similar in the two groups (29% vs 23% [$p = 0.717$] and 43 vs 46 years [$p = 0.593$] respectively).

Conclusions: In patients with laminopathy, the type of disease onset was a marker for a different natural history. Specifically, patients with neuromuscular presentation had an earlier cardiac involvement, characterized by a linear and progressive evolution from rhythm disorders (AF and/or A-V block) to cardiomyopathy.

Keywords: Lamin, Emerin, Neuromuscular disorders, Atrial fibrillation, Bradyarrhythmias, Ventricular tachycardias, Familial cardiomyopathies

Introduction

Laminopathies are a group of inherited conditions due to mutations in the *LMNA* gene, that encodes the nuclear envelope proteins lamin A and C, via alternate splicing [1]. Laminopathies are characterized by a high phenotypic heterogeneity including heart disease, neuromuscular disorders, premature aging and metabolic disorders [2–5]. *LMNA* associated cardiac and skeletal muscle disease -

often coexisting in the same patient - are the most frequent clinical manifestations. The spectrum of cardiac involvement ranges from supraventricular tachyarrhythmias and/or conduction system disease to dilated cardiomyopathy (DCM) and ventricular tachyarrhythmias [6–12]. Sudden cardiac death may occur due to bradyarrhythmias or to malignant ventricular arrhythmias [13], even in the presence of mild left ventricle systolic dysfunction. Similarly, *LMNA*-related neuromuscular disorders are characterized by a wide heterogeneity in clinical manifestations, Emery Dreifuss muscular dystrophy (EDMD) being the most common phenotype. EDMD is typically characterized by

* Correspondence: elena.biagini73@gmail.com

¹Cardiology Unit, Cardio-Thoracic-Vascular Department, Sant'Orsola-Malpighi Hospital, University of Bologna, Via G. Massarenti 9, 40138 Bologna, Italy
Full list of author information is available at the end of the article



early onset joint contractures with slowly progressive scapulo-humero-peroneal muscle weakness, and can be caused by mutations in genes other than *LMNA*, mainly *EMD* that encodes emerin.

Although clinical manifestation in patients with *LMNA* mutations have been extensively described, the exact time course of cardiological and neuromuscular disease and their relation remain unclear. Specifically, it is not known if a neuromuscular onset is associated with a different cardiac phenotype or cardiac disease progression. The aim of this study was therefore to investigate differences in cardiac phenotype and natural history in relation to the presence of neuromuscular involvement at presentation, in patients with a diagnosis of laminopathy. Furthermore, in order to test the hypothesis that neuromuscular presentation (phenotype) per se might be associated with a specific cardiac natural history, irrespective of genetics, we compared patients with neuromuscular presentation and *LMNA* or *EMD* mutations.

Methods

In this observational study, we prospectively evaluated all *LMNA* mutation carriers from a single Italian centre (S.Orsola-Malpighi University Hospital, Bologna), between December 1998 and November 2017. We also retrospectively examined clinical, ECG and echocardiographic reports available prior to evaluation at our centre. According to the presence of signs and/or symptoms of skeletal myopathy at clinical presentation (not necessarily in our centre), patients were divided into two groups: “with neuromuscular onset” and “without neuromuscular onset”. Data of 7 patients with *EMD*-related disease were also recorded. All patients underwent periodical clinical, electrocardiographic and echocardiographic monitoring.

DCM was defined as the presence of left ventricular (LV) dilation and systolic dysfunction in the absence of abnormal loading conditions (hypertension or valve disease) or coronary artery disease sufficient to cause global systolic impairment [14]. “Hypokinetic non-dilated cardiomyopathy” (HNDC) was defined as LV ejection fraction (EF) < 45% or biventricular global systolic dysfunction in absence of dilatation [15]. Restrictive cardiomyopathy was defined as a non-dilated LV with normal wall thickness and EF, and severe diastolic dysfunction with restrictive filling pattern, elevated filling pressures and dilated atria [14]. Sustained ventricular tachyarrhythmias (SVT) were defined as ventricular tachyarrhythmias with a rate ≥ 120 /min, lasting > 30 s.

A neurological involvement was investigated on the basis of personal history and/or symptoms including joint contractures, muscle weakness or wasting, orthopaedic surgery, and exercise tolerance. Electromyography (EMG), muscle imaging or muscle biopsy were performed in selected cases. Patients underwent periodical neurological evaluation, even when no skeletal muscle involvement was

recorded at first evaluation. Elevation of serum creatine kinase (CK) in isolation was not considered diagnostic of neuromuscular involvement in absence of clinical, EMG, imaging or histological evidence of skeletal myopathy.

A detailed family history was collected for each proband in order to identify other potentially affected family members. A genetic diagnosis was made by DNA sequencing from peripheral blood and mutations were considered pathogenic if previously described in literature, in the presence of co-segregation or based on the site and the type of mutation. After mutation identification, cascade genetic screening was performed in family members, following informed consent.

Continuous data distribution was assessed with the Shapiro-Wilk test and expressed as median and interquartile range (IQR). Data were compared by the Fisher's exact test for proportions, and Mann Whitney test for continuous variables. Clinical events were reported as counts and percentages (i.e. events/total number of patients $\times 100$). Data were collected following informed consent.

Results

Of the 41 *LMNA* mutation carriers, 40 were clinically affected. Table 1 reports clinical, ECG and echocardiographic characteristics at first evaluation at our centre. Fourteen patients were assigned to the group “with neuromuscular onset” and 26 to the group “without neuromuscular onset”. A single *LMNA* mutation carrier, who did not have any cardiac or neuromuscular phenotypic expression at baseline or during follow up, was excluded from the analysis.

Patients with neuromuscular onset

Among the 14 patients in this group males and females were equally represented. *LMNA* mutations were: 12 missense, 1 splice site, and 1 deletion (Table 2). Median age at first evaluation at our Centre was 31 years (IQR 20–44). The diagnosis of laminopathy occurred following familial screening in 2 patients. At time of genetic diagnosis, overt neuromuscular involvement was present in all cases whereas none had cardiac involvement. Eleven patients (79%) were diagnosed with EDMD in the first or second decade of life and 3 (21%) were diagnosed with a non-specific myopathy in the third decade; median age at diagnosis was 11 years (IQR 8–30).

Nine patients (64%) developed cardiac involvement prior to referral to our centre (Fig. 1a summarizes the spectrum of cardiac phenotypic expression). All had rhythm disturbances: 2 (14%) had atrial fibrillation (AF), 1 (7%) atrioventricular (A-V) block, 1 (7%) sinus node dysfunction, and 5 (36%) had a combination of brady- and atrial tachyarrhythmias (Fig. 2). Cardiomyopathy was also present in 5 patients (36%): 2 DCM, 2 HNDC and 1 isolated right ventricular cardiomyopathy mimicking arrhythmogenic

Table 1 Characteristics at first clinical evaluation at our centre of patients with *LMNA* mutations with and without neuromuscular onset

	Overall	With neurological Onset	Without neurological onset	P value
Number of patients	40	14 (35)	26 (65)	
Number of families	31	12 (39)	19 (61)	
Males	22 (55)	7 (50)	15 (58)	0.744
Age at symptom onset, yrs	33 (21–42)	11 (8–30)	39 (32–46)	< 0.0001
Age at first contact at our center, yrs	39 (29–74)	31 (20–44)	43 (36–49)	
Follow-up duration, months	30 (6–70)	24 (12–101)	32 (8–63)	
Diagnostic pathway				
Signs or symptoms		12 (86)	19 (73)	0.452
Screening		2 (14)	7 (27)	
Cardiomyopathy	24 (60)	5 (36)	19 (73)	0.040
Dilated CMP	13 (32)	2 (14)	11 (42)	0.089
Hypokinetic non dilated CMP	8 (20)	2 (14)	6 (23)	0.688
Restrictive CMP	2 (5)	0	2 (8)	0.533
Right ventricle CMP	1 (2)	1 (7)	0	0.350
History of atrial fibrillation	17 (42)	6 (43)	11 (42)	1.000
Sinus node dysfunction	4 (10)	3 (21)	1 (4)	0.114
Atrio-ventricular block	23 (57)	6 (43)	17 (65)	0.197
1st degree	8 (20)	2 (14)	6 (23)	
2nd degree	7 (17)	2 (14)	5 (19)	
3rd degree/high degree	8 (20)	2 (14)	6 (23)	
Positive familial history for				
Sudden death	7 (17)	3 (21)	4 (15)	0.678
PM implantation (high degree AVB)	11 (27)	3 (21)	8 (30)	0.715
CMP	16 (40)	5 (36)	11 (42)	0.746
NYHA class III- IV	7 (17)	4 (28)	3 (12)	0.214
PM recipients	8 (20)	2 (14)	6 (23)	0.688
ICD recipients	8 (20)	1 (7)	7 (27)	0.221

Values are expressed as N, N (%) or median (interquartile range)

LMNA, *EMD* gene coding for lamin A/C and emerin, respectively, *ICD* implantable cardioverter defibrillator, *PM* pacemaker, *AVB* atrio-ventricular block, *NYHA* New York Heart Association

right ventricular cardiomyopathy. Patients with LV cardiomyopathy had a severe LV dysfunction (LVEF \leq 35%) and 3 had biventricular involvement.

Two patients (14%) had previously undergone pacemaker (PM) implantation for A-V block, while a single patient had a primary prevention implantable cardiac resynchronization therapy defibrillator (CRT-D). Serum CK levels were raised in 65% of the patients, with a mean abnormal value of 631 UI/L.

Patients without neuromuscular onset

Fifteen (58%) of the 26 patients were males, median age at first evaluation at our centre was 43 years (IQR 36–49). Diagnosis was made due to rhythm disturbances or heart failure symptoms in most cases ($n = 19$, 73%). Seven patients (27%) were identified after family screening. *LMNA*

mutations were: 16 missense, 7 splice site, 2 deletion and 1 frameshift (Table 3).

At first clinical evaluation at our centre, 19 patients (73%) had a cardiomyopathy, in isolation ($n = 3$, 11%) or associated with arrhythmias (AF $n = 5$, 19%; A-V block $n = 6$, 23%; both $n = 5$, 19%; Fig. 3). Seven patients (27%) had arrhythmias in absence of cardiomyopathy: 1 (4%) AF, 5 (19%) A-V block and 1 (4%) a combination of sinus node and A-V node dysfunction. Overall, AF was present in 11 patients (42%). Figure 1b summarizes the spectrum of cardiac phenotypic expression. Six patients (23%) had previously undergone PM implantation for A-V block and 7 patients (27%) had received a primary prevention implantable cardioverter defibrillator (ICD).

Cardiomyopathy phenotype included: 11 DCM, 6 HNDC and 2 restrictive cardiomyopathy. Among the

Table 2 Genetics of *LMNA* mutated patients with neurological onset ($N = 14$)

	Gene	Location	Nucleotide Change	Protein Change	Predicted Effect
Family 1					
F; 16 yo	LMNA	Exon 4	c.746G > A	p.Arg249Gln	Missense
Family 2					
F; 50 yo	LMNA	Exon 9	c.1580G > C	p.Arg.527.Pro	Missense
Family 3					
M; 38 yo	LMNA	Exon 11	c.1930C > T	p.Arg644Cys	Missense
M; 38 yo	LMNA	Exon 11	c.1930C > T	p.Arg644Cys	Missense
Family 4					
F; 46 yo	LMNA	Exon 3 Exon 4	c.569G > A; c. 746G > A	p.Arg190Gln p.Arg249Gln	Missense Missense
Family 5					
F; 34 yo	LMNA	Exon 1	c.203_208 (delAGGTGG)	p.Glu68_Val69 del	Deletion
Family 6					
M; 52 yo	LMNA	Exon 4	c.746G > A	p.Arg249Gln	Missense
Family 7					
M; 46 yo	LMNA	Exon 9	c.1567G > A	p.Gly523Arg	Missense
Family 8					
M; 17 yo	LMNA	Exon 4	c.775 T > G	p.Tyr259Asp	Missense
Family 9					
M; 19 yo	LMNA	Exon 4	c.746 G > A	p.Arg249Gln	Missense
Family 10					
F; 29 yo	LMNA	Intron 9	c.1608 + 1G > T	–	Splice site
Family 11					
F; 22 yo	LMNA	Exon 1	c.188 T > A	p.Ile63Asn	Missense
F; 19 yo	LMNA	Exon 1	c.188 T > A	p.Ile63Asn	Missense
Family 12					
M; 27 yo	LMNA	Exon 4	c.746G > A	p.Arg249Gln	Missense

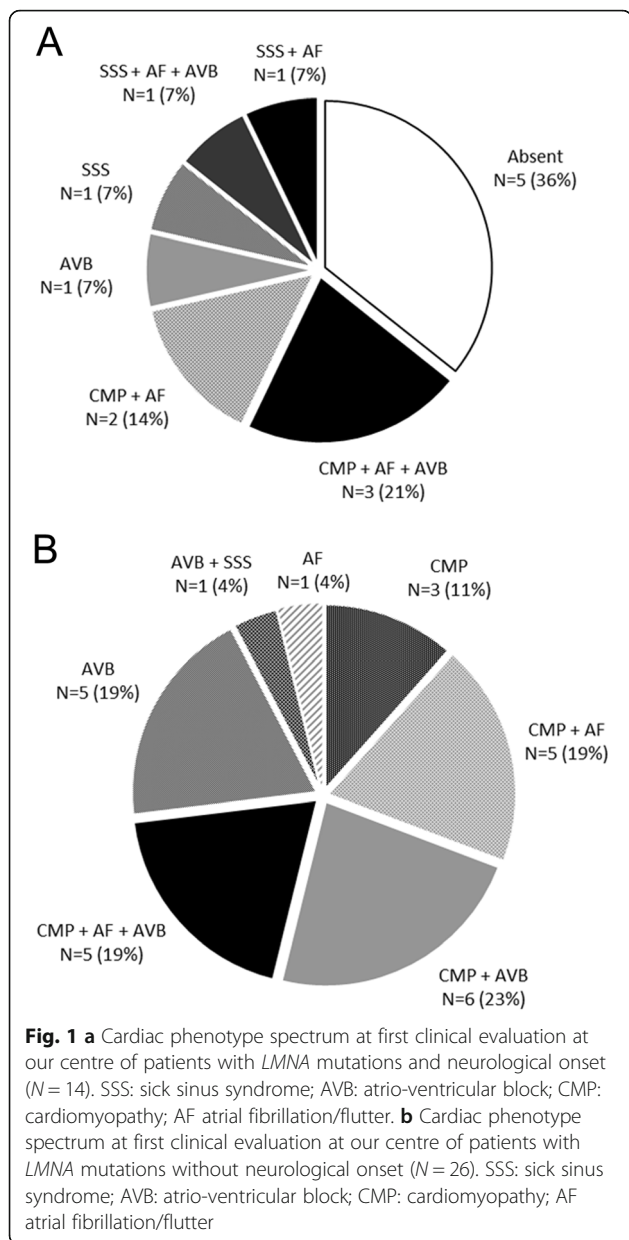
M male, F female, yo years old. The age reported refers to first contact at our centre

17 patients with LV systolic dysfunction, 7 (41%) had a severe impairment (LVEF $\leq 35\%$), 6 (35%) had biventricular involvement and 3 (17%) had increased LV trabeculations. One 54-year old patient with a history of complete A-V block and AF had a biventricular cardiomyopathy with multiple aneurysms in the diaphragmatic and free wall of the right ventricle. Coronary arteries were unobstructed at angiography. Cardiac magnetic resonance showed a severely dilated left ventricle (indexed end diastolic volume: 146 mL/m²) with systolic dysfunction (EF 40%) and mildly dilated right ventricle (indexed end diastolic volume: 111 mL/m²) with reduced EF (40%) and confirmed the wall motion abnormalities (Fig. 4 a-b). Tissue characterization (Fig. 4 c-d) revealed multiple areas of fibro-fatty replacement. In this case, possible phenocopies including desmosomal-related cardiomyopathy and sarcoidosis were excluded by genetic analysis, positron emission tomography, lung CT and, endomyocardial biopsy.

No patient had evidence of neuromuscular involvement. Serum CK levels were raised in 47% of the patients with a mean abnormal value of 217 UI/L.

Follow-up of patients with neuromuscular onset

Median follow up was 24 months (IQR 12–101). New onset AF was recorded in 2 patients, therefore 57% experienced atrial tachyarrhythmias by the end of the follow-up. In one patient, the atrial conduction disease progressed to atrial paralysis. Three patients underwent PM implantation for A-V block ($n = 1$), sinus node disease ($n = 1$) or both ($n = 1$). A primary prevention CRT-D was implanted in a patient with new onset HNDC due to positive family history for sudden death, high inducibility of VT on electrophysiological study and moderate LV dysfunction. The patient affected by right ventricular cardiomyopathy received a primary prevention ICD, due to severe right ventricular dysfunction, non-sustained ventricular tachycardias and the need of a pacing for sinus and A-V node dysfunction.



Thereafter he experienced an appropriate ICD activation and a progression towards severe biventricular involvement. No sudden death occurred. Five patients with cardiomyopathy had hospital admissions due to heart failure during follow-up and 4 of them subsequently underwent heart transplantation (median age 43 [IQR 34–48]).

Follow-up of patients without neuromuscular onset

New onset AF was reported in 6 patients (23%) during a median follow up of 32 months (IQR 8–63); 65% of patients had atrial tachyarrhythmias at the end of follow up. With the exception of 2 patients with atrial flutter – who were treated successfully with cavo-tricuspid isthmus ablation – the attempts of rhythm control with electrical or pharmacological cardioversion were ineffective. No patients underwent pulmonary vein isolation. Atrial paralysis was documented in a single patient. One patient underwent PM implantation due to A-V block. A primary prevention ICD was implanted in 7 patients (4 new implants and 3 device upgrades) and 1 ICD was implanted for secondary prevention. Four of the ICD recipients (50%) received a CRT-D device. During follow up 6 patients (23%) experienced appropriate shocks and/or antitachycardia pacing for ventricular arrhythmias, with an arrhythmic storm in 3 cases. Six (23%) patients underwent cardiac transplantation (median age 46 [IQR 34–53]) due to end stage heart failure (5/6) or to recurrent ventricular arrhythmias (1/6). One patient developed a mild neuromuscular involvement, with muscle atrophy involving the shoulder girdle. Table 4 compares clinical events reported during follow-up in the two groups.

Differences in clinical manifestations between patients with and without neuromuscular onset

Patients with neuromuscular onset had an earlier presentation, during infancy or adolescence in most of the cases (median age 11 years), mainly as EDMD, followed by the first evidence of cardiac disease by a median age of 13 years (IQR 10–15) (maximum timelag 38 years). In patients without neuromuscular onset, first cardiac symptoms occurred later in life, at a median age of 39

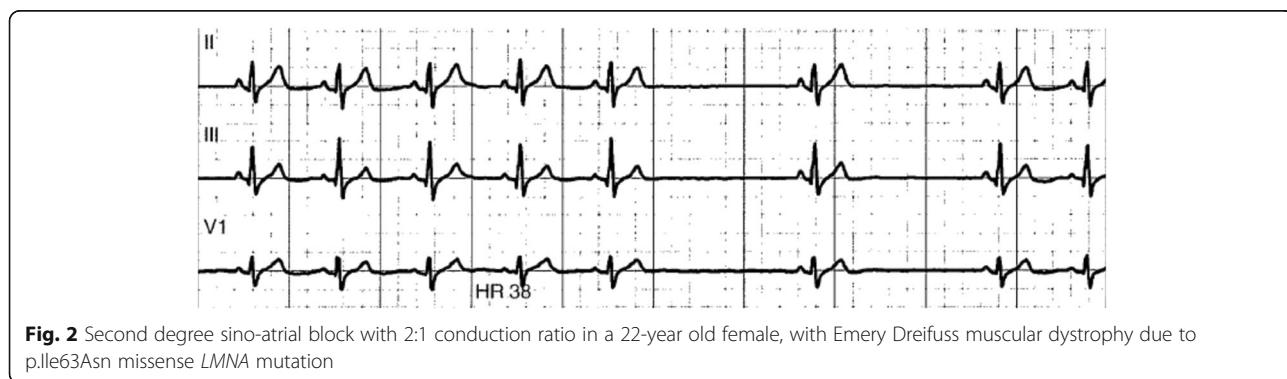


Table 3 Genetics and cardiac manifestations of *LMNA* mutated patients without neurological onset ($N = 26$)

	Gene	Location	Nucleotide Change	Protein Change	Predicted Effect
Family 1					
M; 53 yo	LMNA	Exon 6	c.1004G > A	p.Arg335Gln	Missense
M; 26 yo	LMNA	Exon 6	c.1004G > A	p.Arg335Gln	Missense
Family 2					
F; 47 yo	LMNA	Exon 7	1370delA	p.Lys457SerfsX2	Deletion
Family 3					
M; 19 yo	LMNA	Exon 6	c.1003G > A	p.Arg335Glu	Missense
Family 4					
F; 55 yo	LMNA	Exon 11	c.1912G > A	p.Gly638Arg	Missense
Family 5					
M; 54 yo	LMNA	Exon 7	c.1202G > A	p.Arg401His	Missense
Family 6					
M; 42 yo	LMNA	Exon 1	n/a	p.Arg72Alafs*24	Frame shift
Family 7					
F; 51 yo	LMNA	Exon 4	c.752A > C	p.Gln251Pro	Missense
Family 8					
M; 46 yo	LMNA	Exon 9	c.1517 A > C	p.His506Pro	Missense
Family 9					
F; 38 yo	LMNA	Intron 9	c1608 + 1G > T	–	Splice site
M; 35 yo	LMNA	Intron 9	c1608 + 1G > T	–	Splice site
Family 10					
F; 29 yo	LMNA	Exon 3	c.548 T > C	p.Leu183Pro	Missense
Family 11					
F; 41 yo	LMNA	Exon 6	c.1007G > A	p.Arg336Gln	Missense
Family 12					
M; 60 yo	LMNA	Intron 1	c.357-1G > A IVS1-1G > A	–	Splice site
F; 46 yo	LMNA	Intron 1	c.357-1G > A IVS1-1G > A	–	Splice site
F; 49 yo	LMNA	Intron 1	c.357-1G > A IVS1-1G > A	–	Splice site
F; 49 yo	LMNA	Intron 1	c.357-1G > A IVS1-1G > A	–	Splice site
M; 21 yo	LMNA	Intron 1	c.357-1G > A IVS1-1G > A	–	Splice site
Family 13					
M; 38 yo	LMNA	Exon 6	c.1129C > T	p.Arg377Cys	Missense
Family 14					
M; 50 yo	LMNA	Exon 2	c.481G > A	p.Glu161Lys	Missense
Family 15					
M; 46 yo	LMNA	Exon 2	c.466C > A	p.Arg156Ser	Missense
M; 34 yo	LMNA	Exon 2	c.466C > A	p.Arg156Ser	Missense
Family 16					
M; 44 yo	LMNA	Exon 4	c.671 C > T	p.Thr224Ile	Missense
Family 17					
F; 39 yo	LMNA	Exon 2	c.481G > A	p.Glu161Lys	Missense

Table 3 Genetics and cardiac manifestations of *LMNA* mutated patients without neurological onset ($N = 26$) (Continued)

	Gene	Location	Nucleotide Change	Protein Change	Predicted Effect
Family 18					
F; 37 yo	<i>LMNA</i>	Exon 2	c.513G > A	p.Lys171Asn	Missense
Family 19					
F; 36 yo	<i>LMNA</i>	Exon 5	c.855delG	p.Ala287LeufsX191	Deletion

M male, F female, yo years old. The age reported refers to first contact at our centre. n/a not available

years ($p < 0.0001$). Regarding arrhythmias, at the end of the follow-up A-V block (of any degree) and AF had a similar prevalence between the two groups (50% vs 65%, $p = 0.500$ and 57% vs 65%; $p = 0.735$ respectively). Sinus node dysfunction was more frequent in patients with skeletal myopathy (21% vs 4%; $p = 0.114$), whereas atrial paralysis was reported in one patient for each group. Patients with neuromuscular presentation (Fig. 5) experienced earlier AF (age 28 vs 41, $p = 0.013$) and PM implantation (age 30 vs 44; $p = 0.086$). The percentage of patients requiring permanent pacing (including PM recipients and those who received an ICD due to a concomitant indication for prevention of ventricular arrhythmias) was equal in the two groups (42% vs 42%; $p = 1.000$).

Patients without neuromuscular presentation had a higher prevalence of cardiomyopathy (73% vs 43%, $p = 0.089$) and were older at diagnosis (age 42 vs 35, $p = 0.259$). DCM was the dominant phenotype in this group (58% of

all cardiomyopathies), whereas DCM and HNDC were equally represented in the other group. The higher prevalence of heart muscle involvement in patients without neuromuscular onset was associated with a higher number of implanted ICDs (58% vs 21%, $p = 0.045$) and a higher burden of SVT (23% vs 7%, $p = 0.387$). Despite this, no significant differences were reported in the prevalence of heart transplantation (23% vs 29%; $p = 0.717$) or in the median recipient age (43 vs 46; $p = 0.593$).

All patients with neuromuscular presentation who received a diagnosis of cardiomyopathy had a previous history of rhythm disturbance with the exception of 2 cases, where the diagnosis was concomitant. On the contrary, no pattern of progression from rhythm disturbance to cardiomyopathy was present in those without a neuromuscular presentations: AF and A-V block could precede the diagnosis of cardiomyopathy, be diagnosed at the same time or later. Figure 6 shows the different

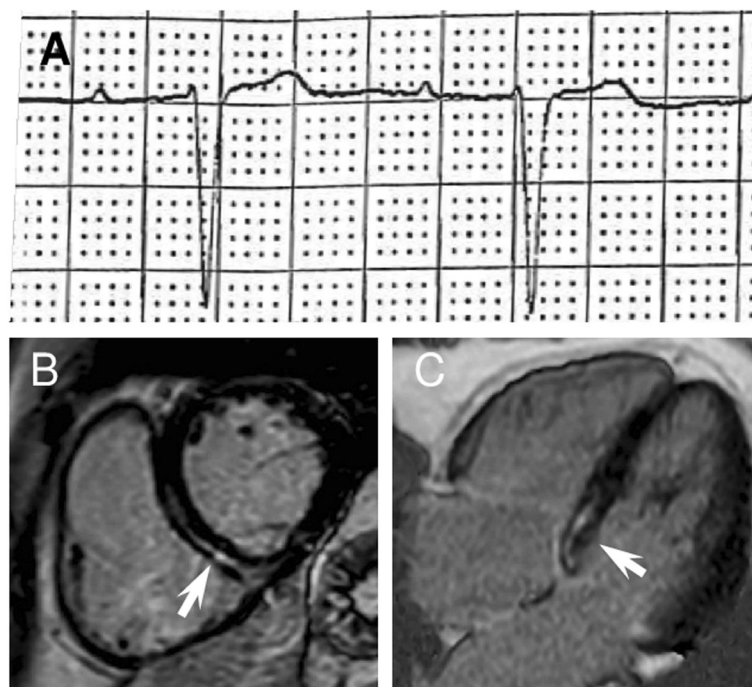


Fig. 3 43-year old male with a *LMNA* frameshift mutation without neuromuscular presentation. **a** V1 lead ECG showing first degree atrioventricular block, **b-c** cardiac magnetic resonance showing midwall late gadolinium enhancement in the basal interventricular septum. Suggestive for myocardial fibrosis

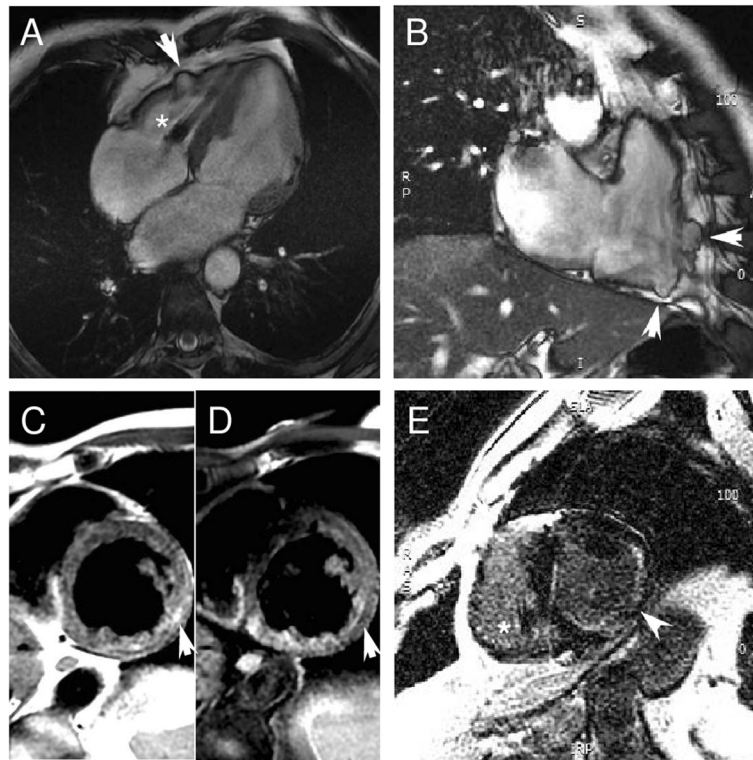


Fig. 4 CMR of a 54-year male, carrier of p.Arg401His missense *LMNA* mutation, affected by DCM. (a-b) Four chamber and RV long axis SSFP images show biventricular dilation, bulging of the RV free wall (white arrow, panel a-b) and diaphragmatic wall (white arrow, panel b). (c) Two chamber T1-weighted and (d) fat suppressed T1-weighted slices showing LV fatty replacement of mid lateral wall (white arrow). (e) IR LGE slice showing fibrosis in the infero-lateral wall (with focal transmural pattern) and in the interventricular septum (image quality was due to respiratory artifacts and to the presence of pacemaker [*]). CMR: cardiac magnetic resonance. DCM: dilated cardiomyopathy. SSFP: steady-state free precession. LV-RV: left-right ventricle. IR LGE: inversion recovery late gadolinium enhancement

overall prevalence of clinical events between the two populations.

Clinical characteristics and follow up of patients with emerlinopathy

Seven male patients (4 families) affected by X-linked EDMD were referred to our Centre at a median age of 26 years (IQR 14–30) and followed for a median time of 108 months (IQR 72–172). All had neuromuscular symptoms as first evaluation, with a median age of 6 years (IQR 5–8). At last follow up 6 patients (85%) had

cardiac involvement. All developed AF at a median age of 27 [IQR 23–37]) and 5 required PM implantation at a median age of 23 [IQR 22–24] due to A-V block ($n = 1$), sinus node dysfunction ($n = 1$) or both ($n = 3$). A single patient developed cardiomyopathy with mild systolic dysfunction; none had ventricular arrhythmias. The time interval from neurological to cardiac disease onset was of 14,5 years (IQR 14–15). Compared to patients with *LMNA* mutations and a neurological onset, patients with emerlinopathy presented a higher burden of AF (85% vs 57%; $p = 0.337$) that occurred an earlier age (27 vs 31

Table 4 Clinical events reported during follow-up in *LMNA* mutated patients

	Patients with neurological onset ($N = 14$)	Patients without neurological onset ($N = 26$)	P value
New onset of atrial fibrillation (any form)	2 (14)	6 (23)	0.688
PM implantation	3 (21)	1 (4)	0.114
ICD implantation	2 (14)	8 (31)	0.445
SVT/arrhythmic storm	1 (7)	6 (23)	0.387
Admission for heart failure	5 (36)	11 (42)	0.746
Heart transplantation	4 (29)	6 (23)	0.717
Thromboembolic events	0	0	

Values are expressed as N or N (%). SVT sustained ventricular tachyarrhythmia, PM pacemaker, ICD implantable cardioverter defibrillator

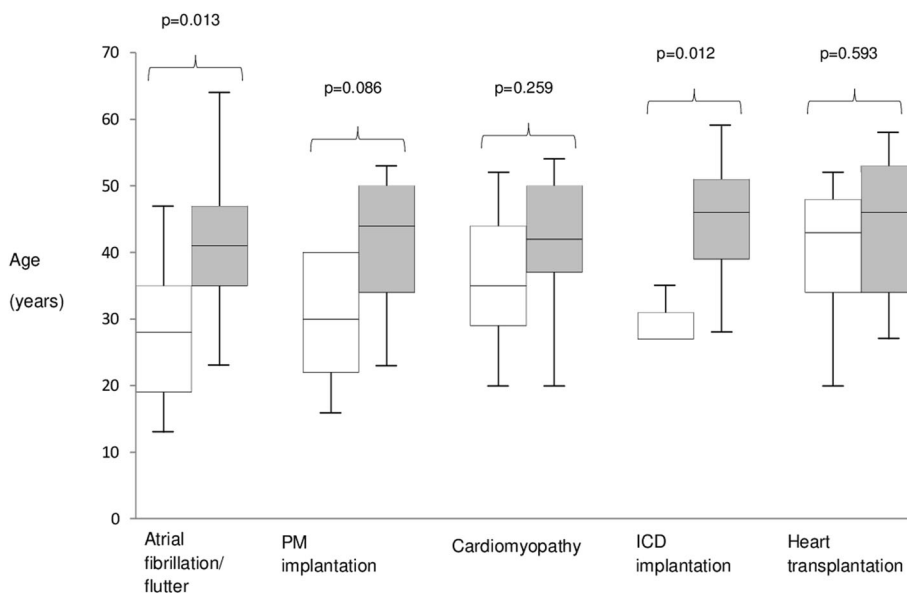


Fig. 5 Box and whiskers plot showing age distribution of different clinical events in *LMNA* patients with (white) and without (gray) neuromuscular onset. Middle horizontal line inside box indicates median. Bottom and top of the box are 25th and 75th percentiles, the whiskers indicate the lowest and highest value. PM: pacemaker. ICD: implantable cardioverter defibrillator

$p = 0.746$), and a higher rate of PM implantation (71 vs 36%; $p = 0.182$) at an earlier age (23 vs 28; $p = 0.461$). Differently, heart muscle involvement was rare (a single case of cardiomyopathy) and no SVT was documented.

Discussion

The main findings of our study are: 1) neuromuscular onset is a marker for a specific natural history in laminopathy patients. Specifically, these patients have a linear and predictable progression over time, from muscular dystrophy to rhythm disturbances and finally cardiomyopathy. 2) With the exception of sinus node dysfunction, that was more frequent in EDMD patients, the prevalence of A-V block and AF was similar between the two groups,

but patients with a neuromuscular presentation had earlier arrhythmias. 3) Prevalence of cardiomyopathy (particularly DCM) and SVT was higher among patients without neuromuscular onset, although the two groups had a similar rate and age of cardiac transplantation.

Most of the patients with neuromuscular presentation (64%) developed cardiac involvement later in life: the delay between neuromuscular and cardiac symptom onset was variable and sometimes very long. These findings suggest that serial reassessment of cardiac status in patients with a diagnosis of EDMD is mandatory. On the other hand, patients without neuromuscular onset did not develop an overt skeletal myopathy (with a single exception). The possibility that these patients could develop neuromuscular

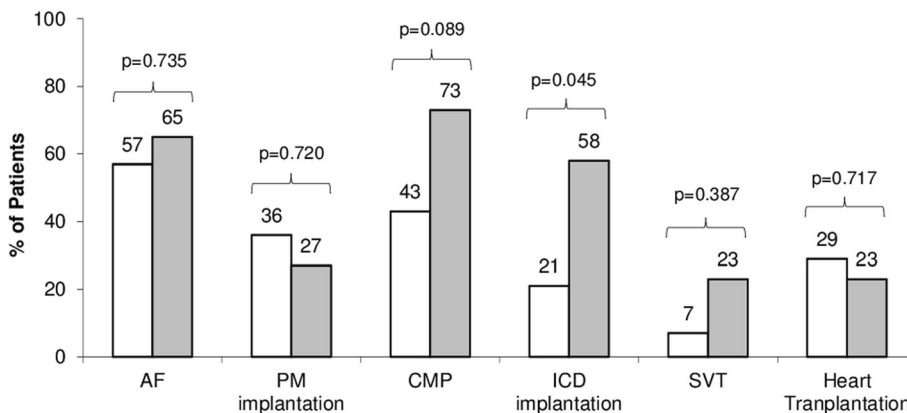


Fig. 6 Different overall prevalence at the end of follow-up of clinical events in *LMNA* patients with (white) and without (gray) neuromuscular presentation. AF: atrial fibrillation; PM: pacemaker; CMP: cardiomyopathy; SVT: sustained ventricular tachycardias

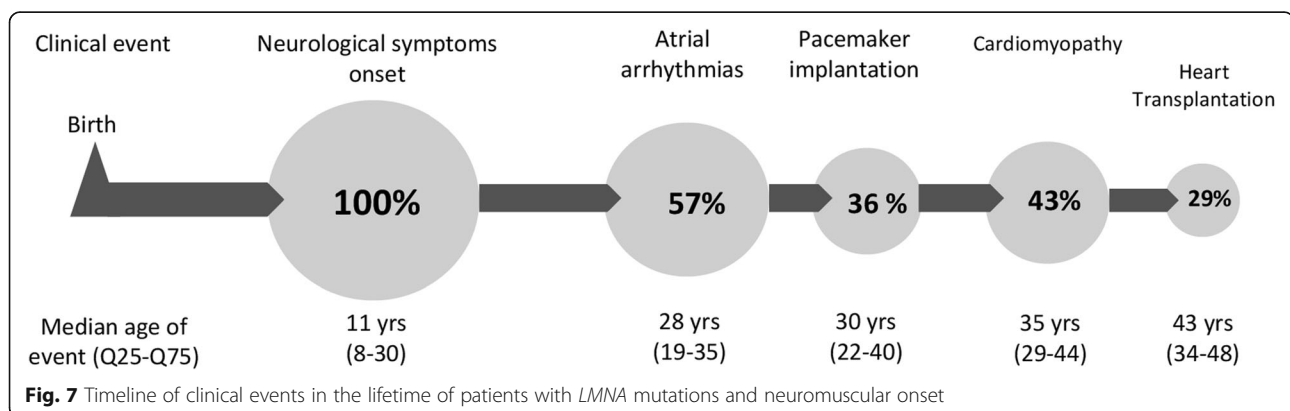
involvement in the future cannot however be entirely ruled out due to the limited observation time. Our results are in line with the phenotypic clustering reported by *Benedetti et al.* [16] in a cohort of patients with *LMNA* mutations, where those with childhood onset had an almost exclusively skeletal muscle involvement (predominantly EDMD), while patients with adult onset developed cardiac disorders or muscle weakness with a limb-girdle distribution. With the limitation of the small size of the screened families in our study population and the limited numbers of relatives who carried the mutation, all the affected relatives of probands with neuromuscular presentation had a skeletal muscle involvement as clinical onset. At the same time, all the affected relatives of patients with an exclusive cardiac phenotype had an isolated cardiological involvement. Differently from our findings, *Bonne et al.* and *Brodsky et al.* [17, 18] have previously described the possibility of the coexistence of both phenotypes as clinical onset within the same family.

Our data confirm the high frequency of AF in laminopathies, as well as advanced A-V block, requiring PM implantation at a young age. Although the prevalence of high degree A-V block and AF was similar, irrespective of clinical presentation, patients with neuromuscular onset experienced arrhythmia earlier in life (on average AF and PM implantation occurred more than 10 years earlier). On the other hand, sinus node dysfunction was more frequent in patients with EDMD (21% vs 4%). Regarding heart muscle involvement, patients without neuromuscular onset had a prevalence of cardiomyopathy that was almost twice that of the other group (42% vs 73%; $p = 0.089$), mostly DCM. On the contrary DCM and HNDC were equally distributed in patients with neuromuscular presentation. A progression from HNDC to DCM was not observed in this study, suggesting that they could be the expression of two different pathophysiologic models; however, a limited follow-up duration (median 41 months) and heart failure therapy could have masked this progression. We described two cases, 1 in each group, with a cardiac phenotype that mimicked arrhythmogenic cardiomyopathy. *LMNA* carriers have

been described with clinical, morphological and histological phenotypes overlapping with arrhythmogenic cardiomyopathy [19], in the absence of desmosomal gene mutations, with conduction disease being the sole 'red flag' for the correct diagnosis. These findings may justify the need to exclude *LMNA* mutations in patients with suspected arrhythmogenic cardiomyopathy, particularly when conduction disease is present.

This study confirms the malignant nature of laminopathies in terms of ventricular arrhythmias and progression to advanced heart failure. In our series sustained SVTs during the follow-up were more frequent in patients without neuromuscular involvement (23% vs 7%) with just 1 EDMD patient experiencing SVT. The low incidence of events in patients with skeletal myopathy differs from previous reports. *Van Rijsingen et al.* [10] reported that in patients with *LMNA* mutations, the diagnosis of muscular dystrophy or a positive family history of muscular dystrophy was not associated with a different incidence of ventricular arrhythmias. The rate of SVT reported by the Authors was of 17% in EDMD patients and 19% in non-EDMD patients. More than 20% of the whole population of this study required cardiac transplantation during follow-up and this is consistent with previous reports. *Hasselberg et al.* [11] reported that 19% of genotyped *LMNA* patients underwent heart transplantation during a follow up of 8 years (median age 46 years). The need for heart transplantation in our series was independent from the involvement of the skeletal muscle and occurred at a median age of 45 years. Differently from what observed for other clinical events, neuromuscular involvement did not lead to an anticipation in the timeline and heart transplant was performed at a similar age in the two groups (median 43 vs 46 years).

In this series, patients with a neuromuscular presentation had a linear predictable progression over time (Fig. 7). Specifically, skeletal myopathy developed first, followed by arrhythmias (A-V block, sick sinus syndrome and AF in various combinations) and eventually, cardiomyopathy. This pattern of progression was not observed in the other patients.



The cardiac involvement in X-linked EDMD patients of our study, compared to patients with LMNA mutations and a neurological onset, was characterized by higher burden of supraventricular tachyarrhythmias and bradyarrhythmias that occurred at a younger age and a lower frequency of cardiomyopathy.

Limitations

Referral bias cannot be excluded since this is a study from a single tertiary centre with a cardiac transplant program and expertise for management of complex ventricular tachycardias.

Conclusion

In patients with laminopathy, the type of disease onset was a marker for a different natural history. Specifically, patients with neuromuscular presentation had an earlier cardiac involvement, characterized by a linear and progressive evolution from rhythm disorders (AF and/or A-V block) to cardiomyopathy. Prevalence of AF and A-V block was similar, regardless of clinical onset, whereas sinus node dysfunction was more frequent in EDMD patients. Patients with neuromuscular onset had a lower prevalence of cardiomyopathy and ventricular arrhythmias, but a similar prevalence of heart transplantation at a similar age.

Abbreviations

AF: Atrial fibrillation/flutter; AVB: Atrio-ventricular block; CK: Creatine kinase; CRT-D: Implantable cardiac resynchronization therapy defibrillator; DCM: Dilated cardiomyopathy; EDMD: Emery Dreifuss muscular dystrophy; EMG: Electromyography; HNDC: Hypokinetic non dilated cardiomyopathy; HT: Heart transplantation; ICD: Implantable cardioverter defibrillator; IQR: Interquartile range; LV: Left ventricle; LVEF: Left ventricle ejection fraction; NYHA: New York Heart Association; PM: Pacemaker; SVT: Sustained ventricular tachyarrhythmias

Acknowledgements

None.

Authors' contributions

EB, RD and CR wrote the initial manuscript. EB, CR, MB, GB, RD and ML provided critical discussion of research. All Authors participated in clinical data collection, read and approved the final manuscript.

Funding

This work was supported by the University of Bologna and "Fondazione Luisa Fanti Melloni".

Availability of data and materials

The datasets used and analysed during the current study are available from the corresponding Author on reasonable request.

Ethics approval and consent to participate

Informed consent was obtained from patients for collection of anonymised clinical data.

Consent for publication

All participants gave consent for publication of anonymised individual personal data.

Competing interests

The authors declare that they have no competing interests.

Author details

¹Cardiology Unit, Cardio-Thoracic-Vascular Department, Sant'Orsola-Malpighi Hospital, University of Bologna, Via G. Massarenti 9, 40138 Bologna, Italy. ²Cardiology Division, Department of Biomedical, Metabolic and Neural Sciences, University of Modena and Reggio Emilia, Policlinico di Modena, Modena, Italy. ³University College London Institute for Cardiovascular Science and Barts Heart Centre, St. Bartholomew's Hospital, London, UK. ⁴Neurology Unit, Sant'Orsola-Malpighi University Hospital, Bologna, Italy. ⁵Italian National Research Council (CNR), Institute of Molecular Genetics IGM Bologna, Bologna, Italy.

Received: 21 May 2019 Accepted: 29 October 2019

Published online: 19 November 2019

References

- Mounkes L, Kozlov S, Burke B, Stewart CL. The laminopathies: nuclear structure meets disease. *Curr Opin Genet Dev.* 2003;13:223–30.
- Shackleton S, et al. LMNA, encoding Lamin a/C, is mutated in partial lipodystrophy. *Nat Genet.* 2000;24:153–6.
- Boriani G, et al. Clinical relevance of atrial fibrillation/flutter, stroke, pacemaker implant, and heart failure in Emery-Dreifuss muscular dystrophy: a long-term longitudinal study. *Stroke.* 2003;34:901–8.
- Eriksson M, et al. Recurrent de novo point mutations in Lamin a cause Hutchinson-Gilford progeria syndrome. *Nature.* 2003;423:293–8.
- Bonne G, et al. Mutations in the gene encoding Lamin a/C cause autosomal dominant Emery-Dreifuss muscular dystrophy. *Nat Genet.* 1999;21:285–8.
- Arbustini E, et al. Autosomal dominant dilated cardiomyopathy with atrioventricular block: a Lamin a/C defect-related disease. *J Am Coll Cardiol.* 2002;39:981–90.
- Kumar S, et al. Long-term arrhythmic and nonarrhythmic outcomes of Lamin a/C mutation carriers. *J Am Coll Cardiol.* 2016;68:2299–307.
- Pasotti M, et al. Long-term outcome and risk stratification in dilated cardiomyopathies. *J Am Coll Cardiol.* 2008;52:1250–60.
- Taylor MR, et al. Natural history of dilated cardiomyopathy due to Lamin a/C gene mutations. *J Am Coll Cardiol.* 2003;41:771–80.
- van Rijsingen IA, et al. Risk factors for malignant ventricular arrhythmias in Lamin a/C mutation carriers: a European cohort study. *J Am Coll Cardiol.* 2012;59:493–500.
- Hasselberg NE, et al. Lamin a/C cardiomyopathy: young onset, high penetrance, and frequent need for heart transplantation. *Eur Heart J.* 2018;39:853–60.
- Captur G, et al. Lamin and the heart. *Heart.* 2018;104:468–79.
- Wahbi K, et al. Development and validation of a new risk prediction score for life-threatening ventricular Tachyarrhythmias in Laminopathies. *Circulation.* 2019;140:293–302.
- Elliott P, et al. Classification of the cardiomyopathies: a position statement from the European Society of Cardiology working group on myocardial and pericardial diseases. *Eur Heart J.* 2008;29:270–6.
- Pinto YM, et al. Proposal for a revised definition of dilated cardiomyopathy, hypokinetic non-dilated cardiomyopathy, and its implications for clinical practice: a position statement of the ESC working group on myocardial and pericardial diseases. *Eur Heart J.* 2016;37:1850–8.
- Benedetti S, et al. Phenotypic clustering of Lamin a/C mutations in neuromuscular patients. *Neurology.* 2007;69:1285–92.
- Bonne G, et al. Clinical and molecular genetic spectrum of autosomal dominant Emery-Dreifuss muscular dystrophy due to mutations of the Lamin a/C gene. *Ann Neurol.* 2000;48:170–80.
- Brodsky GL, et al. Lamin a/C gene mutation associated with dilated cardiomyopathy with variable skeletal muscle involvement. *Circulation.* 2000;101:473–6.
- Quarta G, et al. Mutations in the Lamin a/C gene mimic arrhythmogenic right ventricular cardiomyopathy. *Eur Heart J.* 2012;33:1128–36.

Publisher's Note

Springer Nature remains neutral with regard to jurisdictional claims in published maps and institutional affiliations.



Pediatric Restrictive Cardiomyopathies

Raffaello Ditaranto^{1†}, Angelo Giuseppe Caponetti^{1†}, Valentina Ferrara¹, Vanda Parisi¹, Matteo Minnucci¹, Chiara Chiti¹, Riccardo Baldassarre¹, Federico Di Nicola¹, Simone Bonetti², Tammam Hasan², Luciano Potena¹, Nazzareno Galì¹, Luca Ragni^{2*} and Elena Biagini^{1*}

¹ Cardiology Unit, Department of Experimental, Diagnostic and Specialty Medicine, IRCCS, Sant'Orsola Hospital, University of Bologna, Bologna, Italy, ² Pediatric Cardiac Surgery and GUCH Unit, IRCCS, Sant'Orsola Hospital, University of Bologna, Bologna, Italy

OPEN ACCESS

Edited by:

Giuseppe Limongelli,
Second University of Naples, Italy

Reviewed by:

Gianfranco Sinagra,
University of Trieste, Italy
Hirofumi Saiki,
Iwate Medical University, Japan

*Correspondence:

Luca Ragni
luca.ragni@aosp.bo.it
Elena Biagini
elena.biagini73@gmail.com

[†]These authors have contributed
equally to this work

Specialty section:

This article was submitted to
Pediatric Cardiology,
a section of the journal
Frontiers in Pediatrics

Received: 21 July 2021

Accepted: 28 December 2021

Published: 25 January 2022

Citation:

Ditaranto R, Caponetti AG, Ferrara V,
Parisi V, Minnucci M, Chiti C,
Baldassarre R, Di Nicola F, Bonetti S,
Hasan T, Potena L, Galì N, Ragni L
and Biagini E (2022) Pediatric
Restrictive Cardiomyopathies.
Front. Pediatr. 9:745365.
doi: 10.3389/fped.2021.745365

Restrictive cardiomyopathy (RCM) is the least frequent phenotype among pediatric heart muscle diseases, representing only 2.5–3% of all cardiomyopathies diagnosed during childhood. Pediatric RCM has a poor prognosis, high incidence of pulmonary hypertension (PH), thromboembolic events, and sudden death, is less amenable to medical or surgical treatment with high mortality rates. In this *scenario*, heart transplantation remains the only successful therapeutic option. Despite a shared hemodynamic profile, characterized by severe diastolic dysfunction and restrictive ventricular filling, with normal ventricle ejection fraction and wall thickness, RCM recognizes a broad etiological spectrum, consisting of genetic/familial and acquired causes, each of which has a distinct pathophysiology and natural course. Hence, the aim of this review is to cover the causes, clinical presentation, diagnostic evaluation, treatment, and prognosis of pediatric RCM.

Keywords: cardiomyopathy, restrictive cardiomyopathy (RCM), sarcomeric cardiomyopathy, pediatric cardiomyopathies, heart transplant (HTx)

INTRODUCTION

Restrictive cardiomyopathy (RCM) is a heart muscle disease characterized by abnormal diastolic function with restrictive filling and normal ventricular size, wall thickness, and ejection fraction. Differently from hypertrophic, dilated and right ventricle arrhythmogenic cardiomyopathy, where definition is based on morphology, RCM is defined based on physiology. However, under this common denominator, a wide spectrum of diseases are enclosed, with different causes, natural history, prognosis, and management. Furthermore, a restrictive hemodynamic profile can appear during the natural course of dilated and hypertrophic cardiomyopathy (HCM), being predictor of poor prognosis.

Among pediatric cardiomyopathies, RCM is the least common phenotype, representing only 2.5–3% of cardiomyopathies diagnosed during childhood (1). Unfortunately, compared to other pediatric cardiomyopathies, RCM is less amenable to medical or surgical treatment with higher mortality rates: 63% within 3 years of diagnosis and 75% within 6 years of diagnosis (2). As a consequence, rate for heart transplantation is relatively higher. Accordingly, within the Pediatric Heart Transplant Study Group, patients affected by RCM represents 12% of whole group of patients with cardiomyopathy undergoing heart transplantation.

Purpose of the present review is to summarize the causes of pediatric RCMs, their pathophysiology, clinical presentation and management.

DEFINITION AND EPIDEMIOLOGY

According to European Society of Cardiology position statement, RCM is defined as a myocardial disease characterized by impaired ventricular filling and normal/reduced diastolic volumes in the presence of (near) normal ejection fraction and myocardial thickness (3). Decreased active relaxation and increased parietal stiffness cause pressure within the ventricles to rise precipitously during diastolic filling, with only small increases in volumes. Although systolic function was classically said to be preserved in RCM, contractility is rarely normal, indeed. Furthermore, restrictive physiology can also occur in other scenarios, namely end stage HCM and dilated cardiomyopathy (DCM). However, it is suggested to consider these two entities apart. Restrictive cardiomyopathy is the least common among pediatric cardiomyopathies, accounting for only 2–5% of all cases, although the incidence may be higher in tropical areas of Africa, Asia, and South America, where endomyocardial fibrosis (EMF) is endemic (4). Its prognosis is poor with a 2-year survival <50%, being heart transplantation the only effective treatment (5, 6). Restrictive cardiomyopathy has been described in children of all ages, with mean age at diagnosis ranging from 6 to 11 years old in recent studies.

ETIOLOGY

Restrictive cardiomyopathies represent a heterogeneous group of cardiomyopathies which recognize several etiologies, including inherited and acquired causes. The term of idiopathic RCM is probably no longer appropriate in a large group of patients: in fact, genetics has identified mutations in various genes, above all sarcomeric genes. **Figure 1** summarizes the main causes of pediatric RCMs.

Idiopathic/Genetic RCMs

Although in the past decades pediatric RCMs were most commonly considered idiopathic in origin, the technical progress in genetics and the introduction and diffusion of next-generation sequencing technology into clinical practice have broadened the genetic spectrum of RCMs, discovering disease-causing genes among affected children. The Pediatric Cardiomyopathy Registry Investigators, through whole-exome sequencing of 36 genes involved in cardiomyopathies, reported pathogenic or likely pathogenic variants in 50% of children with RCM (7). Furthermore, not infrequently, they found patients with multiple candidate causal alleles, suggesting that the interaction effects from several alleles may be clinically relevant in pediatric cardiomyopathies.

RCM Caused by Sarcomeric Gene Mutation

Hereditary sarcomeric contractile protein disease finds expression in a broad spectrum of phenotypes. In pediatric RCM, sarcomeric mutations represent the most frequently identified genetic defect, accounting for one-third of children with idiopathic RCM (8). Particularly the genes reported are: myosin-binding protein (*MYBPC3*), β -myosin heavy chain (*MYH7*),

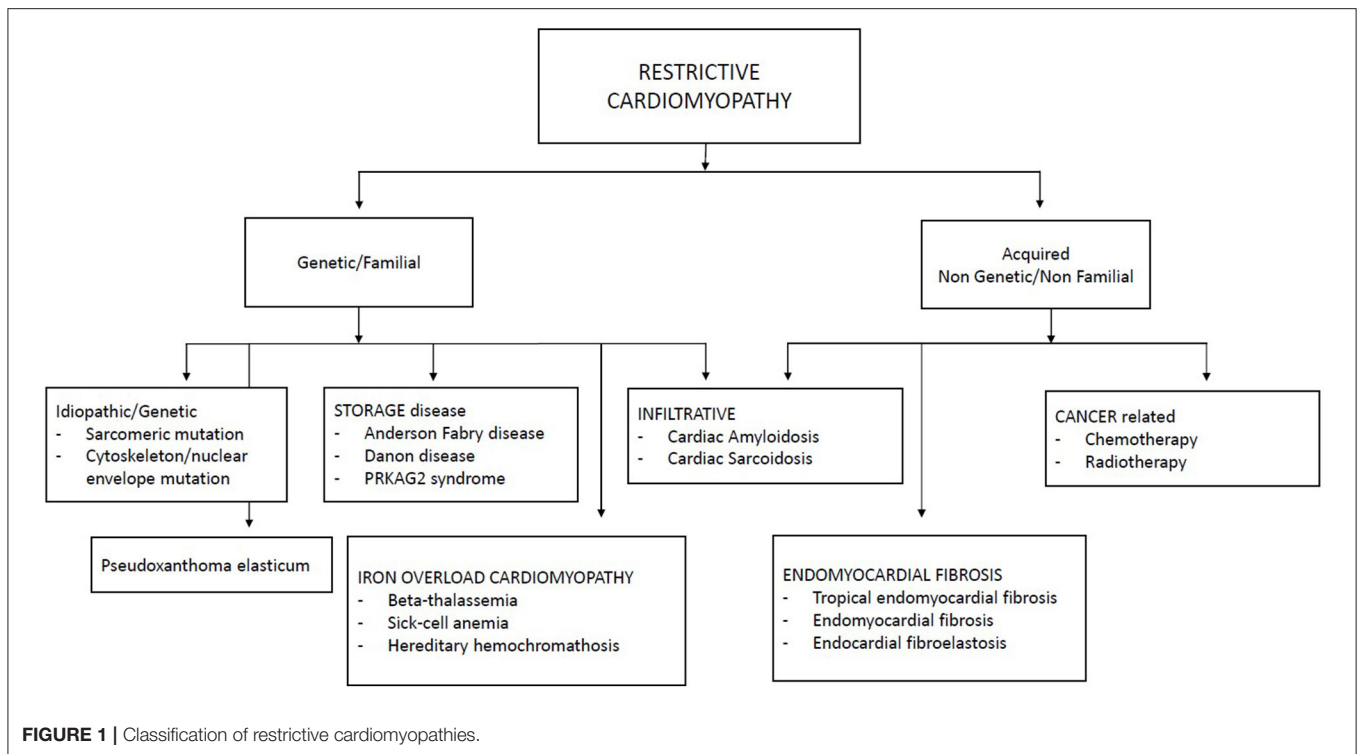
myosin light chain genes, titin (*TTN*), troponin I (*TNNI3*), troponin T (*TNNT2*), and α -cardiac actin (*ACTC*) (8–13).

Although the primary molecular pathways dysregulated in RCM are poorly understood, some hypotheses have been advanced in last years based on experimental models. Sarcomeric gene defects may increase Ca^{2+} sensitivity for force development, impair the inhibitory properties of troponin, activate thin-filament-mediated sarcomeric contraction at submaximal calcium concentrations, resulting in increased muscle tension during diastole and in abnormalities of cardiac relaxation (14). A striking variability in the phenotype, age of onset, and disease severity, even within the same family with a definite sarcomeric mutation, is often documented (**Figure 2**) (15). The basis of this phenotypic plasticity is unknown: probably is multifactorial and not solely dependent from the consequence of the mutated protein on the sarcomere structure/function (16). This suggests that—differently from a pure Mendelian inheritance disorder—a group of modifier genes, each exerting a modest effect, together with epigenetic, post-transcriptional, and translational modifications of expressed protein and environmental factors are responsible for phenotype definition (15). Therefore, the clinical phenotype of a genetic disorder is not simply determined by the information contained in the causal deoxyribonucleic acid sequence: this has relevant consequences, not only for pathophysiological understanding of cardiomyopathies but also to unravel molecular pathways to propel molecular based treatment strategies.

RCM Caused by Cytoskeletal/Nuclear Gene Mutation

Desmin, lamin, and filamin C mutations share a wide heterogeneity in clinical presentation and, particularly, the possibility to determine a RCM, sometimes associated with skeletal muscle involvement and atrio-ventricular conduction disturbances early in the course of disease.

Desmin is a muscle-specific type III intermediate filament, important for the stability and correct cellular function, codified by *DES* gene (2q35). Notably, the spectrum of cardiac phenotypes associated with *DES* mutations ranges from dilated, arrhythmogenic, non-compaction, hypertrophic and, in rare cases, restrictive cardiomyopathies (17). Most of the known *DES* mutations are missense or small in-frame deletions. Many missense mutations introduce prolines that interfere with the hydrogen bonds within the peptide bonds of α -helices, thus destabilizing the protein structure. The majority of *DES* mutations are heterozygously inherited, indicating a dominant negative genetic mechanism or haploinsufficiency (18). However, a recessive autosomal transmission was reported in rare cases with compound heterozygous or homozygous *DES* truncating mutations (17). *DES*-related RCM may be associated with distal skeletal myopathy, atrio-ventricular blocks requiring pacemaker implantation and ventricular arrhythmias (19, 20). The ultrastructural characteristic is represented by granulofilamentous deposits in cardiac and skeletal muscle causing structural disorganization of the cytoskeleton leading to impairment of both myocyte relaxation and contraction (**Figure 3**).



Filamin C (or γ -filamin), coded by the *FLNC* gene (7q32.1), is member of a family of cross-link actin filaments expressed in cardiac and skeletal muscle, whose main role is to anchor membrane proteins to the cytoskeleton. Furthermore, filamin C is involved in protein degradation and autophagy control. The first association between RCM and *FLNC* mutations was described by Brodehl et al. in two unrelated Caucasian families with autosomal-dominant transmission, associated to atrial fibrillation and conduction disorders needing PM implantation (21). Cardiac histology showed myocytes hypertrophy with eosinophilic cytoplasmic aggregates due to mutated protein deposition, fibrosis, and mild disarray. Subsequent works by other groups reported families carrying *FLNC* missense mutations associated to variable degrees of a skeletal myofibrillar myopathy characterized by filamentous intracellular aggregates, combined with mild CK elevation, supraventricular arrhythmias, and RCM with early onset, often in childhood (22). Differently from missense mutation, *FLNC* truncating variants, were found in patients with a cardiac-restricted arrhythmogenic DCM phenotype characterized by a high risk of life-threatening ventricular arrhythmias (23).

Laminopathies are a heterogeneous group of diseases including heart disease, neuromuscular disorders, premature aging, and metabolic disorders, caused by mutation of *LMNA* gene (1q22), coding the nuclear envelope proteins lamin A and C, via alternate splicing. The spectrum of cardiac involvement ranges from supraventricular tachyarrhythmias and/or conduction system disease to DCM and ventricular tachyarrhythmias. Rarely *LMNA* can present as RCM in second decade of life, associated with atrio-ventricular blocks and requiring heart transplantation (24).

Storage Cardiomyopathies

Among lysosomal storage disorders, Anderson Fabry disease (AFD), Danon disease, and PRKAG2 are the most frequently associated with cardiac involvement, generally presenting as HCM.

Anderson Fabry disease is caused by a reduced or absent activity of alpha-galactosidase A due to mutations in the *GLA* gene, mapping on X-chromosome (Xq22). This results in progressive globotriaosylceramide accumulation, in different cytotypes and tissues, with consequent organs dysfunction. Overt heart involvement is rare in childhood and may determine ECG abnormalities and initial diastolic dysfunction (25).

Danon disease is an X-linked multisystemic disorder caused by a defect in the lysosome-associated membrane protein 2 (*LAMP2*) gene (Xq24), encoding the LAMP2 protein, leading to progressive accumulation of autophagic material. Clinical phenotype is characterized by heart and skeletal myopathy, cardiac conduction abnormalities, mild intellectual difficulties, and retinal disease. Men are typically affected earlier and more severely than women. Cardiomyopathy had classically a hypertrophic phenotype, with high risk of end stage evolution and need for heart transplantation at early age (26).

PRKAG2 syndrome is a rare, early-onset autosomal dominant inherited glycogen storage disease, due to *PRKAG2* gene mutation (7q36.1), coding for the c subunit of the AMP-activated protein kinase. It is characterized by ventricular pre-excitation, supraventricular arrhythmias, and cardiac hypertrophy. It is frequently accompanied by chronotropic incompetence and advanced heart blocks, leading to premature PM implantation (27, 28).

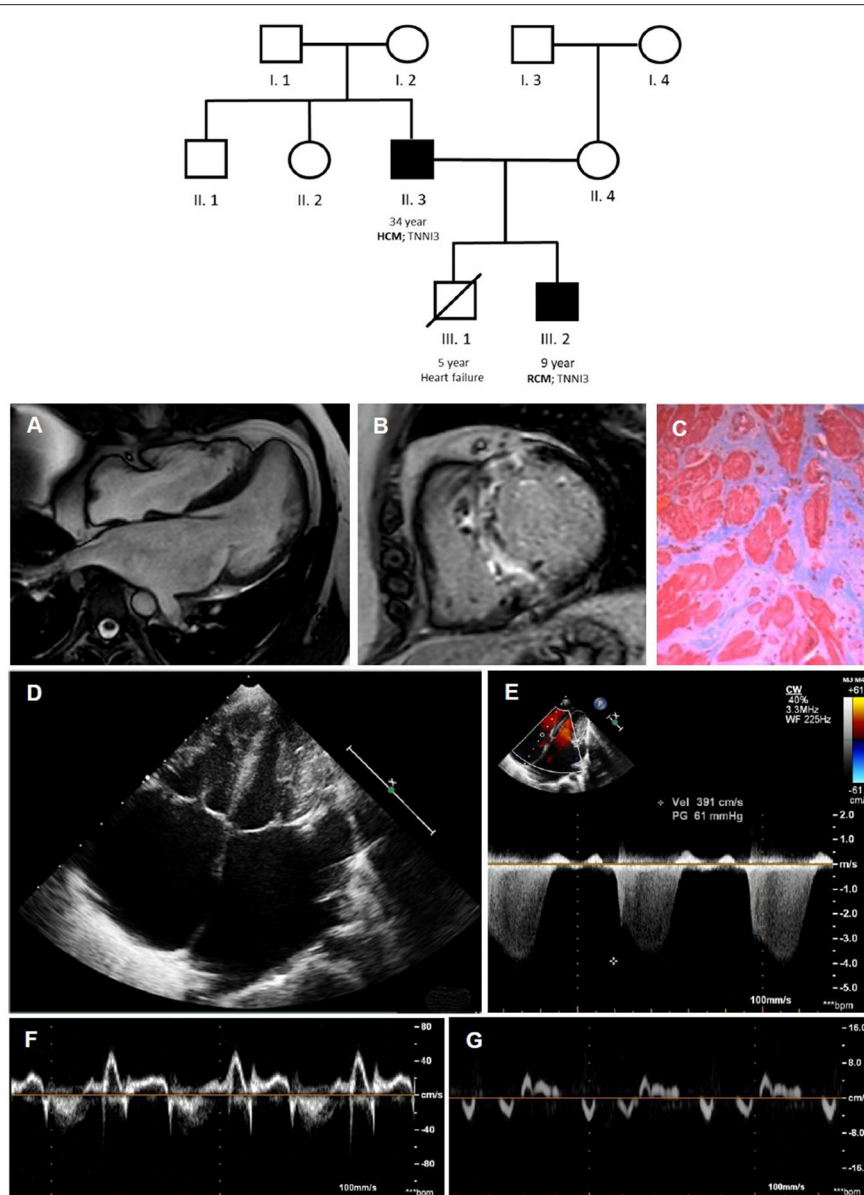


FIGURE 2 | Coexistence of HCM [father; II.3; (A–C)] and RCM [son; III.2; (D–G)] within the same family, due to a pathogenic troponin I mutation. In the family tree, black filled symbols stand for affected carriers. Cardiac magnetic resonance shows mild septum hypertrophy with mild left atrial enlargement (A) and septal late gadolinium enhancement (B) and replacement fibrosis at optical microscopy (C). The echocardiogram (D–G) shows a pediatric RCM with severe biatrial enlargement and small left ventricular volume (D) with signs of increased filling pressures at Doppler and TDI evaluation. HCM, hypertrophic cardiomyopathy; RCM, restrictive cardiomyopathy.

RCM Caused by Infiltrative Diseases

Amyloidosis is caused by deposition of an insoluble fibrillar protein called “amyloid” in the interstitium. It is extremely rare in childhood and is mostly seen late in life. Cardiac involvement is more commonly seen in transthyretin amyloidosis or light-chain amyloidosis, being mutated transthyretin amyloidosis (ATTRm) the earliest to occur in life, having been reported in the third decade of life (1).

Sarcoidosis is a multisystem, granulomatous disease of unknown etiology, characterized by non-caseating granulomas.

Pediatric sarcoidosis is an extremely rare disease, with an estimated incidence of 0.6–1.02/100,000 children and a mean age at diagnosis of 11–13 years (29). Pediatric cardiac sarcoidosis is even rarer, though anecdotal cases were reported (30).

Iron Overload Cardiomyopathy

Iron overload cardiomyopathy (IOC) results from iron accumulation as a consequence of excessive iron intake or absorption. Increased iron intake is generally caused by multiple red blood cell transfusions for chronic anemia (e.g., thalassemia,

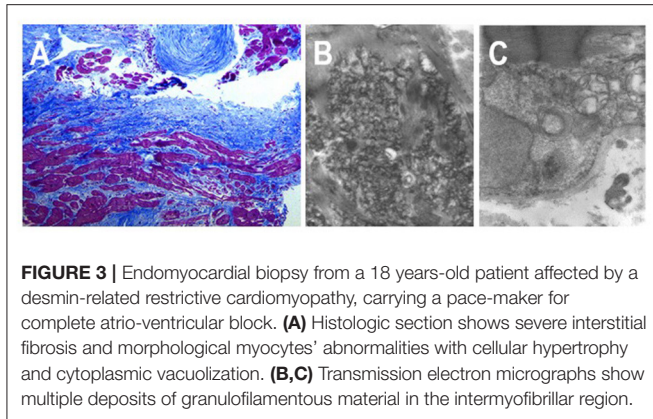


FIGURE 3 | Endomyocardial biopsy from a 18 years-old patient affected by a desmin-related restrictive cardiomyopathy, carrying a pace-maker for complete atrio-ventricular block. **(A)** Histologic section shows severe interstitial fibrosis and morphological myocytes' abnormalities with cellular hypertrophy and cytoplasmic vacuolization. **(B,C)** Transmission electron micrographs show multiple deposits of granulofilamentous material in the intermyofibrillar region.

sickle cell disease, hemolytic anemias, inherited bone marrow failure syndrome, myelodysplastic syndrome) or less commonly by infusions of iron-containing products used to treat certain porphyrias. Increased iron absorption is mainly caused by hereditary hemochromatosis (HH), due to mutations in genes involved in iron metabolism, increasing gastro-intestinal absorption. Among the known four HH subtypes, type 2 (also called juvenile hemochromatosis) typically presents by the second decade with a more severe phenotype accompanied, in addition to cardiomyopathy, by hypogonadotropic hypogonadism, arthropathy, and liver fibrosis or cirrhosis. Type 2 HH can be caused by two different genes: *HFE2* gene mutation, encoding hemojuvelin, a protein that interacts with hepcidin (subtype 1A) or *HAMP* gene, coding for hepcidin, a key regulator of circulating iron (subtype 2B). Regardless of its origin, IOC is characterized by a RCM with prominent early diastolic dysfunction which progressively evolve to an end-stage DCM (31). Although immunoinflammatory and inherited component may contribute to cardiac injury, iron overload plays a central role in the pathophysiology of IOC. Iron toxicity has been attributed to the production of free oxygen radicals, as a result of free iron availability. Excessive circulating free iron (i.e., not bound to transferrin) enters the cardiomyocytes, mainly through voltage-dependent L-type Ca^{2+} channels, in the form of Fe^{2+} (ferrous iron). Inside the cardiomyocytes, free iron induces the formation of reactive oxygen species, hence causing peroxidative damage of cellular structures (lipids, proteins, nucleic acids), cellular apoptosis, and finally cardiac dysfunction (32). Furthermore, iron overload increases calcium influx, which might impair, in its turn, diastolic function. A post-mortem hearts series (comprising two children) from patients with severe cardiac siderosis and heart failure leading to death or heart transplantation, except the severe granular iron deposition on Perl's stain, did not reveal replacement fibrosis and minor interstitial fibrosis was also unusual and very limited in extent, underlining the potential reversibility of heart failure in IOC (33). The best validated method for quantifying myocardial iron overload *in vivo* is T2^* mapping with CMR. A T2^* value of <20 ms at 1.5 T, typically measured in the interventricular septum, is used as a conservative cut-off for segmental and global

heart iron overload and patients with the lowest T2^* values have the highest risk of developing arrhythmia and heart failure (34).

RCM Caused by Fibrotic Process

- Tropical EMF is the most common cause of RCM, affecting more than 12 million people worldwide. Initially described in Uganda, EMF is commonly reported in rural populations of equatorial developing countries, where exhibits a bimodal distribution, peaking at 10 and 30 years of age. Many etiological hypotheses, not mutually exclusive, have been proposed: malnutrition, parasitic infections, environmental factors, and genetics. Due to regional differences in disease prevalence, a geochemical basis has been advanced as unifying hypothesis (35). Despite different possible candidates (magnesium deficiency, cerium toxicity, cyanogenic glycosides, high vitamin D, serotonin toxicity, herbal preparations), for none of them definitive evidence is available. The natural history of EMF is characterized by recurrent hot phases with inflammation and eosinophilia, progressing to a chronic phase where a biventricular RCM, caused by deposition of fibrous tissue in the endomyocardium, affects both ventricles or less frequently exclusively the right ventricle. In this last case, chronic venous hypertension causes facial edema and exophthalmos, jugular venous distention, hepatomegaly, and ascites, often out of proportion to peripheral edema (36).
- Eosinophilic EMF is a rare cause of RCM, resulting from toxicity of eosinophils toward cardiac tissues in patients with a hypereosinophilic syndrome (HES). Although the causes for eosinophilic infiltration of myocardium are various (hypersensitivity, parasitic infestation, systemic diseases, myeloproliferative syndrome, and idiopathic HES), pediatric HES is commonly associated with chromosomal abnormalities, and in 40% of the cases, it has been associated with acute leukemia (37). Eosinophil-mediated heart damage evolves through three stages, although these stages may be overlapping and not clearly sequential. The *acute necrotic stage* is characterized by infiltration of eosinophils and release of their granules' contents in the myocardium (eosinophilic myocarditis). Thereafter, an *intermediate phase* follows, with thrombus formation along the damaged endocardium (more often in the apex of the left ventricle) and finally a *fibrotic stage* characterized by reduced ventricular compliance and RMC. At this stage, entrapment of the chordae tendineae can lead to mitral and tricuspid regurgitation (38).
- Endocardial fibroelastosis is a congenital disease characterized by diffuse thickening of the LV endocardium secondary to proliferation of fibrous and elastic tissue, leading to early death. It manifests with a DCM phenotype or with a RCM phenotype with a small LV cavity. Most forms of endocardial fibroelastosis are associated with congenital heart diseases, first of all hypoplastic left heart syndrome and aortic stenosis/atresia, but also coarctation of the aorta, patent ductus arteriosus and, mitral regurgitation. In the minority of cases, a familial recurrence is seen, with all possible pattern of inheritance reported (39). Despite various attempts to unravel its origin, a definite mechanism could

not be identified. Genetic predisposition, viral infection (particularly mumps virus), and hypoxia during fetal cardiac development have been proposed as putative causes. Cardiac transplantation is required for end-stage heart failure (39). A promising surgical approach to remove endomyocardial layer showed improvement in the restrictive physiology together with growth of the left ventricle in parallel with somatic growth (40).

- Pseudoxanthoma elasticum is an inherited systemic disease of connective tissue, affecting skin, retina, and cardiovascular system. It is transmitted in an autosomal recessive manner and is caused by mutations in the *ABCC6* (ATP binding cassette subtype C number 6) gene (41). Histology of affected tissues exhibits elastic fiber mineralisation and fragmentation (so called “elastorrhexia”) (42). Restrictive cardiomyopathy in relation to diffuse endocardial fibroelastosis is very rare (43).

Oncological Cardiomyopathy

Progress in cancer therapeutics over the past years has significantly improved survival rates for most childhood malignancies. Unfortunately, the developing cardiovascular system of children and adolescents is particularly vulnerable to most pediatric cancer protocols, relying on cytotoxic chemotherapy and radiation. Indeed, cardiac-specific disease is the most common non-cancer cause of death among long-term childhood cancer survivors, only second to the recurrence of primary cancer and the development of second cancers (44).

Anthracyclines (such as doxorubicin, daunorubicin, and epirubicin), used to treat hematologic cancers and solid tumors, are among the most used chemotherapeutic agents causing cardiotoxicity. Although the typical manifestation of cancer drug induced cardiomyopathy is a DCM, with LV dilation and thinning of myocardial wall, with “restrictive” physiology in the more advanced stages, a not negligible proportion of long-term survivors will eventually develop a RCM. Importantly, patients may present cardiotoxicity many years after treatment completion, needing carefully monitoring for years by echocardiography. However, despite the adverse cardiac effects of anthracyclines, these drugs are fundamental components and standard of care for many types of cancer. Risk factors identified for cardiotoxicity include: female sex, younger age at diagnosis, black race, trisomy 21, and certain lifestyle behaviors (1). Although a total cumulative anthracycline dose $>300 \text{ mg/m}^2$ was identified as significant risk factor for late-occurring anthracycline-induced cardiotoxicity, adverse effects were reported also with lower cumulative doses (45).

Radiotherapy is frequently used together with surgery/chemotherapy in thoracic malignancies and lymphomas. Cardiac exposure is generally due to “stray” radiation as the heart is almost never the actual target, except for rare sarcomas or metastases (46). Although modern planning and irradiation techniques have significantly improved, radiation induced cardiac injury represents an actual issue, and combination with chemotherapy and novel agents increase cardiac toxicity. Restrictive cardiomyopathy is the consequence of a diffuse biventricular fibrosis, most often with a non-ischemic pattern, which reduces myocardial compliance. However, coexistent

radiation induced micro and macrovascular disease can result in ischemia/infarction and regional fibrosis.

In the next years the number of the long-term cancer survivors is expected to rise, not only for improved long-term survival rates but—unfortunately—also for the increased incidence of many histological subtypes of childhood cancer: consequently, amelioration of prevention and treatment strategies is needed.

EMODINAMICS

Restrictive cardiomyopathy recognizes a unique hemodynamic profile, independently from the specific cause at the basis of diastolic dysfunction. In RCM impairment of diastole can be related both to the abnormal myocardial relaxation (i.e., the active actin-myosin cross-bridge detachment) and to the increased myocardial stiffness due to the myocardial cells (e.g., titin) and the interstitial matrix (fibrosis) alterations, determining elevated left and right-sided filling pressure. Although left ventricular ejection fraction is typically preserved, systolic contractility is often impaired as showed by tissue Doppler imaging and speckle tracking. Systo-diastolic dysfunction leads to reduced stroke volume. In the protodiastole—despite delayed active relaxation—there is an unusually early rapid filling of the ventricles, due to high atrial pressures, halted by incompliant ventricular walls from the end of the first third of diastole onward—reflecting myocardial stiffness. This results in a prominent “y” descent on the atrial pressure curves and, sometimes, in the *square root* or *dip and plateau sign* on ventricular pressure curves, consisting in an early decrease in ventricular diastolic pressure followed by a rapid rise to a plateau phase. During the following atrial contraction, the stiff ventricles are unable to easily accept additional blood volume, and thus the contribution from atrial contraction is often minimal. Differently from constrictive pericarditis (CP), in patients with RCM there is not enhanced ventricular interdependence, with concordant left and right ventricular pressures during the respiratory cycle and parallel changes in their pressure curve areas. Moreover, atria progressively enlarge, due to high intracavitary pressures and thin and distensible walls, predisposing to atrial arrhythmias and thromboembolic episodes. A relevant proportion of patients develop pulmonary hypertension (PH) with elevated pulmonary vascular resistances, unresponsive to vasodilator testing, precluding them from orthotopic heart transplantation (47).

CLINICAL PRESENTATION

The clinical presentation of RCM can be highly variable in children population, ranging from asymptomatic to right and/or left heart failure with PH.

Biventricular systolic function is typically normal until advanced stages of the disease, leading to heart failure with preserved ejection fraction (HFpEF). Consequently, clinical presentation is characterized by dyspnoea, poor appetite, ascites, peripheral edema, and hepatomegaly. However, while in adults with RCM symptoms and signs of heart failure are easy to detect, clinical evaluation in children is challenging because of the non-specific findings, resulting in some delay

in correct diagnosis. Besides, children with RCM may have a history of frequent respiratory infections. Progressive atrial enlargement can also lead to atrial arrhythmias such as atrial fibrillation and thromboembolic complications, with mitral and tricuspid functional regurgitation frequently associated, due to anulus dilatation. Wolff Parkinson-White syndrome with supraventricular tachycardia has also been reported.

Sudden death occurs in $\approx 25\%$ of pediatric RCM patients, with an annual mortality rate reported of 7%, being cardiac ischemia, arrhythmias, and thromboembolic events the main responsible. Various risk factors for sudden death in pediatric RCM have been identified in previous studies: cardiomegaly, thromboembolism, raised pulmonary vascular resistance, pulmonary venous congestion, syncope, chest pain, left atrial size, PR and QRS duration. Albeit inconsistently sometimes, the main limitation of these studies is their retrospective nature and the intrinsic bias associated. Rivenes et al. evaluated a cohort of 18 pediatric patients with RCM who had sudden, unanticipated cardiac arrests, identifying chest pain, and syncope as risk factors for sudden death (48). Histopathologic evidence for ischemia was found in the majority of patients who died and the evidence of ischemia at Holter monitoring (i.e., ST depression) predicted death within several months. They proposed lethal ventricular arrhythmias as cause of death, showing examples of ventricular tachycardia/fibrillation recorded during resuscitation attempts (48). Complementary, Walsh et al. in a 16 pediatric RCMs cohort reported five sudden cardiac events, with three patients having complete heart block. In one of them, ST-segment elevation was documented before the onset of complete heart block, suggesting an underlying ischemic process as trigger of the bradyarrhythmia. Older age at presentation, longer PR interval and QRS duration were associated with sudden cardiac events (49).

DIAGNOSIS

Approximately 98% of RCM patients have an abnormal electrocardiogram (ECG) (50). The most common abnormalities are right and/or left atrial enlargement (91% of patients) (Figure 4). ST-T segment and T waves abnormalities are also frequently present and may be most evident at higher heart rates. In a small cohort of 12 children affected by RCM, Hayashi et al. found that obliquely elevated ST-T segments and notched or biphasic T waves were the most frequent ventricular repolarization abnormalities (67% of patients). Besides, the criteria for biventricular hypertrophy based on QRS voltage were achieved in seven patients (although three of them actually had some degree of hypertrophy at echocardiogram) (51). ST-T depression is usually mild and non-specific, but in some cases can be pronounced, mimicking a left main or proximal left anterior descending artery occlusion or a multivessel coronary disease. This was associated with high risk of sudden cardiac death (48) and Selvaganesh et al. hypothesized that marked ST depression can be caused by high end-diastolic pressure, impairing perfusion in the subendocardial region or stretching the myocardium and activating stretch sensitive channels (52).

Conduction abnormalities can also be seen, as well as right or left ventricular hypertrophy signs (48). Furthermore, serial ECG-Holter monitoring is useful for the evaluation of rhythm disturbances and ST segment analysis.

Chest X-ray is abnormal in nearly 90% of cases and usually show cardiomegaly and pulmonary venous congestion (51).

Echocardiography plays a key role in RCM diagnosis. Marked biatrial enlargement with a normal or slightly decreased LV ejection fraction are widely considered as pathognomonic findings (Figure 5). Regardless of etiology, the considerable elevation in filling pressures in patients with RCM is reflected in abnormal mitral inflow and tissue Doppler variables. A short (<140 ms) mitral deceleration time, increased pulsed wave (PW) Doppler mitral E/A ratio (>2.5) and $E/e' >15$ are markers of significantly elevated left filling pressures (53). Although IVRT (isovolumic relaxation time) is prolonged when myocardial relaxation is impaired, due to delayed LV pressure falling during the isovolumic relaxation, a short LV IVRT of <50 ms is frequently detected in RCM, as consequence of the high LA pressure (53). Typically plethoric inferior vena cava and hepatic veins are seen and, with inspiration, diastolic flow reversal in the hepatic veins is documented due to the inability of a non-compliant right ventricle to accommodate the increased venous return. Echocardiography is helpful in differential diagnosis between RCM and CP. Although both conditions shares E-wave predominance and short deceleration time, respirophasic shifting of the interventricular septum, caused by exaggerated interventricular dependence, is characteristic of CP. Accordingly respiratory flow variations consisting in increasing $>25\%$ in mitral inflow during expiration and $>40\%$ in tricuspid inflow after inspiration are absent in RCM but frequently noted in CP (54). However, among all echocardiographic parameters, the most useful to distinguish RCM from CP are those of tissue Doppler imaging. In fact a normal tissue Doppler e' velocity (>8 cm/s) indicating normal LV relaxation virtually excludes RCM. In patients affected by CP, where diastolic dysfunction is due to pericardial constraint, e' is normal or even increased since the longitudinal movement of the myocardium is enhanced because of constricted radial motion. Furthermore, in patients with pericardial constriction, lateral mitral annular e' is usually lower than e' from the medial annulus (so called “*annulus reversus*”) (55). This finding, absent in RCM, reflects the tethering of the lateral mitral annulus to the adjacent fibrotic and scarred pericardium. In this regard, speckle tracking may add even higher diagnostic accuracy in differentiating constriction from restriction: in fact while in RCM both radial and longitudinal strains are reduced due to a diseased myocardium, in CP reduction mainly involve circumferential strain, reflecting the subepicardial tethering offered by the fibrous pericardium (55, 56). The myocardial performance index (MPI) or Tei index may provide further information of both LV diastole and systole, with normal value of 0.33 ± 0.02 from 3 to 18 years old. It is defined as the sum of the isovolumic contraction and relaxation times divided by the ejection time, and it can be calculated from PW Doppler at the mitral and aortic valve simultaneously or using TDI at mitral valve annulus (57).

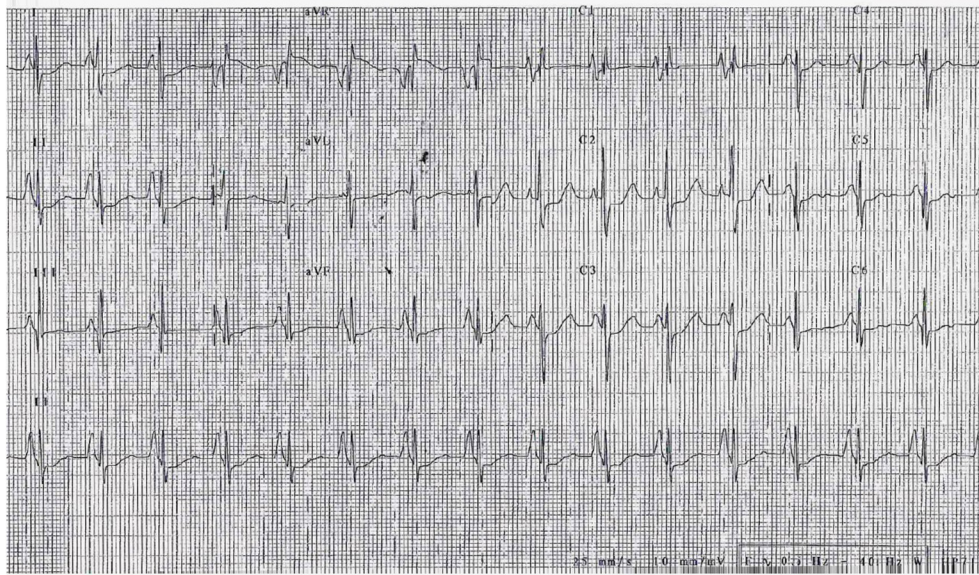


FIGURE 4 | ECG of a 3-year-old girl, affected by restrictive cardiomyopathy, showing biatrial enlargement and diffuse repolarization abnormalities. In the peripheral leads, please note the *monstre* atrial enlargement.

Moreover, lateral a' velocity (cut-off ≤ 0.042 m/s) and pulmonary vein A wave duration (cut-off ≥ 156 m/s) both have sensitivity and specificity $\geq 80\%$ for LVEDP ≥ 20 mmHg measured on right heart catheterization (58). Ancillary methods such as pulmonary regurgitant flow velocity, color M-mode flow propagation, and myocardial velocity gradient have been proposed for differential diagnosis between RCM and CP, however data in pediatric age are lacking. Finally, the performance and interpretation of diastolic measurements in children are challenging, given the higher heart rates, potential need for sedation, together with conflicting and limited data on the relationships among the diastolic variables and the degree of dysfunction (1). Indeed, in the assessment of diastolic dysfunction among 175 children with cardiomyopathy, the percentage of normal diastolic variables in children with overt cardiac dysfunction was high, with discordance between e' and left atrium (LA) volume criteria. Patients with RCM were best identified with mitral E deceleration time, which was found to be abnormal in 75% of patients (59). In another study, Sasaki et al. described the LA area indexed to body surface area as the most useful measurement to differentiate between healthy children and RCM patients (60).

Cardiac magnetic resonance (CMR) offers a better spatial resolution than echocardiography, providing detailed information about anatomic structures, ventricular function, perfusion, and tissue characterization (61). For instance, T2*-weighted CMR is the diagnostic gold standard to detect and quantify myocardial iron content in IOC (62). Late gadolinium enhancement (LGE) can show peculiar patterns of replacement and reactive fibrosis, which can direct the diagnosis to specific subtypes of RCM. In AFD, LGE is typically localized in the infero-lateral mid-basal wall of left ventricle, and because of the distinctive fatty nature of the intracellular deposits, native

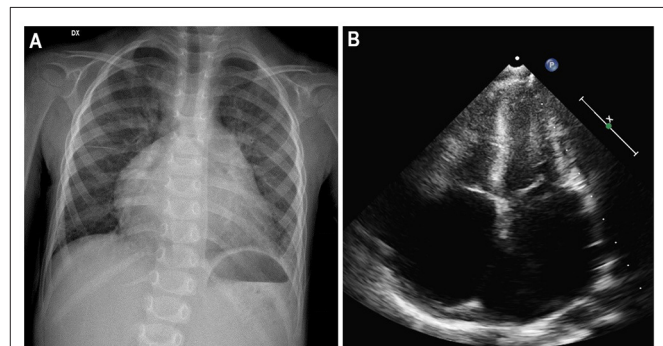
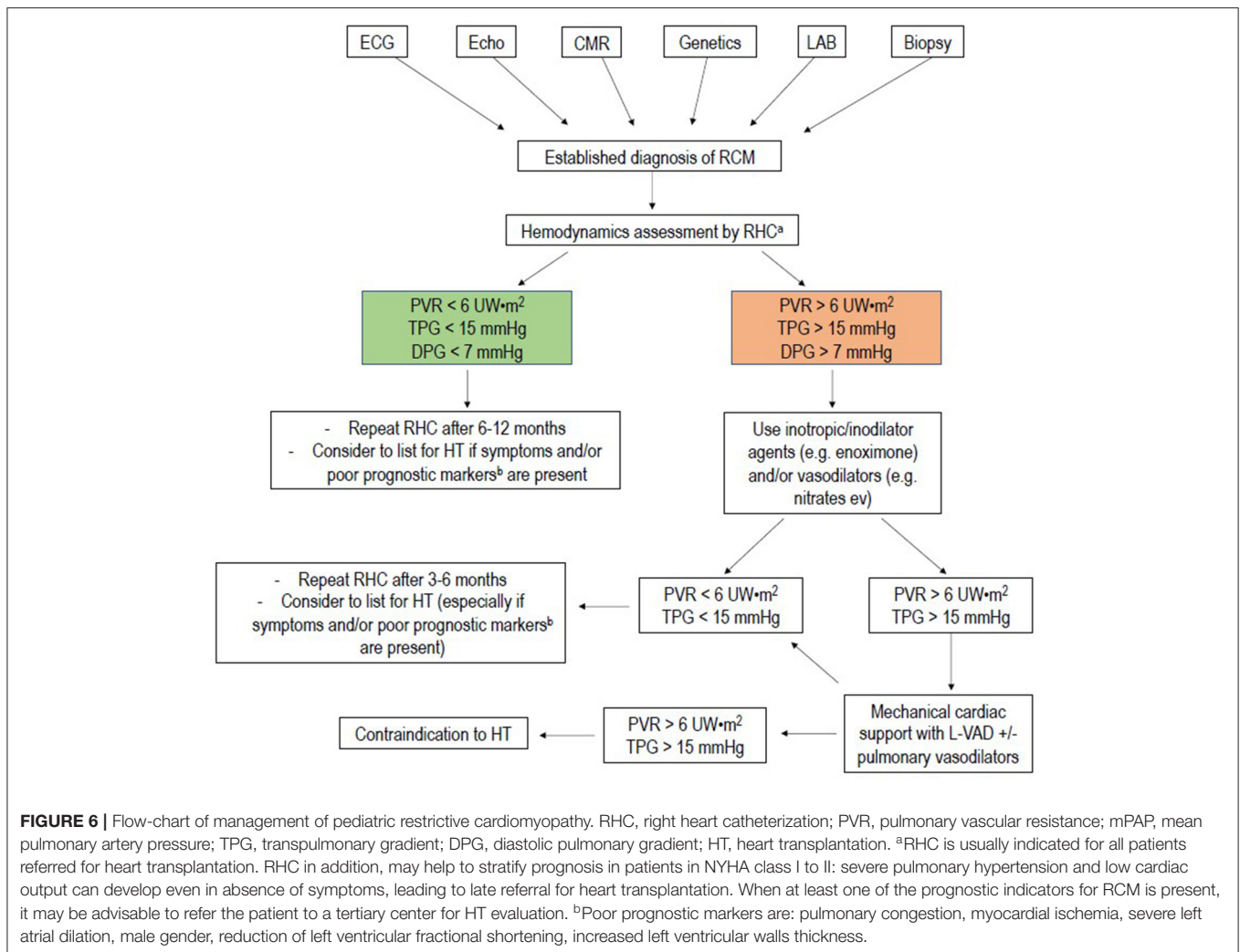


FIGURE 5 | Three-year-old girl affected by restrictive cardiomyopathy. Antero-posterior chest radiograph (A) showing massive cardiomegaly due to severe biatrial enlargement, as confirmed by apical four-chamber echocardiography (B).

T1 mapping has typically a low value, in contrast to most of other infiltrative or storage cardiomyopathies (63). In cardiac sarcoidosis LGE distribution is patchy, often with multifocal distribution, not following a coronary artery topography, sparing the endomyocardial layer, and involving mainly the basal and lateral LV walls (64). When performing CMR, it must be considered that the young patients must hold still in the scanner and follow the instructions to minimize motion artifacts during image acquisition. Whereas, this is possible in older children (more than 6–8 years of age), it requires sedation and anesthesia for younger patients, with different possible strategies, often depending on institutional preference and availability of resources such as pediatric anesthesiologists (65).



Whole-body scintigraphy or SPECT with bone-seeking tracers [(99mTc)-labeled bisphosphonate compounds: pyrophosphate (PYP); 3,3-diphosphono-1,2-propanodicarboxylic acid (DPD), and hydroxydiphosphonate (HDP)] can reveal amyloid deposits (especially in ATTR subtype) in the heart, as well as PET with [¹⁸F] FDG can detect inflammatory cells in some pathological processes such as cardiac sarcoidosis. However, due to the rarity of the aforementioned diseases and due to the concern for radiation exposure in childhood, nuclear imaging has very limited applications in the diagnostic work-up of pediatric RCMs.

Cardiac catheterization is usually not necessary for RCM diagnosis, but it can be useful to distinguish between restrictive and constrictive physiology and to determine the severity of the diastolic dysfunction by directly measuring the filling pressures of both ventricles (Figure 6). In RCM left ventricular end-diastolic pressures are usually higher than right end-diastolic pressure, whereas are equal or very nearly equal in CP. Furthermore, specular discordance between RV and LV peak systolic pressures during inspiration are typical of CP, with an increase in RV pressure occurring during peak inspiration, when LV pressure

is lowest. Cardiac catheterization can also reveal the presence of PH, detect the presence of elevated pulmonary vascular resistance, evaluate the cardiac index and test for pulmonary vasculature reactivity.

Plasma levels of natriuretic peptides can be helpful in the diagnostic pathway of RCM, especially in the differential diagnosis with CP. A study of 49 adults (20 with RCM and 29 with CP) showed that median plasma NT-proBNP was 1,775 (208–7,500) pg/ml in those with RCM vs. 124 (68–718) pg/ml in those with CP ($P = 0.001$) (66). Specific etiologies may require additional laboratory exams such as angiotensin converting enzyme dosage in sarcoidosis, complete blood count to establish eosinophilia in HESs, serum iron concentrations, total iron-binding capacity, and ferritin levels in hemochromatosis, alpha-galactosidase activity, and lyso-Gb3 levels in AFD, immunoglobulin free light chain testing, and serum and urine immunofixation in AL amyloidosis.

The endomyocardial biopsy can be valuable in doubtful cases, when non-invasive tests are inconclusive. Unfortunately, in idiopathic RCM it often demonstrates non-specific findings such

TABLE 1 | Differential diagnosis of constrictive pericarditis and restrictive cardiomyopathy.

	Constrictive pericarditis	Restrictive cardiomyopathy
Clinical examination	Kussmaul's sign, usually present Pulsus paradoxus (may be present) Pericardial knock	Kussmaul's sign, may be present Pulsus paradoxus (infrequent) S3; Systolic murmur due to mitral and tricuspidal regurgitation
Echocardiogram		
Pericardial appearance	Thickened/bright	Normal
Atrial size	Minor enlargement	Major enlargement
Septal motion	Respiratory shift	Normal
Mitral inflow respiratory variation	Usually present (>25%)	Absent
TDI septal S' wave, cm/s	>5	<5
Speckle tracking	↓ Circumferential strain	↓ Radial and longitudinal strain
Biomarkers		
NT-proBNP	Normal or slightly abnormal	Abnormal
Cardiac catheterization		
Right and left ventricular end-diastolic pressures comparison	Equal or ≤5 mm Hg	Usually left > right
Dip-plateau waveform	Typically present	Can be present
CT scan/MRI		
Pericardial thickening	Present	Absent

as myocyte hypertrophy, interstitial and/or endocardial fibrosis. Furthermore, periprocedural risks in fragile affected children should be considered (50).

Restrictive cardiomyopathy should be distinguished from CP, since the two diseases have different treatments and outcomes. In some cases—namely, radiation induced cardiac disease—restriction and constriction may coexist in the same patient, making final diagnosis even more challenging. In **Table 1** the main instrumental features of each condition are summarized.

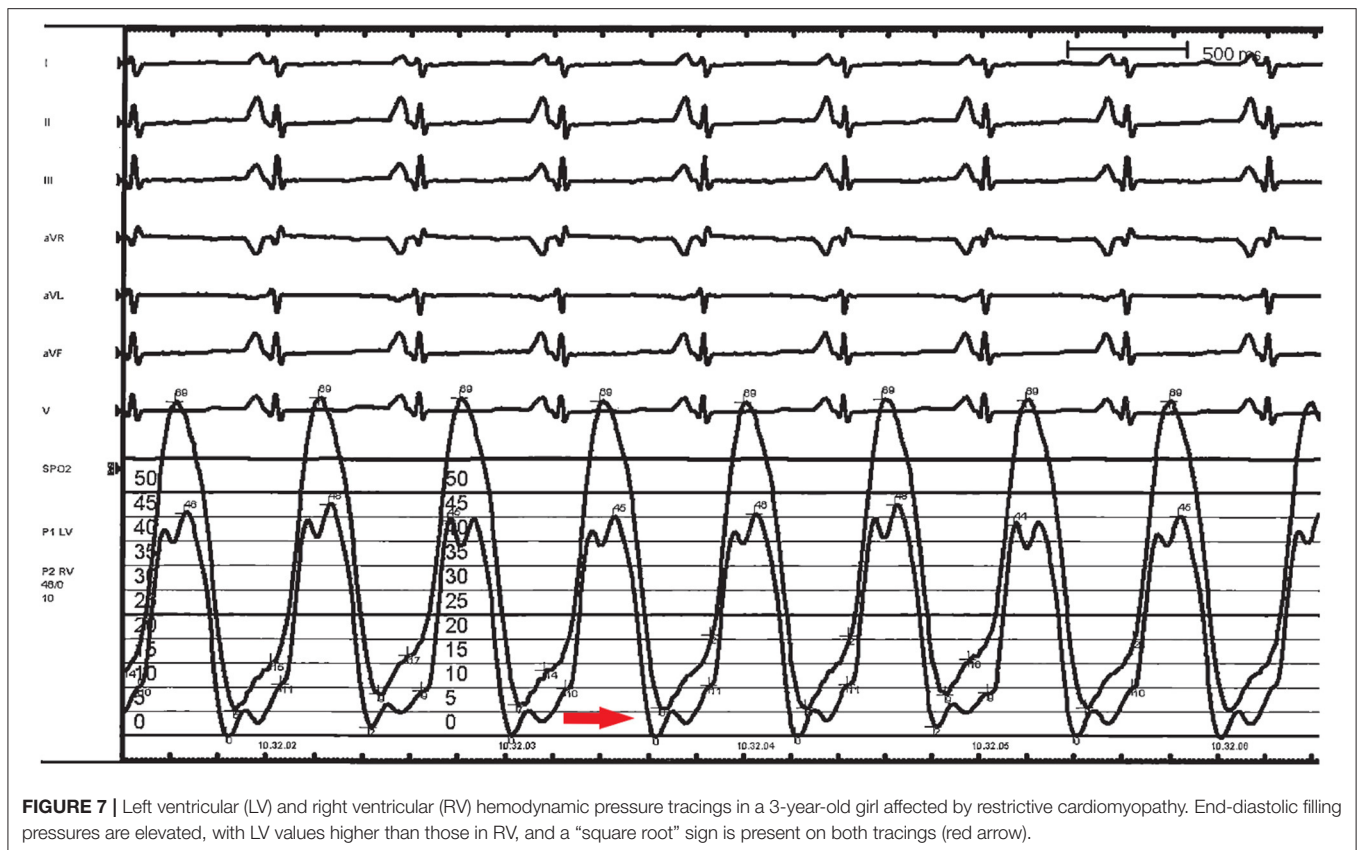
MANAGEMENT

Current medical therapy for RCM is primarily supportive and is in large part limited to diuretics in patients with signs and symptoms of systemic or pulmonary venous congestion. The International Society for Heart and Lung Transplantation (ISHLT) guidelines for the management of pediatric heart failure published in 2014 recommend in class I the diuretic therapy to establish a clinically euvolemic state, with a close monitoring of renal function and blood pressure during initiation and up-titration (67). Diuretic therapy reduces signs of systemic congestion, with beneficial effect on symptoms as dyspnea, fatigue, peripheral edema, and cough. However, excessive diuresis should be avoided because these patients are sensitive to alterations in preload. Furthermore, diuretics

can mask an underlying PH or increased biventricular filling pressures, therefore this aspect must be considered before performing a hemodynamics invasive assessment (particularly prior to candidacy to heart transplantation). Restrictive cardiomyopathy has a unique pathophysiology: small ventricular cavity dimensions and rapid increase of filling pressures significantly compromise stroke volume (according to pressure-volume loop). Therefore, cardiac output is strongly influenced by heart rate, which must be kept at relatively high values to guarantee adequate systemic perfusion. For these reasons β -blockers and calcium channel blockers are not currently recommended in pediatric RCM, unless for a different indication (67). Angiotensin converting enzyme inhibitors and angiotensin receptor blockers may be considered if coexisting systemic arterial hypertension is present (class IIb recommendation). Similarly, digoxin (unless for rate control of atrial arrhythmias), intravenous inotropes (such as dopamine, dobutamine, and epinephrine), and pulmonary vasodilators (prostaglandins and endothelin receptor antagonists to treat secondary PH) are generally not recommended (Class III).

Although atrial thrombosis has been linked to atrial fibrillation, abnormal hemodynamics, and to a possible hypercoagulable state in adults with RCM, dedicated studies in pediatric populations are lacking (68). The incidence of intracardiac thrombus in the reviewed literature ranges from 0 to 42%, with rates of embolism between 12 and 33%. The risk of embolism appears to be much greater in children with RCM than to DCM; therefore, antithrombotic or anticoagulation therapy should be considered at the time of diagnosis (47, 69). However, there are no studies comparing the effectiveness of antiplatelet agents, vitamin K antagonists or enoxaparin in preventing embolism in children with RCM (70).

Conduction system disease recognize different etiologies, such as ischemic injury of the atrio-ventricular node and His-Purkinje system, mechanical stretching due to atrial and ventricular dilation or genetically determined mechanisms (71–73). In addition, prolonged PR interval and wide QRS complex at ECG were associated with acute cardiac event (49). The 2014 ISHLT guidelines recommend in Class I permanent PM for advanced second- or third-degree atrioventricular block associated with ventricular dysfunction. On the basis of available data, the presence of conduction system disease should trigger increased surveillance through baseline ECG and ECG Holter monitoring with ST-segment analysis together with a routine screening for research of clinical (chest pain or syncope) and instrumental ischemia (ST-segment variations). Some Authors suggest in the presence of PR prolongation, QRS widening, and left bundle-branch block particular attention and to consider prophylactic pacing, eventually as part of an implantable-cardioverter defibrillators (ICD) system (48). However, it should be noticed that there are no studies documenting the efficacy of defibrillator systems in large pediatric cohorts, and case to case evaluation, assessing the individual risk factors (including the specific etiology) should be carried out, in order to avoid inappropriate and detrimental therapies (49). At moment, without unanimous criteria, ICD should be considered in the subset of pediatric RCM patients with evidence of ischemia and



ventricular arrhythmia, where also β -blockers may be beneficial (48). In a single center experience of pediatric patients with RCM, 40% of them with an ICD or PM, device therapies were relatively rare and inappropriate therapies were exceedingly rare (6).

These gaps in evidence are partly to ascribe to the low prevalence of RCM and its poor prognosis, with half patients dying or being referred to cardiac transplantation within 3 years from the diagnosis (74). Medical treatment has not shown any significant long term benefit and cardiac transplantation is the only effective therapy with survival rates between 70 and 60% at 5 and 10 year, respectively, in children listed for heart transplant (75). Orthotopic heart transplantation is preferred to heart-lung or heterotopic heart transplant and has a better survival rate than the other two options (76). In 2012 Singh et al. analyzed 1,436 children <18 years of age with a diagnosis of cardiomyopathy listed for heart transplant in the United States between 2004 and 2010, of which 167 with RCM. In adjusted analysis, children with non-DCM (83%) had a higher risk of wait-list mortality only if supported by a ventilator at listing. Post-transplant 30-days and at 1-year survival were similar between children with dilated and non-DCM ($p = 0.17$) (77). In another cohort of children with RCM from the American Pediatric Cardiomyopathy Registry database, about two thirds of children had a pure RCM phenotype, and the rest had a mixed RCM/HCM phenotype. Rate of survival at 5 year was 20 and 28%,

respectively, but patients with pure RCM phenotype underwent heart transplantation more frequently (58 vs. 30%) (5).

The majority of deaths in children awaiting heart transplantation is due to progressive heart and multi-organ failure. Hence, in this context, mechanical circulatory support (MCS), as bridge to transplantation or candidacy, may be a precious weapon. At the moment the experience with MCS in children is quite limited, and this is particularly true for RCM. The most used pediatric long-term support device, is the pneumatically driven, pulsatile EXCOR[®] Berlin Heart, with a variety of pump sizes, covering almost all pediatric patients, and the only long-term device for neonates and infants approved in Europe and USA. Few case series of successful bridging to cardiac transplantation with the Berlin EXCOR[®] left ventricular assist device (LVAD) have been described (78, 79). Conventional LV apical cannulation of a non-compliant left ventricle often results in insufficient drainage and poor pump performance, with residual high left atrial pressures and consequent pulmonary congestion. Left atrial cannulation (such as in EXCOR[®] Berlin Heart) is therefore an interesting option in patient with small ventricular cavity, preserved systolic function, and enlarged atria (80). A recent review of the American registry of EXCOR[®] Berlin Heart implantation in pediatric patients affected by RCM showed a survival rate of 50%, which is significantly less than that of the overall EXCOR[®] pediatric population (75%) (81). Primary

causes of death included stroke, infection, acidosis, multisystem organ failure, and bleeding. It is of note that these patients tended to be sicker than the whole population (INTERMACS class 1 and with ECMO support) and this can explain at least partly, the worst outcome. In summary, long-term MCS implantation is a high-risk procedure that can be considered in advanced stages of the disease as bridge to transplantation or to candidacy by improving hemodynamics, with the reduction of post-capillary PH. Further studies are needed to determine the best timing for the procedure and the best anticoagulant strategy to reduce the risk of thromboembolic events that are the main cause of adverse outcome in these patients.

Considering all these major concerns about the poor efficacy of medical treatment, the identification of the right time to list for heart transplantation a patient affected by RCM during the clinical follow-up becomes both challenging and crucial. Although some clinical and instrumental factors such as pulmonary congestion at diagnosis, severe left atrial dilation, or increased ventricular wall thickness have been identified as potential predictors of poor prognosis, there are no established criteria for listing and the decision is often dependent on individual experienced centers (82). A multi-modal instrumental approach is essential, particularly based on a regular assessment of right heart hemodynamics with or without use of inotropic agents and vasodilators, to detect at the proper time the

development of irreversible PH. Some pediatric institutions consider the development of PH an indication for listing, regardless of heart failure symptoms. Accordingly, right heart catheterization is mandatory at first evaluation, since up to 50% of patients have PH at diagnosis (47, 83). The flow-chart illustrated in **Figure 7** summarizes the experienced approach for pediatric RCM, developed in our tertiary center, with a dedicated program for pediatric cardiomyopathies and pediatric heart transplantation.

CONCLUSION

Pediatric RCM is a rare disorder, due to a large heterogeneous group of causes. As a result of its poor prognosis, RCM contributes disproportionately to mortality in children with cardiomyopathy, being heart transplantation the only effective treatment. Therefore, early referral to a third-level cardiomyopathy center is warranted for careful observation, to avoid the development of irreversible PH and to avoid a delay in listing for heart transplantation when indicated.

AUTHOR CONTRIBUTIONS

All authors listed have made a substantial, direct, and intellectual contribution to the work and approved it for publication.

REFERENCES

- Lipshultz SE, Law YM, Asante-Korang A, Austin ED, Dipchand AI, Everitt MD, et al. Cardiomyopathy in children: classification and diagnosis: a scientific statement from the American Heart Association. *Circulation*. (2019) 140:e9–68. doi: 10.1161/CIR.0000000000000682
- Canter CE, Shaddy RE, Bernstein D, Hsu DT, Chrisant MR, Kirklín JK, et al. Indications for heart transplantation in pediatric heart disease: a scientific statement from the American Heart Association Council on Cardiovascular Disease in the Young; the Councils on Clinical Cardiology, Cardiovascular Nursing, and Cardiovascular Surgery and Anesthesia; and the Quality of Care and Outcomes Research Interdisciplinary Working Group. *Circulation*. (2007) 115:658–76. doi: 10.1161/CIRCULATIONAHA.106.180449
- Elliott P, Andersson B, Arbustini E, Bilinska Z, Cecchi F, Charron P, et al. Classification of the cardiomyopathies: a position statement from the European Society Of Cardiology Working Group on Myocardial and Pericardial Diseases. *Eur Heart J*. (2008) 29:270–6. doi: 10.1093/eurheartj/ehm342
- Bukhman G, Ziegler J, Parry E. Endomyocardial fibrosis: still a mystery after 60 years. *PLoS Negl Trop Dis*. (2008) 2:e97. doi: 10.1371/journal.pntd.0000097
- Webber SA, Lipshultz SE, Sleeper LA, Lu M, Wilkinson JD, Addonizio LJ, et al. Pediatric Cardiomyopathy Registry, outcomes of restrictive cardiomyopathy in childhood and the influence of phenotype: a report from the Pediatric Cardiomyopathy Registry. *Circulation*. (2012) 126:1237–44. doi: 10.1161/CIRCULATIONAHA.112.104638
- Wittekind SG, Ryan TD, Gao Z, Zafar F, Czosek RJ, Chin CW, et al. Contemporary outcomes of pediatric restrictive cardiomyopathy: a single-center experience. *Pediatr Cardiol*. (2019) 40:694–704. doi: 10.1007/s00246-018-2043-0
- Ware SM, Wilkinson JD, Tariq M, Schubert JA, Sridhar A, Colan SD, et al. Genetic causes of cardiomyopathy in children: first results from the pediatric cardiomyopathy genes study. *J Am Heart Assoc*. (2021) 10:e017731. doi: 10.1161/JAHA.121.028040
- Kaski JB, Syrris P, Burch M, Tome-Esteban MT, Fenton M, Christiansen M, et al. Idiopathic restrictive cardiomyopathy in children is caused by mutations in cardiac sarcomere protein genes. *Heart*. (2008) 94:1478–84. doi: 10.1136/hrt.2007.134684
- Ware SM, Quinn ME, Ballard ET, Miller E, Uzark K, Spicer RL. Pediatric restrictive cardiomyopathy associated with a mutation in beta-myosin heavy chain. *Clin Genet*. (2008) 73:165–70. doi: 10.1111/j.1399-0004.2007.00939.x
- Olson TM, Karst ML, Whitby FG, Driscoll DJ. Myosin light chain mutation causes autosomal recessive cardiomyopathy with mid-cavitary hypertrophy and restrictive physiology. *Circulation*. (2002) 105:2337–40. doi: 10.1161/01.CIR.0000018444.47798.94
- Peled Y, Gramlich M, Yoskovitz G, Feinberg MS, Afek A, Polak-Charcon S, et al. Titin mutation in familial restrictive cardiomyopathy. *Int J Cardiol*. (2014) 171:24–30. doi: 10.1016/j.ijcard.2013.11.037
- Mogensen J, Kubo T, Duque M, Uribe W, Shaw A, Murphy R, et al. Idiopathic restrictive cardiomyopathy is part of the clinical expression of cardiac troponin I mutations. *J Clin Invest*. (2003) 111:209–16. doi: 10.1172/JCI200316336
- Ezekian JE, Clippinger SR, Garcia JM, Yang Q, Denfield S, Jeewa A, et al. Variant R94C in TNNT2-encoded troponin T predisposes to pediatric restrictive cardiomyopathy and sudden death through impaired thin filament relaxation resulting in myocardial diastolic dysfunction. *J Am Heart Assoc*. (2020) 9:e015111. doi: 10.1161/JAHA.119.015111
- Pinto JR, Parvatiyar MS, Jones MA, Liang J, Potter JD. A troponin T mutation that causes infantile restrictive cardiomyopathy increases Ca²⁺ sensitivity of force development and impairs the inhibitory properties of troponin. *J Biol Chem*. (2008) 283:2156–66. doi: 10.1074/jbc.M707066200
- Rindler TN, Hinton RB, Salomonis N, Ware SM. Molecular characterization of pediatric restrictive cardiomyopathy from integrative genomics. *Sci Rep*. (2017) 7:39276. doi: 10.1038/srep39276
- Marian AJ. Phenotypic plasticity of sarcomeric protein mutations. *J Am Coll Cardiol*. (2007) 49:2427–9. doi: 10.1016/j.jacc.2007.04.016
- Brodehl A, Pour Hakimi SA, Stanasiuk C, Ratnavadivel S, Hendig D, Gaertner A, et al. Restrictive cardiomyopathy is caused by a novel homozygous Desmin (DES) mutation p.Y122H leading to a severe filament assembly defect. *Genes*. (2019) 10:918. doi: 10.3390/genes10110918

18. Brodehl A, Gaertner-Rommel A, Milting H. Molecular insights into cardiomyopathies associated with desmin (DES) mutations. *Biophys Rev.* (2018) 10:983–1006. doi: 10.1007/s12551-018-0429-0
19. Arbustini E, Pasotti M, Pilotto A, Pellegrini C, Grasso M, Previtali S, et al. Desmin accumulation restrictive cardiomyopathy and atrioventricular block associated with desmin gene defects. *Eur J Heart Fail.* (2006) 8:477–83. doi: 10.1016/j.ejheart.2005.11.003
20. Wahbi K, Behin A, Charron P, Dunand M, Richard P, Meune C, et al. High cardiovascular morbidity and mortality in myofibrillar myopathies due to DES gene mutations: a 10-year longitudinal study. *Neuromuscul Disord.* (2012) 22:211–8. doi: 10.1016/j.nmd.2011.10.019
21. Brodehl A, Ferrier RA, Hamilton SJ, Greenway SC, Brundler MA, Yu W, et al. Mutations in FLNC are associated with familial restrictive cardiomyopathy. *Hum Mutat.* (2016) 37:269–79. doi: 10.1002/humu.22942
22. Schubert J, Tariq M, Geddes G, Kindel S, Miller EM, Ware SM. Novel pathogenic variants in filamin C identified in pediatric restrictive cardiomyopathy. *Hum Mutat.* (2018) 39:2083–96. doi: 10.1002/humu.23661
23. Ortiz-Genga MF, Cuenca S, Dal Ferro M, Zorio E, Salgado-Aranda R, Climent V, et al. Truncating FLNC mutations are associated with high-risk dilated and arrhythmogenic cardiomyopathies. *J Am Coll Cardiol.* (2016) 68:2440–51. doi: 10.1016/j.jacc.2016.09.927
24. Ditaranto R, Boriani G, Biffi M, Lorenzini M, Graziosi M, Ziacchi M, et al. Differences in cardiac phenotype and natural history of laminopathies with and without neuromuscular onset. *Orphanet J Rare Dis.* (2019) 14:263. doi: 10.1186/s13023-019-1245-8
25. Havranek S, Linhart A, Urbanova Z, Ramaswami U. Early cardiac changes in children with anderson-fabry disease. *JIMD Rep.* (2013) 11:53–64. doi: 10.1007/8904_2013_222
26. Lotan D, Salazar-Mendiguchia J, Mogensen J, Rathore F, Anastakis A, Kaski J, et al. Cooperating investigators double, clinical profile of cardiac involvement in Danon disease: a Multicenter European Registry. *Circ Genom Precis Med.* (2020) 13:e003117. doi: 10.1161/CIRCGEN.120.003117
27. Porto AG, Brun F, Severini GM, Losurdo P, Fabris E, Taylor RGM, et al. Clinical spectrum of PRKAG2 syndrome. *Circ Arrhythm Electrophysiol.* (2016) 9:e003121. doi: 10.1161/CIRCEP.115.003121
28. Fabris E, Brun F, Porto AG, Losurdo P, Vitali Serdoz L, Zecchin M, et al. Cardiac hypertrophy, accessory pathway, and conduction system disease in an adolescent: the PRKAG2 cardiac syndrome. *J Am Coll Cardiol.* (2013) 62:e17. doi: 10.1016/j.jacc.2013.02.099
29. Nathan N, Sileo C, Calender A, Pacheco Y, Rosental PA, Cavalin C, et al. Paediatric sarcoidosis. *Paediatr Respir Rev.* (2019) 29:53–9. doi: 10.1016/j.prrv.2018.05.003
30. Hafner R, Vogel P. Sarcoidosis of early onset. A challenge for the pediatric rheumatologist. *Clin Exp Rheumatol.* (1993) 11:685–91.
31. Murphy CJ, Oudit GY. Iron-overload cardiomyopathy: pathophysiology, diagnosis, and treatment. *J Card Fail.* (2010) 16:888–900. doi: 10.1016/j.cardfail.2010.05.009
32. Kremastinos DT, Farmakis D, Aessopos A, Hahalis G, Hamodraka E, Tsiapras D, et al. Beta-thalassemia cardiomyopathy: history, present considerations, and future perspectives. *Circ Heart Fail.* (2010) 3:451–8. doi: 10.1161/CIRCHEARTFAILURE.109.913863
33. Kirk P, Sheppard M, Carpenter JP, Anderson L, He T, St Pierre T, et al. Post-mortem study of the association between cardiac iron and fibrosis in transfusion dependent anaemia. *J Cardiovasc Magn Reson.* (2017) 19:36. doi: 10.1186/s12968-017-0349-3
34. Pennell DJ, Udelson JE, Arai AE, Bozkurt B, Cohen AR, Galanello R, et al. Cardiovascular function and treatment in beta-thalassemia major: a consensus statement from the American Heart Association. *Circulation.* (2013) 128:281–308. doi: 10.1161/CIR.0b013e31829b2be6
35. Valiathan MS, Kartha CC, Eapen JT, Dang HS, Sunta CM. A geochemical basis for endomyocardial fibrosis. *Cardiovasc Res.* (1989) 23:647–8. doi: 10.1093/cvr/23.7.647
36. Grimaldi A, Mocumbi AO, Freers J, Lachaud M, Mirabel M, Ferreira B, et al. Tropical endomyocardial fibrosis: natural history, challenges, and perspectives. *Circulation.* (2016) 133:2503–15. doi: 10.1161/CIRCULATIONAHA.115.021178
37. Katz HT, Haque SJ, Hsieh FH. Pediatric hypereosinophilic syndrome (HES) differs from adult HES. *J Pediatr.* (2005) 146:134–6. doi: 10.1016/j.jpeds.2004.09.014
38. Pereira NL, Grogan M, Dec GW. Spectrum of restrictive and infiltrative cardiomyopathies: part 2 of a 2-part series. *J Am Coll Cardiol.* (2018) 71:1149–66. doi: 10.1016/j.jacc.2018.01.017
39. Steger CM, Antretter H, Moser PL. Endocardial fibroelastosis of the heart. *Lancet.* (2012) 379:932. doi: 10.1016/S0140-6736(11)61418-9
40. Xu X, Friehs I, Zhong Hu T, Melnychenko I, Tampe B, Alnour F, et al. Endocardial fibroelastosis is caused by aberrant endothelial to mesenchymal transition. *Circ Res.* (2015) 116:857–66. doi: 10.1161/CIRCRESAHA.116.305629
41. Bergen AA, Plomp AS, Schuurman EJ, Terry S, Breuning M, Dauwerse H, et al. Mutations in ABCC6 cause pseudoxanthoma elasticum. *Nat Genet.* (2000) 25:228–31. doi: 10.1038/76109
42. Chassaing N, Martin L, Calvas P, Le Bert M, Hovnanian A. *Pseudoxanthoma elasticum*: a clinical, pathophysiological and genetic update including 11 novel ABCC6 mutations. *J Med Genet.* (2005) 42:881–92. doi: 10.1136/jmg.2004.030171
43. Navarro-Lopez F, Llorian A, Ferrer-Roca O, Betriu A, Sanz G. Restrictive cardiomyopathy in pseudoxanthoma elasticum. *Chest.* (1980) 78:113–5. doi: 10.1378/chest.78.1.113
44. Lipshultz SE, Adams MJ, Colan SD, Constine LS, Herman EH, Hsu DT, et al. Long-term cardiovascular toxicity in children, adolescents, and young adults who receive cancer therapy: pathophysiology, course, monitoring, management, prevention, and research directions: a scientific statement from the American Heart Association. *Circulation.* (2013) 128:1927–95. doi: 10.1161/CIR.0b013e3182a88099
45. Lipshultz SE, Diamond MB, Franco VI, Aggarwal S, Leger K, Santos MV, et al. Managing chemotherapy-related cardiotoxicity in survivors of childhood cancers. *Paediatr Drugs.* (2014) 16:373–89. doi: 10.1007/s40272-014-0085-1
46. Desai MY, Windecker S, Lancellotti P, Bax JJ, Griffin BP, Cahlon O, et al. Prevention, diagnosis, and management of radiation-associated cardiac disease: JACC scientific expert panel. *J Am Coll Cardiol.* (2019) 74:905–27. doi: 10.1016/j.jacc.2019.07.006
47. Weller RJ, Weintraub R, Addonizio LJ, Chrisant MR, Gersony WM, Hsu DT. Outcome of idiopathic restrictive cardiomyopathy in children. *Am J Cardiol.* (2002) 90:501–6. doi: 10.1016/S0002-9149(02)02522-5
48. Rivenes SM, Kearney DL, Smith EO, Towbin JA, Denfield SW. Sudden death and cardiovascular collapse in children with restrictive cardiomyopathy. *Circulation.* (2000) 102:876–82. doi: 10.1161/01.CIR.102.8.876
49. Walsh MA, Grenier MA, Jefferies JL, Towbin JA, Lorts A, Czosek RJ. Conduction abnormalities in pediatric patients with restrictive cardiomyopathy. *Circ Heart Fail.* (2012) 5:267–73. doi: 10.1161/CIRCHEARTFAILURE.111.964395
50. Denfield SW, Rosenthal G, Gajarski RJ, Bricker JT, Schowengerdt KO, Price JK, et al. Restrictive cardiomyopathies in childhood. Etiologies and natural history. *Tex Heart Inst J.* (1997) 24:38–44.
51. Hayashi T, Tsuda E, Kurosaki K, Ueda H, Yamada O, Echigo S. Electrocardiographic and clinical characteristics of idiopathic restrictive cardiomyopathy in children. *Circ J.* (2007) 71:1534–9. doi: 10.1253/circj.71.1534
52. Selvaganesh M, Arul AS, Balasubramanian S, Ganesan N, Naina Mohammed S, Sivakumar GS, et al. An unusual ECG pattern in restrictive cardiomyopathy. *Indian Heart J.* (2015) 67:362–7. doi: 10.1016/j.ihj.2015.05.012
53. Nagueh SF, Smiseth OA, Appleton CP, Byrd BF III, Dokainish H, Edvardsen T, et al. Recommendations for the evaluation of left ventricular diastolic function by echocardiography: an update from the American Society of Echocardiography and the European Association of Cardiovascular Imaging. *Eur Heart J Cardiovasc Imaging.* (2016) 17:1321–60. doi: 10.1093/ehjci/jew082
54. Alajaji W, Xu B, Sripariwuth A, Menon V, Kumar A, Schleicher M, et al. Noninvasive multimodality imaging for the diagnosis of constrictive pericarditis. *Circ Cardiovasc Imaging.* (2018) 11:e007878. doi: 10.1161/CIRCIMAGING.118.007878
55. Reuss CS, Wilansky SM, Lester SJ, Lusk JL, Grill DE, Oh JK, et al. Using mitral 'annulus reversus' to diagnose constrictive pericarditis. *Eur J Echocardiogr.* (2009) 10:372–5. doi: 10.1093/ejehoccardj/enj258

56. Kusunose K, Dahiya A, Popovic ZB, Motoki H, Alraies MC, Zurick AO, et al. Biventricular mechanics in constrictive pericarditis comparison with restrictive cardiomyopathy and impact of pericardiectomy. *Circ Cardiovasc Imaging*. (2013) 6:399–406. doi: 10.1161/CIRCIMAGING.112.000078
57. Tissot C, Singh Y, Sekarski N. Echocardiographic evaluation of ventricular function-for the neonatologist and pediatric intensivist. *Front Pediatrics*. (2018) 6:79. doi: 10.3389/fped.2018.00079
58. Ryan TD, Madueme PC, Jefferies JL, Michelfelder EC, Towbin JA, Woo JG, et al. Utility of echocardiography in the assessment of left ventricular diastolic function and restrictive physiology in children and young adults with restrictive cardiomyopathy: a comparative echocardiography-catheterization study. *Pediatr Cardiol*. (2017) 38:381–9. doi: 10.1007/s00246-016-1526-0
59. Dragulescu A, Mertens L, Friedberg MK. Interpretation of left ventricular diastolic dysfunction in children with cardiomyopathy by echocardiography: problems and limitations. *Circ Cardiovasc Imaging*. (2013) 6:254–61. doi: 10.1161/CIRCIMAGING.112.000175
60. Sasaki N, Garcia M, Ko HH, Sharma S, Parness IA, Srivastava S. Applicability of published guidelines for assessment of left ventricular diastolic function in adults to children with restrictive cardiomyopathy: an observational study. *Pediatr Cardiol*. (2015) 36:386–92. doi: 10.1007/s00246-014-1018-z
61. Quarta G, Sado DM, Moon JC. Cardiomyopathies: focus on cardiovascular magnetic resonance. *Br J Radiol*. (2011) 84:S296–305. doi: 10.1259/bjr/67212179
62. Anderson LJ, Holden S, Davis B, Prescott E, Charrier CC, Bunce NH, et al. Cardiovascular T2-star (T2*) magnetic resonance for the early diagnosis of myocardial iron overload. *Eur Heart J*. (2001) 22:2171–9. doi: 10.1053/ehj.2001.2822
63. Sado DM, White SK, Piechnik SK, Banyersad SM, Treibel T, Captur G, et al. Identification and assessment of Anderson-Fabry disease by cardiovascular magnetic resonance noncontrast myocardial T1 mapping. *Circ Cardiovasc Imaging*. (2013) 6:392–8. doi: 10.1161/CIRCIMAGING.112.000070
64. Habib G, Bucciarelli-Ducci CA, Caforio LP, Cardim N, Charron P, et al. Multimodality imaging in restrictive cardiomyopathies: an EACVI expert consensus document in collaboration with the “Working Group on myocardial and pericardial diseases” of the European Society of Cardiology Endorsed by The Indian Academy of Echocardiography. *Eur Heart J Cardiovasc Imaging*. (2017) 18:1090–121. doi: 10.1093/ehjci/jex034
65. Fratz S, Chung T, Greil GF, Samyn MM, Taylor AM, Valsangiacomo Buechel ER, et al. Guidelines and protocols for cardiovascular magnetic resonance in children and adults with congenital heart disease: SCMR expert consensus group on congenital heart disease. *J Cardiovasc Magn Reson*. (2013) 15:51. doi: 10.1186/1532-429X-15-51
66. Parakh N, Mehrotra S, Seth S, Ramakrishnan S, Kothari SS, Bhargava B, et al. NT pro B type natriuretic peptide levels in constrictive pericarditis and restrictive cardiomyopathy. *Indian Heart J*. (2015) 67:40–4. doi: 10.1016/j.ihj.2015.02.008
67. Kirk R, Dipchand AI, Rosenthal DN, Addonizio L, Burch M, Chrisant M, et al. The International Society for Heart and Lung Transplantation Guidelines for the management of pediatric heart failure: executive summary. *J Heart Lung Transplant*. (2014) 33:888–909. doi: 10.1016/j.healun.2014.06.002
68. Arslan S, Sevimli S, Gundogdu F. Fatal biatrial thrombus in a patient with idiopathic restrictive cardiomyopathy during sinus rhythm. *Int J Cardiol*. (2007) 117:e68–70. doi: 10.1016/j.ijcard.2006.11.141
69. Lewis AB. Clinical profile and outcome of restrictive cardiomyopathy in children. *Am Heart J*. (1992) 123:1589–93. doi: 10.1016/0002-8703(92)90814-C
70. Chen K, Williams S, Chan AK, Mondal TK. Thrombosis and embolism in pediatric cardiomyopathy. *Blood Coagul Fibrinolysis*. (2013) 24:221–30. doi: 10.1097/MBC.0b013e32835bfd85
71. Kozhevnikov D, Caref EB, El-Sherif N. Mechanisms of enhanced arrhythmogenicity of regional ischemia in the hypertrophied heart. *Heart Rhythm*. (2009) 6:522–7. doi: 10.1016/j.hrthm.2008.12.021
72. Petrich BG, Eloff BC, Lerner DL, Kovacs A, Saffitz JE, Rosenbaum DS, et al. Targeted activation of c-Jun N-terminal kinase in vivo induces restrictive cardiomyopathy and conduction defects. *J Biol Chem*. (2004) 279:15330–8. doi: 10.1074/jbc.M314142200
73. Gehmlich K, Lambiase PD, Asimaki A, Ciaccio EJ, Ehler E, Syrris P, et al. A novel desmocollin-2 mutation reveals insights into the molecular link between desmosomes and gap junctions. *Heart Rhythm*. (2011) 8:711–8. doi: 10.1016/j.hrthm.2011.01.010
74. Russo LM, Webber SA. Idiopathic restrictive cardiomyopathy in children. *Heart*. (2005) 91:1199–202. doi: 10.1136/hrt.2004.043869
75. Zangwill SD, Naftel D, L’Ecuyer T, Rosenthal D, Robinson B, Kirklin JK, et al. Outcomes of children with restrictive cardiomyopathy listed for heart transplant: a multi-institutional study. *J Heart Lung Transplant*. (2009) 28:1335–40. doi: 10.1016/j.healun.2009.06.028
76. Fenton MJ, Chubb H, McMahon AM, Rees P, Elliott MJ, Burch M. Heart and heart-lung transplantation for idiopathic restrictive cardiomyopathy in children. *Heart*. (2006) 92:85–9. doi: 10.1136/hrt.2004.049502
77. Singh TP, Almond CS, Piercey G, Gauvreau K. Current outcomes in US children with cardiomyopathy listed for heart transplantation. *Circ Heart Failure*. (2012) 5:594–601. doi: 10.1161/CIRCHEARTFAILURE.112.969980
78. Cassidy J, Dominguez T, Haynes S, Burch M, Kirk R, Hoskote A, et al. A longer waiting game: bridging children to heart transplant with the Berlin Heart EXCOR device—the United Kingdom experience. *J Heart Lung Transplant*. (2013) 32:1101–6. doi: 10.1016/j.healun.2013.08.003
79. Sundararajan S, Thiruchelvam T, Hsia TY, Karimova A. New 15-mL ventricular assist device in children with restrictive physiology of the left ventricle. *J Thorac Cardiovasc Surg*. (2014) 147:e79–80. doi: 10.1016/j.jtcvs.2014.02.083
80. Price JF, Jeewa A, Denfield SW. Clinical characteristics and treatment of cardiomyopathies in children. *Curr Cardiol Rev*. (2016) 12:85–98. doi: 10.2174/1573403X12666160301115543
81. Su JA, Menteeer J. Outcomes of Berlin Heart EXCOR((R)) pediatric ventricular assist device support in patients with restrictive and hypertrophic cardiomyopathy. *Pediatr Transplant*. (2017) 21:13048. doi: 10.1111/petr.13048
82. Mehra MR, Canter CE, Hannan MM, Semigran MJ, Uber PA, Baran DA, et al. The 2016 International Society for Heart Lung Transplantation listing criteria for heart transplantation: a 10-year update. *J Heart Lung Transplant*. (2016) 35:1–23. doi: 10.1016/j.healun.2015.10.023
83. Bograd AJ, Mital S, Schwarzenberger JC, Mosca RS, Quaegebeur JM, Addonizio LJ, et al. Twenty-year experience with heart transplantation for infants and children with restrictive cardiomyopathy: 1986–2006. *Am J Transplant*. (2008) 8:201–7. doi: 10.1111/j.1600-6143.2007.02027.x

Conflict of Interest: The authors declare that the research was conducted in the absence of any commercial or financial relationships that could be construed as a potential conflict of interest.

Publisher’s Note: All claims expressed in this article are solely those of the authors and do not necessarily represent those of their affiliated organizations, or those of the publisher, the editors and the reviewers. Any product that may be evaluated in this article, or claim that may be made by its manufacturer, is not guaranteed or endorsed by the publisher.

Copyright © 2022 Ditaranto, Caponetti, Ferrara, Parisi, Minnucci, Chiti, Baldassarre, Di Nicola, Bonetti, Hasan, Potenza, Galie, Ragni and Biagini. This is an open-access article distributed under the terms of the Creative Commons Attribution License (CC BY). The use, distribution or reproduction in other forums is permitted, provided the original author(s) and the copyright owner(s) are credited and that the original publication in this journal is cited, in accordance with accepted academic practice. No use, distribution or reproduction is permitted which does not comply with these terms.

openheart Clinical presentations leading to arrhythmogenic left ventricular cardiomyopathy

Maddalena Graziosi,¹ Raffaello Ditaranto ^{1,2} Claudio Rapezzi,^{3,4} Ferdinando Pasquale,¹ Luigi Lovato,⁵ Ornella Leone,⁶ Vanda Parisi,² Luciano Potena,¹ Valentina Ferrara,² Matteo Minnucci,² Angelo Giuseppe Caponetti,² Chiara Chiti,² Alessandra Ferlini,⁷ Francesca Gualandi,⁷ Cesare Rossi,⁸ Alessandra Bernardini,¹ Giacomo Tini ⁹, Matteo Bertini ³, Matteo Ziacchi,¹ Mauro Biffi ¹, Nazzareno Galie,^{1,2} Iacopo Olivetto,¹⁰ Elena Biagini ¹

► Additional supplemental material is published online only. To view, please visit the journal online (<http://dx.doi.org/10.1136/openhrt-2021-001914>).

To cite: Graziosi M, Ditaranto R, Rapezzi C, *et al.* Clinical presentations leading to arrhythmogenic left ventricular cardiomyopathy. *Open Heart* 2022;**9**:e001914. doi:10.1136/openhrt-2021-001914

MG and RD contributed equally.

Received 10 November 2021
Accepted 8 February 2022



© Author(s) (or their employer(s)) 2022. Re-use permitted under CC BY-NC. No commercial re-use. See rights and permissions. Published by BMJ.

For numbered affiliations see end of article.

Correspondence to
Dr Elena Biagini; elena.biagini73@gmail.com

ABSTRACT

Objectives To describe a cohort of patients with arrhythmogenic left ventricular cardiomyopathy (ALVC), focusing on the spectrum of the clinical presentations.

Methods Patients were retrospectively evaluated between January 2012 and June 2020. Diagnosis was based on (1) ≥ 3 contiguous segments with subepicardial/midwall late gadolinium enhancement in the left ventricle (LV) at cardiac magnetic resonance *plus* a likely pathogenic/pathogenic arrhythmogenic cardiomyopathy (AC) associated genetic mutation *and/or* familial history of AC *and/or* red flags for ALVC (ie, negative T waves in V4–6/aVL, low voltages in limb leads, right bundle branch block like ventricular tachycardia) or (2) pathology examination of explanted hearts or autopsic cases suffering sudden cardiac death (SCD). Significant right ventricular involvement was an exclusion criterion.

Results Fifty-two patients (63% males, age 45 years (31–53)) composed the study cohort. Twenty-one (41%) had normal echocardiogram, 13 (25%) a hypokinetic non-dilated cardiomyopathy (HNDC) and 17 (33%) a dilated cardiomyopathy (DCM). Of 47 tested patients, 29 (62%) were carriers of a pathogenic/likely pathogenic DNA variant. Clinical contexts leading to diagnosis were SCD in 3 (6%), ventricular arrhythmias in 15 (29%), chest pain in 8 (15%), heart failure in 6 (12%) and familial screening in 20 (38%). Thirty patients (57%) had previously received a diagnosis other than ALVC with a diagnostic delay of 6 years (IQR 1–7).

Conclusions ALVC is hidden in different clinical scenarios with a phenotypic spectrum ranging from normal LV to HNDC and DCM. Ventricular arrhythmias, chest pain, heart failure and SCD are the main clinical presentations, being familial screening essential for the affected relatives' identification.

INTRODUCTION

The recent and rapid expansion of molecular biology and cardiac magnetic resonance (CMR) in the field of cardiomyopathies (CMP) has brought new clinical entities to

Key questions

What is already known about this subject?

► Arrhythmogenic left ventricular cardiomyopathy (ALVC) diagnosis is mainly based on the identification of fibro-fatty left ventricle (LV) replacement at histological analysis or demonstration of typical late gadolinium enhancement pattern with ring-like distribution at cardiac magnetic resonance (CMR) associated with positive genetic test or family history of arrhythmogenic right/left ventricular cardiomyopathy.

What does this study add?

► ALVC is hidden under different clinical scenarios and degree of functional LV impairment.
► Five main clinical contexts may be identified with this study: ventricular arrhythmias, chest pain, heart failure, familial screening and sudden cardiac death (SCD) as presenting event. Shared characteristics between these scenarios are represented by family history of cardiomyopathy/SCD, previous diagnosis of myocarditis, (infero)lateral negative T waves and low QRS voltages at ECG.

How might this impact on clinical practice?

► We describe five diagnostic scenarios of ALVC, underlying common features that may rise clinical suspicion and guide the clinicians to request CMR and depict the typical structural involvement when clinical suspicion is high.

the fore, whose definition goes beyond the 'classical' phenotype recognition. A paradigmatic situation is represented by arrhythmogenic cardiomyopathy (AC), an inherited CMP characterised by fibro-fatty infiltration, life threatening ventricular arrhythmias and sudden cardiac death (SCD). Although originally depicted as exclusive of the right ventricle—the classic arrhythmogenic right

ventricle cardiomyopathy (ARVC)—in the last few years it has become clear that AC can affect either ventricles or predominantly the left ventricle (LV).¹ Key features of arrhythmogenic left ventricular cardiomyopathy (ALVC) are a circumferential fibrous/fibro-fatty band between the middle and subepicardial third of the myocardium, corresponding to a ring-like late gadolinium enhancement (LGE) distribution at CMR, often associated with low QRS voltages and negative T waves in the inferior and/or lateral leads at ECG.² Awareness for this disease is still poor, and diagnosis is often delayed or missed altogether, since this clinical entity can be concealed in different clinical settings both in terms of clinical onset and imaging phenotype. Yet, the highly malignant arrhythmogenic presentation, with ventricular arrhythmias and sudden death occurring irrespective of the degree of LV systolic dysfunction, makes prompt diagnosis essential. Therefore, the aim of this study was to describe the clinical, instrumental and genetic profile of a multicentre ALVC cohort, focusing on the spectrum of clinical presentations.

METHODS

This is a retrospective observational study evaluating 62 consecutive patients with suspected ALVC between January 2012 and June 2020 at three Italian Centres (Cardiology Unit, St. Orsola Hospital, IRCCS Azienda Ospedaliero-Universitaria of Bologna (N=48); Azienda Ospedaliera Careggi, Florence (N=11) and Cardiovascular Center, University Hospital of Cona, Ferrara (=3)).

ALVC diagnosis was based on the following criteria: (1) a ring-like LGE LV pattern at CMR defined as ≥ 3 contiguous segments with subepicardial/midwall LGE in the

same slice (isolated septal junctional LGE was not considered significant) with or without fatty infiltration *plus* a likely pathogenic/pathogenic AC associated genetic mutation *and/or* familial history of AC *and/or* red flags for ALVC (ie, negative T waves in V4-6/aVL, low voltages in limb leads, right bundle branch block-like ventricular tachycardia)¹; (2) LV myocyte degeneration with fat and fibrosis in the same microscopic field, from subepicardial layer inward or within the mid-wall ($>20\%$ in at least two tissue blocks of 4 cm²; H&E stain) defined on microscopic analysis in explanted heart or autopsy examinations.^{2,3} Relatives with LV LGE were included (even if <3 consecutive segments). Significant right ventricle involvement, defined as the presence of systolic dysfunction (fractional area change (FAC) $<30\%$ at echocardiogram or EF $<40\%$ at CMR) or the presence of wall motion abnormalities (a/dyskinesia, bulging), was considered an exclusion criterion. Phenocopies (eight myocarditis and two sarcoidosis) were excluded based on a comprehensive clinical and multi-modality instrumental evaluation including myocardial biopsy and positron emission tomography (PET) when indicated (figure 1). Ischaemic heart disease was ruled out based on low pretest probability (young age, angina free, no cardiovascular risk factors) and where clinically indicated, by coronary anatomy evaluation (angiography n=29; CT scan n=2) or vasodilator stress CMR (n=2). A regional autopsy programme, integrated with molecular analysis, in patients with SCD younger than 55 years is active at St. Orsola University Hospital (Bologna) since 2018.

Definition of clinical scenarios

Based on the clinical setting in which diagnosis was performed, patients were divided into five groups:

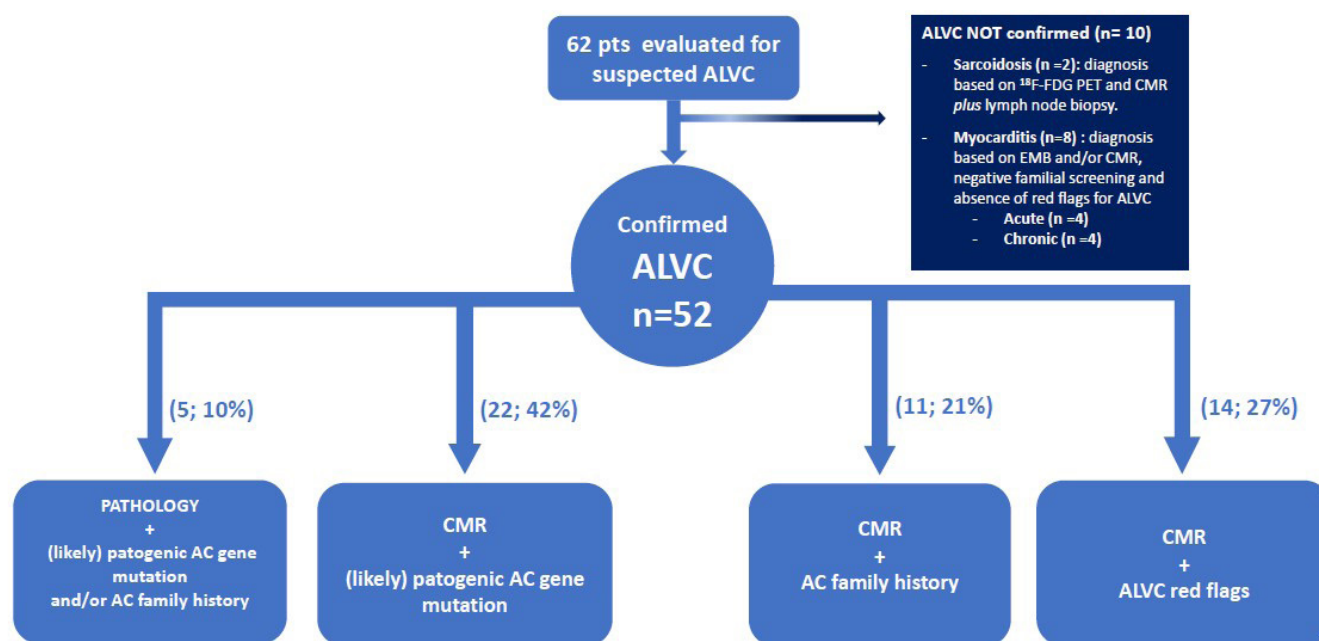


Figure 1 Flow chart summarising the enrolment of the study population according to the met inclusion criteria. AC, arrhythmogenic cardiomyopathy; ALVC, arrhythmogenic left ventricular cardiomyopathy; CMR, cardiac magnetic resonance.

- ▶ SCD: a non-traumatic, unexpected fatal event occurring within 1 hour of the onset of symptoms in an apparently healthy subject (or when the victim was in good health 24 hours before the event, if death was not witnessed).⁴
- ▶ Ventricular arrhythmias: 'high arrhythmic burden' defined as frequent ventricular ectopic beats (>500/24 hours)/non-sustained ventricular tachycardia (NSVT) associated with palpitations, SVT requiring emergency department admission and aborted cardiac arrest due to ventricular fibrillation.
- ▶ Chest pain: patients requiring hospital admission or outpatient evaluation because of acute or chronic chest pain, respectively.
- ▶ Heart failure: signs and symptoms of heart failure with evidence of reduced LV ejection fraction (LVEF).⁵
- ▶ Familial screening: cases identified due to the family history of dilated cardiomyopathy (DCM, ALVC, ARVC or SCD).

Echocardiographic phenotypes were distinguished as normal (in terms of LV dimension and systolic function), hypokinetic non-dilated cardiomyopathy (HNDC) (LVEF <50% without LV dilatation⁶) and DCM (LV dilation and systolic dysfunction in the absence of abnormal loading conditions such as hypertension or valve disease, or coronary artery disease causing global systolic impairment).

CMR was carried out on 1.5 Tesla equipment at each centre using standardised protocols. The presence and location of LGE were assessed: positivity was considered when visible in two phase-encoding directions and two orthogonal planes. Intramyocardial fat replacement was reported by comparing T1-weighted and fat suppressed T1-weighted sequences.

Genetic test was performed by different sequencing technologies, using gene panels reflecting the standard practice at the time of testing in each centre. Identified variants were defined according to recommended guidance for classification.⁷ All patients gave written informed consent for DNA analysis.

Continuous data distribution was assessed with the Shapiro-Wilk test and expressed as median and IQR.

RESULTS

General patient features

Fifty-two patients from 37 families (63% males, median age 45 years (IQR 31–53)) formed the final study cohort (table 1). Echocardiographic patterns were distributed as follows: normal (n=21; 41%), HNDC (n=13; 25%), DCM (n=17; 33%). Diagnosis was based on CMR plus additional criteria in 47 patients (90%). LGE involved most frequently the septum (30; 64%), the inferior (31; 66%) and the infero-lateral (30; 64%) walls, whereas a circumferential distribution was present in 14 patients (30%). Intramyocardial fat infiltration was present in 23 patients (49%) always near to the LGE areas.

Diagnosis was based on whole heart examination in five patients: three patients suffering SCD and two heart

transplant patients affected by end stage heart failure. Pathology revealed LV fibro-fatty replacement predominantly in the postero-lateral wall in the three cases of SCD, while RV was only mildly involved. Regarding the two explanted hearts, a diffuse LV fibro-fatty replacement involving the septum, anterior, postero-lateral wall and the right ventricle was present in first one whereas a fibro-fatty replacement of the LV anterior wall with septal and RV outflow tract extensive fibrosis was detected in the second one. In both of them, RV was not significantly involved in the first clinical evaluation.

Applying the 2010 Task Force Criteria in the group of 47 patients clinically diagnosed (ie, excluding the 5 patients with pathological diagnosis), 11 (23%) had a definite diagnosis, while 3 (6%) had a borderline diagnosis and 20 (42%) a possible diagnosis. One minor criterion was present in 13/47 (28%) patients.

Notably, 29 of the 52 patients (56%) had previously received a diagnosis other than ALVC: 12 idiopathic DCM, 5 post-myocarditis DCM, 7 acute myocarditis, 3 idiopathic sustained ventricular tachyarrhythmias, 1 frequent ventricular ectopic beats and 1 non-ST-elevated myocardial infarction. In particular, in 15 patients ALVC was diagnosed following the introduction of MRI in the diagnostic work-up of patients with DCM and in two cases by pathology examination after heart transplantation. The diagnostic delay was 6 years (IQR 1–7) with a maximum of 21 years.

Genetic testing

Forty-seven (90%) patients underwent genetic test (table 2). All were screened for the exons and flanking intronic sequences of the following desmosomal genes: desmoplakin (*DSP*), plakophilin-2 (*PKP2*), desmoglein-2 (*DSG2*), desmocollin-2 (*DSC2*) and plakoglobin (*JUP*). Of them, 43 (91%) were screened for phospholamban (*PLN*), *TMEM43*, desmin (*DES*), lamin A/C (*LMNA*) and *SCN5A as well*, while 11 patients (23%) for filamin C (*FLNC*). Two patients with negative next-generation sequencing (NGS) panel were tested for multiplex ligation probe amplification and no copy number variation was detected. Pathogenic/likely pathogenic mutations were identified in 29 (62%) patients and *DSP* accounted for the most frequently involved gene (n=23; 49%). It should be noted that a relevant subgroup of patients had a double sequence variant, with VUS/likely benign variation in addition to a pathogenic/likely pathogenic mutation, raising the hypothesis of a digenic contribution or a modifier role (online supplemental table 1).

Clinical presentations

Clinical presentations leading to ALVC diagnosis were: SCD in 3 (6%) patients, ventricular arrhythmias in 15 (29%), chest pain in 8 (15%), heart failure in 6 (12%). Moreover, ALVC was identified through familial screening in 20 (38%). Clinical and instrumental characteristics of the patients according to the clinical context are reported in table 1 and figures 2 and 3.

Table 1 Clinical and instrumental characteristics of patients with ALVC according to the clinical scenario

	Overall	SCD	Ventricular Arrhythmias	Chest Pain	Heart failure	Familial Screening
	52	3 (6)	15 (29)	8 (15)	6 (12)	20 (38)
Age at diagnosis (years)	45 (31–53)	23 (19–36)	50 (40–57)	45 (27–57)	47 (46–59)	36 (30–50)
Males	33 (63)	3 (100)	11 (73)	4 (50%)	5 (83)	10 (50)
Probands	36 (69)	3 (100)	14 (93)	8 (100)	5 (83)	6 (30)
Family history of sudden death	30 (58)	0	10 (67)	4 (50)	3 (50)	13 (65)
≤40 years	17 (33)	0	3 (20)	0	3 (50)	11 (55)
>40 years	13 (25)	0	7 (47)	4 (50)	0	2 (10)
Family history of ALVC/ARVC	19 (4)	0	2 (13)	1 (12)	2 (33)	14 (70)
Family history of DCM	2 (4)	0	1 (6)	0	0	1 (5)
Any previous myocarditis diagnosis	16 (31)	1 (17)	3 (21)	6 (75)	4 (67)	2 (10)
Previous myocarditis	9 (17)	1 (17)	2 (14)	4 (50)	1 (17)	1 (5)
Instrumental diagnosis of previous myocarditis	7 (13)	–	1 (7)	2 (25)	3 (50)	1 (5)
NYHA III/IV	2 (4)	0	0	0	1 (17)	1 (5)
Echocardiogram	51/52	2 (66)	15 (100)	8 (100)	6 (100)	20 (100)
Phenotype						
Normal	21 (41)	2 (100)	3 (20)	4 (50)	0 (0)	12 (60)
HNDC	13 (25)	0	4 (26)	3 (37)	2 (33)	4 (20)
DCM	17 (33)	0	8 (54)	1 (12)	4 (67)	4 (20)
LVEF (%)	50 (45–57)	57	49 (43–50)	50 (46–62)	33 (31–47)	53 (49–60)
LVEF ≤35%	2 (4)	0	0	0	2 (33)	0
LVEDV (mL/m ²)	63 (55–76)	62	75 (61–80)	59 (54–76)	81 (70–117)	57 (52–60)
Severe LV dilation	4 (8)	0	1 (6)	0	2 (33)	1 (5)
High arrhythmic burden	30 (57)	0	12 (80)	2 (24)	4 (67)	12 (60)
VEB >500	11 (21)	0	4 (25)	1 (12)	1 (17)	5 (25)
NSVT	19 (36)	0	8 (50)	1 (12)	3 (50)	7 (35)
Cardiac magnetic resonance	47	–	15	8	4	20
LVEF (%)	50 (43–56)		48 (41–52)	49 (40–57)	39 (36–43)	53 (51–59)
LVEDV (mL/m ²)	101 (88–110)		103 (88–119)	106 (98–112)	102 (98–107)	95 (84–109)
RVEF (%)	57 (53–61)		56 (53–60)	58 (56–60)	45 (40–52)	59 (54–61)
RVEDV (mL/m ²)	83 (68–90)		73 (66–82)	84 (76–90)	89 (72–105)	85 (78–91)
LV fat infiltration	23 (49)		12 (80)	3 (37)	1 (25)	7
RV fat infiltration	0		0	0	0	0
LGE distribution						
Septum	30 (64)		9 (60)	6 (75)	2 (50)	13 (65)
Inferior	31 (66)		7 (47)	7 (87)	1 (25)	16 (80)
Infero-lateral	30 (64)		9 (60)	7 (87)	2 (50)	12 (60)
Lateral	26 (55)		6 (43)	7 (87)	4 (100)	9 (45)
Antero-lateral	17 (37)		2 (13)	6 (75)	2 (50)	7 (35)
Anterior	21 (45)		5 (33)	5 (62)	2 (50)	9 (45)
ECG available	50/52	1 (33)	15 (100)	8 (100)	6 (100)	20 (100)
Normal	4 (8)	0	1 (7)	1 (17)	0	2 (10)
T wave inversion						
Isolated in V1–V3	3 (6)	0	0	0	0	3 (15)
Isolated in V4–V6 or/and D1–aVL	12 (23)	0	2 (13)	2 (25)	3 (50)	5 (25)
Isolated in inferior leads	2 (4)	0	0	0	0	2 (10)
Infero-lateral	6 (12)	0	2 (13)	1 (12)	2 (33)	1 (5)

Continued

Table 1 Continued

	Overall	SCD	Ventricular Arrhythmias	Chest Pain	Heart failure	Familial Screening
	52	3 (6)	15 (29)	8 (15)	6 (12)	20 (38)
Diffuse	1 (2)	0	0	0	1 (17)	0
Low QRS peripheric voltages	23 (47)	1 (100)	10 (67)	3 (37)	2 (33)	7 (35)
Q waves	13 (52)	0	6 (40)	2 (25)	2 (33)	3 (15)
LAFB	4 (8)	0	0	1 (12)	3 (50)	0
LPFB	1 (2)	0	1 (7)	0	0	0
LBBB	0	0	0	0	0	0
RBBB	3 (6)	0	2 (13)	0	0	1 (5)
QRS duration (ms)	100 (90–110)	95	100 (90–114)	110 (100–120)	110 (100–120)	97.5 (88–102)
QRS _≥ 120 ms	6 (12)	0	3 (20)	2 (25)	2 (33)	0
LVH	2 (4)	0	1 (7)	1 (12)	0	0
ICD implantation	29 (56)	–	9 (60)	3 (37)	4 (66)	13 (65)
Primary prevention	20 (38)	–	2 (13)	3 (37)	4 (66)	11 (55)
Secondary prevention	9 (27)	–	7 (47)	0	0	2 (10)

Values are expressed as n, n (%) or median (IQR).

Severe LV dilatation: >100 mL/m² for male and >80 mL/m² for female (*J Am Soc Echocardiogr* 2015;28:1–39).

ALVC, arrhythmogenic left ventricle cardiomyopathy; ARVC, arrhythmogenic right ventricle cardiomyopathy; DCM, dilated cardiomyopathy; HNDC, hypokinetic non-dilated cardiomyopathy; ICD, implantable cardioverter defibrillator; LAFB, left anterior fascicular block; LBBB, left bundle branch block; LVEDV, left ventricle end-diastolic volume; LVEF, left ventricle ejection fraction; LVH, left ventricular hypertrophy (one of Sokolow-Lyon, Cornell, Romhilt-Estes, R wave in aVL); NSVT, non-sustained ventricular tachyarrhythmia; NYHA, New York Heart Association; RBBB, right bundle branch block; SCD, sudden cardiac death; TWI, T wave inversion; VEB, ventricular ectopic beats.

Sudden cardiac death

Of 50 cases of SCD referred to St. Orsola University Hospital of Bologna from 2018 to 2020, 3 (6%) received a diagnosis of ALVC. They were all males and had no family history of SCD or CMP.

The first was a 49-year-old man who died during physical exertion. Normal ECG and echocardiogram were recorded the year before. A likely pathogenic mutation in *DSP* (c.3533 T>G) and a VUS in *TMEM43* (c.1150 C>G)

were identified by molecular analysis. Familial screening led to ALVC diagnosis in his 19-year-old child with mid-wall LGE in the infero-lateral wall at CMR despite a normal ECG and echocardiogram; the same *DSP* gene mutation was identified. The second patient died at the age of 30 years during recreational sport activity. He previously received a diagnosis of myocarditis (chest pain and elevated plasmatic troponins) at the age of 26 years. Low QRS voltages were present on ECG whereas LV

Table 2 Genetic findings in tested patients (n=47)

	Pathogenic	Likely pathogenic	VUS	Likely benign/benign
	24 (52%)	5 (10%)	8 (17%)	3 (6%)
Single desmosome mutation				
DSP	18	1	1	–
DSG2	–	–	2	–
Single non-desmosome mutation				
FLNC	3	–	–	–
RYR2	–	–	1	–
DES	–	1	–	–
Double mutation				
DSP+FLNC	2 (DSP)	–	2 (FLNC)	–
DSP+TMEM43	–	1 (DSP)	1 (TMEM43)	–
PKP2+TMEM43	1 (PKP2)	–	–	1 (TMEM43)
SCN5A+ANK2	–	2 (SCN5A)	–	2 (ANK2)

ANK2, ankirin2; DES, desmin; DSG2, desmoglein 2; DSP, desmoplakin; FLNC, filamin C; PKP2, plakophilin; RYR2, ryanodine receptor 2; SCN5A, sodium voltage-gated channel alpha subunit 5; TMEM43, transmembrane protein 43; VUS, variant of unknown significance.

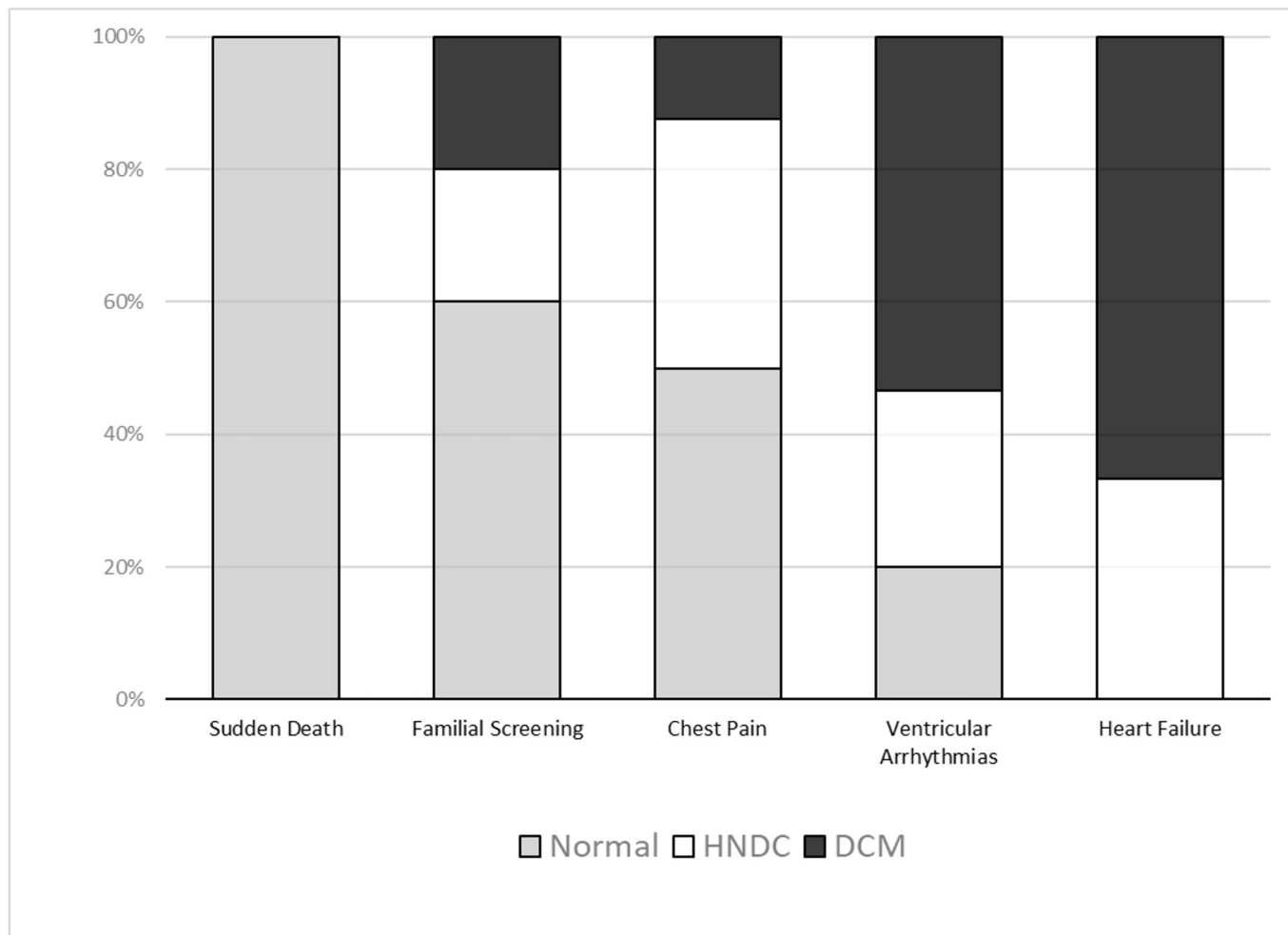


Figure 2 Echocardiographic phenotype according to the clinical scenario. Distribution of normal (grey), hypokinetic non-dilated cardiomyopathy (HNDC, white) and dilated cardiomyopathy phenotypes (DCM, black) among the different diagnostic pathways are shown by stacked bar chart.

volumes and EF were normal at echocardiogram, with no segmental wall motion abnormalities. Familial screening performed after death revealed a DCM in his sister and an HNDC in his mother with a likely pathogenic mutation in *SCN5A* (c.2244G>A) and a VUS in *ANK* (c.10054G>C) in both family members. The last patient was a 15-year-old boy who had SCD at rest. A pathogenic *FLNC* variant (c.8034delC) determining a truncated protein was found by molecular autopsy. Family screening revealed the same *FLNC* variant in his father who presented an HNDC with LVEF 45% and a subepicardial circumferential LGE at CMR.

Ventricular arrhythmias

This was the most common clinical presentation, being present in a third of the study population (n=15, 29%). Aborted cardiac arrest was documented in 2 (4%) patients, SVT in 7 (13%) and high arrhythmic burden in 6 (11%). Family history of SCD was present in 10 patients (67%). Eight patients (54%) had DCM, four (26%) HNDC and three (20%) normal LV volumes and EF. Most (80%) were in New York Heart Association (NYHA) functional class I. A normal ECG was rare (7%) whereas

most tracings were characterised by low QRS voltages in limb leads (67%). Three patients (21%) had a previous clinical or instrumental diagnosis of myocarditis. Of 13 patients tested, 3 had a truncating *DSP* mutation (in 1 case associated with a VUS on *FLNC*), 1 had a truncating *FLNC* mutation, 1 *DSG2*, 1 *RYR2*.

Chest pain

Eight (15%) patients were included in this group characterised by two main clinical scenarios: acute and chronic chest pain. The first setting involved six patients (median age 36 years (27–44); 50% males) accessing the emergency department for acute chest pain with elevated troponins consistent with acute myocardial injury but no coronary arteries obstruction on angiography. The initial diagnosis was acute myocarditis in five and myocardial infarction with non-obstructed coronary arteries (MINOCA) in one. Three of them had been previously hospitalised for similar episodes interpreted as myocarditis (N=2) or MINOCA (N=1). The final diagnosis of ALVC was supported by typical CMR findings and six were successfully genotyped (4 *DSP*). Main clinical and instrumental characteristics in this subgroup were a family

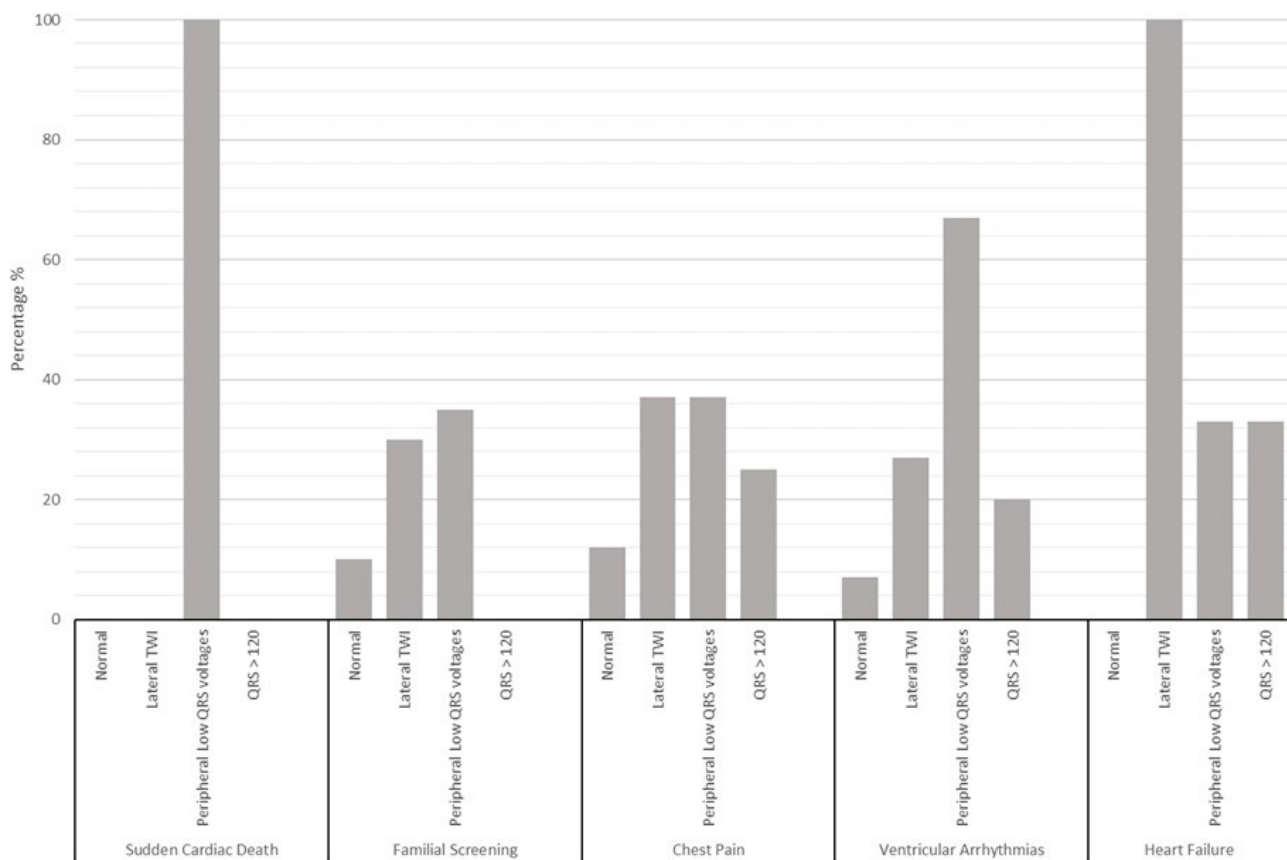


Figure 3 ECG findings according to the clinical scenario. The prevalence of the main ECG characteristics for each clinical scenario shown by histograms. Lateral T wave inversion (TWI) includes: isolated lateral, infero-lateral and diffuse TWI.

history of sudden death (50%), prior acute myocarditis (50%), (infero)lateral T wave inversion (TWI) (33%) and low QRS voltages in limb leads (37%).

In the second setting two outpatients with chronic chest pain atypical for angina, mild LV dysfunction and abnormal ECG at rest were included (a 60-year-old man and a 57-year-old woman). ALVC diagnosis originated from a stress perfusion CMR, performed to exclude an ischaemic aetiology, which unexpectedly showed non-ischaemic ring-like subepicardial fibrosis plus fatty infiltration in the septum and lateral wall.

Heart failure

Six patients (12%) were referred due to exertional dyspnoea (NYHA class II or III) and impaired LVEF. None experienced acute heart failure. The echocardiographic phenotype was characterised by DCM in four patients (67%) and HNDC in two (33%), with a median LVEF of 33% (IQR 31–47) and a median indexed end-diastolic volume of 81 mL/m² (IQR 70–117 mL/m²). The ECG showed prolonged QRS (ie, ≥ 120 ms) in 2 patients (33%), TWI in the (infero)lateral leads in 6 (100%) and low peripheral QRS voltages in 2 (33%). No patient had either left bundle branch block or LV hypertrophy. Three patients had truncating *DSP* mutations and three had a negative genetic test.

Familial screening

Twenty patients (38%) were identified by screening performed due to family history of ALVC (n=10), ARVC (n=2), DCM (n=2) or SCD (n=6). A family history of SCD was frequent (65%) and patients were mainly asymptomatic (90%). Two patients (10%) had normal ECG whereas six (30%) had (infero)lateral TWI and seven (35%) low QRS voltages in limb leads. The echocardiogram was normal in 12 (60%) whereas DCM and HNDC phenotypes were evenly distributed. Frequent ventricular ectopic beats and/or NSVT were recorded in 12 patients (60%) by ECG Holter monitoring. *DSP* variants were reported in 11 patients (55%), alone or with mutations in other genes. It is worth noting that the relatives identified by familial screening had clinical features that might have led to ALVC diagnosis through a different way, as shown in figures 4 and 5.

DISCUSSION

ALVC diagnosis is challenging since this clinical entity is hidden in different clinical contexts and is characterised by a wide phenotypic spectrum ranging from normal LV, to HNDC and classic DCM. In fact, differently from the traditional CMPs phenotypes, ALVC diagnosis mainly relies on typical tissue characterisation and distribution

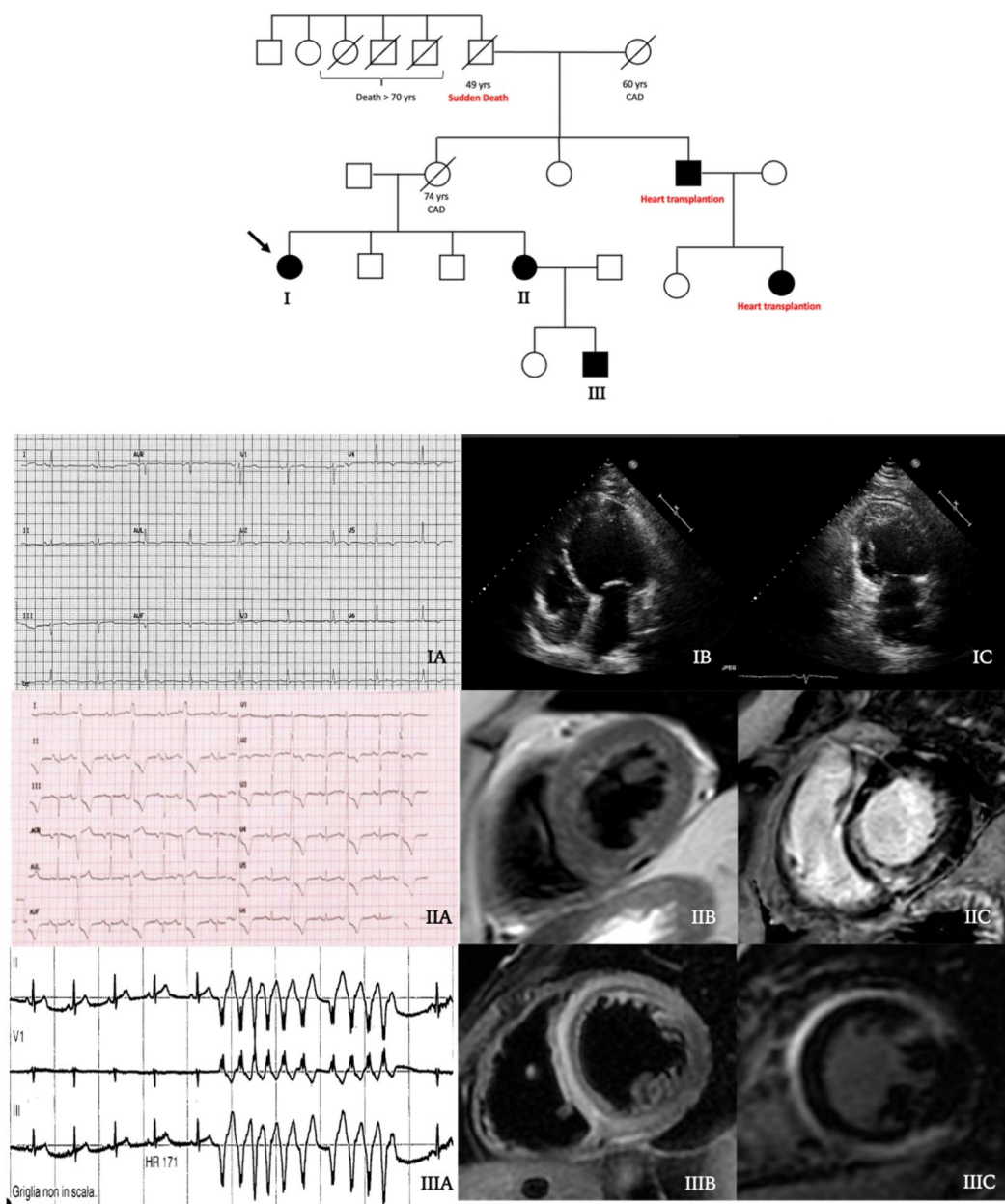


Figure 4 Central illustration: family tree. Black filled symbols stand for affected carriers. The 54-year-old woman proband (patient I, arrow) showed T wave inversion in inferolateral leads at ECG (IA) and a dilated cardiomyopathy at echocardiogram (IB–IC). Her 61-year-old sister (patient II) had a high premature ventricular ectopic beats burden (IB), a hypokinetic non-dilated cardiomyopathy (HNDC) phenotype and an initial subepicardial fatty replacement (IIB) with a semi-circumferential mid-wall distribution of late gadolinium enhancement (LGE) (IIC) at cardiac magnetic resonance (CMR). Patient III had a history of hospital admission at the age of 21 years for chest pain and suspected myocarditis with an HNDC phenotype. During the hospitalisation, non-sustained ventricular tachycardia occurred (IIIA) and CMR showed an extensive intramyocardial oedema at T2-weighted sequences (IIIB) with a mutual mid-wall distribution of LGE (IIIC).

of fibro-fatty replacement, regardless of the degree of LV functional impairment or dilatation. In the present study, we describe five clinical scenarios leading to ALVC diagnosis with the aim to underline common features and discrepancies that may prompt clinical suspicion.

Sudden cardiac death

SCD is not uncommon in AC, especially among male young individuals and athletes, and can be the first disease presentation. We reported three young males

experiencing SCD, two of them during moderate effort. In a large cohort of 5205 SCD cases, Miles *et al*³ collected 202 cases (4%) of AC including 35 (17%) ALVC, whose death occurred during effort or at rest/sleep in equal proportion and generally without preceding symptoms or relevant family history. At initial inspection 20% of the AC cases were macroscopically normal regardless of LV involvement suggesting a concealed phase of the disease. This is in line with the hypothesis that in ALVC,

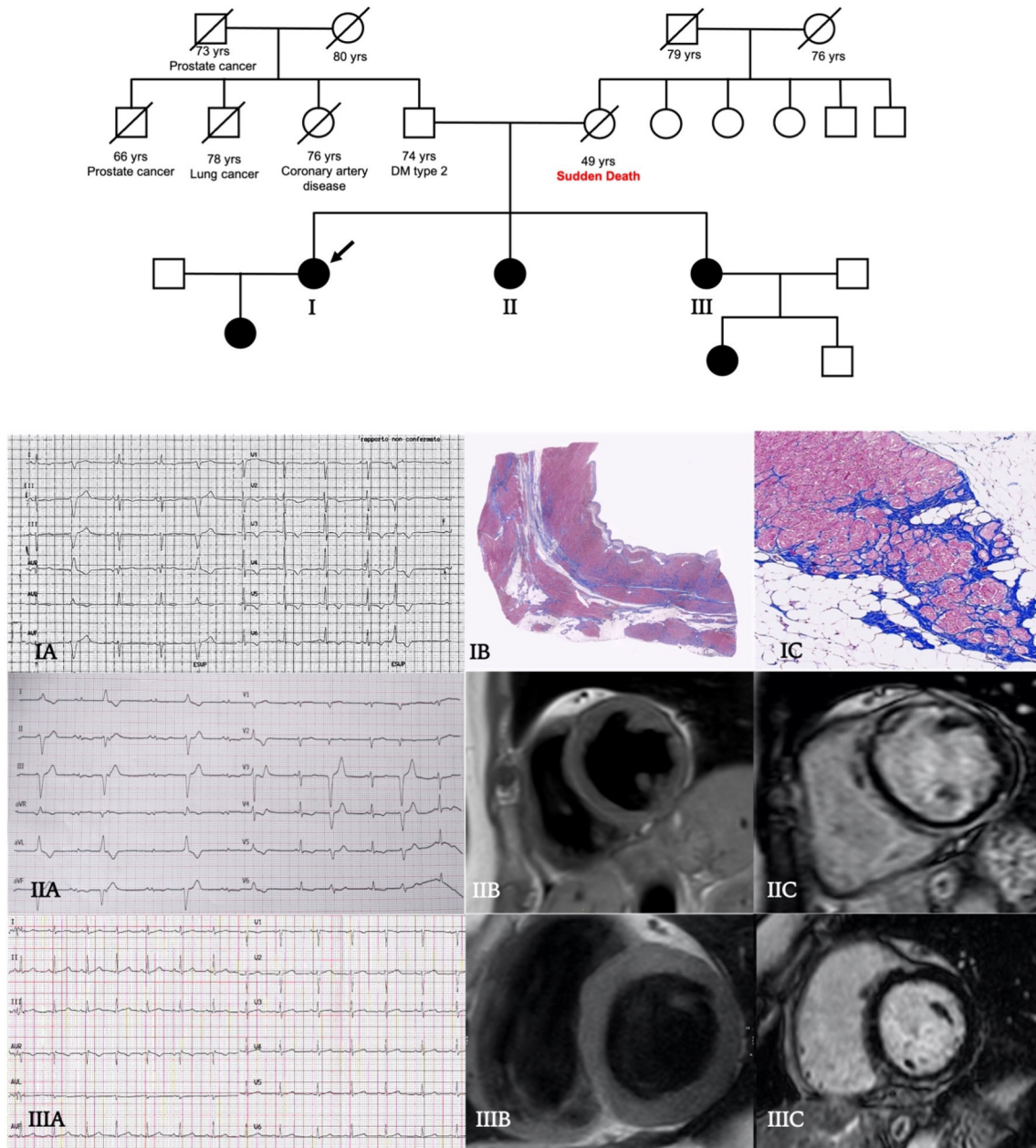


Figure 5 Central illustration: family tree. Affected male (squares) and female subjects (circles) are shown as solid black. The 49-year-old woman proband (patient I, arrow), affected by dilated cardiomyopathy with diffuse T wave inversion at ECG (IA), underwent heart transplantation due to severe heart failure. The histopathological examination of the explanted heart showed extensive mid-wall fibrosis with fibrofatty replacement on the right ventricular side of the septum (IB), hypertrophy and sarcoplasmic vacuolation of cardiomyocytes (IC). Her 47-year-old sister (patient II) showed normal echocardiographic phenotype, frequent premature ventricular beats at ECG, infero-lateral T wave inversion and peripheral low voltages (IIA); at cardiac magnetic resonance (CMR) T1-weighted sequences detected a linear fatty infiltration of mid-wall interventricular septum (IIB) and a diffuse mid-wall/subendocardial and circumferential late gadolinium enhancement (LGE) on anterior, septal and inferior walls of left ventricle (IIC). Patient III was asymptomatic, ECG and echocardiogram were normal (IIIA), but CMR revealed a small area of subepicardial fat on infero-basal septum (IIIB) and a focal mid-wall/subendocardial distribution of LGE on inferior wall (IIIC).

differently from ARVC and biventricular AC, the risk of major cardiac events could be relevant even in absence of evident functional impairment.⁸ Additionally, this finding emphasises the importance of dedicated regional or national cardiac pathology programmes for young SCD victims. When appropriate pathological expertise is lacking, autopsies are often not performed or reach

a non-specific diagnosis of ‘myocarditis’ which does not trigger family screening and hence fails to identify other affected members.

Ventricular arrhythmias

In our population, the most frequent clinical presentation was characterised by symptoms associated with

ventricular arrhythmias. Half of the patients had a DCM whereas normal echocardiogram and HNDC were equally distributed in the other half. On the ECG, low QRS voltages in limb leads were highly prevalent (67%). *DSP* was the most frequent gene involved. In line with our findings, in a cohort of *DSP*-related CMP, ventricular arrhythmias occurred with an LVEF between 35% and 55%, occasionally >55%, confirming that the established LVEF threshold <35% for ICD implantation is a poor event predictor in this setting.⁹ The not negligible risk, even with preserved EF, may be the result of early gap junction remodelling, recurrent inflammatory episodes or extensive LV fibro-fatty replacement that can precede or be discrepant with respect to the degree of LV dysfunction.

Chest pain

Chest pain, mainly with acute onset and troponin release without coronary obstruction on angiography, was the second most frequent clinical presentation. Accordingly, Sen-Chowdhry *et al*⁷ reported that almost one-third of 42 patients with ALVC had recurrent chest pain and a previous diagnosis of presumed viral myocarditis characterised by acute chest pain and angiographically normal coronary arteries. Similarly, in 107 patients with pathogenic *DSP* mutations Smith *et al*⁸ reported chest pain with troponin elevation and normal coronary angiography in 15%, associated with a non-ischaemic LGE mainly in the LV subepicardium. Therefore, when presenting with acute chest pain, ALVC may be misdiagnosed with a first step label of myocarditis or MINOCA. Clinicians should keep in mind AC as possible genetic cause when facing these diagnostic ‘boxes’. In this perspective, both CMR and family history play an important role. Piriou *et al*¹⁰ suggested that the presence of a family history of CMP or SCD, in case of acute myocarditis, should always prompt genetic testing to search for desmosomal mutations.

Heart failure

Patients in this subset were typically middle-aged males, coming to medical attention due to HF symptoms and a moderate–severe reduction of LVEF but mildly dilated LV. Awareness of desmosome gene-related aetiologies among the broad DCM spectrum has gained momentum in the last decade, beyond mere nosography, because of the implications for SCD prevention.^{11–13} Augusto *et al*² compared patients with *DSP/FLNC* mutations to those without desmosomal gene variants in 89 DCM patients and identified the subepicardial ring-like LGE pattern at CMR together with LV regional wall motion abnormalities as the most defining elements in *DSP/FLNC*. Notably, LVEF and global longitudinal strain were on average higher in the *DSP-FLNC* group. This peculiar LGE pattern, confined to the outer layers of the LV wall, has been associated with milder degrees of LV systolic dysfunction in ALVC, differently from classic, non-desmosomal DCM where LV dysfunction is mainly the expression of a primary myocyte contractile dysfunction.¹⁴ Two patients

in our study, with a previous diagnosis of post-myocarditis DCM, received ALVC diagnosis by pathological evaluation after heart transplantation. Similarly, in a recent autopsic series by Miles *et al*³ more than half of the decedents with pathological features of AC at autopsy were diagnosed with DCM in life. High arrhythmic burden, low voltages in limb leads, TWI in the infero-lateral leads and the absence of left bundle branch block at ECG might be useful red flags for ALVC diagnosis.¹⁴

Familiar screening

AC is most commonly inherited by an autosomal dominant pattern and a thorough familial screening is mandatory. Our study underlines the relevance of this strategy to identify affected relatives (being the largest group in the cohort) and contributes to the awareness that AC can express with different clinical presentations and different phenotypes even within the same family. Moreover, the high proportion of patients with normal LV function among relatives remarks the need of tissue characterisation through CMR, that should be considered part of the first level imaging approach to not miss ALVC diagnosis.

LIMITATIONS

A third of the study cohort had a negative genetic test, but the pick-up rate was similar to previous ALVC/ARVC studies.¹⁵ Additionally, molecular analyses mostly relied on next-generation DNA sequencing that does not detect copy number variants of large DNA segments. Finally, although in the recently proposed ‘Padua criteria’ a pathogenic AC-causing mutation is deemed necessary for ALVC diagnosis, phenocopies were excluded based on a comprehensive clinical and multi-modality instrumental evaluation.¹⁶

CONCLUSIONS

ALVC diagnosis is challenging since this clinical entity is hidden in different clinical scenarios with a phenotypic spectrum ranging from normal LV, to HNDC and classic DCM. Five main clinical scenarios leading to ALVC diagnosis may be identified including ventricular arrhythmias, chest pain, heart failure, familial screening and, in 6% of patients, SCD as the presenting event. Family history of CMP/SCD, previous diagnosis of myocarditis, ECG infero-lateral negative T waves and low QRS voltages are common features that may increase clinical suspicion. Normal ECG and echocardiograms cannot rule out ALVC diagnosis and CMR is crucial to exclude typical structural involvement when suspicion is high or in familial screening.

Author affiliations

¹Cardiology Unit, St. Orsola Hospital, IRCCS Azienda Ospedaliero-Universitaria di Bologna, Bologna, Italy

²Department of Experimental, Diagnostic and Specialty Medicine, University of Bologna, Bologna, Italy

³Cardiological Center, University of Ferrara, Ferrara, Italy

⁴Cardiology Unit, Maria Cecilia Hospital SpA, Cotignola, Emilia-Romagna, Italy

⁵Cardio-Thoracic Radiology, IRCCS University Hospital of Bologna S Orsola-Malpighi Polyclinic, Bologna, Italy

⁶Department of Pathology, Cardiovascular and Cardiac Transplant Pathology Unit, Sant'Orsola-Malpighi University Hospital, Bologna, Italy

⁷Department of Medical Sciences, Unit of Medical Genetics, Università degli Studi di Ferrara, Ferrara, Italy

⁸Medical Genetics Unit, IRCCS University Hospital of Bologna S Orsola-Malpighi Polyclinic, Bologna, Italy

⁹Department of Experimental and Clinical Medicine, Cardiomyopathy Unit, University Hospital Careggi, Firenze, Italy

¹⁰Department of Experimental and Clinical Medicine, University Hospital Careggi, Firenze, Italy

Twitter Matteo Bertini @MatteoBertini5

Contributors MG and RD contributed equally to this work. Study design: EB and CR. Collection of data: MG, RD, VP, MM, VF, MB, GT. Data analysis: MG, RD, EB. Statistical analysis: RD, MG. Drafting of the manuscript: MG, RD and EB. Critical revision for important intellectual content: IO, CR. Revision, editing and approval of the final manuscript: all authors. Author responsible for the overall content as the guarantor: MG, RD and EB.

Funding The authors have not declared a specific grant for this research from any funding agency in the public, commercial or not-for-profit sectors.

Competing interests None declared.

Patient consent for publication Consent obtained directly from patient(s).

Ethics approval This study involves human participants and was approved by CMPBO-19CmpiBo. Participants gave informed consent to participate in the study before taking part.

Provenance and peer review Not commissioned; externally peer reviewed.

Data availability statement All data relevant to the study are included in the article or uploaded as supplementary information.

Supplemental material This content has been supplied by the author(s). It has not been vetted by BMJ Publishing Group Limited (BMJ) and may not have been peer-reviewed. Any opinions or recommendations discussed are solely those of the author(s) and are not endorsed by BMJ. BMJ disclaims all liability and responsibility arising from any reliance placed on the content. Where the content includes any translated material, BMJ does not warrant the accuracy and reliability of the translations (including but not limited to local regulations, clinical guidelines, terminology, drug names and drug dosages), and is not responsible for any error and/or omissions arising from translation and adaptation or otherwise.

Open access This is an open access article distributed in accordance with the Creative Commons Attribution Non Commercial (CC BY-NC 4.0) license, which permits others to distribute, remix, adapt, build upon this work non-commercially, and license their derivative works on different terms, provided the original work is properly cited, appropriate credit is given, any changes made indicated, and the use is non-commercial. See: <http://creativecommons.org/licenses/by-nc/4.0/>.

ORCID iDs

Raffaello Ditaranto <http://orcid.org/0000-0001-7025-0679>

Giacomo Tini <http://orcid.org/0000-0001-8520-152X>

Matteo Bertini <http://orcid.org/0000-0002-5285-7140>




Mauro Biffi <http://orcid.org/0000-0003-4590-8584>

Elena Biagini <http://orcid.org/0000-0003-0295-0440>

REFERENCES

- 1 Sen-Chowdhry S, Syrris P, Prasad SK, *et al*. Left-dominant arrhythmogenic cardiomyopathy: an under-recognized clinical entity. *J Am Coll Cardiol* 2008;52:2175–87.
- 2 Augusto JB, Eiros R, Nakou E, *et al*. Dilated cardiomyopathy and arrhythmogenic left ventricular cardiomyopathy: a comprehensive genotype-imaging phenotype study. *Eur Heart J Cardiovasc Imaging* 2020;21:326–36.
- 3 Miles C, Finocchiaro G, Papadakis M, *et al*. Sudden death and left ventricular involvement in arrhythmogenic cardiomyopathy. *Circulation* 2019;139:1786–97.
- 4 Priori SG, Blomström-Lundqvist C, Mazzanti A, *et al*. 2015 ESC guidelines for the management of patients with ventricular arrhythmias and the prevention of sudden cardiac death: the task force for the management of patients with ventricular arrhythmias and the prevention of sudden cardiac death of the European Society of Cardiology (ESC), endorsed by: association for European paediatric and congenital cardiology (AEPC). *Eur Heart J* 2015;36:2793–867.
- 5 Ponikowski P, Voors AA, Anker SD, *et al*. 2016 ESC Guidelines for the diagnosis and treatment of acute and chronic heart failure: The Task Force for the diagnosis and treatment of acute and chronic heart failure of the European Society of Cardiology (ESC)/Developed with the special contribution of the Heart Failure Association (HFA) of the ESC. *Eur Heart J* 2016;37:2129–200.
- 6 Pinto YM, Elliott PM, Arbustini E, *et al*. Proposal for a revised definition of dilated cardiomyopathy, hypokinetic non-dilated cardiomyopathy, and its implications for clinical practice: a position statement of the ESC Working group on myocardial and pericardial diseases. *Eur Heart J* 2016;37:1850–8.
- 7 Richards S, Aziz N, Bale S, *et al*. Standards and guidelines for the interpretation of sequence variants: a joint consensus recommendation of the American College of medical genetics and genomics and the association for molecular pathology. *Genet Med* 2015;17:405–24.
- 8 Aquaro GD, De Luca A, Cappelletto C, *et al*. Prognostic value of magnetic resonance phenotype in patients with arrhythmogenic right ventricular cardiomyopathy. *J Am Coll Cardiol* 2020;75:2753–65.
- 9 Smith ED, Lakdawala NK, Papoutsidakis N, *et al*. Desmoplakin cardiomyopathy, a fibrotic and inflammatory form of cardiomyopathy distinct from typical dilated or arrhythmogenic right ventricular cardiomyopathy. *Circulation* 2020;141:1872–84.
- 10 Piriou N, Marteau L, Kyndt F, *et al*. Familial screening in case of acute myocarditis reveals inherited arrhythmogenic left ventricular cardiomyopathies. *ESC Heart Fail* 2020;7:1520–33.
- 11 Elliott P, O'Mahony C, Syrris P, *et al*. Prevalence of desmosomal protein gene mutations in patients with dilated cardiomyopathy. *Circ Cardiovasc Genet* 2010;3:314–22.
- 12 Garcia-Pavia P, Syrris P, Salas C, *et al*. Desmosomal protein gene mutations in patients with idiopathic dilated cardiomyopathy undergoing cardiac transplantation: a clinicopathological study. *Heart* 2011;97:1744–52.
- 13 Disertori M, Quintarelli S, Mazzola S, *et al*. The need to modify patient selection to improve the benefits of implantable cardioverter-defibrillator for primary prevention of sudden death in non-ischaemic dilated cardiomyopathy. *Europace* 2013;15:1693–701.
- 14 Cipriani A, Bauce B, De Lazzari M, *et al*. Arrhythmogenic right ventricular cardiomyopathy: characterization of left ventricular phenotype and differential diagnosis with dilated cardiomyopathy. *J Am Heart Assoc* 2020;9:e014628.
- 15 Romano S, Judd RM, Kim RJ, *et al*. Feature-Tracking Global Longitudinal Strain Predicts Death in a Multicenter Population of Patients With Ischemic and Nonischemic Dilated Cardiomyopathy Incremental to Ejection Fraction and Late Gadolinium Enhancement. *JACC Cardiovasc Imaging* 2018;11:1419–29.
- 16 Corrado D, Perazzolo Marra M, Zorzi A, *et al*. Diagnosis of arrhythmogenic cardiomyopathy: the Padua criteria. *Int J Cardiol* 2020;319:106–14.

Standard ECG for differential diagnosis between Anderson-Fabry disease and hypertrophic cardiomyopathy

Giovanni Vitale ,¹ Raffaello Ditaranto ,¹ Francesca Graziani,² Ilaria Tanini,³ Antonia Camporeale,⁴ Rosa Lillo,² Marta Rubino,⁵ Elena Panaioli,² Federico Di Nicola,¹ Valentina Ferrara,¹ Rossana Zanoni,¹ Angelo Giuseppe Caponetti,¹ Ferdinando Pasquale,¹ Maddalena Graziosi,¹ Alessandra Berardini,¹ Matteo Ziacchi,¹ Mauro Biffi,¹ Marisa Santostefano,⁶ Rocco Liguori,^{7,8} Nevio Taglieri,¹ Elena Nardi,¹ Ales Linhart ,⁹ Iacopo Olivotto,³ Claudio Rapezzi,^{10,11} Elena Biagini¹

► Additional material is published online only. To view, please visit the journal online (<http://dx.doi.org/10.1136/heartjnl-2020-318271>).

For numbered affiliations see end of article.

Correspondence to

Dr Elena Biagini, Cardiology Unit, IRCCS, Department of Experimental, Diagnostic and Specialty Medicine, Sant'Orsola Hospital, University of Bologna, 40125 Bologna, Emilia-Romagna, Italy; elena.biagini73@gmail.com

GV and RD contributed equally.

Received 20 September 2020
Revised 19 January 2021
Accepted 22 January 2021
Published Online First
9 February 2021

ABSTRACT

Objectives To evaluate the role of the ECG in the differential diagnosis between Anderson-Fabry disease (AFD) and hypertrophic cardiomyopathy (HCM).

Methods In this multicentre retrospective study, 111 AFD patients with left ventricular hypertrophy were compared with 111 patients with HCM, matched for sex, age and maximal wall thickness by propensity score. Independent ECG predictors of AFD were identified by multivariate analysis, and a multiparametric ECG score-based algorithm for differential diagnosis was developed.

Results Short PR interval, prolonged QRS duration, right bundle branch block (RBBB), R in augmented vector left (aVL) ≥ 1.1 mV and inferior ST depression independently predicted AFD diagnosis. A point-by-point ECG score was then derived with the following diagnostic performances: c-statistic 0.80 (95% CI 0.74 to 0.86) for discrimination, the Hosmel-Lemeshow χ^2 6.14 ($p=0.189$) for calibration, sensitivity 69%, specificity 84%, positive predictive value 82% and negative predictive value 72%. After bootstrap resampling, the mean optimism was 0.025, and the internal validated c-statistic for the score was 0.78.

Conclusions Standard ECG can help to differentiate AFD from HCM while investigating unexplained left ventricular hypertrophy. Short PR interval, prolonged QRS duration, RBBB, R in aVL ≥ 1.1 mV and inferior ST depression independently predicted AFD. Their systematic evaluation and the integration in a multiparametric ECG score can support AFD diagnosis.

INTRODUCTION

Hypertrophic cardiomyopathy (HCM) is the most common genetically determined cardiomyopathy, with an estimated clinical prevalence of 1:200 or greater.¹ In most cases, HCM is due to sarcomeric genes mutations; however, a proportion of unexplained left ventricular (LV) hypertrophy (LVH) is caused by other aetiologies. In the *mare magnum* of different possible HCM phenocopies, Anderson-Fabry disease (AFD), an X-linked lysosomal storage disorder due to α -galactosidase (*GLA*) gene mutations, has gained increasing relevance, thanks to the improved pathophysiological understanding

and the availability of therapeutic options. The heterogeneity in clinical spectrum is influenced by sex, age and residual enzymatic activity and ranges from a more severe and earlier classic phenotype to a late-onset presentation. Correct diagnosis is clinically relevant due to the different management of HCM and AFD. In this regard, the old-fashioned ECG remains the first diagnostic outpost when approaching patients with LVH. Although peculiar features such as short PR interval without pre-excitation, atrioventricular and intraventricular blocks have been reported in AFD, a systematic comparison of the ECG findings between HCM and AFD in order to identify useful clues for differential diagnosis has not been performed. Thus, the purpose of the present study was to describe the spectrum of ECG abnormalities in AFD cardiomyopathy compared with patients with HCM, determine independent ECG predictors of AFD and, accordingly, derive and internally validate an ECG score for differential diagnosis.

METHODS

Study design

In this multicentre observational retrospective cohort study, we analysed 167 AFD patients ≥ 18 years of age, evaluated between 2003 and 2019 at four Italian centres (IRCCS, University Sant'Orsola Hospital, Bologna ($n=38$; 23%); Fondazione Policlinico Universitario Agostino Gemelli, Rome ($n=51$; 30%); Azienda Ospedaliera Careggi, Florence ($n=52$; 31%) and Policlinico Universitario San Donato, Milan ($n=26$; 16%)). Five patients were excluded due to unfeasible ECG interpretation (ventricular paced rhythm: $n=1$; previous septal myomectomy: $n=3$; and previous myocardial infarction: $n=1$). AFD diagnosis was based on the measurement of the enzyme activity in leucocytes (in male patients) and/or plasmatic lyso-Gb3 levels with dried blood spot method. Diagnosis was confirmed by genetic analysis. Endomyocardial biopsy was performed in cases of doubt (new *GLA* variants and variants of uncertain significance). Fifty-one patients had no evidence of LVH (defined



© Author(s) (or their employer(s)) 2022. No commercial re-use. See rights and permissions. Published by BMJ.

To cite: Vitale G, Ditaranto R, Graziani F, et al. *Heart* 2022;**108**:54–60.

as an echocardiographic LV maximal wall thickness (MWT) >12 mm) and were also excluded.² Therefore, 111 patients formed the final AFD population. Baseline characteristics and demographics are reported in online supplemental table 1. AFD patients with LVH were compared with 111 patients with HCM, recruited from a database of 657 unselected patients with HCM (evaluated between 2000 and 2019) through a 1-to-1 propensity score matching considering age, sex and MWT, using the 'nearest neighbor' method. The diagnosis of HCM—namely sarcomeric or without an identifiable cause—was based on standard international criteria.³ HCM patients with previous septal myectomy, septal alcohol ablation or ventricular paced rhythm on ECG were excluded. The study was conducted in accordance with the principles of the most recent revision of the Declaration of Helsinki.

ECG analysis

The 12-lead ECG (standard calibration 10 mm/1 mV; paper speed of 25 mm/s), performed at first evaluation on commercially available instruments in the supine position, was available for all patients. All ECGs were independently analysed by two investigators (GV and FDN) using a manual calliper; discrepancies were solved by two senior supervisors (CR and EB). Corrected QT (Bazett's formula) was considered pathological if ≥ 450 ms in males and 470 ms in females. Total QRS score was defined by the sum of zenith-to-nadir QRS amplitudes of all 12 leads.⁴ An rSr' pattern in V1 was assumed as incomplete right bundle branch block (RBBB) (and not a normal variant) in the presence of at least one of the following criteria: S wave in DI – aVL >0.1 mV; rSr' morphology in both V1 and V2; S wave deeper in V1 than in V2 (SV1>SV2); a notch in the ascending branch of S wave in V2; QRS duration >100 ms. Electrocardiographic LVH was defined by at least one of the following criteria: Sokolow-Lyon index (SV1 or SV2+RV5 or RV6 ≥ 3.5 mV); Cornell index (SV3+R aVL ≥ 2.0 mV in females and ≥ 2.8 mV in males); R wave amplitude in aVL ≥ 1.1 mV. Sokolow-Lyon and Cornell voltage-duration product were calculated (Sokolow-Lyon and Cornell index multiplied by the QRS duration). Pathological Q waves and low QRS voltages were defined according to previously reported criteria.⁵

Statistical analysis

Continuous data had a non-normal distribution (as assessed with the Shapiro-Wilk test) and were expressed as median and IQR and compared using Mann-Whitney U test. χ^2 test was used for comparison of categorical data. Bivariate correlations between independent ECG predictors and MWT were determined using the Pearson correlation coefficient test.

ECG variables potentially predictive for the AFD diagnosis, selected by univariable analysis ($p < 0.1$), were entered in a backward multivariable logistic regression analysis. Linear association assumption between continuous predictors and outcome was tested by Box-Tidwell transformation method.⁶ In case of non-linearity, variables were opportunely transformed. Interactions between independent predictors of AFD were also tested. Model discrimination was assessed using the area under the receiver operating characteristic curve (ROC, c-statistic). Calibration was evaluated by the Hosmer-Lemeshow test, with a $\chi^2 \geq 20$ ($p < 0.01$) indicating poor calibration.

Clinical risk score construction for AFD prediction

A point risk score was developed based on the results of the multivariate risk model. A weight was assigned to each independent

predictor of AFD diagnosis, as previously described.⁷ The individual score was then obtained by summing those weights for each patient and its discrimination assessed using the area under the ROC curve c-statistic. Calibration was evaluated by the Hosmer-Lemeshow test. In order to estimate the internally validated performance of the score, we applied the regular bootstrap procedure (1000 iterations) and estimated the optimism of each bootstrap sample. The mean optimism was then subtracted from the apparent performance measure (c-statistic).⁸ ROC analysis was used to establish the best score cut-off by evaluating both the diagnostic accuracy of each point (ie, rate of patients correctly classified) and the Youden index.⁹ A p value <0.05 in the two-tailed tests was considered significant. All analyses were performed with STATA V.13.0 software (STATA Corporation, College Station, Texas, USA).

Patient and public involvement

Patients were not involved in designing or conduct of the study.

RESULTS

Baseline characteristics of study populations are shown in table 1. AFD cardiomyopathy showed more frequently a symmetric distribution of LVH (68% vs 22%; $p < 0.001$), while apical phenotype was similarly present in both groups (8% vs 14%; $p = 0.28$). ECG characteristics are summarised in table 2. Patients with AFD showed higher prevalence of atrial fibrillation (12% vs 3%; $p = 0.009$), shorter PR interval (155 (140–180) vs 162 (148–184) ms; $p = 0.009$) and longer QRS duration (110 (100–135) vs 100 (90–106) ms; $p < 0.001$), as well as greater prevalence of complete (22% vs 3%; $p < 0.001$) and incomplete (13% vs 1%; $p < 0.001$) RBBB, and non-specific intraventricular conduction delay (13% vs 4%; $p = 0.014$). Moreover, R in aVL ≥ 1.1 mV (46% vs 23%; $p < 0.001$), total QRS score (20.4

Table 1 Baseline clinical and echocardiographic characteristics in patients with Anderson-Fabry disease (AFD) and hypertrophic cardiomyopathy (HCM), matched for age, gender and LV maximum wall thickness

Variables	AFD with LVH (N=111)	HCM (N=111)	P value
Male sex	65 (59)	65 (59)	1
Age at first evaluation (years)	57(51–67)	58 (51–70)	0.196
NYHA class			
I–II	101 (91)	103 (93)	0.806
III–IV	10 (9)	8 (7)	0.806
History of atrial fibrillation (any form)	30 (27)	14 (13)	0.012
LVOTO	8 (7)	51 (46)	<0.001
Symmetric LVH	75 (68)	24 (22)	<0.001
Asymmetric LVH	27 (24)	72 (65)	<0.001
Apical morphology	9 (8)	15 (14)	0.28
ICD recipients			
Primary prevention	5/6 (83)	9/11 (82)	0.407
Secondary prevention	1/6 (17)	2/11 (18)	0.937
End-stage disease	4 (4)	4 (4)	1
Echocardiography			
IVS at M-mode (mm)	14.5 (13–18)	15 (13–18)	0.585
Maximum wall thickness (mm)	16 (14–19)	17 (15–19)	0.334
End diastolic volume (ml)	86(66–111)	89(70–108)	0.794
LVEF (%)	63(60–67)	69(65–75)	<0.001
Indexed left ventricular mass (g/m ²)	151(124–211)	145(123–182)	0.167

Data are described as medians with IQRs or numbers with percentages. ICD, implantable cardioverter defibrillator; IVS, interventricular septum; LV, left ventricular; LVEF, left ventricular ejection fraction; LVH, left ventricular hypertrophy; LVOTO, left ventricular outflow tract obstruction; NYHA, New York Heart Association.

(15.8–26.8) vs 17.7 (13.8–22.1) mV; $p < 0.001$) and R amplitude in V5 (1.8 (1.1–2.6) vs 1.4 (0.9–2.3) mV; $p = 0.009$) were higher in patients with AFD. No difference was observed for Sokolow-Lyon and Cornell indexes. Notably, low QRS voltages (overall rare) and Q waves in the inferior leads were observed only in patients with HCM. Ventricular repolarisation abnormalities in the inferior leads, namely ST-segment depression (13% vs 1%; $p = 0.001$) and negative T waves (34% vs 19%; $p = 0.01$), were more common in AFD. PR interval ($r = 0.20$, $p = 0.004$), QRS duration ($r = 0.40$, $p < 0.001$) and R wave in aVL ≥ 1.1 mV ($r = 0.27$, $p = 0.001$) showed a mild to moderate correlation with MWT. The main ECG features are depicted in [figure 1](#).

Development of multiparametric electrocardiographic score for AFD identification

Results of univariable analysis are shown in online supplemental table 2). Only the Sokolow-Lyon score did not meet the assumption of linearity so that it was used as transformed variable. Since the presence of low QRS voltages and inferior Q waves were exclusively associated with HCM, they were not included in the score calculation: these parameters, however, were included as the entry criteria for the final flow diagram. At multivariable analysis, independent predictors of AFD were short PR interval, prolonged QRS duration, RBBB (complete or incomplete),

Table 2 Electrocardiographic characteristics in Anderson-Fabry disease (AFD) with left ventricular hypertrophy (LVH) and hypertrophic cardiomyopathy (HCM)

Variables	AFD patients with LVH (n=111)	Patients with HCM (n=111)	P value
Normal ECG	7 (6)	8 (7)	0.789
Sinus rhythm	97 (87)	107 (96)	0.014
Atrial fibrillation	13 (12)	3 (3)	0.009
PR interval (ms)	155 (140–180)	162 (148–184)	0.009
PR <120 ms (n=204)	11/97 (11)	4/107 (4)	0.004
I degree atrioventricular block (n=204)	11/97 (11)	20/107 (19)	0.144
QRS duration (ms)	110 (100–135)	100 (90–106)	<0.001
QRS ≥ 120 ms	41 (37)	8 (7)	<0.001
Incomplete right bundle branch block	15 (13)	1 (1)	<0.001
Complete right bundle branch block	25 (22)	3 (3)	<0.001
Complete or incomplete right bundle branch block	40 (36)	4 (4)	<0.001
Left bundle branch block	1 (1)	1 (1)	1
Non-specific intraventricular block	14 (13)	4 (4)	0.014
Left anterior fascicular block	13 (12)	6 (5)	0.093
Left axis deviation	19 (17)	14 (13)	0.346
Corrected QT interval (ms)	429 (406–447)	420 (405–436)	0.074
Prolonged corrected QT interval	22 (20)	8 (7)	0.006
Left atrial enlargement	37/97 (38)	41/108 (38)	0.979
Right atrial enlargement	3/97 (3)	6/108 (5)	0.39
Low QRS voltages	0	8 (7)	0.004
Sokolow-Lyon criterion	47 (42)	50 (45)	0.685
Sokolow-Lyon score (mV)	3.1 (1.8–4.4)	3.2 (2.2–4)	0.518
Sokolow product (mV)	333 (217–514)	306 (218–416)	0.282
Cornell voltage criterion	29 (26)	26 (23)	0.641
Cornell voltage score (mV)	1.9 (1.2–2.5)	1.7 (1.2–2.4)	0.5
Cornell product (mV)	200 (120–295)	178.5 (108–253)	0.068
R in aVL ≥ 1.1 mV	51 (46)	25 (23)	<0.001
Total QRS score (mV)	20.4 (15.8–26.8)	17.7 (13.8–22.1)	<0.001
R in V5 (mV)	1.8 (1.1–2.6)	1.4 (0.9–2.3)	0.009
Pathological Q waves	10 (9)	18 (16)	0.106
Anterior	2 (2)	8 (7)	0.052
Inferior	0	8 (7)	0.004
Lateral	10 (9)	7 (6)	0.449
Posterior	2 (2)	0	0.155
Negative T waves	67 (60)	61 (55)	0.415
Anterior	35 (31)	26 (23)	0.176
Inferior	38 (34)	21 (19)	0.01
Lateral	64 (58)	55 (49)	0.226
Diffuse	22 (20)	12 (11)	0.093
Negative T waves >10 mm	17 (15)	5 (4)	0.007
ST-segment depression	43 (39)	35 (32)	0.261
Anterior	11 (10)	5 (4)	0.119
Inferior	14 (13)	1 (1)	0.001
Lateral	40 (36)	33 (30)	0.31
ST-segment elevation	8 (7)	13 (12)	0.252

Data are described as medians with IQRs or numbers with percentages.

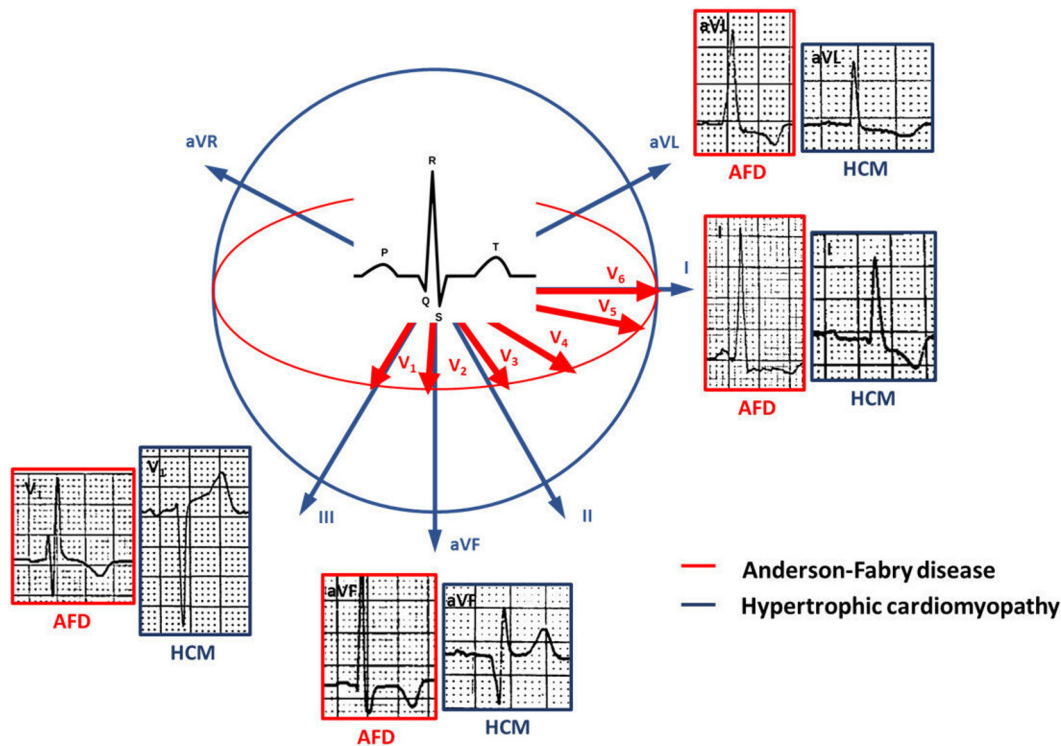


Figure 1 A schematic representation of the main electrocardiographic features in Anderson-Fabry disease (AFD, red frame) and hypertrophic cardiomyopathy (HCM, blue frame). Counterclockwise: V1: QRS complex with right bundle branch block and rSR' morphology (AFD) versus rS complex with J point elevation in V1 (HCM). On frontal plane augmented vector foot (aVF): ST-segment depression and negative T wave (AFD) versus pathological Q wave and discordant T wave (QT discordance, HCM); I: short PR interval (AFD) versus first degree atrioventricular block (HCM); aVL: high R wave (>1.1 mV) and large QRS (AFD) versus normal R wave and narrow QRS (HCM).

R wave in aVL ≥ 1.1 mV and inferior ST-segment depression (table 3). The c-statistic and the Hosmer-Lemeshow χ^2 for the model were 0.83 and 5.68 ($p=0.68$), respectively. Using the adjusted regression coefficients of the final multivariable logistic regression, an integer risk score was developed (table 4). The score did not include patients whose PR interval could not be assessed (due to atrial fibrillation in 16 and supraventricular ectopic rhythms in 2). The distribution of risk score is shown in the online supplemental table 3; the values reported in the study population ranged between -2 and 7 . The OR for each increasing point of the score for a diagnosis of AFD was 2.30 (95% CI 1.76 to 3.00; $p<0.001$). The score c-statistic was 0.80 (95% CI 0.74 to 0.86) and the Hosmer-Lemeshow χ^2 6.14 ($p=0.189$), indicating good discrimination and calibration, respectively. After bootstrap resampling, the mean optimism was 0.025, and the internal validated c-statistic for the score was 0.78. Based on the results of the ROC analysis (online supplemental table 4 and figure 2), a score cut-off ≥ 2 was associated with the best diagnostic accuracy correctly classifying 76% of patients. For this cut-off sensitivity, specificity, positive predictive

value and negative predictive value for AFD were 69%, 84%, 82% and 72%, respectively. These findings were consistent with the Youden statistics (online supplemental table 4). In figure 3, a flow diagram is reported with a step-by-step analysis of the ECG.

DISCUSSION

This study aimed to describe the ECG abnormalities in a large AFD population with LVH and to establish their usefulness for differential diagnosis with HCM. The main findings were that short PR interval, prolonged QRS duration, RBBB (either incomplete and complete), R in aVL ≥ 1.1 mV and inferior ST-segment depression were independent ECG predictors of AFD. These

Table 3 Independent ECG predictors of Anderson-Fabry disease at multivariable logistic regression

Variables	OR	95% CI	P >(z)
PR interval	0.98	0.98 to 0.99	0.001
QRS duration	1.04	1.02 to 1.06	0.001
Right bundle branch block	9.82	2.5 to 37.81	0.001
Inferior ST-segment depression	17.29	1.95 to 153.22	0.01
R in aVL ≥ 1.1 mV	2.35	1.10 to 4.99	0.027

Table 4 Anderson-Fabry ECG score

Parameters	B coefficient	Points
Score calculation		
PR interval	<120 ms	-0.020
	120–199 ms	0
	≥ 200 ms	-2
QRS duration	<100 ms	0
	100–119 ms	1
	120–139 ms	2
	≥ 140 ms	3
Right bundle branch block (complete or incomplete)	Yes	2.284
	No	0
R in aVL ≥ 1.1 mV	Yes	0.853
	No	0
Inferior ST-segment depression	Yes	2.850
	No	0

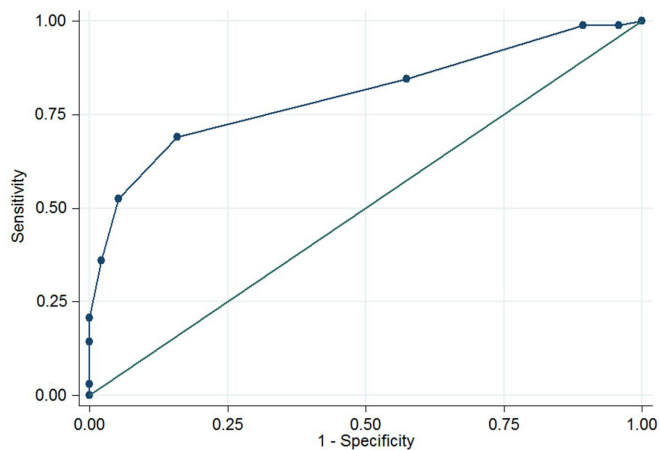


Figure 2 Receiver operating characteristics curve analysis evaluating the diagnostic performance of the ECG score for Anderson-Fabry disease diagnosis. The Anderson-Fabry ECG score shows a 69% sensitivity and 84% specificity at a cut-off value of 2 (area under the curve 0.80 (95% CI 0.74-0.86)).

variables, included in a point-by-point ECG score, differentiated AFD from HCM with good predictive accuracy, discrimination and calibration.

PR interval and intraventricular conduction abnormalities

In AFD, the atrioventricular and intraventricular conduction are known to exhibit a biphasic trend, with a faster conduction in the early stages and PR and QRS prolongation with ageing and disease progression.^{10 11} Although short PR interval is a red flag for AFD diagnosis, it cannot be considered a sensitive sign for AFD due to its low prevalence in patients with and without LVH.¹²⁻¹⁵ However, when compared with age and heart rate-matched controls, patients with early-stage AFD (ie, those without LVH) have a shorter PR interval, even if in the 'normal'

range (ie, 120–200 ms).¹⁰ In our study, patients with AFD (all with LVH) had significantly shorter median PR values—but still in the normal range—compared with patients with HCM, and short PR values proved to be a strong predictor for AFD diagnosis. Increased cells diameter, Gb3 interactions with membrane ion channels and circulating metabolites have been supposed as potential mechanisms of this supranormal conduction.¹⁶ Thereafter, additional factors such as LVH, ischaemia, inflammation and fibrosis slow down the electrical pulse conduction and overrule the aforesaid mechanisms.¹⁷ Differently from what observed for PR, our patients with AFD had longer QRS duration compared with HCM group, and QRS width was identified as an independent predictor of AFD diagnosis. Namely, a peculiar predilection for right bundle branch conduction disturbances emerged in our study. This could reflect a greater vulnerability of this branch due to the thin cord-like structure and superficial localisation, compared with the left bundle. In HCM RBBB is uncommon, except in the context of prior alcohol septal ablation. The behaviour of PR and QRS intervals in our patients with AFD may express a different effect of the disease burden at the two different sites, particularly the delayed activation of the increased ventricular mass. Accordingly, the correlation with MWT was higher for QRS interval compared with PR interval.

Left ventricular hypertrophy

Patients with AFD demonstrated a higher prevalence of R wave in aVL ≥ 1.1 mV, higher values of R wave in V5 and total QRS score compared with HCM. Conversely, no significant difference was seen for Sokolow-Lyon and Cornell criteria. These findings may partly reflect differences in the distribution and amount of anatomic LV mass in the two diseases. LVH is more often symmetric in AFD than in HCM (68% vs 22% in our cohorts; $p < 0.001$) that typically presents an asymmetric septal hypertrophy (65% vs 24% in our cohorts; $p < 0.001$).^{18 19} Enhanced wall thickness involving the left and posterior wall—rather than being confined to the septum—may determine leftward and posterior displacement of electrical vectors, justifying a taller R wave in aVL in AFD as well as higher values of R wave in V5. The R wave in aVL was previously shown to correlate more closely with LV mass measured at echocardiography, compared with Sokolow-Lyon or Cornell indexes, in hypertensive patients.²⁰ Consistent with this hypothesis, R wave amplitude in V5 was higher among AFD patients, expressing the increased leftward QRS forces in the transverse plane, because of different LV mass distribution, even if this parameter did not emerge as an independent predictor for AFD. Likewise, the uniform distribution of hypertrophy may explain superior QRS amplitudes and higher total QRS score in AFD. Although the two groups were matched for MWT, differences in terms of cellular mass and/or volume may further explain ECG differences. Among other findings we found that a small but not negligible subset of patients in each aetiology had a normal ECG despite LVH at echocardiogram, confirming that normal ECG cannot rule out the diagnosis of either HCM or AFD.

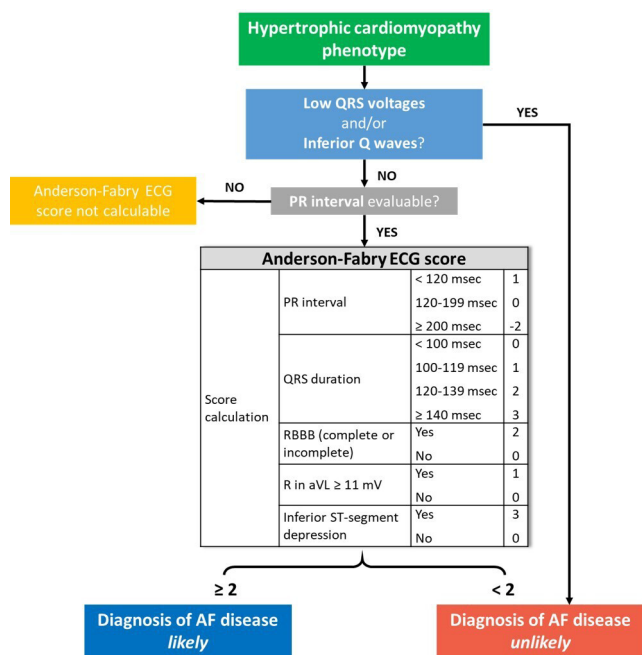


Figure 3 Flow diagram showing the proposed ECG score for differential diagnosis between Anderson-Fabry disease and hypertrophic cardiomyopathy. AF, Anderson-Fabry; RBBB, right bundle branch block.

Inferior abnormal Q waves and repolarisation abnormalities

Inferior leads emerged as a crucial diagnostic key for the differential diagnosis between AFD and HCM. Though abnormal Q waves were found in both groups, inferior Q waves exclusively characterised HCM. It is well known that abnormal Q waves, mainly in the infero-lateral leads, sometimes associated with positive T wave (so-called QT discordance), are often the initial ECG findings in HCM, frequently preceding echocardiographic

abnormalities.^{21 22} The electrogenesis of abnormal Q waves in HCM is not completely understood and could have two possible mechanisms: loss of electrical force due to transmural myocardial fibrosis and abnormal electrical activations of hypertrophied ventricular septum causing unbalance of the electrical vectors.²³ However, inferior negative T waves and ST-segment depression were more frequent in AFD and the latter a predictor for such a diagnosis. It may be supposed that abnormalities in repolarisation are expression of fibrosis in the infero-lateral wall, which is preferentially involved by progressive fibrosis in AFD.²⁴ Conversely, in HCM late gadolinium enhancement is typically located at the midwall of the most hypertrophied areas and at the anterior and posterior right ventricle insertion points.²⁵ This speculation is indirectly supported by the observation of Niemann *et al*²⁶ that the absence of ST-segment or T wave alterations seems to exclude late enhancement in patients with AFD. Instead, repolarisation abnormalities in lateral leads, though associated with fibrosis at CMR in AFD, did not provide diagnostic benefit, being present in both groups with similar frequencies.²⁶

Low QRS voltages

Low QRS voltages are rare in HCM and typically limited to the end-stage phase. Conversely, AFD hearts generally preserve high voltages over time, even in the more advanced phases.²⁷ Accordingly, low QRS voltages were totally absent in our AFD cohort, despite an equal prevalence of end-stage cardiomyopathy compared with the HCM subset. This might be the consequence of higher baseline voltages in AFD compared with HCM, preventing low QRS complexes occurrence, due to the higher myocardial mass and the progressive pathologic accumulation within myocytes.

Clinical utility of the ECG score

Among patients with unexplained LVH, early identification of AFD is crucial. However, in clinical practice, the rate of missed or delayed diagnosis in AFD is still significant, especially in the late-onset variants.^{28 29} We propose an electrocardiographic multiparametric score system for differential diagnosis between HCM and AFD; therefore, the score does not consider that some ECG clues could be shared with other hypertrophic phenocopies. Indeed, short PR interval is a common feature of storage diseases (Pompe disease, PRKAG2 mutations, Danon disease) and mitochondrial (MELAS and MERFF) disorders, whereas low QRS voltages and atrioventricular blocks are frequent in cardiac amyloidosis.¹⁵

Limitations

Given its retrospective nature, the study is not immune to sources of biases. Results of the present study are not generalisable in suspected AFD patients without LVH. Furthermore, the score should be used with caution in patients with advanced disease, as patients with LV outflow tract obstruction, since they are under-represented in our cohort (7%). Nonetheless, our results could prompt future investigations aimed at evaluating its applicability in both early and late stage of AFD. More than half of the patients with AFD were already on specific therapy, whose effects on the ECG are unknown. Additionally, not all patients with HCM received genetic investigation; although rare, non-sarcomeric phenocopies were excluded to the best of contemporary clinical and instrumental evaluation. HCM group was selected by propensity score matching with cases of AFD. Therefore, it may, not represent an average HCM population. Indeed, a lower rate of atrial fibrillation and lower degree of

Key messages

What is already known on this subject?

- ▶ In Anderson-Fabry disease (AFD), some electrocardiographic features like short PR interval without pre-excitation, atrioventricular and intraventricular blocks have been reported. However, a systematic comparison of the ECG findings between hypertrophic cardiomyopathy (HCM) and AFD has not been performed.

What might this study add?

- ▶ Short PR interval, prolonged QRS duration, right bundle branch block, R in aVL ≥ 1.1 mV and inferior ST-segment depression were found more frequently in AFD and independently predicted AFD diagnosis. On the contrary, inferior Q waves and low QRS voltages suggested HCM diagnosis. The combination of these electrocardiographic findings enabled the construction of a multiparametric ECG score, in which a score cut-off of ≥ 2 suggested AFD diagnosis with good predictive accuracy and discrimination.

How might this impact on clinical practice?

- ▶ The present study shows that the calculation of an easily ECG-based score for patients with unexplained left ventricular hypertrophy may distinguish between HCM and AFD with a good diagnostic performance, providing consequent clinical and therapeutic implications.

LVH was observed compared with larger cohorts.³⁰ Finally, due to the limited sample size, we were unable to perform a more robust internal validation of the ECG score. An external validation cohort would be desirable to confirm the good diagnostic accuracy of ECG variables.

CONCLUSIONS

The present study emphasises the role of the ECG in the differential diagnosis between AFD and HCM. Short PR interval, prolonged QRS duration, RBBB, LVH expressed as R in aVL ≥ 1.1 mV and inferior ST-segment depression proved to be independent predictors of AFD diagnosis. A stepwise approach, based on a multiparametric ECG score system, is proposed as instrument for discrimination of these two diseases in the scenario of an unexplained LVH.

Author affiliations

¹Cardiology Unit, IRCCS, Department of Experimental, Diagnostic and Specialty Medicine, Sant'Orsola Hospital, University of Bologna, Bologna, Emilia-Romagna, Italy

²Department of Cardiovascular and Thoracic Sciences, Fondazione Policlinico Universitario A. Gemelli IRCCS, Roma, Lazio, Italy

³Cardiomyopathy Unit, Careggi University Hospital, Firenze, Toscana, Italy

⁴Multimodality Cardiac Imaging Section, IRCCS Policlinico San Donato, San Donato Milanese, Milano, Lombardia, Italy

⁵Inherited and Rare Cardiovascular Diseases, Department of Translational Medical Sciences, University of Campania "Luigi Vanvitelli", Monaldi Hospital, Napoli, Campania, Italy

⁶Division of Nephrology, Azienda Ospedaliero Universitaria - Policlinico di St. Orsola, Bologna, Emilia-Romagna, Italy

⁷Department of Biomedical and Neuromotor Sciences, University of Bologna, Bologna, Emilia-Romagna, Italy

⁸IRCCS Istituto delle Scienze Neurologiche di Bologna, UOC Clinica Neurologica, Bologna, Emilia-Romagna, Italy

⁹2nd Department of Medicine-Department of Cardiovascular Medicine, First Faculty of Medicine, Charles University and General University Hospital, Praha, Czech Republic

¹⁰Cardiovascular Center, University of Ferrara, Azienda Ospedaliero Universitaria di Ferrara Ospedale Sant'Anna, Cona, Emilia-Romagna, Italy

¹¹Maria Cecilia Hospital, GVM Care & Research, Cotignola, Ravenna, Emilia-Romagna, Italy

Twitter Rosa Lillo @RosaLillo14 and Elena Biagini @elena.biagini73@gmail.com

Contributors GV and RD contributed equally to this work. Study design: EB and NT. Collection of data: GV and FDN. Data analysis: GV, RD, FDN, NT and EB. Statistical analysis: GV, RD, NT and EN. Drafting of the manuscript: GV, RD, NT and EB. Critical revision for important intellectual content: IO, AL and CR. Revision, editing and approval of the final manuscript: all authors.

Funding The authors have not declared a specific grant for this research from any funding agency in the public, commercial or not-for-profit sectors.

Competing interests None declared.

Patient consent for publication Obtained.

Ethics approval The study was approved by the Ethics Committee of the St. Orsola-Malpighi Hospital (478/2019/Oss/AOUBO).

Provenance and peer review Not commissioned; externally peer reviewed.

Data availability statement All data relevant to the study are included in the article or uploaded as supplementary material. The authors from each center guarantee the integrity of data from their institution. All provided data included in the article cannot be traced back to individuals that participated in the study.

Supplemental material This content has been supplied by the author(s). It has not been vetted by BMJ Publishing Group Limited (BMJ) and may not have been peer-reviewed. Any opinions or recommendations discussed are solely those of the author(s) and are not endorsed by BMJ. BMJ disclaims all liability and responsibility arising from any reliance placed on the content. Where the content includes any translated material, BMJ does not warrant the accuracy and reliability of the translations (including but not limited to local regulations, clinical guidelines, terminology, drug names and drug dosages), and is not responsible for any error and/or omissions arising from translation and adaptation or otherwise.

ORCID iDs

Giovanni Vitale <http://orcid.org/0000-0002-5416-7645>

Raffaello Ditaranto <http://orcid.org/0000-0001-7025-0679>

Ales Linhart <http://orcid.org/0000-0002-3372-7850>

REFERENCES

- Semsarian C, Ingles J, Maron MS, *et al.* New perspectives on the prevalence of hypertrophic cardiomyopathy. *J Am Coll Cardiol* 2015;65:1249–54.
- Eng CM, Germain DP, Banikazemi M, *et al.* Fabry disease: guidelines for the evaluation and management of multi-organ system involvement. *Genet Med* 2006;8:539–48.
- Authors/Task Force members, Elliott PM, Anastasakis A, *et al.* 2014 ESC guidelines on diagnosis and management of hypertrophic cardiomyopathy: the task force for the diagnosis and management of hypertrophic cardiomyopathy of the European Society of cardiology (ESC). *Eur Heart J* 2014;35:2733–79.
- Dollar AL, Roberts WC. Usefulness of total 12-lead QRS voltage compared with other criteria for determining left ventricular hypertrophy in hypertrophic cardiomyopathy: analysis of 57 patients studied at necropsy. *Am J Med* 1989;87:377–81.
- Biagini E, Pazzi C, Olivetto I, *et al.* Usefulness of electrocardiographic patterns at presentation to predict long-term risk of cardiac death in patients with hypertrophic cardiomyopathy. *Am J Cardiol* 2016;118:432–9.
- Box GEP, Tidwell PW. Transformation of the independent variables. *Technometrics* 1962;4:531–50.
- Sullivan LM, Massaro JM, D'Agostino RB. Presentation of multivariate data for clinical use: the Framingham study risk score functions. *Stat Med* 2004;23:1631–60.
- Steyerberg EW, Harrell FE, Borsboom GJ, *et al.* Internal validation of predictive models: efficiency of some procedures for logistic regression analysis. *J Clin Epidemiol* 2001;54:774–81.
- Youden WJ. Index for rating diagnostic tests. *Cancer* 1950;3:32–5.
- Namdar M, Steffel J, Vidovic M, *et al.* Electrocardiographic changes in early recognition of Fabry disease. *Heart* 2011;97:485–90.
- O'Mahony C, Coats C, Cardona M, *et al.* Incidence and predictors of anti-bradycardia pacing in patients with Anderson-Fabry disease. *Europace* 2011;13:1781–8.
- Namdar M, Kampmann C, Steffel J, *et al.* Pq interval in patients with Fabry disease. *Am J Cardiol* 2010;105:753–6.
- Roudebush CP, Foerster JM, Bing OH. The abbreviated PR interval of Fabry's disease. *N Engl J Med* 1973;289:357–8.
- Linhart A, Elliott PM. The heart in Anderson-Fabry disease and other lysosomal storage disorders. *Heart* 2007;93:528–35.
- Rapezzi C, Arbustini E, Caforio ALP, *et al.* Diagnostic work-up in cardiomyopathies: bridging the gap between clinical phenotypes and final diagnosis. A position statement from the ESC Working group on myocardial and pericardial diseases. *Eur Heart J* 2013;34:1448–58.
- Namdar M. Electrocardiographic changes and arrhythmia in Fabry disease. *Front Cardiovasc Med* 2016;3:7.
- Frustaci A, Morgante E, Russo MA, *et al.* Pathology and function of conduction tissue in Fabry disease cardiomyopathy. *Circ Arrhythm Electrophysiol* 2015;8:799–805.
- Wu JC, Ho CY, Skali H, *et al.* Cardiovascular manifestations of Fabry disease: relationships between left ventricular hypertrophy, disease severity, and alpha-galactosidase A activity. *Eur Heart J* 2010;31:1088–97.
- Neubauer S, Kolm P, Ho CY, *et al.* Distinct subgroups in hypertrophic cardiomyopathy in the NHLBI HCM registry. *J Am Coll Cardiol* 2019;74:2333–45.
- Gosse P, Jan E, Coulon P, *et al.* ECG detection of left ventricular hypertrophy: the simpler, the better? *J Hypertens* 2012;30:990–6.
- Lakdawala NK, Thune JJ, Maron BJ, *et al.* Electrocardiographic features of sarcomere mutation carriers with and without clinically overt hypertrophic cardiomyopathy. *Am J Cardiol* 2011;108:1606–13.
- al-Mahdawi S, Chamberlain S, Chojnowska L, *et al.* The electrocardiogram is a more sensitive indicator than echocardiography of hypertrophic cardiomyopathy in families with a mutation in the MYH7 gene. *Br Heart J* 1994;72:105–11.
- Dumont CA, Monserrat L, Soler R, *et al.* Interpretation of electrocardiographic abnormalities in hypertrophic cardiomyopathy with cardiac magnetic resonance. *Eur Heart J* 2006;27:1725–31.
- Moon JCC, Sachdev B, Elkington AG, *et al.* Gadolinium enhanced cardiovascular magnetic resonance in Anderson-Fabry disease. Evidence for a disease specific abnormality of the myocardial interstitium. *Eur Heart J* 2003;24:2151–5.
- Quarta G, Aquaro GD, Pedrotti P, *et al.* Cardiovascular magnetic resonance imaging in hypertrophic cardiomyopathy: the importance of clinical context. *Eur Heart J Cardiovasc Imaging* 2018;19:601–10.
- Niemann M, Hartmann T, Namdar M, *et al.* Cross-sectional baseline analysis of electrocardiography in a large cohort of patients with untreated Fabry disease. *J Inherit Metab Dis* 2013;36:873–9.
- Takenaka T, Teraguchi H, Yoshida A, *et al.* Terminal stage cardiac findings in patients with cardiac Fabry disease: an electrocardiographic, echocardiographic, and autopsy study. *J Cardiol* 2008;51:50–9.
- Mehta A, Ricci R, Widmer U, *et al.* Fabry disease defined: baseline clinical manifestations of 366 patients in the Fabry outcome survey. *Eur J Clin Invest* 2004;34:236–42.
- Maurizi N, Rella V, Fumagalli C, *et al.* Prevalence of cardiac amyloidosis among adult patients referred to tertiary centres with an initial diagnosis of hypertrophic cardiomyopathy. *Int J Cardiol* 2020;300:191–5.
- Guttmann OP, Rahman MS, O'Mahony C, *et al.* Atrial fibrillation and thromboembolism in patients with hypertrophic cardiomyopathy: systematic review. *Heart* 2014;100:465–72.

The complex interplay between fitness, genetics, lifestyle, and inflammation in the pathogenesis of coronary atherosclerosis: lessons from the Amazon rainforest

Raffaello Ditaranto, Giovanni Vitale, Massimiliano Lorenzini, and Claudio Rapezzi

Cardiology, Department of Experimental, Diagnostic and Specialty Medicine, Alma Mater Studiorum-University of Bologna, Italy

KEYWORDS

Atherosclerosis;
Inflammation;
Environment;
Genetics

Far from only being a modern disease, atherosclerosis has also been reported also in ancient civilizations, as shown in some studies conducted on Mummies from different latitudes. Conventional cardiovascular (CV) risk factors can explain more than 90% of the attributable risk of coronary artery disease (CAD). In this regard, Tsimane Aborigenous of Amazon rainforest, conducting a subsistence lifestyle with low prevalence of CV risk factors, present the lowest reported prevalence of CAD in the world, despite an elevated inflammatory burden. Experimental and clinical studies have supported the theory that other factors, like genetics and inflammation, are involved in atherosclerosis. Indeed, a large clinical randomized study (CANTOS trial) tested the anti-inflammatory properties of canakinumab, and provided the first evidence to support the 'inflammation hypothesis'. Another field of research, based on Mendelian randomization studies, supports the appealing hypothesis that correcting CV risk factors earlier in life, may prevent or delay the progression of CAD. All these data prove that atherosclerosis is the expression of a complex, dynamic, and continuous interaction between environment and genetics that begins at conception and continues through adulthood.

Introduction

Throughout human history life expectancy has progressively increased. Infection and famine, reported for millennia as the primary causes of death in the world, still represent the main cause of death in developing countries. On the contrary, in recent centuries, cardiovascular (CV) death has become the main mortality cause in industrialized Countries. Conventional CV risk factors (cholesterol, smoking, arterial hypertension, and diabetes) can explain more than 90% of the attributable risk of coronary artery disease (CAD).¹ For this reason, international health organizations have been trying to design and implement different intervention strategies. Primary prevention with

meticulous risk factor control leads to a significant, consistent, and dose-related reduction in major adverse cardiac events. Nevertheless, other factors, such as genetic predisposition or inflammatory state, that are only partially modifiable, seem to be relevant determinants of CV risk.

Messages from Amazon rainforest

Despite a process of wild industrialization, there are still small populations around the world with a preindustrial lifestyle. The Tsimane of Bolivia are one of these groups, living in Amazon rainforest, maintaining a subsistence lifestyle of hunting, fishing, gathering, and farming. The Tsimane Health and Life History Project team (THLHP) has

been working with this population to understand the correlation between preindustrial lifestyle and low prevalence of CAD. A recent THLHP study, published on *Lancet*, evaluated prevalence of coronary atherosclerosis in the Tsimane, measured by coronary artery calcium (CAC) scoring with non-contrast computed tomography (CT).² Of 705 Tsimane indigenous considered (mean age: 57 years, male: 349, 50%), about 85% had no CAC, and only 3% had CAC scores higher than 100, suggestive of significant atherosclerotic disease. For individuals older than 75 years, 65% were free from atherosclerosis, and only 8% had CAC scores of 100 or more, with a five-fold lower prevalence than industrialized population ($P \leq 0.0001$). The prevalence of CV risk factors were low in all age groups. However, high-sensitivity C reactive protein (hs-CRP) was elevated (>3 mg/L) in about half the population (360, 51%), without differences across age groups. These data prove that Tsimane aborigines are the population with the lowest reported levels of CAD in the world. This seems to be related to subsistence lifestyle, intense physical activity, low prevalence of CV risk factors, a diet with low processed carbohydrates, and saturated fats. However, the Tsimane aborigines have a high inflammatory burden, related to infections and environmental exposure. The results of Kaplan *et al.*² partly contrast other studies according to which inflammation plays a central role in atherosclerosis. It is however possible, that inflammation, in presence of lifelong low LDL levels, might not potentiate atherosclerotic disease. From the Amazon rainforest, a number of lessons can be learnt:

- (1) Some populations with very low LDL levels from birth have a very low prevalence of CAD.
- (2) Age is an intrinsic and unmodifiable risk factor related to atherosclerosis, although with a smaller order of magnitude.
- (3) A healthy lifestyle is crucial for CV protection, even in the presence of a high inflammatory burden.
- (4) Inflammation is able to potentiate atherogenic effects of CV risk factors, but it is not able to determine atherosclerotic disease alone.

This study does not consider the possibility of a favourable genetic predisposition, and the hypothesis that environment and healthy lifestyle are only the tip of the iceberg of CV disease protection remains.

Messages from the past

The low prevalence of atherosclerosis described in a Bolivian population should not get our hopes up regarding the existence of a Paradise lost in the past where CV disease was absent. Far from being only a modern disease, atherosclerosis has been reported in ancient civilizations. To support this hypothesis, the Horus group first studied 52 ancient Egyptian adult mummies (mean estimated age: 38 years) by performing whole body multislice CT to identify arterial calcific deposits in arterial bed as equivalent of atherosclerosis.³ Among 44 mummies with identifiable CV structures, 20 (45%) had arterial calcifications, especially in the aortic wall, but also in coronary, iliac, femoral,

carotid, and peripheral arteries, with no significant gender differences (55% male, 45% female). Mummies with atherosclerotic calcification were generally older, and multivessel involvement (≥ 3 beds) was significantly more frequent in patients with ≥ 40 years.

The prevalence of CV risk factors in ancient Egypt is very difficult, nay impossible to evaluate: hypertension and diabetes mellitus cannot be estimated, and tobacco smoke was not present. Furthermore, mummification in ancient Egypt was reserved for elite members of society, Royals, and clergy. Based on the interpretation of hieroglyphs and representations, the authors suggest that a sedentary lifestyle and a lipid rich diet, especially amongst the clergy, played a central role in atherogenesis. However, we have to be careful to not extend these hypotheses to the entire population of ancient Egypt since these data belong to a small elite of society.

The Horus Team also conducted a similar, larger study, considering 137 mummies from different Ages through four millennia and from four different parts of the world (ancient Egypt, ancient Peru, Ancestral Puebloans of southwest America, and the Unangans of the modern-day Aleutian Islands), with a mean age of about 36-years.⁴ Once again, probable or definite atherosclerotic calcifications were found in a high number of mummies (47, 34%) using total body CT, especially in the aorta, without statistically significant differences among the four populations (38% in the Egyptians, 25% in the Peruvians, 40% in the Ancestral Puebloans, and 60% in the Unangans; $P = \text{NS}$). Atherosclerosis extension and severity were directly related to age, while there was not significant correlation to sex or historical period. Regarding atherosclerotic risk factors, there were differences in diet, climate and environment amongst these four populations. Tobacco was unavailable in these civilizations, but the authors speculated that inhalation of fire smoke could have had a part in the pathogenesis of atherosclerosis. However, chronic infections were common in all civilties, and it is likely that inflammation played a crucial role in the development of CAD. Again, the past can give us some interesting messages:

- (1) Atherosclerosis is not exclusively a disease of modern society, but it affected different ancient civilizations around the world. It seems to be a loyal companion of humankind throughout history, and not a characteristic of any specific diet or lifestyle.
- (2) A linear correlation exists between age and atherosclerotic disease. Older age mummies often present vascular calcification and more frequently show multivessel involvement.

Inflammation

Several lines of evidence (experimental models and population studies) support the notion that inflammation is involved in all stages of atherosclerosis. Different statin trials (REVERSAL, PROVE-IT and JUPITER) over the last decade have taught us that a reduction in hs-CRP levels—a marker of subclinical inflammation—is associated with improved CV outcomes, independently of modification of traditional risk factors. However, due to the duplicity of statin

drug action, affecting both LDL cholesterol and inflammatory pathways, it is not possible to state that therapy targeting inflammation *per se* can reduce CV events.

The first successful large scale clinical trial that addressed the 'inflammation hypothesis' was the CANTOS trial (Canakinumab Anti-Inflammatory Thrombosis Outcome Study).⁵ This randomized, double-blind trial enrolled 10 061 patients with previous myocardial infarction (MI) and a hs-CRP level ≥ 2 mg/L despite the use of aggressive secondary prevention strategies. Patients randomly received placebo or one of three doses of canakinumab, a fully human monoclonal antibody targeting interleukin-1 β , with an anti-inflammatory effect, that was previously approved for clinical use in rheumatologic disorders. The primary endpoint included non-fatal MI, non-fatal stroke, or CV death. In the canakinumab group, there was a significantly reduction of hs-CRP levels from baseline compared to the placebo group, without reduction of LDL cholesterol levels but only the 150 mg dose resulted in a significant reduction (15%) of the primary endpoint. These open the way to an era of 'precision medicine', where specific therapeutic strategies are tailored according to the single patient's needs, based on simple biomarkers. Currently, the standard of care for secondary prevention in survivors of acute coronary syndromes includes high-dose statins (plus ezetimibe when needed), anti-platelet drugs, beta-blockers, and myocardial revascularization. Despite optimal medical therapy, many patients continue to experience life-threatening CV events—due to what is known as 'residual risk'—partly due to the insufficient LDL-C lowering ('residual cholesterol risk'), and partly due to an inflammatory component ('residual inflammatory risk').⁶ Nowadays we can face residual risk by lowering LDL-C further with the use of proprotein convertase subtilisin/kexin type 9 (PCSK9) inhibitors—as shown in FOURIER trial⁷—in patients with suboptimal cholesterol control and, in near future possibly further reduce the residual inflammatory risk by inhibiting inflammation downstream.

Genetics and environment

Cardiovascular diseases are the expression of a complex and dynamic interaction between environment and genetics that begins at conception and continues through adulthood. Several environmental variables, such as tobacco exposure, diet, psychosocial stressors, alcohol consumption, and physical inactivity, increase CV risk; however, quantifying the impact of each one, with any precision, is difficult. On the other hand, genetic background influences the atherogenic process: with the exception of monogenic familial hypercholesterolaemias, atherosclerosis is generally a polygenic disease. Genome-wide association studies have recently identified more than 60 genomic regions where single nucleotide polymorphisms affect inherited CV risk. At any particular point in life, each genotype can lead to different phenotypes, according to the particular individual's environmental niche: a patient with a low-risk genotype might develop disease because of adverse environmental exposures. On the other hand, an individual with a high-risk genotype might remain healthy thanks to

beneficial exogenous elements. During lifetime, environmental factors might modify CV risk through epigenetic or transcriptional mechanisms that regulate gene expression, or by directly affecting metabolic pathways. The study by Allam *et al.*³ on the Tsimane does not consider the genetic substratum. However, it is likely that not only a healthy lifestyle but also a protective genetic background, perpetuated generation by generation thanks to the Tsimane's isolation, can explain the extreme low prevalence of atherosclerosis in these aborigines.

Mendelian randomization and lifetime exposure to cardiovascular risk factors

Investigators have recently developed a novel epidemiological study design that can be used to investigate potential risk factors for specific outcomes: Mendelian randomization (MR). These studies were designed to demonstrate whether an outcome of interest (e.g. CV events) is more common in individuals with a risk allele (e.g. LDLR genetic variant) than in those without the allele. Because the risk allele is strictly associated with a risk factor (intermediate variable) of interest (e.g. LDL cholesterol blood levels), it can be shown that the presence of the risk factor is likely a causal factor for the outcome of interest. Anyway, thanks to the experience from families carrying LDL receptor mutations and from the multiple epidemiological and interventional studies, the causal role for LDL in promoting CV diseases had been well-established long before MR studies were conducted. However, an advantage of the MR approach is that it can provide information on the impact of a lifetime modulation of a biomarker, unlike clinical trials that often follow their patients only for a few years.

In this respect, MR studies showed that variants in the LDL receptor gene, increasing LDL cholesterol level from childhood, result in stronger effects on CV risk than predicted by epidemiological or clinical studies. On the contrary, individuals carrying a rare PCSK9 allele, which lowers LDL levels below population average, have a significantly lower incidence of MI. Ference *et al.*⁸ have recently estimated the effect of long-term exposure to lower LDL-C on the risk of CV disease, mediated by nine polymorphisms in six different genes known to be associated with lower LDL-C. They found that prolonged exposure to lower LDL-C, beginning early in life, is associated with a substantially greater reduction in the risk of CV disease than that observed in clinical trials involving statin therapies given over shorter periods of time and later in life. All this evidence demonstrates that both the magnitude and lengths of exposure to low LDL-C have an important effect on the risk of CV disease, confirming not only the rule that the lower the better but also the earlier the better. In fact, it is known that coronary atherosclerosis is a chronic and progressive disease that begins early in life and develops slowly over several decades before becoming clinically manifest.

Conclusions

The interesting findings from the Tsimane study need to be integrated with the current knowledge of traditional CV

risk factors in western countries, the findings from MR studies and from intervention trials focusing on lipid lowering therapies and anti-inflammatory drugs.

The genetic profile of this population was not investigated, so it remains unknown whether the low prevalence of atherosclerosis is a consequence of the peculiar lifestyle or of genetic background. Despite the fact that the hypothesis of a protective genetic heritage is attractive, a widespread protection against atherosclerosis in the Tsimanes probably depends on their healthy lifestyle. Prevention strategies should therefore be encouraged and started from a young age with educational strategies promoting a healthy lifestyle.

Conflict of interest: none declared.

References

1. Yusuf S, Hawken S, Ounpuu S, Dans T, Avezum A, Lanas F, McQueen M, Budaj A, Pais P, Varigos J, Lisheng L. Effect of potentially modifiable risk factors associated with myocardial infarction in 52 countries (the INTERHEART study): case-control study. *Lancet* 2004;**364**: 937-952.
2. Kaplan H, Thompson RC, Trumble BC, Wann LS, Allam AH, Beheim B, Frohlich B, Sutherland ML, Sutherland JD, Stieglitz J, Rodriguez DE, Michalik DE, Rowan CJ, Lombardi GP, Bedi R, Garcia AR, Min JK, Narula J, Finch CE, Gurven M, Thomas GS. Coronary atherosclerosis in indigenous South American Tsimane: a cross-sectional cohort study. *Lancet* 2017;**389**:1730-1739.
3. Allam AH, Thompson RC, Wann LS, Miyamoto MI, Nur el-Din A. e-H, el-Maksoud GA, Al-Tohamy Soliman M, Badr I, el-Rahman Amer HA, Sutherland ML, Sutherland JD, Thomas GS. Atherosclerosis in ancient Egyptian Mummies. The Horus Study. *JACC Cardiovasc Imaging* 2011;**4**:315-327.
4. Thompson RC, Allam AH, Lombardi GP, Wann LS, Sutherland ML, Sutherland JD, Soliman MA-T, Frohlich B, Mininberg DT, Monge JM, Vallodolid CM, Cox SL, Abd el-Maksoud G, Badr I, Miyamoto MI, el-Halim Nur el-Din A, Narula J, Finch CE, Thomas GS. Atherosclerosis across 4000 years of human history: the Horus study of four ancient populations. *Lancet* 2013;**381**:1211-1222.
5. Ridker PM, Everett BM, Thuren T, MacFadyen JG, Chang WH, Ballantyne C, Fonseca F, Nicolau J, Koenig W, Anker SD, Kastelein JJP, Cornel JH, Pais P, Pella D, Genest J, Cifkova R, Lorenzatti A, Forster T, Kobalava Z, Vida-Simiti L, Flather M, Shimokawa H, Ogawa H, Dellborg M, Rossi PRF, Troquay RPT, Libby P, Glynn RJ. Antiinflammatory therapy with canakinumab for atherosclerotic disease. *N Engl J Med* 2017;**377**:1119-1131.
6. Ridker PM. Residual inflammatory risk: addressing the obverse side of the atherosclerosis prevention coin. *Eur Heart J* 2016;**37**:1720-1722.
7. Sabatine MS, Giugliano RP, Keech AC, Honarpour N, Wiviott SD, Murphy SA, Kuder JF, Wang H, Liu T, Wasserman SM, Sever PS, Pedersen TR. Evolocumab and clinical outcomes in patients with cardiovascular disease. *N Engl J Med* 2017;**376**:1713-1722.
8. Ference BA, Yoo W, Alesh I, Mahajan N, Mirowska KK, Mewada A, Kahn J, Afonso L, Williams KA, Flack JM. Effect of long-term exposure to lower low-density lipoprotein cholesterol beginning early in life on the risk of coronary heart disease: a Mendelian randomization analysis. *J Am Coll Cardiol* 2012;**60**:2631-2639.

CARDIOVASCULAR IMAGES

Cum Grano Salis

Cardiac Sarcoidosis as a Perfect Mimic of Arrhythmogenic Right Ventricular Cardiomyopathy

Giulia Saturi, MD*; Angelo Giuseppe Caponetti, MD*; Ornella Leone, MD; Luigi Lovato, MD; Simone Longhi¹, MD, PhD; Maddalena Graziosi, MD, PhD; Raffaello Ditaranto, MD; Mauro Biffi¹, MD; Nazzareno Galiè, MD; Elena Biagini¹, MD, PhD

A forty-four-year-old man, overweight (body mass index, 27.5 kg/m²), former smoker, and with hypertension came to medical attention for dyspnea and reduced exercise tolerance. No comorbidities or family history for cardiac disease or sudden death were present. Physical examination and blood tests were normal. The ECG showed respiratory sinus arrhythmia, anterior and inferior pseudonecrosis pattern, incomplete right bundle branch block with terminal activation delay detectable as positive terminal wave in V₁ through V₃ in III and aVR, small and round s wave in the lateral leads (I, aVL, and V₆), and negative T waves in V₁ through V₆ (Figure 1A). The echocardiogram showed mild left ventricular (LV) hypertrophy with systolic dysfunction (interventricular septum [IVS] and posterior wall, 13 and 12 mm, respectively; indexed end-diastolic volume, 51 mL/m²; ejection fraction [EF], 48%) and severe right ventricular (RV) dilation and dysfunction (end-diastolic area, 49 cm²; fractional area change, 17%; tricuspid annular plane systolic excursion, 10 mm; Figure 1B through 1D). Coronary angiography excluded significant coronary artery disease. Cardiac magnetic resonance confirmed severe RV dilation (132 mL/m²) and systolic dysfunction (RV EF, 32%) with localized dyskinetic areas in the free and diaphragmatic walls, as well as in the outflow tract. The LV was moderately hypokinetic (LV EF, 44%) with a moderate increase of septal and lateral wall thickness (IVS, 14 mm; Movies I and II in the [Data Supplement](#)).

Native T1 mapping, performed using a modified Look-Locker inversion recovery sequence, showed increased values particularly in the medium IVS (1100 ms; normal values, 980±25 ms). T2-weighted images (short-tau inversion recovery) showed diffuse edema of the RV and right side of the IVS, whereas a patchy distribution was present in the left side of the IVS and in the LV lateral and inferior walls. Late gadolinium enhancement using a phase-sensitive inversion recovery was present in all the aforementioned segments. Rest perfusion-weighted images documented septal hypoperfusion (Figures 2A through 2F and 3A). Patient phenotype fulfilled the diagnostic 2010 Task Force criteria for arrhythmogenic RV cardiomyopathy with mild LV involvement and signs of acute myocarditis. However, the unusual high inflammatory burden at cardiac magnetic resonance and the patchy, focal LV involvement triggered further diagnostic workup and an endomyocardial biopsy (EMB) was performed. Unexpectedly, severe diffuse inflammatory process characterized by non-necrotizing granulomas and isolated giant cells was detected, compatible with cardiac sarcoidosis; moderate-to-severe myocardial fibrosis was also present (Figure 4A through 4H). High-resolution computed tomography scan showed no signs of pulmonary or lymph node involvement. After administering a high dose of corticosteroid therapy, the patient underwent a positron emission tomography with 18F-fluorodeoxyglucose that showed no signs of active inflammation.

Key Words: arrhythmogenic right ventricular dysplasia ■ exercise tolerance ■ inflammation ■ myocarditis ■ sarcoidosis

Correspondence to: Elena Biagini, MD, PhD, Cardiology Unit, St. Orsola Hospital, IRCCS Azienda Ospedaliero-Universitaria di Bologna, Via Giuseppe Massarenti N9, Bologna 40138, Italy. Email elena.biagini73@gmail.com

*G. Saturi and A. Giuseppe Caponetti contributed equally.

The Data Supplement is available at <https://www.ahajournals.org/doi/suppl/10.1161/CIRCIMAGING.120.012355>.

For Sources of Funding and Disclosures, see page 664.

© 2021 American Heart Association, Inc.

Circulation: Cardiovascular Imaging is available at www.ahajournals.org/journal/circimaging

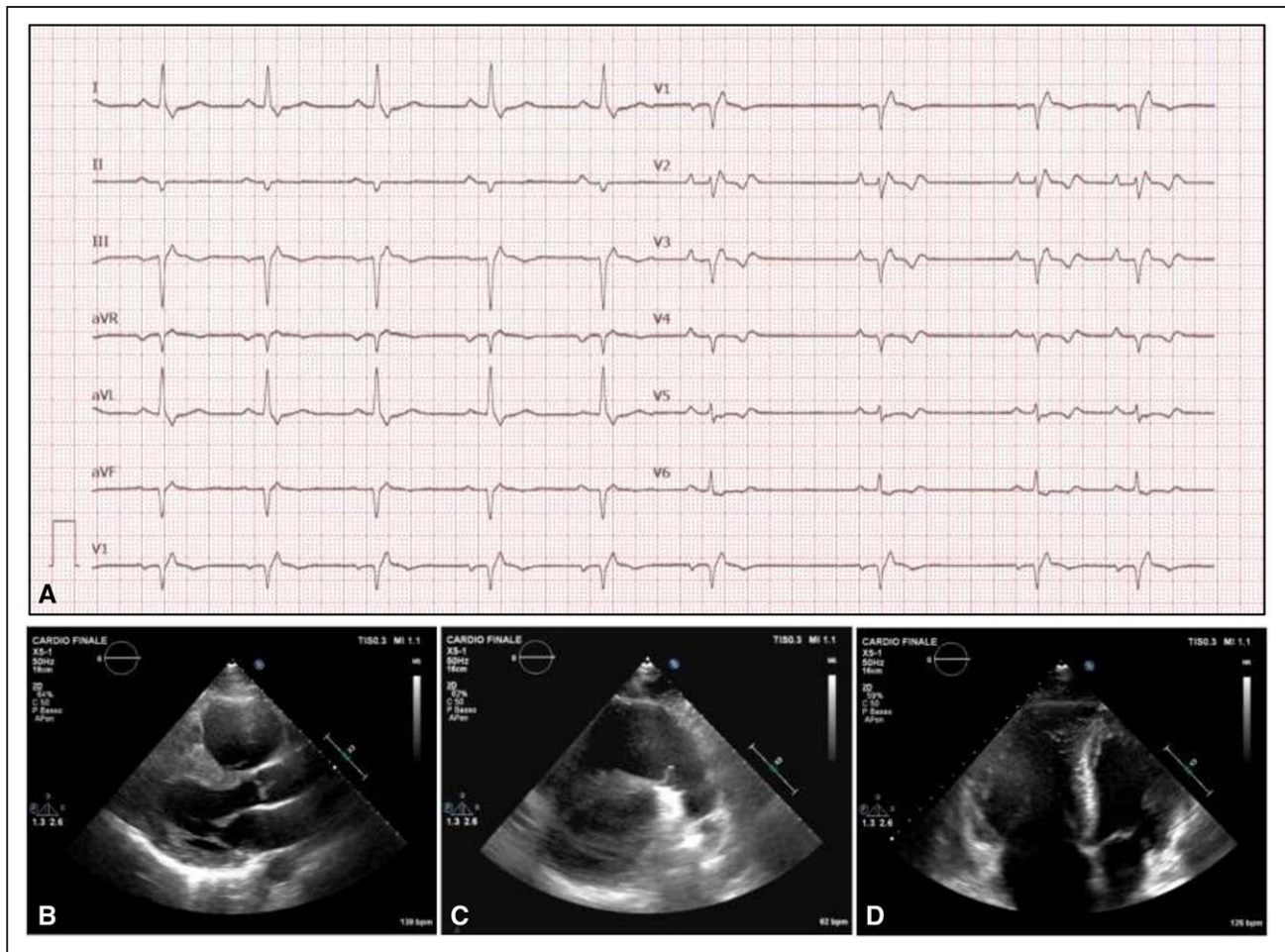


Figure 1. Electrocardiogram and echocardiogram at first evaluation.

A, Standard 12-lead ECG. **B**, Echocardiogram parasternal long-axis view. **C**, Parasternal short-axis view focusing the right ventricular outflow tract. **D**, Apical 4-chamber view.

The patient was discharged, and after 1 month, cardiac magnetic resonance and EMB were repeated. Mild improvement of biventricular function (RV EF, 38%; LV EF, 52%) and an important global reduction of edema were detected. In particular, there was a marked reduction of wall thickness (IVS, 11 mm) and a decrease of native T1 mapping values (mean value, 990 ms with a maximum value of 1042 ms in the IVS; Figure 3B) with normal T2 mapping values confirming the edema resolution (mean value, 57 ms; normal values, <60 ms). Persistent patchy late gadolinium enhancement indicated the presence of myocardial fibrosis in the RV, IVS, and inferior LV wall (Figure 5A through 5F). EMB showed resolution of granulomatous myocarditis: only few focal macrophages and mild-to-moderate myocardial and sub-endocardial fibrosis were detected (Figure 6A through 6C). Due to the persistence of RV dysfunction and the presence of diffuse fibrosis, a dual-chamber implantable cardioverter defibrillator was implanted for primary prevention of sudden cardiac death. At 1-year follow-up, the patient was New York Heart Association class II, LV EF was 50%, and RV fractional area change was 28%.

Interrogation of the implantable defibrillator showed periods of nonsustained ventricular tachycardia.

Sarcoidosis is a multisystem inflammatory disorder characterized by epithelioid noncaseating granulomas as histological hallmark. Lungs are frequently involved, but heart, skin, eyes, kidney, lymph nodes, and central nervous system can be affected as well. Cardiac involvement has been reported in 25% of patients with systemic sarcoidosis although the isolated cardiac presentation is rare but possible. Cardiac sarcoidosis foreshadows a worse prognosis and accounts for substantial mortality and morbidity. It predominantly involves the LV, and clinical features include atrioventricular blocks, arrhythmias, or heart failure; primary RV involvement is rare and difficult to diagnose.¹

Arrhythmogenic right ventricular cardiomyopathy is a primary, genetically based, heart muscle disease that shares with sarcoidosis a challenging diagnosis due to the rarity of these conditions, the patchy and nonischemic regional wall motion abnormalities, and the inflammatory phase fluctuations.² Furthermore, a possible interplay in the molecular substrate has been reported since sarcoidosis may exhibit a similar pattern of reduced plakoglobin

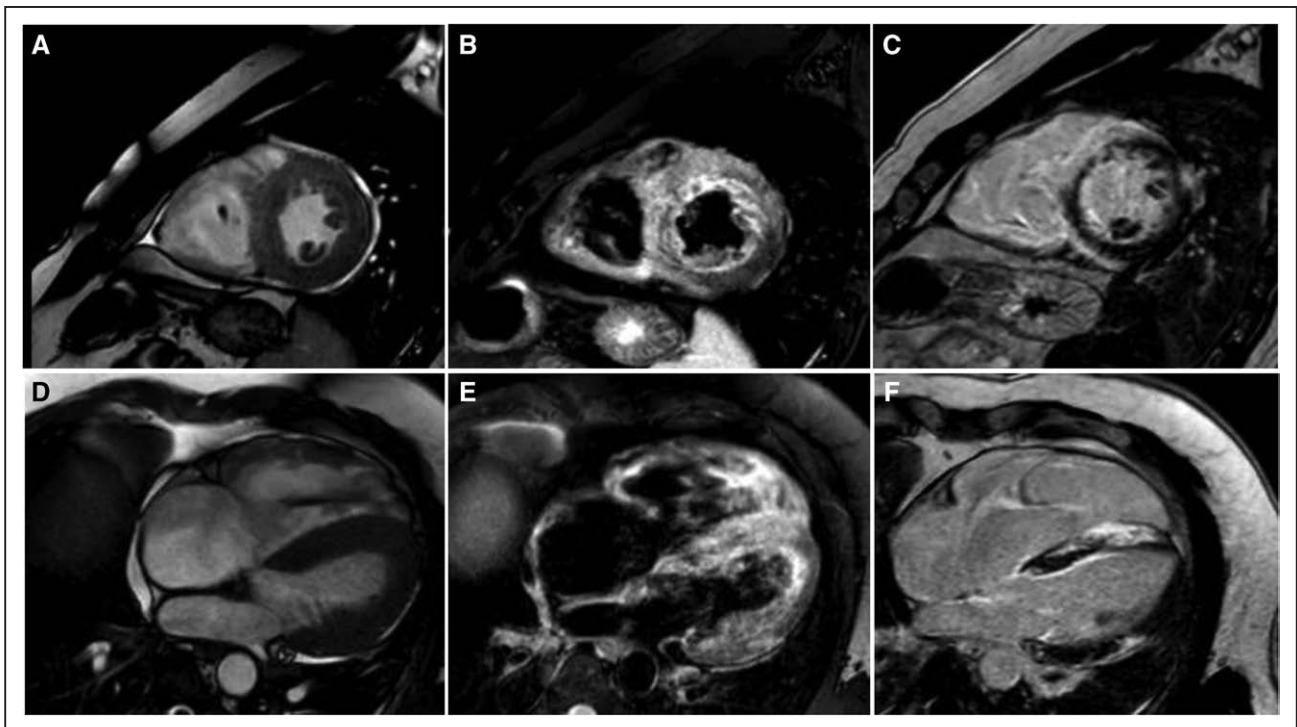


Figure 2. Cardiac magnetic resonance at first clinical presentation.

A, Short-axis end-diastolic cine image. **B,** T2-weighted short-axis view. **C,** Late gadolinium enhancement short-axis view. **D,** Four-chamber end-diastolic cine image. **E,** T2-weighted 4-chamber view. **F,** Late gadolinium enhancement 4-chamber view.

staining in the absence of any mutations linked to ARVC. Moreover, several studies have demonstrated the leading role of inflammation in ARVC as trigger for fibrofatty infiltration or consequence of the apoptotic process. This inflammatory theory has been confirmed by histology (inflammatory cell infiltrates in 60%–74% of ARVC) and by resonance imaging studies. The diagnosis of ARVC is based on a scoring system that combines clinical,

instrumental, histopathologic, and genetic tools.² However, none of these findings have a specific or unique diagnostic value, and the algorithm identifies more a right-sided cardiomyopathy phenotype rather than a definite etiology. Cardiac sarcoidosis can closely mimic ARVC, and in doubtful cases, EMB can provide the definite diagnosis. In a prospective study conducted by Vasaiwala et al³ on consecutive patients with suspected

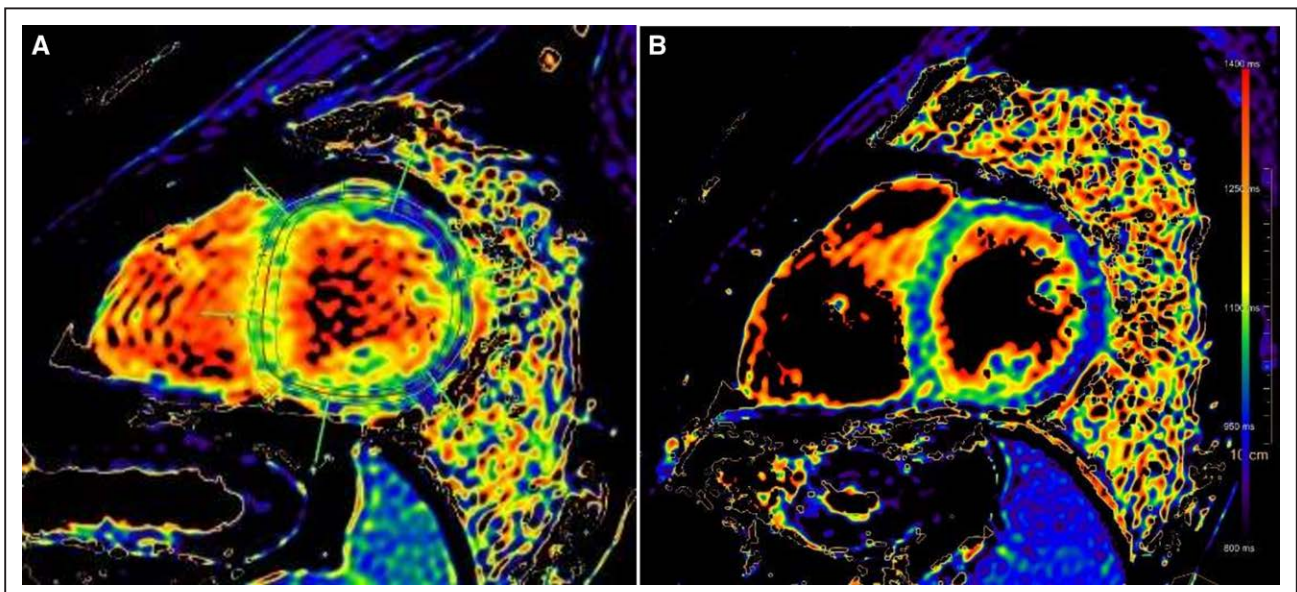


Figure 3. Cardiac magnetic resonance T1 mapping sequence.

A, First cardiac magnetic resonance. **B,** Cardiac magnetic resonance at 1-mo follow-up.

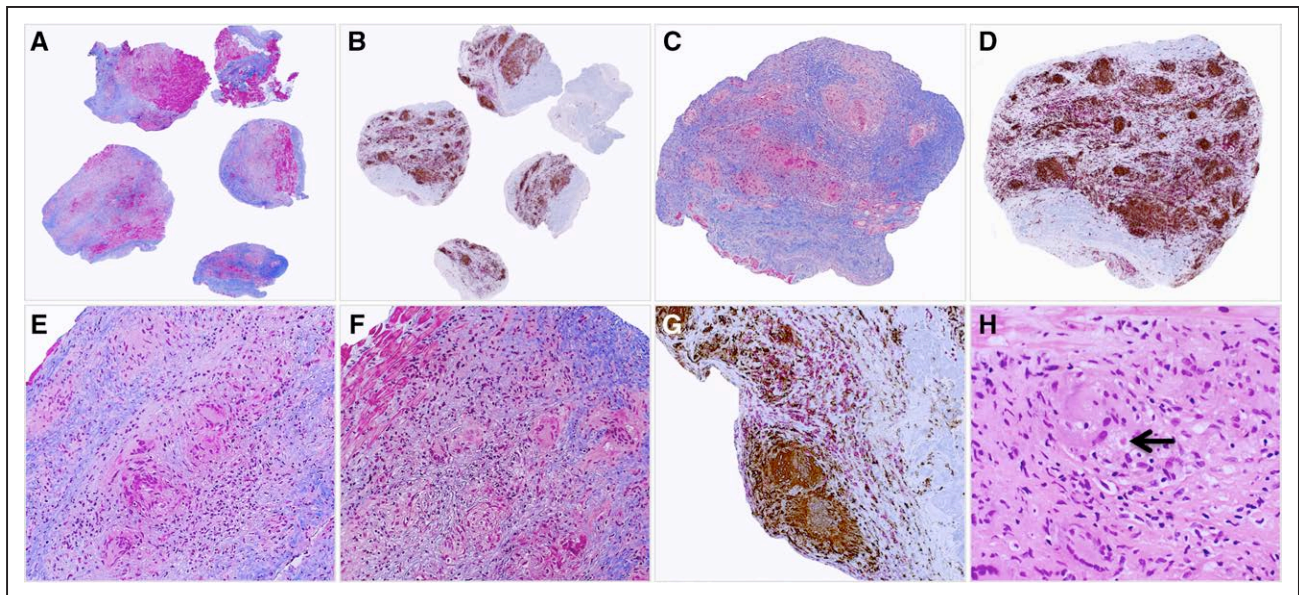


Figure 4. Endomyocardial biopsy.

A and **B**, Severe and diffuse inflammatory process: (**A**) Azan Mallory trichrome 25 \times and (**B**) CD68+ macrophages in brown, CD3 T lymphocytes in red 25 \times . **C** and **D**, Macrophagic granulomas and giant cells, surrounded by T lymphocytes and severe myocardial fibrosis: (**C**) Azan Mallory trichrome 50 \times and (**D**) double CD68/CD3 immunostaining 50 \times . **E–G**, Isolated and well-defined granulomas with epithelioid pattern and absence of necrotizing or caseating areas: (**E** and **F**) Azan Mallory trichrome 200 \times and (**G**) double CD68/CD3 immunostaining 200 \times . **H**, Giant cells show asteroid bodies (arrow) in the cytoplasm, hematoxylin-eosin: H 400 \times . CD indicates cluster differentiation.

ARVC evaluated by a standard protocol including EMB, a histological evidence of sarcoidosis was found in 15% of the patients with a definite diagnosis of ARVC.

In this clinical case, a disproportionate inflammation and the patchy LV and IVS distribution at cardiac

magnetic resonance raised the suspicion of an alternative etiology and led to the correct diagnosis of cardiac sarcoidosis.

Keeping in mind a global vision of the patient with a cardiomyopathy-oriented attitude and identifying red

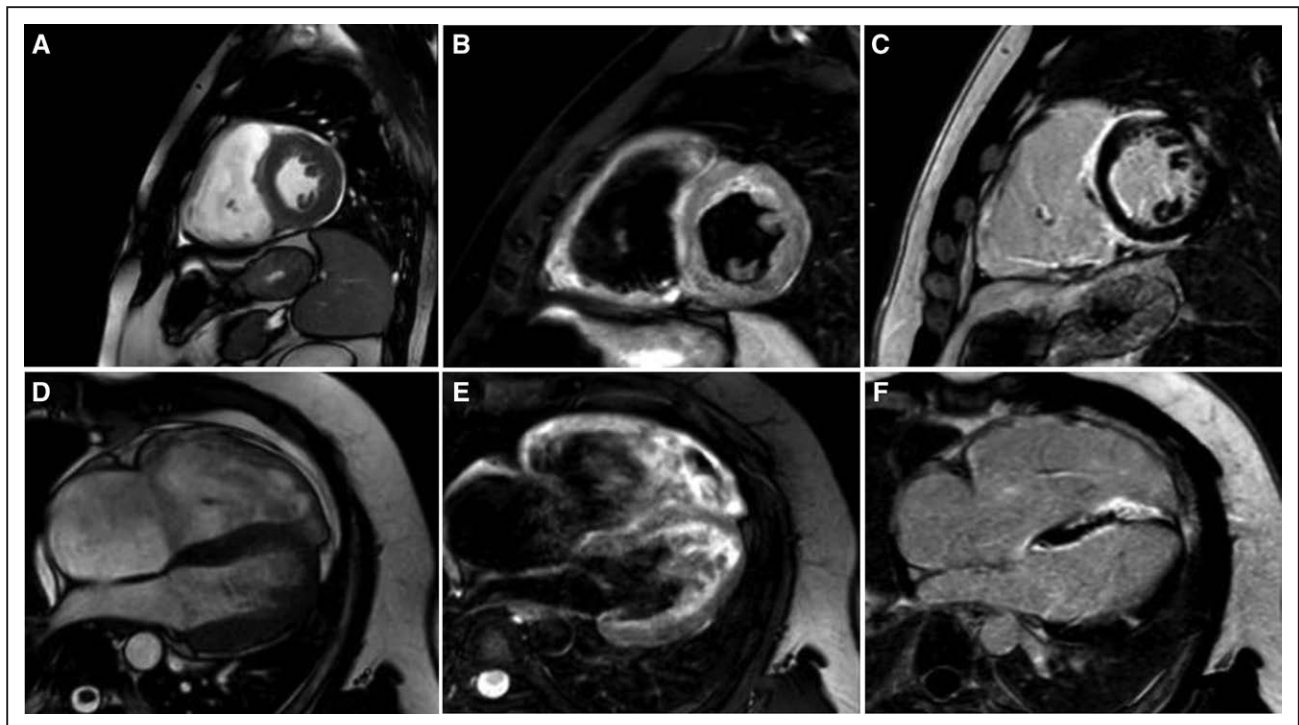


Figure 5. Cardiac magnetic resonance at 1-mo follow-up.

A, Short-axis end-diastolic cine image. **B**, T2-weighted short-axis view. **C**, Late gadolinium enhancement short-axis view. **D**, Four-chamber end-diastolic cine image. **E**, T2-weighted 4-chamber view. **F**, Late gadolinium enhancement 4-chamber view.

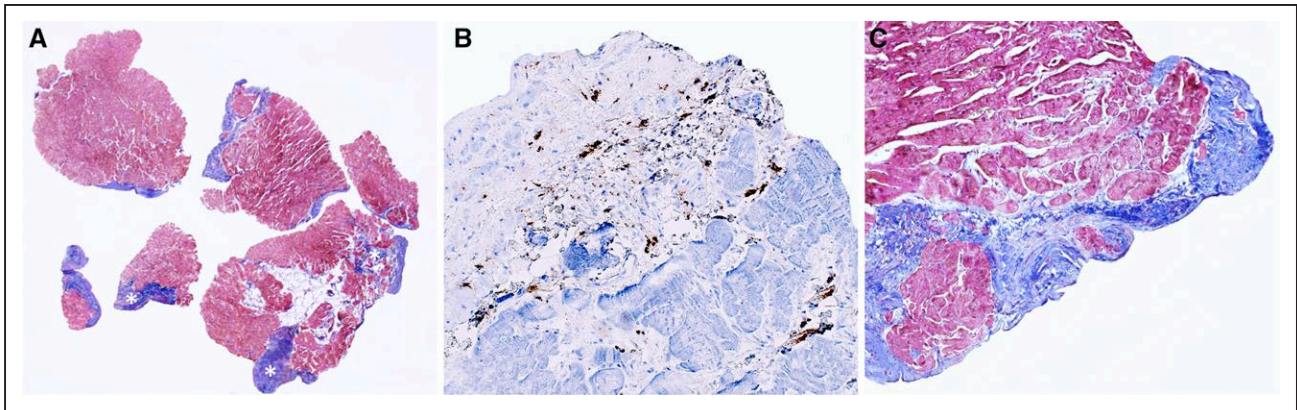


Figure 6. Endomyocardial biopsy at 1-mo follow-up.

A and **B**, Moderate subendocardial and mild myocardial fibrosis: (**A**) Azan Mallory trichrome, 25 \times and (**B**) Azan Mallory trichrome, 100 \times . **C**, Inflammation resolution with only few residual macrophages (in brown) in a limited fibrotic area, CD68 immunostaining, 200 \times . CD indicates cluster differentiation.

flags and discrepancies in the different phenotypes can be crucial to guide the clinical decision-making.⁴

Supplemental Materials

Data Supplement Movies I and II

ARTICLE INFORMATION

Affiliations

Cardiology Unit, Cardio-Thoracic-Vascular Department, St. Orsola Hospital, IRCCS Azienda Ospedaliero-Universitaria di Bologna, Italy (G.S., A.G.C., S.L., M.G., R.D., M.B., N.G., E.B.). Department of Experimental, Diagnostic and Specialty Medicine, University of Bologna, Italy (G.S., A.G.C., R.D., N.G.) Cardio-Thoracic Radiology Unit, Cardio-Thoracic-Vascular Department, St. Orsola Hospital, IRCCS Azienda Ospedaliero-Universitaria di Bologna, Italy (L.L.), Cardiovascular Pathology Unit, Department of Pathology, St. Orsola Hospital, IRCCS Azienda Ospedaliero-Universitaria di Bologna, Italy (O.L.).

Sources of Funding

None.

Disclosures

None.

REFERENCES

1. Birnie DH, Nery PB, Ha AC, Beanlands RS. Cardiac sarcoidosis. *J Am Coll Cardiol*. 2016;68:411–421. doi: 10.1016/j.jacc.2016.03.605
2. Marcus FI, McKenna WJ, Sherrill D, Basso C, Bauce B, Bluemke DA, Calkins H, Corrado D, Cox MG, Daubert JP, et al. Diagnosis of arrhythmogenic right ventricular cardiomyopathy/dysplasia: proposed modification of the task force criteria. *Circulation*. 2010;121:1533–1541. doi: 10.1161/CIRCULATIONAHA.108.840827
3. Vasaiwala SC, Finn C, Delpriore J, Leya F, Gagermeier J, Akar JG, Santucci P, Dajani K, Bova D, Picken MM, et al. Prospective study of cardiac sarcoid mimicking arrhythmogenic right ventricular dysplasia. *J Cardiovasc Electrophysiol*. 2009;20:473–476. doi: 10.1111/j.1540-8167.2008.01351.x
4. Protonotarios A, Elliott PM. Arrhythmogenic cardiomyopathy: a disease or Merely a phenotype? *Eur Cardiol*. 2020;15:1–5. doi: 10.15420/ecr.2019.05

ARTICLE OPEN



Circulating miR-184 is a potential predictive biomarker of cardiac damage in Anderson–Fabry disease

Irene Salamon ^{1,2,12}, Elena Biagini^{3,12}, Paolo Kunderfranco ¹, Roberta Roncarati^{4,5}, Manuela Ferracin ⁶, Nevio Taglieri³, Elena Nardi ^{3,6}, Noemi Laprovitera ⁶, Luciana Tomasi⁶, Marisa Santostefano⁷, Raffaello Ditaranto^{3,6}, Giovanni Vitale^{3,6}, Elena Cavarretta^{8,9}, Antonio Pisani¹⁰, Eleonora Riccio¹⁰, Valeria Aiello^{6,7}, Irene Capelli^{6,7}, Gaetano La Manna^{6,7}, Nazzareno Galie^{3,6}, Letizia Spinelli ¹¹✉ and Gianluigi Condorelli ^{1,2}✉

© The Author(s) 2021

Enzyme replacement therapy (ERT) is a mainstay of treatment for Anderson–Fabry disease (AFD), a pathology with negative effects on the heart and kidneys. However, no reliable biomarkers are available to monitor its efficacy. Therefore, we tested a panel of four microRNAs linked with cardiac and renal damage in order to identify a novel biomarker associated with AFD and modulated by ERT. To this end, 60 patients with a definite diagnosis of AFD and on chronic ERT, and 29 age- and sex-matched healthy individuals, were enrolled by two Italian university hospitals. Only miR-184 met both conditions: its level discriminated untreated AFD patients from healthy individuals (c -statistic = 0.7522), and it was upregulated upon ERT ($P < 0.001$). On multivariable analysis, miR-184 was independently and inversely associated with a higher risk of cardiac damage (odds ratio = 0.86; 95% confidence interval [CI] = 0.76–0.98; $P = 0.026$). Adding miR-184 to a comprehensive clinical model improved the prediction of cardiac damage in terms of global model fit, calibration, discrimination, and classification accuracy (continuous net reclassification improvement = 0.917, $P < 0.001$; integrated discrimination improvement [IDI] = 0.105, $P = 0.017$; relative IDI = 0.221, 95% CI = 0.002–0.356). Thus, miR-184 is a circulating biomarker of AFD that changes after ERT. Assessment of its level in plasma could be clinically valuable in improving the prediction of cardiac damage in AFD patients.

Cell Death and Disease (2021)12:1150; <https://doi.org/10.1038/s41419-021-04438-5>

INTRODUCTION

Anderson–Fabry disease (AFD) is a rare X-linked lysosomal storage disorder caused by mutations of the alpha-galactosidase A gene (GLA), located on the X chromosome (Xq22.1). Deficiency of GLA causes accumulation of a neutral glycosphingolipid, globotriaosylceramide (Gb3), in the lysosomes of various tissues and organs, including the vascular endothelium, kidneys, heart, eyes, skin, and nervous system [1]. The spectrum of clinical presentation is extremely broad. The disease has an early onset, usually in childhood, and its classical phenotype is characterized by neuropathic pain, angiokeratomas, cornea verticillata, and gastrointestinal disturbances [2]; after the third decade of life, cardiac involvement, renal failure, and cerebrovascular events may occur and are the major causes of morbidity and mortality [3]. In contrast, non-classical AFD presents with a milder, later onset and a variable phenotype, usually with the manifestation of cardiac disease. In addition, as a consequence of random X-chromosome inactivation (lyonization), heterozygous females present with

variable clinical manifestations, ranging from an almost absence of symptoms to very severe pathologies similar to those observed in males, albeit usually with a later onset [4].

Enzyme replacement therapy (ERT) and oral pharmacologic chaperones are the specific treatments for AFD. The most-used recombinant enzyme (either agalsidase alpha or beta) is intravenously administered to restore missing enzymatic function, so reducing the accumulation of Gb3 in tissues and slowing down disease progression [5]. Pharmacologic intervention before the occurrence of irreversible manifestations is crucial for improving biochemical response and outcome [6]. Indeed, organ transplant may represent the only therapeutic option for advanced AFD.

Recently, globotriaosylsphingosine (lyso-Gb3), which accumulates in the plasma of AFD patients, has been proposed as a diagnostic biomarker [7] and has become part of a panel of variables used to decide the optimal time to initiate therapy [8–10]. However, the relationship between lyso-Gb3 and organ damage is still uncertain [11]. The discovery of circulating

¹Humanitas Research Hospital – IRCCS, 20089 Rozzano, (MI), Italy. ²Department of Biomedical Sciences, Humanitas University, 20090 Pieve Emanuele, (MI), Italy. ³Cardiology Unit, St. Orsola Hospital, IRCCS Azienda Ospedaliero-Universitaria di Bologna, 40138 Bologna, Italy. ⁴Institute of Genetics and Biomedical Research – Milan Unit, National Research Council of Italy, 20089 Rozzano, (MI), Italy. ⁵Department of Morphology, Surgery and Experimental Medicine, University of Ferrara, 44121 Ferrara, Italy. ⁶Department of Experimental, Diagnostic and Specialty Medicine (DIMES), University of Bologna, 40138 Bologna, Italy. ⁷Nephrology, Dialysis and Renal Transplant Unit, St. Orsola Hospital, IRCCS Azienda Ospedaliero-Universitaria di Bologna, 40138 Bologna, Italy. ⁸Department of Medico-Surgical Sciences and Biotechnologies, University of Rome Sapienza, 04100 Latina, Italy. ⁹Mediterranea Cardiocentro, 80122 Naples, Italy. ¹⁰Department of Public Health – Nephrology Unit, University of Naples Federico II, 80131 Naples, Italy. ¹¹Department of Advanced Biomedical Sciences, University of Naples Federico II, 80131 Naples, Italy. ¹²These authors contributed equally: Irene Salamon, Elena Biagini. ✉email: letspine@unina.it; gianluigi.condorelli@hunimed.eu

Edited by Professor Sergio Lavandero

Received: 1 July 2021 Revised: 17 November 2021 Accepted: 25 November 2021

Published online: 11 December 2021

biomarkers associated with organ damage and modulated by ERT could be clinically useful in improving risk stratification and monitoring ERT efficacy in AFD patients. Small non-coding RNAs, such as microRNAs (miRNAs), could be used for this purpose. They are acknowledged to regulate gene expression and have been implicated in many physiological and pathological processes, like cell regulation [12], cancer [13], cardiovascular diseases [14], and renal dysfunction [15]. Several miRNAs have been shown to contribute to the development and progression of cardiovascular diseases, including heart failure [16], myocardial infarction [17], cardiomyopathies [18], arrhythmias [19], and atherosclerosis [20], as well as renal conditions [21]. Moreover, miRNAs are secreted as part of the cargo of microvesicles or exosomes from a variety of cell types, are released from damaged cells, and can be taken up by recipient cells [22]. Importantly, when they are released into body fluids, they are protected from RNase-mediated degradation by multiple mechanisms (e.g., formation of miRNA–protein complexes), leading them to be stable and, hence, detectable [23]. For this reason, they have been proposed as biomarkers of cardiovascular pathology [24], including those associated with AFD [25, 26].

Here, we selected a panel of miRNAs potentially associated with cardiac and renal damage as candidate biomarkers of AFD and ERT response. We first assessed if the circulating levels of these miRNAs were associated with AFD and modulated by ERT. Then, we evaluated the independent association of any promising miRNAs with organ damage and any additional predictive value when added to a clinical model of AFD.

MATERIALS AND METHODS

Setting

Sixty patients (35 males; 25 females) with a definitive diagnosis of AFD [27] comprised the whole study cohort: 37 were enrolled by Azienda Ospedaliero-Universitaria Policlinico Federico II, Naples, and 23 by the Cardiology Unit, IRCCS Azienda Ospedaliero-Universitaria di Bologna, Bologna, Italy. Except for those enrolled at first diagnosis ($N = 16$), all patients were already on chronic ERT. At the time of enrollment, all subjects underwent a complete clinical examination. Blood samples were systematically collected and analyzed for high-sensitivity troponin I (TnI) and pro-B-type natriuretic peptide (pro-BNP) levels [28]. Plasma lyso-Gb3 levels were measured by liquid chromatography-mass spectroscopy. The study protocol conformed to the ethical guidelines of the 1975 Declaration of Helsinki and was approved by the review board of the institutions involved (protocol #ICH-967); written informed consent was obtained from all enrolled individuals.

Blood collection for RNA purification

Five ml of peripheral blood was collected in EDTA-containing Vacutainer tubes for plasma separation. Total RNA, including miRNA, was extracted from plasma with the miRNeasy Mini Kit (cat. no. 217004, Qiagen), as described elsewhere [29], and used for droplet digital PCR (ddPCR) testing.

Reverse transcription and droplet digital PCR

Reverse transcription of 8 μ l of RNA was performed using the miRCURY LNA RT Kit (Qiagen, cat. no. 339340), following the manufacturer's protocol. Absolute levels of circulating miR-184 were quantified using ddPCR (Bio-Rad). The QX200 AutoDG Droplet Digital PCR System was used for the amplification and detection of the target miRNA, following a protocol we developed [30]. An EvaGreen-based assay, in association with an LNA primer (Exiqon-Qiagen), was chosen to test miRNA expression. We used the following miRCURY LNA PCR primer set (Exiqon-Qiagen): hsa-miR-1-3p (YP00204344); hsa-miR-133a-3p (YP00204788), hsa-miR-146a-5p (YP00204688), hsa-miR-184 (YP00204601). PCR was performed using constant RT volumes in a 20 μ l reaction volume.

Study endpoint and definitions

The study's primary endpoint was cardiac damage, defined as increased LV mass. LV mass was normalized for the height-to-allometric signals (LVMh) parameter: a cut-off of 50 $\text{g}/\text{m}^{2.7}$ for males (M) and 47 $\text{g}/\text{m}^{2.7}$ for females (F) was used to discriminate patients with or without cardiac damage [31, 32].

Other echocardiographic parameters were defined as follows: left ventricular hypertrophy (LVH) upon the presence of a maximum LV wall thickness ≥ 13 mm in end-diastole in the absence of any other systemic or cardiac process capable of producing LVH [33], on standard trans-thoracic echocardiography; maximal wall thickness (MWT) was defined as the greatest ventricular thickness, obtained at end-diastole and in short-axis views, measured at any site in the LV wall; LV mass indexed for body surface area (LVMI) was calculated by the Devereux formula on the basis of echocardiographic measurements; ejection fraction (EF) was calculated using the modified Simpson method; blood pool pulsed Doppler of mitral valve inflow was used to extract the ratio of early-to-late diastolic flow velocity and the deceleration time [34]; left atrial volume indexed for body surface area (LAVI) was measured by Simpson's biplane method, with a cut-off of 34 ml/m^2 considered to indicate left atrial enlargement [35]; and LV longitudinal function was assessed by two-dimensional speckle tracking measurements of LV global longitudinal strain (GLS) taken in the 2-, 3-, and 4-chamber apical views [36]. The endocardial border was traced at end-systole and manually adjusted to include the entire myocardial wall.

Renal function was evaluated via estimated glomerular filtration rate (eGFR) and amount of protein excretion in urine: eGFR was calculated using the CKD-EPI formula for adults and the Schwartz formula for children up to 18 years of age; albuminuria and proteinuria excretion were categorized following Kidney Disease Improving Global Outcomes guidelines [37–39].

Classical AFD phenotype was defined based on *GLA* mutation type, organ or multi-organ involvement, and time of disease onset.

Statistical analyses

Categorical data are expressed as proportions, and continuous variables are reported as medians and interquartile ranges (25th–75th percentiles). For comparisons between groups, the Mann–Whitney test was used for continuous variables and the Chi-square test for categorical variables. In the validation cohort, the area under the receiver operating characteristic (ROC) curves (c-statistic) was used to evaluate the diagnostic performance of candidate miRNAs in differentiating AFD from control patients. Non-parametric Wilcoxon matched-paired signed-rank test was used to compare continuous variables before and after ERT. For the whole study cohort, we also used Spearman's rank correlation coefficient to evaluate the correlation between a selected miRNA and clinical variables.

The relation between a selected miRNA and cardiac damage was investigated with the use of a backward multivariable logistic regression model adjusted for variables selected at univariable analysis ($P < 0.1$). The additional contribution of the selected miRNA to the model for the prediction of study end-point was evaluated in terms of global model fit, calibration, discrimination, and classification accuracy. The likelihood-ratio test was used for global model fit. Model discrimination was assessed using the c-statistic. Calibration was evaluated by the Hosmer Lemeshow test, with a $\chi^2 \geq 20$ ($P < 0.01$) indicating poor calibration. Classification accuracy was evaluated by measuring continuous net reclassification improvement (NRI) > 0 , integrated discrimination improvement (IDI), and relative IDI (rIDI) [40]. For the last index, 95% confidence intervals (CIs) were calculated using bootstraps estimation. Continuous NRI defined any change in predicted probability as either upward or downward movement, depending on the direction, whereas IDI took into account a weight for each movement and was equal to the difference in discrimination slopes [41]. The rIDI indicated the increase in discrimination slopes divided by the slope of the model without the selected miRNA. A $P < 0.05$ in the two-tailed tests was considered significant. All analyses were performed with STATA 14.0 software (STATA Corporation).

RESULTS

Identification of candidate circulating miRNA biomarkers

Four miRNAs were selected as potential biomarkers for AFD due to their role in cardiac and renal damage: hsa-miR-1-3p [42, 43], hsa-miR-133a-3p [44, 45], hsa-miR-146a-5p [46], and hsa-miR-184 [47, 48]. A pilot screening conducted on a group of patients sampled before and after ERT administration ($N = 12$) led to the selection of miR-184 as the most promising biomarker of response to ERT (Supplementary Fig. S1). Quantification of the miRNAs in all patients revealed that miR-184 and miR-146a-5p were differentially expressed in AFD patients vs. control individuals (respectively, $N = 60$ and $N = 42$) (Supplementary Fig. S2). Accordingly,

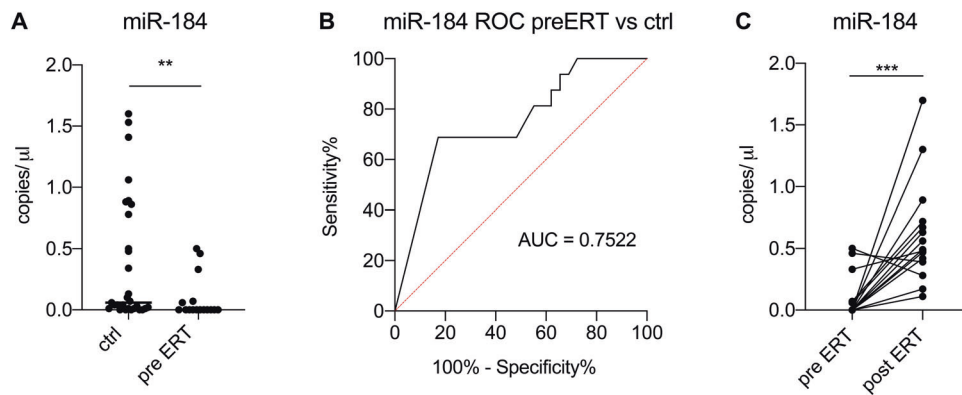


Fig. 1 miR-184 as a biomarker in AFD. **A** Circulating levels of miR-184, measured by ddPCR, in AFD patients before starting treatment (pre-ERT) and in healthy controls (ctrl) ($N = 16$ pre-ERT patients; $N = 29$ healthy controls). $**P < 0.05$ (non-parametric Mann–Whitney test). **B** ROC curve and relative area under the curve calculation for miR-184 as a biomarker of AFD. **C** miR-184 is modulated by ERT. The circulating level of miR-184, measured by ddPCR, in 16 AFD patients before (pre-ERT) and after (post-ERT) the start of ERT. $***P = 0.0004$ (non-parametric Wilcoxon matched-paired signed-rank test).

miR-184 was selected as the candidate biomarker for further analyses, being both associated with AFD and modulated by ERT.

Validation of miR-184 as an AFD biomarker

Circulating levels of miR-184 were quantified by ddPCR in 16 AFD patients before and after ERT and in 29 healthy individuals. ROC curve analysis and relative AUC were used to evaluate the diagnostic performance of miR-184 in discriminating AFD patients from healthy controls (Fig. 1A, B). Paired analysis of pre- vs. post-ERT clinical characteristics and laboratory variables, including miR-184 level, revealed that the miRNA was significantly increased upon therapy and that there were no significant changes in any other clinical variable except for lyso-Gb3, which was modulated to a minor extent (Table 1 and Fig. 1C). Therefore, miR-184 was confirmed to be associated with AFD and modulated by ERT.

Prognostic significance of miR-184 and its additional value in predicting cardiac damage in AFD

Spearman's correlation analyses revealed that miR-184 negatively correlated with myocardial mass (LVMI: $r = -0.31$, $P = 0.02$; LVMh: $r = -0.30$, $P = 0.02$), LAVi ($r = -0.24$, $P = 0.065$) and Tnl ($r = -0.6$, $P < 0.01$), and positively correlated with kidney function (eGFR: $r = 0.29$, $P = 0.04$); no correlation was observed between miR-184 and lyso-Gb3 (Supplementary Fig. S3).

In our cohort, only 11 patients had clinically relevant renal impairment ($eGFR \leq 60$ ml/min); in contrast, the presence of cardiac damage was around 60%. Patients with cardiac damage were older, had a lower level of miR-184, and were on ERT longer compared to patients without cardiac damage (Table 2). As expected, cardiac mass and function parameters were consistently worse in the former. There was no difference in lyso-Gb3 level between these two sub-groups.

Multivariable logistic analyses revealed an independent and inverse relationship between miR-184 and the risk of cardiac damage (Table 3). Of note, although not associated with the study endpoint at the bivariate level, we forced lyso-Gb3 level into the multivariable model. The variable was not retained by the backward stepwise selection method, and the main study findings did not change.

Finally, we estimated the contribution of miR-184 to a clinical model for the prediction of cardiac impairment. The addition of miR-184 to other variables independently associated with cardiac damage (disease phenotype, eGFR, and ERT duration) improved the model's performance in terms of global fit, discrimination power (although not to a statistically significant extent), and classification accuracy (Table 4). In this regard, classification accuracy improved by 66% in patients with cardiac damage and

Table 1. Clinical characteristics of 16 AFD patients before and after ERT.

Variable	pre-ERT ^a	post-ERT ^a	P Value
HR, bpm	73 [64–85]	74 [66–82]	0.349
SBP, mmHg	120 [110–130]	120 [110–125]	0.287
DBP, mmHg	75 [70–80]	75 [70–80]	0.903
BMI, kg/m ²	24.2 [22.2–26.47]	24.2 [22.7–27.4]	0.059
miR-184, copies/μl	0 [0–0.065]	0.525 [0.404–0.805]	0.001
proBNP, pg/ml	34.1 [9.1–234.1]	23.84 [14.12–104.3]	0.570
eGFR, ml/min	120.5 [107–125]	120 [107–129]	0.195
lysoGb3, ng/ml	3.1 [1.2–9.3]	2.2 [0.7–3.5]	0.010
tdIVS, mm	10 [8.5–12]	11 [9–13]	0.156
tdPW, mm	9 [8–12]	9 [8–13]	0.739
EDV, ml	120 [81–143]	120 [93–134]	0.594
ESV, ml	43 [30–51]	41 [37–50]	0.533
EF, %	0.64 [0.59–0.69]	0.62 [0.55–0.65]	0.539
LVMI, g/m ²	90 [77–118]	91.2 [86.1–106]	0.753
LVMh, g/m ^{2.7}	39.0 [32.0–51.5]	39.1 [36.8–50.3]	0.799
LAVi, ml/m ²	28 [22.98–31]	30 [28–33]	0.074
sPAP, mmHg	26 [25–35]	26 [25–28]	0.144
GLS, %	−17.61 [−19.76– −14.95]	−15.8 [−19.04– −11.62]	0.433
Tnl, ng/l	0.007 [0.004–0.07]	0.03 [0.003–1.53]	0.230
months of ERT	0	14 [9.5–22]	–

Abbreviations: *MI* Body mass index, *bpm* Beats per minute, *DBP* Diastolic blood pressure, *EDV* End-diastolic volume, *EF* Ejection fraction, *eGFR* Estimated glomerular filtration rate, *ESV* End-systolic volume, *GLS* Global longitudinal strain, *HR* Heart rate, *LAVi* Left atrial volume index; *LVEDDI*, indexed left ventricular end-diastolic diameter; *LVMI/h*, left ventricular mass indexed for body surface area/height^{2.7}; *RWT*, relative wall thickness, *SBP* Systolic blood pressure, *sPAP* Systolic pulmonary arterial pressure, *tdIVS* Tele-diastolic interventricular septum, *tdPW* Tele-diastolic posterior wall, *Tnl* Troponin. ^aData are median [interquartile range].

by 25% in patients without damage, leading to a continuous NRI (> 0) of 91.7%. Although improvement in classification accuracy was mitigated by indexes that took into account the weight of any change in predicted probabilities, such as IDI and rIDI, it remained statistically significant.

DISCUSSION

In this study, we determine whether miR-184 could serve as a biomarker for risk stratification and the monitoring of treatment

Table 2. Clinical characteristics of 60 AFD patients under chronic ERT stratified for the presence of cardiac damage.

Variable	All population ^a (N = 60)	Cardiac damage ^a (N = 33)	No cardiac damage ^a (N = 27)	P Value
Age, years	45 [32–55]	54 [42–62]	35 [23–47]	<0.001
Males, n (%)	35 (58.3)	22 (66.7)	13 (48.1)	0.191
Months on ERT	23 [14–60]	36 [22–68]	15 [10–24]	<0.001
HR, bpm	70 [63–80]	67 [60–80]	70 [65–80]	0.203
SBP, mmHg	120 [110–130]	120 [110–130]	120 [115–130]	0.798
DBP, mmHg	80 [70–80]	80 [70–80]	80 [70–80]	0.607
BMI, kg/m ²	25.5 [23.0–28.4]	26.8 [23.9–29.1]	23.9 [22.3–26.7]	0.022
BSA, m ²	1.8 [1.7–2.0]	1.85 [1.73–1.93]	1.8 [1.6–2.0]	0.275
miR-184, copies/ μ l	0.40 [0.01–4.50]	0.03 [0.00–3.0]	0.63 [0.11–10.5]	0.014
proBNP, pg/ml	103.7 [76.8–355.1]	258.3 [101.0–1713.4]	84 [23.84–104.30]	<0.001
eGFR, ml/min	90.5 [72.8–111.0]	81.0 [51.8–91.0]	110 [98.5–123.0]	<0.001
lysoGb3, ng/ml	2.6 [1.3–8.1]	4.55 [1.25–10.85]	2.20 [1.30–3.70]	0.140
tdIVS, mm	12 [10–15]	15 [13–17]	10 [9–11]	<0.001
tdPW, mm	11 [9–13]	13 [12–15]	9.0 [8.8–9.8]	<0.001
EDV, ml	98 [79–120]	100 [82–130]	95.0 [73.5–108.0]	0.190
ESV, ml	35 [27–42]	38 [27–47]	31.5 [26.5–40.5]	0.244
EF, %	0.67 [0.63–60]	0.67 [0.63–62.0]	0.66 [0.64–30.36]	0.668
LVMi, g/m ²	127.6 [91.7–167.0]	161 [134–194]	90.8 [80.9–98.0]	<0.001
LVMh, g/m ^{2.7}	51.2 [40.6–70.3]	66.8 [54.3–88.0]	39 [34.8–44.2]	<0.001
LAVi, ml/m ²	33.9 [28.0–43.0]	41 [37–60]	28.5 [25.1–32.3]	<0.001
sPAP, mmHg	29.5 [25.0–36.0]	35 [28–40]	26.0 [25.0–29.5]	<0.001
GLS, %	–15.8 [–19.0–11.8]	–12.7 [–16.6–8.5]	–18.3 [–20.8–15.8]	<0.001
Tnl, ng/l	0.09 [0.01–5.50]	0.20 [0.07–26.0]	0.01 [0.00–0.83]	<0.001

Abbreviations: As in Table 1.

^aData are median [interquartile range], unless stated otherwise.

Table 3. Independent predictors of cardiac damage in 60 AFD patients on ERT (multivariable logistic regression).

	Odds ratio	95% Conf. interval	P Value
miR-184	0.864	0.7598–0.983	0.026
Classical phenotype	10.691	1.379–82.908	0.023
Months of ERT	1.017	0.997–1.038	0.089
eGFR	0.922	0.877–0.970	0.002

efficacy. The main findings of the present study were as follows: (1) the level of miR-184 is associated with AFD and is also modulated by ERT; (2) a higher circulating level of miR-184 is independently associated with a lower risk of cardiac damage in AFD patients; and (3) adding miR-184 to a comprehensive clinical model improves the prediction of cardiac damage in AFD patients. These results suggest that assessment of the plasma level of miR-184 could be of use for assessing response to ERT and the prognosis of AFD.

AFD manifests with a range of severities and a heterogeneous spectrum of phenotypes: whereas hemizygous male patients typically present with severe symptoms, the clinical manifestations of heterozygous female patients depend on the *GLA* variant and the lyonization pattern in tissues [49]. Premature death occurs mostly due to cardiac complications and end-stage renal disease. ERT—which is based on intravenous infusions of recombinant forms of alpha-galactosidase—is an expensive and lifelong treatment option that has been available since 2001 [50]. The timing of treatment initiation is critical: indeed, although ERT can slow disease progression, it cannot reverse permanent damage, at which point organ transplant is the only therapeutic option. Thus, initiating therapy prior to irreversible cellular impairment is crucial for

mitigating damage caused by Gb3 deposition [51]. As a matter of fact, supplementing GLA activity in order to improve Gb3 clearance was not sufficient to rescue profibrotic signaling and dysregulated autophagy in a podocyte culture model of AFD [52, 53]. The use of lyso-Gb3 as a biomarker of AFD and for monitoring of ERT outcome needs to be better investigated since additional mechanisms besides Gb3 accumulation may be taking place in AFD [54]. Recently, elevated plasma levels of several proteins, including inflammatory and cardiac remodeling biomarkers, have been reported in AFD patients [55]. Among circulating nucleic acids, some miRNAs were proposed as circulating biomarkers for AFD diagnosis and prognosis, either in plasma [26] or serum [25], but the number of samples in the studies was low, and no coupled analysis of pre- and post-ERT patients were reported.

Here, we conducted a discovery study on a panel of four candidate miRNAs. In our cohort of 60 patients enrolled at two different hospitals, we found miR-184 to be significantly reduced in untreated AFD patients vs. healthy individuals. Moreover, this miRNA was modulated by ERT when other clinical variables were still mostly unaltered shortly after initiation of ERT. Therefore, miR-184 is a sensitive circulating biomarker that is modulated in response to ERT administration. Furthermore, we found that a lower miR-184 level is independently associated with the risk of cardiac damage, and that the incorporation of miR-184 into a clinical model improves risk prediction of impaired cardiac function, as assessed by statistical metrics. These results indicate that miR-184 is a circulating biomarker that could be employed in the clinic for assessing the response to ERT as well as the severity of the disease.

MiR-184 has been reported in several studies to have a role in response to the stress of cardiac and renal tissue. The miRNA was found downregulated in cardiac hypertrophy. Indeed, through competitive binding with the long noncoding RNA *UCA1*, miR-184

Table 4. Additional contribution of miRNA-184 to a clinical model for the prediction of cardiac damage.

	Model without miR-184	Model with miR-184
Global model fit:		
Likelihood ratio chi-square test	30.31	37.56
Likelihood ratio test	$P = 0.007$	
Calibration:		
Hosmer–Lemeshow, chi-square	14.48 $P = 0.070$	10.78 $P = 0.214$
Discrimination:		
c-statistic	0.889	0.925
Δ c-statistic	0.036 ($P = 0.250$)	
Classification accuracy:		
Continuous NRI (> 0)	0.917 ($P < 0.001$)	
IDI	0.105 ($P = 0.017$)	
Relative IDI (95% bootstrap C.I.)	0.221 (0.002–0.356)	

Global model fit, calibration, discrimination, and classification accuracy of logistic regression models.

Abbreviations: *IDI* Integrated discrimination improvement, *NRI* Net reclassification improvement.

controls the mRNA level of homeobox A9, inducing upregulation of atrial and brain natriuretic peptide genes in hypertrophic cardiomyocytes [56]. Exposure to radical oxygen species was found to induce oxidation-dependent modification of the miR-184 level to regulate apoptosis through the downregulation of Bcl-xL and Bcl-w in a mouse model of myocardial ischemia–reperfusion [47]. The miRNA was also found expressed in renal tubules, in which it induced fibrosis through downregulation of the phospholipid phosphatase three gene, and its expression was found to be controlled by albumin, triggering the recruitment of NF- κ B to the miR-184 promoter in diabetic nephropathy [48]. Importantly, miR-184 is released into the circulation, so it can serve as a disease biomarker [57].

In our study cohort, we did not observe any relationship between the circulating level of lyso-Gb3 and the risk of cardiac damage. The reason for this finding is unclear, but it may be related to our small sample size. Indeed, lyso-Gb3 is a powerful diagnostic biomarker and has been shown to correlate with phenotype and organ damage severity in patients with AFD [58, 59]. However, a relation between lyso-Gb3 changes over time and treatment outcome (such as in LV mass or eGFR) has not been validated until now. Neither lyso-Gb3 concentration at baseline or during treatment nor its absolute decrease have been shown to predict clinical events or changes in organ damage [2]. Additionally, the baseline lyso-Gb3 has not emerged as a predictor of myocardial fibrosis during follow-up in untreated patients [60]. Therefore, prognostic biomarkers for AFD progression and clinical response to guide treatment decisions are not available at the moment.

AFD induces multi-organ failure via progressive deposition of unprocessed material inside the lysosome, which in the heart leads to hypertrophy and activation of other intracellular processes associated with inflammation, apoptosis, and pro-oxidative molecule production [61]. Given that our patient cohort presented mainly with the classical form of the pathology and showed predominantly cardiac involvement, with only mild kidney damage, we put forward that the circulating level of miR-184 is at least a sensitive and early sensor of cardiac impairment, and therefore that its measurement could be clinically relevant for discriminating patients with cardiac damage due to chronic intracellular glycosphingolipid accumulation.

Limitations

Owing to our small sample size, we could have missed some other significant relationships, such as that between lyso-Gb3 and cardiac damage (as mentioned above). However, to the best of

our knowledge, the present study comprises more patients than previous ones and introduces the novelty of measuring a panel of miRNAs pre- and post-ERT. Moreover, AFD is associated with the risk of cardiac and renal impairment. Although we found that miR-184 level positively correlated with eGFR, the number of patients with clinically relevant renal dysfunction was very low ($N = 11$). This prevented us from building a multivariable model for renal damage prediction because of the risk of overfitting.

Finally, our observation period of post-ERT samples was limited to one time-point, so the complete picture of disease progression is still needed. Future investigations will include multiple samplings throughout the course of the disease, a dose–response analysis of ERT, and a longer clinical follow-up to establish the relationship between changes in circulating miR-184 level and disease progression. Furthermore, more studies are required to elucidate whether this miRNA targets specific molecular pathways inside cells, playing a role in AFD pathogenesis.

Perspectives

Monitoring the efficacy of ERT is still problematic in the management of AFD. Indeed, we know of no circulating biomarker that can strongly indicate whether and how ERT is working, anticipating the mid- to long-term clinical outcomes of the therapy. In the present study, we have identified a circulating microRNA, namely miR-184, as a sensitive biomarker of ERT that adds value to clinical and biochemical parameters in discriminating significant cardiac involvement in disease progression. Whether changes in the miR-184 level associated with ERT could translate into better clinical outcome should be investigated in properly powerful studies.

DATA AVAILABILITY

The droplet digital PCR data analyzed in the current study are available from the corresponding authors on reasonable request.

REFERENCES

- Lidove O, West ML, Pintos-Morell G, Reisin R, Nicholls K, Figuera LE, et al. Effects of enzyme replacement therapy in Fabry disease—a comprehensive review of the medical literature. *Genet Med*. 2010;12:668–79.
- Arends M, Wanner C, Hughes D, Mehta A, Oder D, Watkinson OT, et al. Characterization of classical and nonclassical Fabry disease: a multicenter study. *J Am Soc Nephrol*. 2017;28:1631–41.
- Breunig F, Weidemann F, Beer M, Eggert A, Krane V, Spindler M, et al. Fabry disease: diagnosis and treatment. *Kidney Int Suppl*. 2003;63:S181–5.

4. Redonnet-Vernhet I, Ploos van Amstel JK, Jansen RP, Wevers RA, Salvayre R, Levade T. Uneven X inactivation in a female monozygotic twin pair with Fabry disease and discordant expression of a novel mutation in the alpha-galactosidase A gene. *J Med Genet.* 1996;33:682–8.
5. Eng CM, Banikazemi M, Gordon RE, Goldman M, Phelps R, Kim L, et al. A phase 1/2 clinical trial of enzyme replacement in fabry disease: pharmacokinetic, substrate clearance, and safety studies. *Am J Hum Genet.* 2001;68:711–22.
6. Eng CM, Germain DP, Banikazemi M, Warnock DG, Wanner C, Hopkin RJ, et al. Fabry disease: guidelines for the evaluation and management of multi-organ system involvement. *Genet Med.* 2006;8:539–48.
7. Rombach SM, Dekker N, Bouwman MG, Linthorst GE, Zwiderman AH, Wijburg FA, et al. Plasma globotriaosylsphingosine: Diagnostic value and relation to clinical manifestations of Fabry disease. *Biochimica Et Biophysica Acta-Mol Basis Dis.* 2010;1802:741–8.
8. Biegstraaten M, Arngrimsson R, Barbey F, Boks L, Cecchi F, Deegan PB, et al. Recommendations for initiation and cessation of enzyme replacement therapy in patients with Fabry disease: the European Fabry Working Group consensus document. *Orphanet J Rare Dis.* 2015;10:36.
9. Smid BE, van der Tol L, Biegstraaten M, Linthorst GE, Hollak CE, Poorthuis BJ. Plasma globotriaosylsphingosine in relation to phenotypes of Fabry disease. *J Med Genet.* 2015;52:262–8.
10. Arends M, Wijburg FA, Wanner C, Vaz FM, van Kuilenburg ABP, Hughes DA, et al. Favourable effect of early versus late start of enzyme replacement therapy on plasma globotriaosylsphingosine levels in men with classical Fabry disease. *Mol Genet Metab.* 2017;121:157–61.
11. Bichet DG, Aerts JM, Auray-Blais C, Maruyama H, Mehta AB, Skuban N, et al. Assessment of plasma lyso-Gb3 for clinical monitoring of treatment response in migalastat-treated patients with Fabry disease. *Genet Med.* 2021;23:192–201.
12. Krol J, Loedige I, Filipowicz W. The widespread regulation of microRNA biogenesis, function and decay. *Nat Rev Genet.* 2010;11:597–610.
13. Anfossi S, Babayan A, Pantel K, Calin GA. Clinical utility of circulating non-coding RNAs—an update. *Nat Rev Clin Oncol.* 2018;15:541–63.
14. Colpaert RMW, Calore M. MicroRNAs in cardiac diseases. *Cells* 2019;8:737.
15. Neal CS, Michael MZ, Pimlott LK, Yong TY, Li JY, Gleadle JM. Circulating microRNA expression is reduced in chronic kidney disease. *Nephrol Dial Transpl.* 2011;26:3794–802.
16. Belevych AE, Sansom SE, Terentyeva R, Ho HT, Nishijima Y, Martin MM, et al. MicroRNA-1 and -133 increase arrhythmogenesis in heart failure by dissociating phosphatase activity from RyR2 complex. *PLoS One.* 2011;6:e28324.
17. Yu Y, Liu H, Yang D, He F, Yuan Y, Guo J, et al. Aloe-emodin attenuates myocardial infarction and apoptosis via up-regulating miR-133 expression. *Pharm Res.* 2019;146:104315.
18. Calore M, Lorenzon A, Vitiello L, Poloni G, Khan MAF, Beffagna G, et al. A novel murine model for arrhythmogenic cardiomyopathy points to a pathogenic role of Wnt signalling and miRNA dysregulation. *Cardiovasc Res.* 2019;115:739–51.
19. Yamada S, Hsiao YW, Chang SL, Lin YJ, Lo LW, Chung FP, et al. Circulating microRNAs in arrhythmogenic right ventricular cardiomyopathy with ventricular arrhythmia. *Europace.* 2018;20:f37–f45.
20. Di Gregoli K, Mohamad Anuar NN, Bianco R, White SJ, Newby AC, George SJ, et al. MicroRNA-181b controls atherosclerosis and aneurysms through regulation of TIMP-3 and elastin. *Circ Res.* 2017;120:49–65.
21. Chung AC, Huang XR, Meng X, Lan HY. miR-192 mediates TGF-beta/Smad3-driven renal fibrosis. *J Am Soc Nephrol.* 2010;21:1317–25.
22. Alexander M, Hu R, Runtsch MC, Kagele DA, Mosbrugger TL, Tolmachova T, et al. Exosome-delivered microRNAs modulate the inflammatory response to endotoxin. *Nat Commun.* 2015;6:7321.
23. Schwarzenbach H, Nishida N, Calin GA, Pantel K. Clinical relevance of circulating cell-free microRNAs in cancer. *Nat Rev Clin Oncol.* 2014;11:145–56.
24. Yang Y, Cheng HW, Qiu Y, Dupee D, Noonan M, Lin YD, et al. MicroRNA-34a plays a key role in cardiac repair and regeneration following myocardial infarction. *Circ Res.* 2015;117:450–9.
25. Xiao K, Lu D, Hoepfner J, Santer L, Gupta S, Pfanne A, et al. Circulating microRNAs in Fabry Disease. *Sci Rep.* 2019;9:15277.
26. Cammarata G, Scalia S, Colomba P, Zizzo C, Pisani A, Riccio E, et al. A pilot study of circulating microRNAs as potential biomarkers of Fabry disease. *Oncotarget* 2018;9:27333–45.
27. Smid BE, van der Tol L, Cecchi F, Elliott PM, Hughes DA, Linthorst GE, et al. Uncertain diagnosis of Fabry disease: consensus recommendation on diagnosis in adults with left ventricular hypertrophy and genetic variants of unknown significance. *Int J Cardiol.* 2014;177:400–8.
28. Coats CJ, Parisi V, Ramos M, Janagarajan K, O'Mahony C, Dawney A, et al. Role of serum N-terminal pro-brain natriuretic peptide measurement in diagnosis of cardiac involvement in patients with Anderson–Fabry disease. *Am J Cardiol.* 2013;111:111–7.
29. Roncarati R, Viviani Anselmi C, Losi MA, Papa L, Cavarretta E, Da Costa Martins P, et al. Circulating miR-29a, among other up-regulated microRNAs, is the only biomarker for both hypertrophy and fibrosis in patients with hypertrophic cardiomyopathy. *J Am Coll Cardiol.* 2014;63:920–7.
30. Ferracin M, Salamon I, Lupini L, Miotto E, Sabbioni S, Negrini M. Circulating microRNA quantification using DNA-binding dye chemistry and droplet digital PCR. *J Vis Exp.* 2016. <https://doi.org/10.3791/54102>.
31. de Simone G, Devereux RB, Daniels SR, Koren MJ, Meyer RA, Laragh JH. Effect of growth on variability of left ventricular mass: assessment of allometric signals in adults and children and their capacity to predict cardiovascular risk. *J Am Coll Cardiol.* 1995;25:1056–62.
32. de Simone G, Kizer JR, Chinali M, Roman MJ, Bella JN, Best LG, et al. Normalization for body size and population-attributable risk of left ventricular hypertrophy: the Strong Heart Study. *Am J Hypertens.* 2005;18:191–6.
33. Yousef Z, Elliott PM, Cecchi F, Escoubet B, Linhart A, Monserrat L, et al. Left ventricular hypertrophy in Fabry disease: a practical approach to diagnosis. *Eur Heart J.* 2013;34:802–8.
34. Lang RM, Bierig M, Devereux RB, Flachskampf FA, Foster E, Pellikka PA, et al. Recommendations for chamber quantification: a report from the American Society of Echocardiography's Guidelines and Standards Committee and the Chamber Quantification Writing Group, developed in conjunction with the European Association of Echocardiography, a branch of the European Society of Cardiology. *J Am Soc Echocardiogr.* 2005;18:1440–63.
35. Nagueh SF, Appleton CP, Gillebert TC, Marino PN, Oh JK, Smiseth OA, et al. Recommendations for the evaluation of left ventricular diastolic function by echocardiography. *Eur J Echocardiogr.* 2009;10:165–93.
36. Vijapurapu R, Nordin S, Baig S, Liu B, Rosmini S, Augusto J, et al. Global longitudinal strain, myocardial storage and hypertrophy in Fabry disease. *Heart* 2019;105:470–6.
37. Levey AS, Stevens LA, Schmid CH, Zhang YL, Castro AF 3rd, Feldman HI, et al. A new equation to estimate glomerular filtration rate. *Ann Intern Med.* 2009;150:604–12.
38. Kidney Disease: Improving Global Outcomes (KDIGO) CKD-MBD Update Work Group. KDIGO 2017 clinical practice guideline update for the diagnosis, evaluation, prevention, and treatment of chronic kidney disease-mineral and bone disorder (CKD-MBD). *Kidney Int Suppl* (2011). 2017;7:1–59.
39. Nilsson-Ehle P. Iohexol clearance for the determination of glomerular filtration rate: 15 years' experience in clinical practice. *EJIFCC* 2001;13:48–52.
40. Pencina MJ, D'Agostino RB Sr, D'Agostino RB, Vasan RS Jr. Evaluating the added predictive ability of a new marker: from area under the ROC curve to reclassification and beyond. *Stat Med.* 2008;27:157–72.
41. Yates JF. External correspondence: decompositions of the mean probability score. *Organ Behav Hum Perform.* 1982;30:132–56.
42. Elia L, Contu R, Quintavalle M, Varrone F, Chimenti C, Russo MA, et al. Reciprocal regulation of microRNA-1 and insulin-like growth factor-1 signal transduction cascade in cardiac and skeletal muscle in physiological and pathological conditions. *Circulation* 2009;120:2377–85.
43. Seok H, Lee H, Lee S, Ahn SH, Lee HS, Kim GD, et al. Position-specific oxidation of miR-1 encodes cardiac hypertrophy. *Nature* 2020;584:279–85.
44. Care A, Catalucci D, Felicetti F, Bonci D, Addario A, Gallo P, et al. MicroRNA-133 controls cardiac hypertrophy. *Nat Med.* 2007;13:613–8.
45. Romaine SP, Tomaszewski M, Condorelli G, Samani NJ. MicroRNAs in cardiovascular disease: an introduction for clinicians. *Heart* 2015;101:921–8.
46. Shimada BK, Yang Y, Zhu J, Wang S, Suen A, Kronstadt SM, et al. Extracellular miR-146a-5p induces cardiac innate immune response and cardiomyocyte dysfunction. *Immunohorizons.* 2020;4:561–72.
47. Wang JX, Gao J, Ding SL, Wang K, Jiao JQ, Wang Y, et al. Oxidative modification of miR-184 enables it to target Bcl-xL and Bcl-w. *Mol Cell.* 2015;59:50–61.
48. Zanchi C, Macconi D, Trionfani P, Tomasoni S, Rottoli D, Locatelli M, et al. MicroRNA-184 is a downstream effector of albuminuria driving renal fibrosis in rats with diabetic nephropathy. *Diabetologia* 2017;60:1114–25.
49. Germain DP, Fouilhoux A, Decramer S, Tardieu M, Pillet P, Fila M, et al. Consensus recommendations for diagnosis, management and treatment of Fabry disease in paediatric patients. *Clin Genet.* 2019;96:107–17.
50. Alegria T, Vairo F, de Souza MV, Krug BC, Schwartz IV. Enzyme replacement therapy for Fabry disease: a systematic review and meta-analysis. *Genet Mol Biol.* 2012;35:947–54.
51. Ortiz A, Germain DP, Desnick RJ, Politei J, Mauer M, Burlina A, et al. Fabry disease revisited: management and treatment recommendations for adult patients. *Mol Genet Metab.* 2018;123:416–27.
52. Liebau MC, Braun F, Hopker K, Weitbrecht C, Bartels V, Muller RU, et al. Dysregulated autophagy contributes to podocyte damage in Fabry's disease. *PLoS One.* 2013;8:e63506.
53. Braun F, Blomberg L, Brodesser S, Liebau MC, Schermer B, Benzing T, et al. Enzyme replacement therapy clears Gb3 deposits from a podocyte cell culture

- model of Fabry disease but fails to restore altered cellular signaling. *Cell Physiol Biochem.* 2019;52:1139–50.
54. Namdar M, Gebhard C, Studiger R, Shi Y, Mocharla P, Schmied C, et al. Globotriaosylsphingosine accumulation and not alpha-galactosidase-A deficiency causes endothelial dysfunction in Fabry disease. *PLoS One.* 2012;7:e36373.
 55. Yogasundaram H, Nikhanj A, Putko BN, Boutin M, Jain-Ghai S, Khan A, et al. Elevated inflammatory plasma biomarkers in patients with Fabry disease: a critical link to heart failure with preserved ejection fraction. *J Am Heart Assoc.* 2018;7:e009098.
 56. Zhou G, Li C, Feng J, Zhang J, Fang Y. lncRNA UCA1 is a novel regulator in cardiomyocyte hypertrophy through targeting the miR-184/HOXA9 axis. *Cardiorenal Med.* 2018;8:130–9.
 57. Cuk K, Zucknick M, Heil J, Madhavan D, Schott S, Turchinovich A, et al. Circulating microRNAs in plasma as early detection markers for breast cancer. *Int J Cancer.* 2013;132:1602–12.
 58. Nowak A, Mechtler TP, Hornemann T, Gawinecka J, Theswet E, Hilz MJ, et al. Genotype, phenotype and disease severity reflected by serum LysoGb3 levels in patients with Fabry disease. *Mol Genet Metab.* 2018;123:148–53.
 59. Auray-Blais C, Lavoie P, Boutin M, Ntwari A, Hsu TR, Huang CK, et al. Biomarkers associated with clinical manifestations in Fabry disease patients with a late-onset cardiac variant mutation. *Clin Chim Acta.* 2017;466:185–93.
 60. Weidemann F, Beer M, Kralewski M, Siwy J, Kampmann C. Early detection of organ involvement in Fabry disease by biomarker assessment in conjunction with LGE cardiac MRI: results from the SOPHIA study. *Mol Genet Metab.* 2019;126:169–82.
 61. Rozenfeld P, Feriozzi S. Contribution of inflammatory pathways to Fabry disease pathogenesis. *Mol Genet Metab.* 2017;122:19–27.

AUTHOR CONTRIBUTIONS

IS and NL performed experiments; EB, MS, AP, ER, LT, RD, VA, IC, GLM, NG, and LS acquired samples and clinical data; EN, GV, EC, PK, and MF performed statistical analyses of clinical data; IS, EB, NT, and GC wrote the manuscript; IS prepared the figures; EB, MF, RR, LS, and GC revised the work critically; GC conceived the research and provided funding.

FUNDING

This work was supported by the Italian Ministry of Health (PE-2013-02356818) to GC

COMPETING INTERESTS

The authors declare no competing interests.

ETHICS APPROVAL AND CONSENT TO PARTICIPATE

The study protocol conformed to the ethical guidelines of the 1975 Declaration of Helsinki and was approved by the review board of the institutions involved (protocol #, ICH-967); written informed consent was obtained from all enrolled individuals.

ADDITIONAL INFORMATION

Supplementary information The online version contains supplementary material available at <https://doi.org/10.1038/s41419-021-04438-5>.

Correspondence and requests for materials should be addressed to Letizia Spinelli or Gianluigi Condorelli.

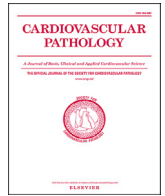
Reprints and permission information is available at <http://www.nature.com/reprints>

Publisher's note Springer Nature remains neutral with regard to jurisdictional claims in published maps and institutional affiliations.



Open Access This article is licensed under a Creative Commons Attribution 4.0 International License, which permits use, sharing, adaptation, distribution and reproduction in any medium or format, as long as you give appropriate credit to the original author(s) and the source, provide a link to the Creative Commons license, and indicate if changes were made. The images or other third party material in this article are included in the article's Creative Commons license, unless indicated otherwise in a credit line to the material. If material is not included in the article's Creative Commons license and your intended use is not permitted by statutory regulation or exceeds the permitted use, you will need to obtain permission directly from the copyright holder. To view a copy of this license, visit <http://creativecommons.org/licenses/by/4.0/>.

© The Author(s) 2021



Case Report

Postmortem diagnosis of left dominant arrhythmogenic cardiomyopathy: the importance of a multidisciplinary network for sudden death victims. “HIC mors gaudet succurere vitae”



Maddalena Graziosi^a, Ornella Leone^b, Alberto Foà^a, Valentina Agostini^b,
Raffaello Ditaranto^a, Marco Foroni^a, Cesare Rossi^c, Luigi Lovato^d, Marco Seri^c,
Claudio Rapezzi^{a,*}

^a Cardiology, Department of Experimental Diagnostic and Specialty Medicine, Alma Mater Studiorum-University of Bologna, Bologna, Italy

^b Cardiovascular Pathology Unit, Department of Pathology, S.Orsola Hospital, Bologna, Italy

^c Medical Genetics Unit, S.Orsola Hospital and University of Bologna, Bologna, Italy

^d Cardiovascular Radiology Department, S.Orsola Hospital, Bologna, Italy

ARTICLE INFO

Article history:

Received 22 July 2019

Received in revised form

17 September 2019

Accepted 27 September 2019

Keywords:

Sudden death

Cardiovascular pathology

Molecular autopsy

Multidisciplinary network

Arrhythmogenic left ventricular

cardiomyopathy

Familial screening

ABSTRACT

An apparently healthy man died suddenly at the age of 49 during physical activity. The heart was referred to our Cardiovascular Pathology Unit for valve tissue banking. Pathology findings led to the diagnosis of arrhythmogenic left ventricular cardiomyopathy. Molecular autopsy was performed and two variants of interest were identified in genes associated with arrhythmogenic cardiomyopathy. The 19-year-old son underwent a cardiac screening comprehensive of electrocardiogram (ECG), echocardiogram, cardiac magnetic resonance and genetic testing, and the diagnosis of arrhythmogenic left ventricular cardiomyopathy was achieved.

This case report highlights the need of a systematic evaluation of all sudden death victims with autopsy performed by expert cardiovascular pathologists and implemented by molecular analysis, aiming to identify also rare hereditary diseases and activate proper family screening.

© 2019 Elsevier Inc. All rights reserved.

1. Introduction

Accurate autopsy examination in cases of sudden death (SD) is essential to identify the underlying disease and screen relatives. However, forensic autopsy may be inconclusive especially in cases of mild and/or uncommon abnormalities. A multidisciplinary approach specifically dedicated to SD victims increases the diagnostic yield as the cooperation between expert cardiovascular pathologists and clinicians may identify the cause of death. Moreover, an integrated postmortem examination combining autopsy with molecular biology testing (molecular autopsies) has been proposed to identify genetic diseases that may cause SD [1–4].

We report the case of a postmortem examination integrated with molecular autopsy leading to the diagnosis of arrhythmogenic

left ventricular cardiomyopathy (ALVC) due to a previously unreported desmoplakin (DSP) variant in a dead proband and in his living son, who received a defibrillator for SD primary prevention.

2. Case report

A 49-year-old man died suddenly during physical activity. Personal and familial anamnesis was silent. The patient had undergone a routine presport cardiologic evaluation – comprehensive of ECG and echocardiogram – the previous year at another center, and no abnormal findings were reported.

The heart was explanted to remove the valves for tissue banking and then examined at our Cardiovascular Pathology Unit.

Macroscopic examination of the heart revealed moderate left ventricular (LV) dilatation (Fig. 1B–E). The LV subepicardial myocardial border was irregular and scalloped due to the presence of multiple fibro-fatty areas infiltrating/replacing the myocardium, mainly in the midbasal anterolateral (Fig. 1B–D) and apical inferolateral walls (Fig. 1E). In the anterior septum, an area of fatty tissue originating from the subepicardium layer and progressing

* Corresponding author. Cardiology, Department of Experimental Diagnostic and Specialty Medicine, Alma Mater Studiorum-University of Bologna, Via G. Massarenti 9, 40138 Bologna, Italy. Tel: +39 051 349858; fax: +39 051 344859.

E-mail address: claudio.rapezzi@unibo.it (C. Rapezzi).

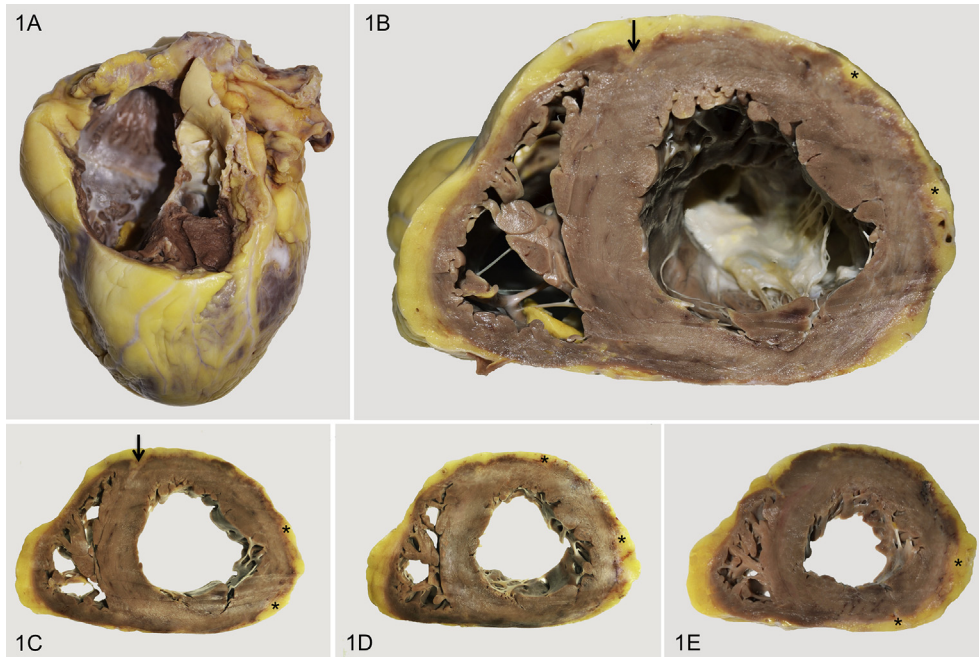


Fig. 1. Macroscopy of the heart. Heart is mildly dilated and altered in shape because of rounded apex (A). On short-axis slices (B, C, D, E) obtained from the apex to the mid-ventricular level, the presence of fibro-fatty areas infiltrating/replacing the myocardium makes the left ventricular (LV) subepicardial myocardial border irregular (asterisks). A layer of fatty tissue progressing from the subepicardium towards the midmural area is evident in the anterior septum too (arrows).

toward the midmural section was evident (Fig. 1B–C). The right ventricle (RV) was mildly dilated in the inflow tract, with a near-regular subepicardial border.

Histology findings were striking and confirmed the extensive and diffuse fibro-fatty replacement of the LV myocardium, originating from the subepicardial layer and spreading toward the midmural layer without any involvement of the subendocardial layer; the inferolateral wall showed the most extensive fibro-fatty replacement. Fibro-fatty replacement also involved the midbasal anterior septum whereas the RV had only mild fatty infiltration with no significant fibrosis. The myocardium showed severe myocyte alterations such as increased size (Fig. 2C), attenuation (Fig. 2D),

vacuolization, and irregular-shaped nuclei (Fig. 2E–F). No inflammation was found. At histology, the coronary arteries had only mild subintimal hyperplasia.

2.1. Pathology diagnosis was left dominant arrhythmogenic cardiomyopathy

Genetic testing with next-generation sequencing was performed on DNA isolated from explanted heart paraffin samples (174 candidate genes for channelopathies and cardiomyopathies were analyzed, [Supplementary material](#)). Two variants of interest were identified in genes associated with arrhythmogenic cardiomyopathy

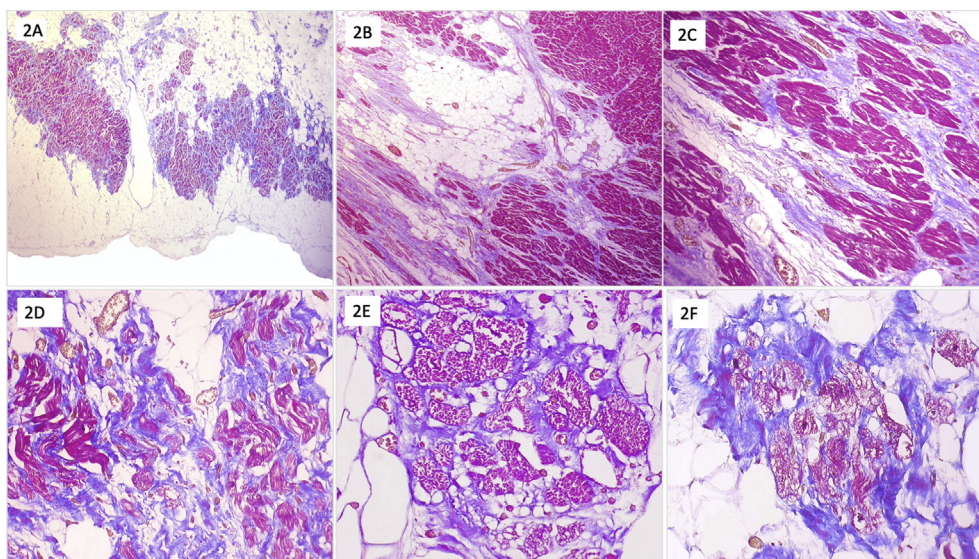


Fig. 2. Histology of the heart. Dense fibrosis is admixed to fatty tissue and to residual myocardium (A–B, Azan Mallory trichrome, 50 x, 100 x) and severe myocyte alterations are evident: increased size (C, Azan Mallory trichrome, 100 x), attenuation (D, Azan Mallory trichrome, 200 x) and cytoplasmic vacuolization (E–F, Azan Mallory trichrome, 400 x).

Table 1
Features of the variants identified in this study in the TMEM43 and DSP genes

Gene and variant	Cytogenetic location, genomic position (GRCh38) and reference sequence	MIM phenotype	gnomAD frequency	Exome variant server	SIFT	Poly Phen	CADD	Mutation taster
TMEM43 c.1150 C > G p.Leu384Val	3p25.1 3:14183242C > G NM_0243342	Arrhythmogenic right ventricular dysplasia familial 5; ARVD5 [#604400]	3.19e-5	Absent	Tolerated 0.96	Benign 0.003	7.57	Polymorphism
DSP c.3533 T > G p.Leu1178Arg	6p24.3 6:7579723T > G NM_004415.4	Arrhythmogenic right ventricular dysplasia familial 8; ARVD8 [#607450]	Absent	Absent	Deleterious 0.01	Probably damaging 0.996	26.9	Disease causing

DSP, desmoplakin, TMEM43, Transmembrane Protein 43, gnomAD, Genome Aggregation Database <https://gnomad.broadinstitute.org>.

(AC), both confirmed by Sanger sequencing: a heterozygous mutation c.1150C > G (p.Leu384Val) in exon 12 of the TMEM43 (transmembrane protein 43) gene, and a heterozygous mutation c.3533 T > G (p.Leu1178Arg) in exon 23 of the DSP gene. Table 1 summarizes the cytogenetic and genomic locations of the two variants, their frequency in the gnomAD and Exon Variant Server databases and the prediction of their impact in accordance with four different algorithms. The available information about the DSP variant can be classified following the criteria set by the American College of Medical Genetics and Genomics (ACMG) Standards and Guidelines [5]; this results in the following evidence of pathogenicity: two moderate [(a) absent in population databases and (b) novel missense change at an amino acid residue where a different pathogenic missense change has been seen before [6]] and three supporting evidence [(a) in silico prediction of deleterious effect, (b) co-segregation with disease in multiple family members, (c) patient's phenotype highly specific for gene involved]. On this basis, the DSP variant must be considered "likely pathogenic" (2 moderate and ≥ 2 Supporting evidence). Evaluation of the TMEM43 variant by the same criteria leads to no

definitive classification; therefore, its status is confirmed as variant of unknown significance (VUS).

2.2. Family screening

A targeted familial screening was activated. Both parents of the proband died of natural causes although the only brother is living abroad and is unavailable for clinical/genetic evaluation. The proband had one child, a 19-year-old asymptomatic boy who underwent cardiac screening. ECG and echocardiography were normal (Fig. 3). Cardiac magnetic resonance (CMR) showed normal biventricular volumes and function without any regional abnormalities. At T2 weighted analysis, a hypointense area was identified in the LV inferolateral segment. On postcontrast sequencing, a long mid-mural stria of late gadolinium enhancement (LGE) was identified in the inferolateral wall both in 4 chambers and in short-axis images (Fig. 3). Diagnostic workup was completed with an exercise stress test and a Holter monitoring, which were unremarkable; in particular, no arrhythmias were recorded. Genetic testing was

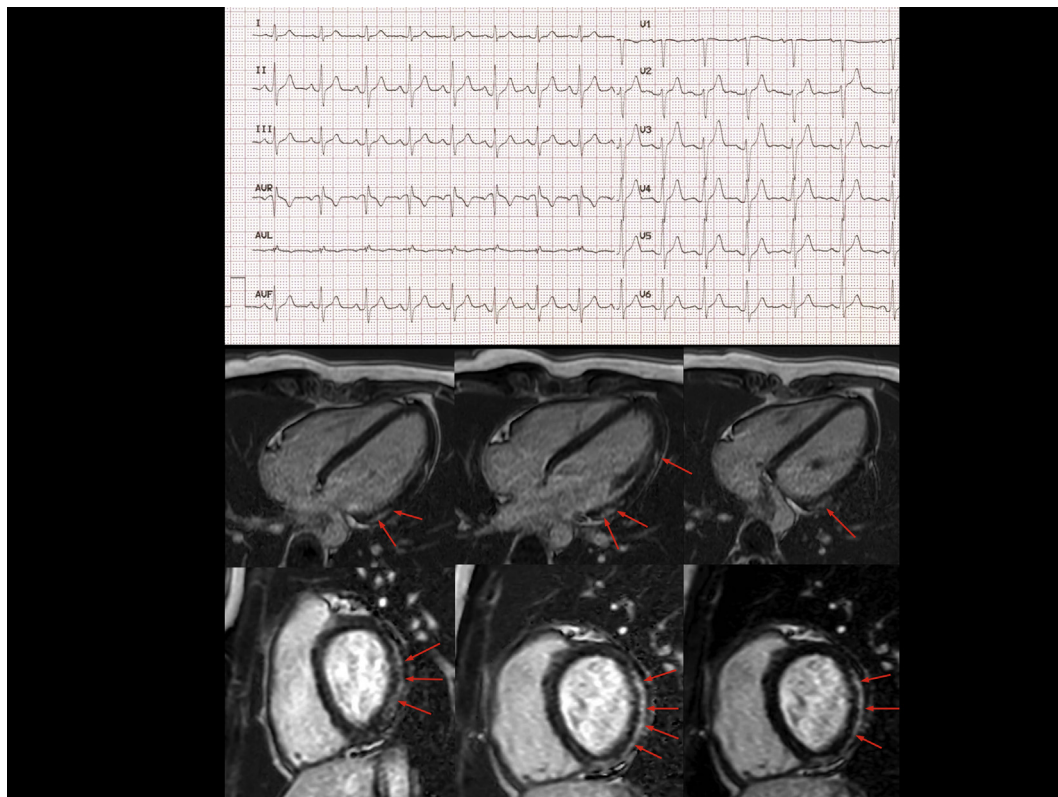


Fig. 3. Instrumental tests of the 19-year-old proband's son. Normal ECG. Linear LGE in subepicardial midwall region of the left ventricular inferolateral wall. LGE, late gadolinium enhancement (arrows).

performed and only the DSP variant was detected. Therefore, the young patient was diagnosed with ALVC. Given the history of sudden cardiac death in a first-degree relative, the possibility of defibrillator implantation for sudden cardiac death (SCD) primary prevention was thoroughly discussed with the boy and his mother, clearly explaining the lack of solid evidence in this context [7] as well as the benefits and the risks of such strategy. They both expressed a strong opinion in favor of the implantation, and this factor importantly influenced the final decision. As a result, the young patient gave his informed consent to the implant of a subcutaneous defibrillator.

3. Discussion

Our case report highlights the use of a regional network with a diagnostic pathway specifically dedicated to SD victims where clinicians, cardiovascular pathologists, and geneticists cooperate to identify the cause of death and activate a targeted familial screening.

We reported the case of a middle-aged man who died suddenly during moderate physical activity and whose heart was centralized to our Institution as part of a valve tissue banking regional protocol. The histopathological examination of the heart revealed abnormalities suggestive of ALVC; genetic testing results, albeit not conclusive, supported this hypothesis.

Clinical and genetic evaluation of the only son identified CMR signs suggestive of the same disease (ALVC) leading to the final decision of a subcutaneous defibrillator implantation for SCD primary prevention.

Left dominant AC is the most rare and recently described AC variant. Precise diagnostic guidelines are still lacking, and this cardiomyopathy is probably clinically underrecognized as the abnormal LV myocardial substrate not necessarily causes contractile dysfunction or electrocardiographic abnormalities [8,9].

The relationship between SD and LV involvement in AC has been recently investigated in detail [10]. In fact, in a large cohort of 202 SCD victims with a histopathological diagnosis of AC, authors reported a biventricular disease in 141 hearts (70%) and an isolated LV involvement in 35 cases (17%). In our case, SD was the first clinical expression of the disease in the absence of previous symptoms or medical records. This should not be surprising, given the non-transmural extension of the pathological process as well as the limited circumferential distribution. On the other hand, also the son's ECG and echocardiogram were normal but a CMR revealed LGE aspects highly specific for ALVC, with a topographic distribution that matched the histopathological abnormalities found in the father [11]. Therefore, we speculate that without such a thorough postmortem evaluation, the boy would have been considered healthy with potentially tragic implications [12–14].

The proband carried two variants of interest in genes associated with AC [15]. Importantly, the DSP variant – exon 23, c.3533T > G (p.Leu1178Arg) – was detected also in the living son. Whereas the causative link between several DSP variants and ALVC is well established [16–18], the pathogenic role of TMEM43 mutations has been poorly investigated. In fact, to date, the few described TMEM43 variants have been detected exclusively among patients with arrhythmogenic right ventricular cardiomyopathy whereas the role in ALVC is still unclear [19–23]. On the basis of the available information, the TMEM43 c.1150C > G p. Leu384Val variant is a VUS because it is not possible to assign it to one of the ACMG categories. On the other hand, the DSP variant is “likely pathogenic” in accordance with the ACMG Guidelines; in particular, we noted its absence in public databases of human genetic variation, such as gnomAD – consisting of 125,748 exomes and 15,708 genomes to date – and the fact that a variant involving the same amino acid in DSP was reported in a family with AC. It is also relevant that the DSP

gene has only two protein-coding transcripts reported in ENSEMBL (ENST00000379802.8 and ENST00000418664.2) and in both cases, the p.Leu1178 amino acid is present in the resulting protein [5,6].

As genetic testing of AC enters standard care, it is likely that the status of either or both variants will be confirmed or updated; it should also be noted that formally we cannot exclude a digenic contribution (with TMEM43 as modifier) to the genesis of SCD [24,25].

In our case, the opportunity of a defibrillator implantation for SCD prevention was thoroughly discussed. Currently, it is impossible to stratify the risk of major arrhythmic events for patients with ALVC due to the scarce evidence, derived mainly from case reports and small series. Therefore, in this scenario, the possibility of a defibrillator implantation should be considered on a case-by-case basis, taking into account the psychological impact and the patient's preference.

“Hic mors gaudet succurrere vitae: here death is delighted to aid life” is the classic plaque exhibited in many anatomical theaters around Europe [26,27]. Our case report embodies a model of multidisciplinary approach to SD where an accurate cardiopathological postmortem examination was implemented by molecular testing leading to the diagnosis of a rare hereditary disease, subsequently detected also in the proband's living son as a result of a targeted familial screening.

Funding sources

“Fondazione Luisa Fanti Melloni”, University of Bologna, Italy.

Conflicts of interest

The authors declare no conflict of interest.

Appendix A. Supplementary data

Supplementary data to this article can be found online at <https://doi.org/10.1016/j.carpath.2019.107157>.

References

- [1] Basso C, Carturan E, Pilichou K, Rizzo S, Corrado D, Thiene G. Sudden cardiac death with normal heart: molecular autopsy. *Cardiovasc Pathol* 2010. <https://doi.org/10.1016/j.carpath.2010.02.003>.
- [2] Basso C, Aguilera B, Banner J, Cohle S, d'Amati G, de Gouveia RH, et al. Guidelines for autopsy investigation of sudden cardiac death: 2017 update from the Association for European Cardiovascular Pathology. *Virchows Arch* 2017. <https://doi.org/10.1007/s00428-017-2221-0>.
- [3] Shanks GW, Tester DJ, Ackerman JP, Simpson MA, Behr ER, White SM, et al. Importance of variant interpretation in whole-exome molecular autopsy. *Circulation* 2018. <https://doi.org/10.1161/circulationaha.117.031053>.
- [4] Lahrouchi N, Raju H, Lodder EM, Papatheodorou E, Ware JS, Papadakis M, et al. Utility of post-mortem genetic testing in cases of sudden arrhythmic death syndrome. *J Am Coll Cardiol* 2017. <https://doi.org/10.1016/j.jacc.2017.02.046>.
- [5] Richards S, Aziz N, Bale S, Bick D, Das S, Gastier-Foster J, et al., ACMG Laboratory Quality Assurance Committee. Standards and guidelines for the interpretation of sequence variants: a joint consensus recommendation of the American College of medical genetics and genomics and the association for molecular pathology. *Genet Med* 2015;405–24. <https://doi.org/10.1038/gim.2015.30>.
- [6] G1 Quarta, Muir A, Pantazis A, Syrris P, Gehmlich K, Garcia-Pavia P, et al. Familial evaluation in arrhythmogenic right ventricular cardiomyopathy: impact of genetics and revised task force criteria. *Circulation* 2011. <https://doi.org/10.1161/CIRCULATIONAHA.110.976936>.
- [7] Towbin JA, McKenna WJ, Abrams DJ, Ackerman MJ, Calkins H, Darrieux FCC, et al. 2019 HRS expert consensus statement on evaluation, risk stratification, and management of arrhythmogenic cardiomyopathy. *Heart Rhythm* 2019. <https://doi.org/10.1016/j.hrthm.2019.05.007>.
- [8] Sen-Chowdhry S, Syrris P, Prasad SK, Hughes SE, Merrifield R, Ward D, et al. Left-dominant arrhythmogenic cardiomyopathy. An under-recognized clinical entity. *J Am Coll Cardiol* 2008. <https://doi.org/10.1016/j.jacc.2008.09.019>.
- [9] Coats CJ, Quarta G, Flett AS, Pantazis AA, McKenna WJ, Moon JC. Arrhythmogenic left ventricular cardiomyopathy. *Circulation* 2009. <https://doi.org/10.1161/circulationaha.109.874628>.

- [10] Miles C, Finocchiaro G, Papadakis M, Gray B, Westaby J, Ensam B, et al. Sudden death and left ventricular involvement in arrhythmogenic cardiomyopathy. *Circulation* 2019. <https://doi.org/10.1161/CIRCULATIONAHA.118.037230>.
- [11] Zorzi A, Marra MP, Rigato I, De Lazzari M, Susana A, Niero A, et al. Non-ischemic left ventricular scar as a substrate of life-threatening ventricular arrhythmias and sudden cardiac death in competitive athletes. *Circ Arrhythmia Electrophysiol* 2016. <https://doi.org/10.1161/CIRCEP.116.004229>.
- [12] Pilichou K, Mancini M, Rigato I, Lazzarini E, Giorgi B, Carturan E, et al. Non-ischemic left ventricular scar sporadic or familial? Screen the genes, scan the mutation carriers. *Circulation* 2014. <https://doi.org/10.1161/CIRCULATIONAHA.114.012515>.
- [13] Sen-Chowdhry S, McKenna WJ. Sudden cardiac death in the young: a strategy for prevention by targeted evaluation. *Cardiology* 2006. <https://doi.org/10.1159/000091640>.
- [14] Behr ER, Dalageorgou C, Christiansen M, Syrris P, Hughes S, Tome Esteban MT, et al. Sudden arrhythmic death syndrome: familial evaluation identifies inheritable heart disease in the majority of families. *Eur Heart J* 2008. <https://doi.org/10.1093/eurheartj/ehn219>.
- [15] Karmouch J, Protonotarios A, Syrris P. Genetic basis of arrhythmogenic cardiomyopathy. *Curr Opin Cardiol* 2018. <https://doi.org/10.1097/HCO.0000000000000509>.
- [16] López-Ayala JM, Gómez-Milanés I, Muñoz JJ, Ruiz-Espejo F, Ortíz M, González-Carrillo J, et al. Desmoplakin truncations and arrhythmogenic left ventricular cardiomyopathy: characterizing a phenotype. *Europace* 2014. <https://doi.org/10.1093/europace/euu128>.
- [17] Castelletti S, Vischer AS, Syrris P, Crotti L, Spazzolini C, Ghidoni A, et al. Desmoplakin missense and non-missense mutations in arrhythmogenic right ventricular cardiomyopathy: genotype-phenotype correlation. *Int J Cardiol* 2017. <https://doi.org/10.1016/j.ijcard.2017.05.018>.
- [18] Tsatsopoulou A. Desmoplakin: highlights on a left ventricular arrhythmogenic disorder. *Int J Cardiol* 2017. <https://doi.org/10.1016/j.ijcard.2017.09.030>.
- [19] Christensen A, Andersen C, Tybjaerg-Hansen A, Haunso S, Svendsen J. Mutation analysis and evaluation of the cardiac localization of TMEM43 in arrhythmogenic right ventricular cardiomyopathy. *Clin Genet* 2011. <https://doi.org/10.1111/j.1399-0004.2011.01623.x>.
- [20] Milting H, Klauke B, Christensen AH, Müsebeck J, Walhorn V, Grannemann S, et al. The TMEM43 Newfoundland mutation p.S358L causing ARVC-5 was imported from Europe and increases the stiffness of the cell nucleus. *Eur Heart J* 2015. <https://doi.org/10.1093/eurheartj/ehu077>.
- [21] Klauke B, Baecker C, Müsebeck J, Schulze-Bahr E, Gerdes D, Gaertner A, et al. Deleterious effects of the TMEM43 mutation p.S358L found in a German family with arrhythmogenic right ventricular cardiomyopathy and sudden cardiac death. *Cell Tissue Res* 2012;348:368.
- [22] Merner ND, Hodgkinson KA, Haywood AFM, Connors S, French VM, Drenckhahn JD, et al. Arrhythmogenic right ventricular cardiomyopathy type 5 is a fully penetrant, lethal arrhythmic disorder caused by a missense mutation in the TMEM43 gene. *Am J Hum Genet* 2008. <https://doi.org/10.1016/j.ajhg.2008.01.010>.
- [23] Haywood AFM, Merner ND, Hodgkinson KA, Houston J, Syrris P, Booth V, et al. Recurrent missense mutations in TMEM43 (ARVD5) due to founder effects cause arrhythmogenic cardiomyopathies in the UK and Canada. *Eur Heart J* 2013. <https://doi.org/10.1093/eurheartj/ehs383>.
- [24] Rigato I, Bauce B, Rampazzo A, Zorzi A, Pilichou K, Mazzotti E, et al. Compound and digenic heterozygosity predicts lifetime arrhythmic outcome and sudden cardiac death in desmosomal gene-related arrhythmogenic right ventricular cardiomyopathy. *Circ Cardiovasc Genet* 2013. <https://doi.org/10.1161/CIRCGENETICS.113.000288>.
- [25] Bauce B, Nava A, Beffagna G, Basso C, Lorenzon A, Smaniotto G, et al. Multiple mutations in desmosomal proteins encoding genes in arrhythmogenic right ventricular cardiomyopathy/dysplasia. *Heart Rhythm* 2010. <https://doi.org/10.1016/j.hrthm.2009.09.070>.
- [26] Thiene G. Sudden cardiac death and cardiovascular pathology: from anatomic theater to double helix. *Am J Cardiol* 2014. <https://doi.org/10.1016/j.amjcard.2014.09.037>.
- [27] Thiene G, Saffitz JE. Autopsy as a source of discovery in cardiovascular medicine: then and now. *Circulation* 2018. <https://doi.org/10.1161/CIRCULATIONAHA.118.033234>.

Case Report

A Pathogenic Galactosidase A Mutation Coexisting With an MYBPC3 Mutation in a Female Patient With Hypertrophic Cardiomyopathy

Giovanni Vitale, MD,^a Ferdinando Pasquale, MD, PhD,^a Ornella Leone, MD,^b
Giovanna Cenacchi, MD,^c Fabio Niro, MD,^d Mario Torrado, PhD,^c Emilia Maneiro, PhD,^f
Maddalena Graziosi, MD, PhD,^a Raffaello Ditaranto, MD,^a Irene Capelli, MD, PhD,^g
Lorenzo Monserrat, MD, PhD,^f Claudio Rapezzi, MD,^{h,i} and Elena Biagini, MD, PhD^a

^a Azienda Ospedaliero Universitaria - Policlinico di St. Orsola, Cardiology Unit, Cardio-Thoracic-Vascular Department, Bologna, Italy

^b Cardiovascular Pathology Unit, Sant'Orsola-Malpighi Hospital, Bologna, Italy

^c Department of Biomedical and Neuromotor Science, University of Bologna, Bologna, Italy

^d Cardiothoracic Radiology Unit, Sant'Orsola-Malpighi Hospital, Bologna, Italy

^e Institute of Health Sciences, University of A Coruña, A Coruña, Spain

^f Health in Code, A Coruña, Spain

^g Nephrology, Department of Experimental, Diagnostic, and Specialty Medicine, University of Bologna, Bologna, Italy

^h Cardiology, University of Ferrara and Maria Cecilia Hospital, Cotignola, Italy

ⁱ GVM Care and Research, Cotignola, Italy

ABSTRACT

The coexistence of *GLA* (Pro259Ser, c.775C>T) and *MYBPC3* (c.1351+2T>C) mutations was found in a female patient with hypertrophic cardiomyopathy. Histology documented abundant vacuolisation with osmiophilic lamellar bodies and positive Gb3 immunohistochemistry. In the presence of a hypertrophic cardiomyopathy phenotype, the systematic search for unusual findings is mandatory to rule out a phenocopy.

RÉSUMÉ

On a observé la coexistence de mutations des gènes *GLA* (Pro259Ser, c.775C>T) et *MYBPC3* (c.1351+2T>C) chez une patiente atteinte d'une cardiomyopathie hypertrophique. L'examen histologique a révélé une vacuolisation importante et la présence de corps lamellaires osmiophiles, et l'analyse par immunohistochimie a mis au jour la présence de globotriaosylcéramides (Gb3). En présence d'un phénotype de cardiomyopathie hypertrophique, il est impératif de rechercher systématiquement les anomalies afin d'écartier la possibilité d'une phénocopie.

Case

A 63-year-old Italian woman with history of juvenile asymptomatic paroxysmal Mobitz type I second-degree atrioventricular (AV) block was admitted to our hospital for atypical chest pain. Standard 12-lead electrocardiography showed sinus rhythm with right bundle branch block and negative lateral T waves. Cardiac troponin I variation was not indicative of acute myocardial injury (232-227-224 ng/L, reference range [RR] < 40 ng/L), and coronary arteries

appeared normal on angiography. Echocardiography showed left ventricular (LV) hypertrophy with maximal wall thickness (MWT) of 13 mm at the anterior basal septum and hypertrophy of the LV papillary muscles. Cardiac magnetic resonance, performed with a 1.5-T magnet (Ingenia; Philips), confirmed LV hypertrophy (LV mass index 72 g/m², RR 52 ± 7.4 g/m²; MWT at anterior basal septum 15 mm). Intramyocardial late gadolinium enhancement (LGE) was detected in the basal posterolateral wall, and native T1 was reduced in the posterobasal septum (878 ms, RR 1003 ± 46 ms) at modified Look-Locker inversion recovery sequence (Fig. 1).

Because of the association among hypertrophic cardiomyopathy (HCM), history of AV block, posterolateral LGE, and confined septal low T1, a genetic analysis including the most frequent phenocopies was performed, with the following

Received for publication June 17, 2019. Accepted April 6, 2020.

Corresponding author: Dr Elena Biagini, Via G. Massarenti 9, 40138, Bologna, Italy. Tel.: (+39)051-2144483; fax: (+39)051-6363411.

E-mail: elena.biagini73@gmail.com

See page 1554.e3 for disclosure information.

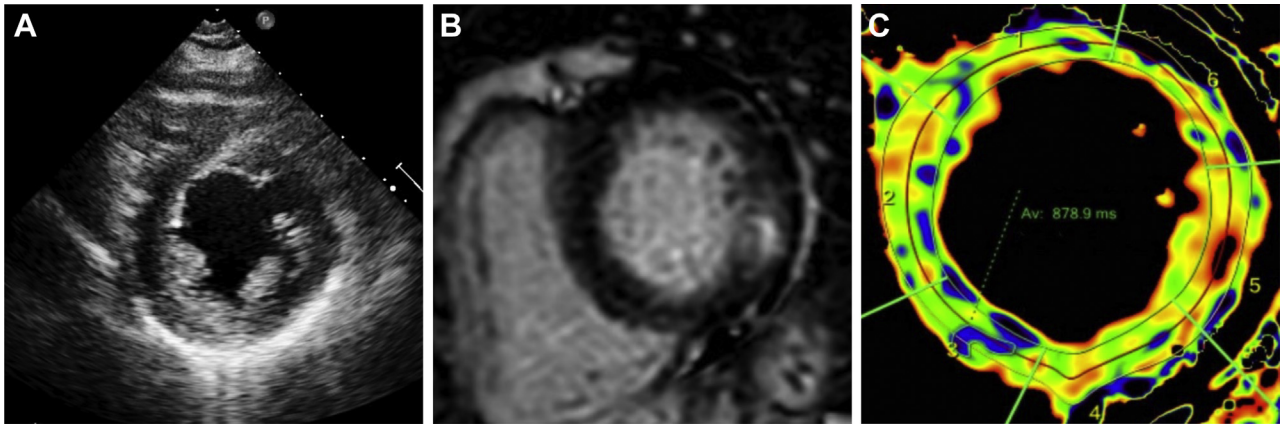


Figure 1. (A) Echocardiogram showing hypertrophy of papillary muscles. (B, C) Cardiac magnetic resonance with (B) posterolateral late enhancement and (C) low native T1 at posterobasal septum.

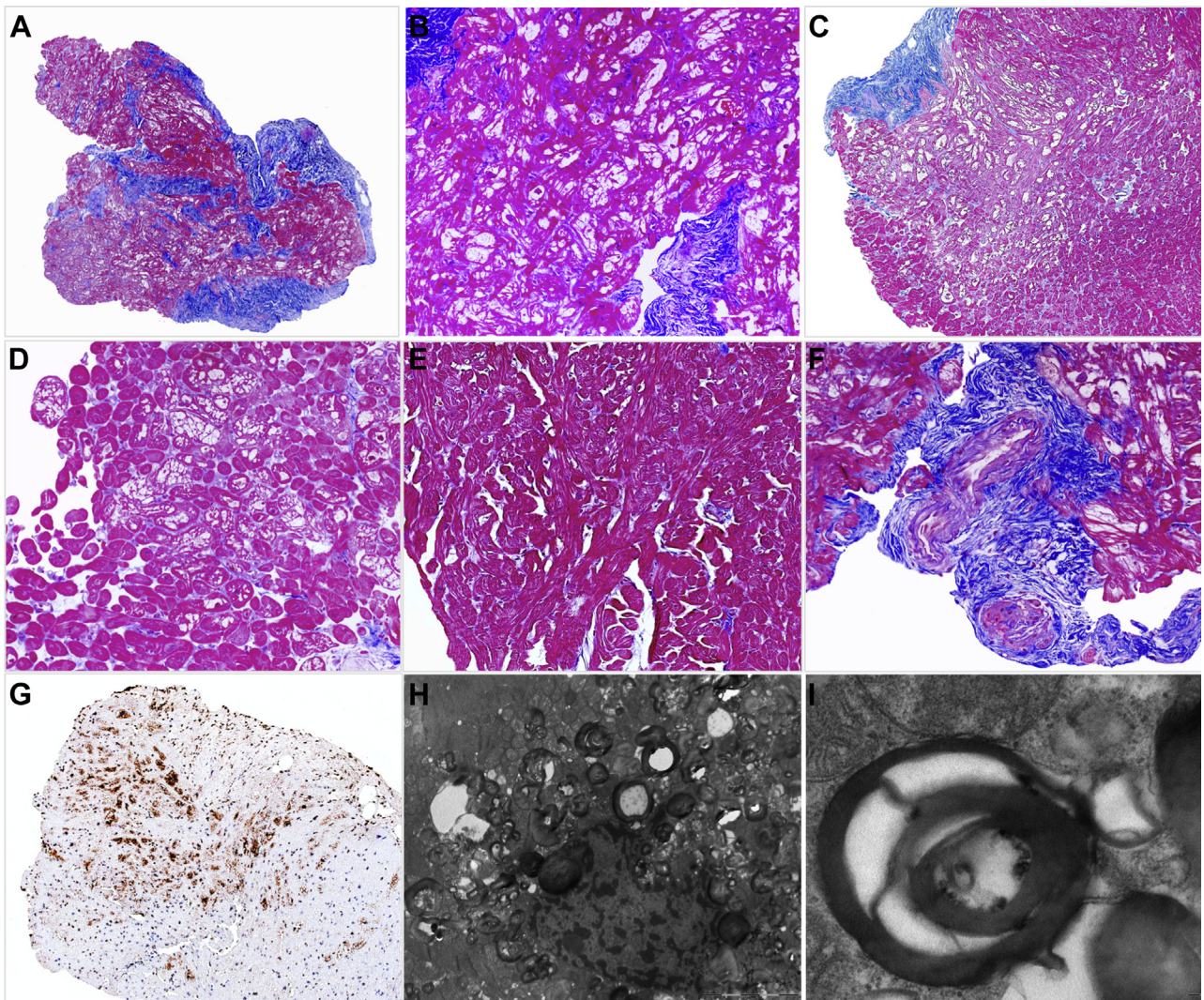


Figure 2. Histology of endomyocardial biopsy with Mallory trichrome stain showing (A, $\times 50$) moderate myocardial fibrosis, (B, $200\times$) marked myocyte vacuolisation with (C, $\times 100$; D, $\times 200$) patchy distribution, (E, $\times 200$) enlarged myocytes with myocardial disarray, and (F, $\times 200$) small vessels disease. (G) Gb3 immunohistochemistry with strong staining of the vacuolated myocytes ($\times 100$). (H, I) Ultrastructural features of lysosomal inclusion with a concentric-lamellar pattern.

genes: *MYH7*, *MYBPC3*, *TNNT2*, *TNNI3*, *TPM1*, *ACTC1*, *MYL2*, *MYL3*, *TTR*, *GLA*, *PRKAG2*, and *LAMP2*. Heterozygous mutations in 2 different genes were found: the splice-site mutation NM_000256.3:c.1351+2T>C in *MYBPC3* and the missense mutation NM_000169.2:c.775C>T [p.(Pro259Ser)] in *GLA*.¹ Plasma lyso-Gb3 levels were 3.0 ng/mL (RR ≤ 1.8 ng/mL). Dermatologic and neurologic screenings were negative, renal function was normal except for Maltese cross-like crystals in urinary sediment, and cornea verticillata was excluded.

Endomyocardial biopsy showed diffuse myocyte hypertrophy with multiple areas of myocardial and myofibrillar disarray and moderate subendocardial interstitial fibrosis. Small arteries with medial hypertrophy and fibrosis of the wall were also present. Marked sarcoplasmic vacuolisation consisting of small periodic acid–Schiff–negative and Pearls–negative confluent vacuoles was evident in some myocardial areas alongside others without, according to a “patchy” distribution. At ultrastructural examination, large vacuoles containing osmiophilic myelinoid lamellar bodies suitable for complex lipid storage were detected (Fig. 2). Enzyme replacement therapy with agalsidase alpha was started, and cascade genetic testing performed in all first-degree relatives had negative results except for the sarcomeric mutation in the son, without clinical expression.

Discussion

Cardiac involvement in Anderson-Fabry (AF) disease is one of the most disabling organ damages, causing HCM, conduction disturbances, and arrhythmias. Different missense mutations in the *GLA* gene with replacement of the Pro259 amino acid have been reported to cause either the classic or the late-onset phenotype and suggesting a relevant role of this amino acid in the protein function.^{2,3} Pro259Ser mutation was reported by Kwon et al. in a 59-year-old man with HCM and perinucleolar vacuolisation at endomyocardial biopsy, albeit without ultrastructural characterisation.⁴ In the present case, the typical zebra bodies at electron microscopy along with positive Gb3 immunohistochemistry provided evidence of Gb3 storage in myocytes. The patchy distribution of myocyte vacuolization as well as the confined septal low T1 at T1 mapping could be related to the random X-chromosome inactivation in female patients. Troponin I elevation, already reported in AF disease, could be the expression of chronic cardiac damage in which proapoptotic and inflammatory pathways are probably involved.⁵

Regarding the intronic *MYBPC3* variant, *in silico* and *in vivo* specific genetic analyses confirmed its pathogenicity,

leading to frameshift change and premature stop codon (Supplementary Material).

Coexistence of sarcomeric and AF mutations is uncommon but possible in HCM. Differential diagnosis is mandatory, because a specific therapy for AF disease is available. Moreover, differences in terms of sudden death risk stratification and genetic counselling of relatives are implied. In the presence of an HCM phenotype, unusual findings, such as AV blocks, papillary muscle hypertrophy, and posterolateral fibrosis, are important red flags that require careful evaluation to rule out a phenocopy.

Funding Sources

The authors have no funding sources to declare.

Disclosures

F.P. received speaker fees from Shire. C.R. and E.B. received speaker fees from Shire Italia Spa (now named Takeda) and Sanofi-Genzyme, Italia. The other authors have no conflicts of interest to disclose.

References

1. Alfares AA, Kelly MA, McDermott G, et al. Results of clinical genetic testing of 2,912 probands with hypertrophic cardiomyopathy: expanded panels offer limited additional sensitivity. *Genet Med* 2015;17:880-8.
2. Topaloglu AK, Ashley GA, Tong B, et al. Twenty novel mutations in the alpha-galactosidase A gene causing Fabry disease. *Mol Med* 1999;5:806-11.
3. Ashley GA, Shabbeer J, Yasuda M, Eng CM, Desnick RJ. Fabry disease: twenty novel alpha-galactosidase A mutations causing the classical phenotype. *J Hum Genet* 2001;46:192-6.
4. Kwon S, Lee SP, Park SS, et al. Fabry disease that phenocopies hypertrophic cardiomyopathy: a thorough genetic “detective” identifies the “rogue” hidden in the *GLA* gene. *Korean Circ J* 2019;49:464-7.
5. Feustel A, Hahn A, Schneider C, et al. Continuous cardiac troponin I release in Fabry disease. *PLoS One* 2014;9:e91757.

Supplementary Material

To access the supplementary material accompanying this article, visit the online version of the *Canadian Journal of Cardiology* at www.onlinecjc.ca and at <https://doi.org/10.1016/j.cjca.2020.04.008>.



Claudio Rapezzi, Alberto Foà, and Raffaello Ditaranto

7.1 Introduction

Standard ECG is one of the essential diagnostic tools when approaching a patient with suspected myocarditis. Most of the knowledge on ECG correlates was mainly collected in the 1970s when myocarditis was diagnosed on the basis of endomyocardial biopsy (EMB) findings.

Over the last two decades, the introduction and the widespread use of cardiac magnetic resonance (CMR) has broadened the number of myocarditis diagnoses, especially among patients with mild forms who might have not received an EMB according to current indications.

Myocarditis is no longer considered a single entity, but rather a spectrum of clinical conditions, so that diagnostic work-up, risk stratification, and therapeutic management are nowadays challenging. Namely, the 2013 ESC myocarditis Task Force position statement [1] identified four main clinical scenarios of myocarditis presentation: acute coronary syndrome (ACS) like, new onset or worsening heart failure, chronic heart failure, life threatening condition (i.e. life threatening arrhythmias/aborted sudden death, cardiogenic shock, and severely impaired left ventricle [LV] function).

This chapter summarizes the available data on ECG characteristics of acute, sub-acute, and chronic myocarditis according to clinical presentation as well as the underlying etiology, trying to identify the most relevant findings that may be useful for differential diagnosis and prognostic stratification.

C. Rapezzi (✉) · A. Foà · R. Ditaranto
Cardiology, Department of Experimental Diagnostic and Specialty Medicine, Alma Mater
Studiorum-University of Bologna, Bologna, Italy
e-mail: claudio.rapezzi@unibo.it; alberto.foa@gmail.com, alberto.foa2@unibo.it;
raffaello.ditaranto@studio.unibo.it

7.2 The Spectrum of ECG Findings in Different Clinical Presentations of Myocarditis: Prevalence, Electrogenesis, Diagnostic Implications, and Differential Diagnosis

A wide spectrum of ECG findings can be found in acute myocarditis [2] including ST elevation and depression, atrioventricular blocks of different degrees, PR segment depression/elevation, QRS enlargement and bundle branch blocks, abnormal Q waves, reduced QRS voltage, T wave inversion, and QT interval prolongation. Furthermore, atrial and ventricular arrhythmias frequently coexist. Nevertheless, it should be noted that patients affected by acute myocarditis might have a normal ECG [3] at first medical contact and develop only mild abnormalities throughout the disease.

The correct ECG interpretation cannot be detached from clinical background. In this regard the current myocarditis classification [1], differentiated according to clinical presentation, meets this requirement.

7.2.1 Acute Coronary Syndrome (ACS)

Acute myocarditis can mimic an ACS, with chest pain (frequently starting within 1–4 weeks from a respiratory or gastrointestinal infection), ST/T wave changes, increased serum troponin levels (more commonly with prolonged and sustained release over several weeks or months). Global or regional LV or right ventricular (RV) dysfunction can be observed at imaging. Viral lymphocytic myocarditis is presumed to be the most frequent cause, although other infectious/inflammatory causes might be responsible of the scenario. These ECG findings are thought to be the result of a combination of inflammation, necrosis and, in some circumstances, coronary vasospasm as shown in parvovirus B19 (PVB19) endothelial cells infection [4], causing vascular dysfunction.

The presence of ST elevation (STE) in patients with acute myocarditis might lead to a wrong ST-segment elevation myocardial infarction (STEMI) diagnosis. Typically, in these cases, myocarditis causes isolated saddle-shaped (concave) STE without specular repolarization changes, or a widespread STE with diffuse distribution (except for aVR). However, STE topography may be localized and associated with specular ST depression, perfectly mimicking a coronary pattern, and ST may have a convex aspect (Fig. 7.1). A long-lasting STE (paralleling troponin kinetics) with a slow regression of ECG abnormalities is in favor of acute myocarditis. On the other hand, in anterior STEMI due to distal or mid-level left descendent anterior coronary occlusion (after the first diagonal branch), reciprocal ST depression in the inferior leads is absent and ST segment can even be elevated in both anterior and inferior leads [5, 6] (Fig. 7.2). The electrocardiographic ambiguity of myocarditis and ACS contributes to a relevant risk of diagnostic mistakes, even in specialized and ultra-specialized settings [7–12]. This is clearly evident in data coming from different PCI networks [7–13], showing a high frequency (up to 39%) of inappropriate cardiac catheterization laboratories' activation for primary PCI. Within these false positives, a relevant percentage of patients received a diagnosis of acute myocarditis at the end of work-up. Awareness of this phenomenon and of the possible role of acute myocarditis is fundamental to avoid the simplistic

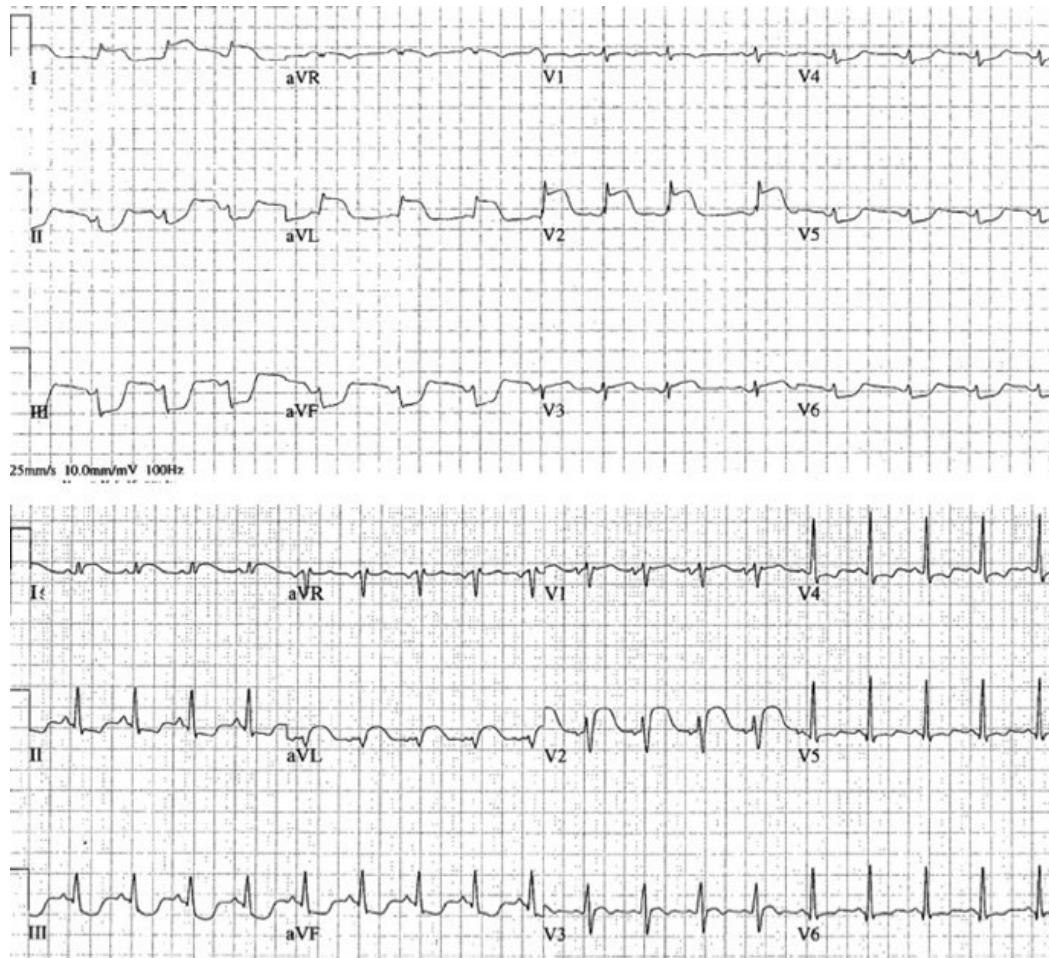


Fig. 7.1 Two cases of acute myocarditis presenting with ST segment elevation in the lateral leads and marked ST depression in the inferior leads. In both cases precordial leads show an “inconsistent” isolated ST elevation in V2

label of ACS with normal coronary arteries or myocardial infarction with nonobstructive coronary arteries (MINOCA) and to address patients towards a tailored diagnostic evaluation and appropriate management.

While in STEMI the value of ECG in localizing the affected regions is unquestionable, ECG is an unreliable tool to localize involved heart muscle sites in acute myocarditis. Different studies [3, 14, 15] tried to assess the ability of ECG to predict inflammatory process localization, using cardiac magnetic resonance as reference for in vivo tissue characterization. All available data showed poor correlation. Particularly, Meléndez-Ramírez et al. [14] found only a moderate agreement for the inferolateral localization of late gadolinium enhancement (LGE) and STE, but not in the other regions. Nucifora et al. [15] reported a topographic agreement between LGE and STE site in 59% of patients presenting with anterolateral STE, in 46% of those with inferolateral STE, with an overall agreement between the LGE and STE site reaching 68%. These data might reflect a limited resolution of CMR, unable to detect small areas of myocardial damage that are, however, large enough to modify the ECG. Conversely, the magnitude of STE and a late ST normalization were found to be significantly and independently related to the extent of LGE, identifying the

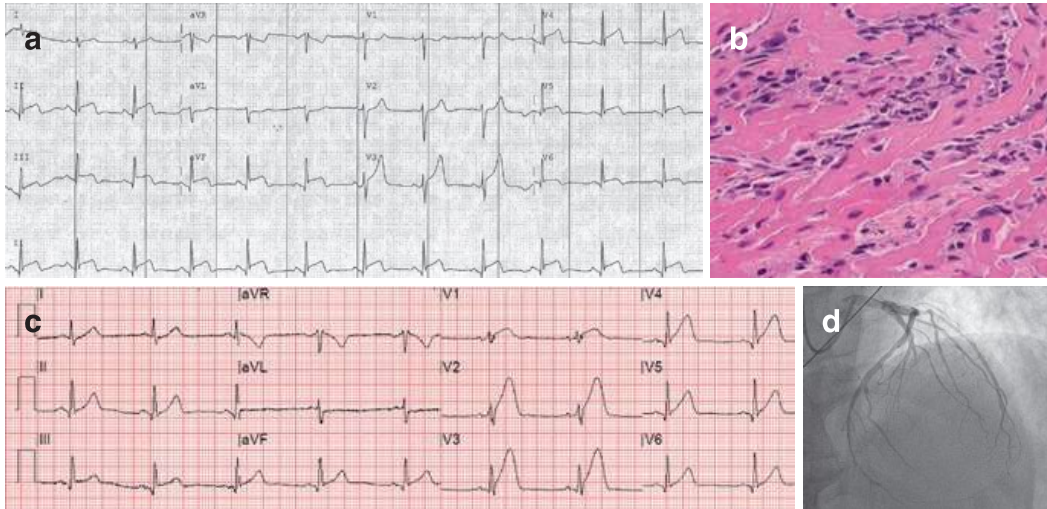


Fig. 7.2 Two examples of anterolateral ST segment elevation without reciprocal changes (a) and (c). In both cases ST elevation involves both anterior and inferior leads. (b) shows the underlying acute myocarditis with lymphocytic infiltrates while in (d) a mid-level occlusion of the left anterior descending artery is evident resulting in the same electrocardiographic pattern. *Courtesy of Dr. Ornella Leone and Dr. Nevio Taglieri*

ECG as an easy bedside tool for predicting the extent of myocardial damage, irrespective of its localization.

Another ECG feature that may be helpful in differential diagnosis is the Q wave. More specifically, although Q waves can be present in the acute phase of myocarditis, they may be overlooked due to their brief appearance. In myocardial infarction Q waves persist indefinitely, due to irreversible myocardial injury, whereas Q waves in myocarditis might disappear along with the inflammatory process resolution. Supposedly, Q waves in myocarditis reflect the transiently decreased electrical and mechanical activity in the inflamed regions, not necessarily implying cellular death. This view is in keeping with the clinical observation that LV function improvement usually occurs when Q waves disappear. Myocarditis patients with Q waves generally have more thickened myocardium, more depressed LV function (with an inverse correlation between the number of leads showing Q waves and reduced LV ejection fraction) and a higher incidence of severe complications, e.g. hemodynamic instability and conduction disturbances.

The ECG in acute myocarditis can also simulate acute myocardial infarction without ST segment elevation (NSTEMI). Inverted symmetric T waves, typically short lasting, may be documented, resembling those seen in coronary artery disease. These findings can be isolated or associated with ST depression (or sometimes following ST elevation), localized at two or more contiguous leads or present in all standard leads except for aVR, the so-called diffuse inversion (Fig. 7.3). The reported prevalence of T-waves inversion (TWI) varies from 9% to 48% and likely reflects the underlying myocardial edema and dyshomogeneity of cardiomyocyte repolarization between spared endocardial and diseased epicardial layers. Similarly to STE, concordance between TWI location at ECG leads and affected LV segments at cardiac imaging is poor. Considering any pattern of myocardial edema, De Lazzari et al. [16] reported an overall topographic agreement not exceeding 57%. However, focusing only on areas affected by transmural myocardial edema, the

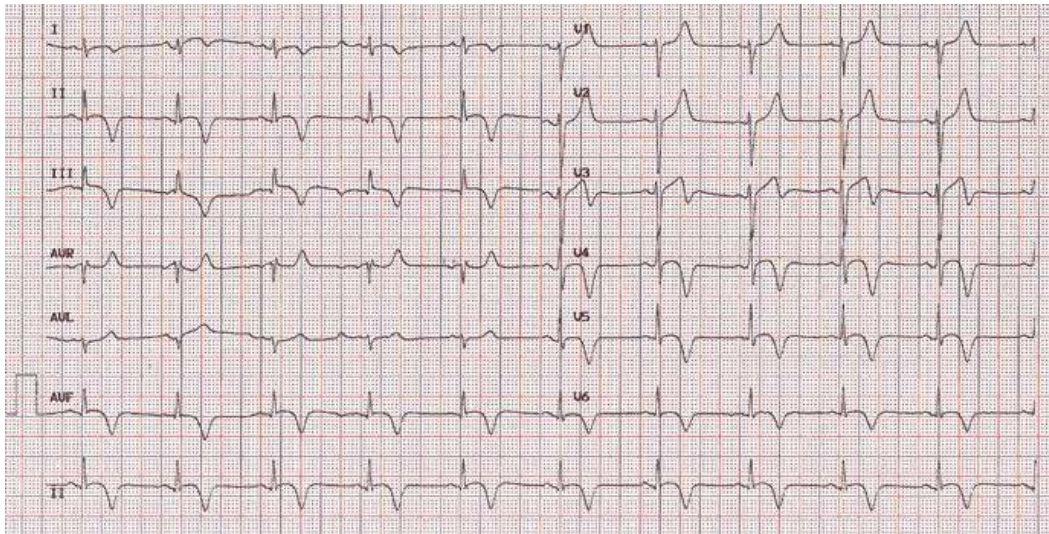


Fig. 7.3 Diffuse (giant) T wave inversion in a young adult with lymphocytic myocarditis presenting with chest pain

overall agreement raised to 88%, supporting the hypothesis that the occurrence of TWI mostly depends on the extent of transmural myocardial edema. Furthermore, the development of TWI was significantly and independently associated with the extent of myocardial LGE. This study underlines the ability of the ECG, once again, to estimate the amount rather than the topography of myocardial damage.

A peculiar form of acute myocarditis often characterized by a pseudo-ACS presentation is represented by *myocarditis associated with pericarditis*, a still widely debated clinical entity. The term indicates a condition in which a typical acute pericarditis is accompanied by echocardiographic or CMR evidence of new onset global/regional wall motion abnormalities or by an abnormal troponin release.

Notably, since the pericardium is electrically silent, the classical ECG changes detected in pericarditis are actually generated in response to myocardial inflammation of subepicardial layers. In this context, the diffuse STE without reciprocal ST segment depression, the PR segment depression and the evolution towards transient negative T waves, reflect an existing “epicarditis.” Accordingly, the magnitude of ST-T abnormalities usually correlates with the extent of myocardial inflammation.

Although various and often non-specific ECG patterns may accompany myocarditis associated with pericarditis, ECG may provide useful clues to identify myocardial involvement among patients with pericarditis. Imazio et al. in a series of 234 cases of isolated acute pericarditis compared with 40 cases of myocarditis associated with pericarditis described in the latter a higher prevalence of ST segment elevation (90 vs 70%) and an “atypical” ECG evolution, not necessarily following the classic 4 stages of pericarditis [17]. In fact, among patients with myocarditis associated with pericarditis, negative T waves may be detected before ST segment normalization. Furthermore, patients with myocarditis associated with pericarditis show a much greater arrhythmogenic burden, mainly characterized by ventricular arrhythmias [17]. Lastly, a prolonged QT interval may be detected as an expression of acute myocardial damage.

7.2.2 New Onset or Worsening Heart Failure

The clinical scenario of acute heart failure associated with imaging evidence of a dilated/hypokinetic cardiomyopathy phenotype underlies two possible conditions: sudden onset symptoms in the context of a pre-existing cardiomyopathy or, alternatively, a new onset ventricular dysfunction. In this setting, ECG findings integrated with clinical characteristics, echocardiography, and eventually CMR imaging may address a differential diagnosis.

Acute Phase Indicators The most typical ECG findings in this setting are ST elevation or depression, low QRS voltages, impaired atrioventricular conduction, prolonged QT interval, and transient Q waves. Notably, reduced QRS voltages, frequently associated with sinus tachycardia, suggest extensive myocardial edema (Fig. 7.4) or pericardial effusion. Differently from what observed in an ischemic setting or in chronic cardiomyopathies, this ECG presentation in the acute phase is not necessarily associated with irreversible muscle loss: in fact, as myocardial inflammation resolves, QRS voltages increase paralleling the improvement in ventricular ejection fraction.

Chronic Phase Indicators Conversely, the absence of relevant repolarization abnormalities, an abnormal QRS duration, left bundle branch block, left ventricular hypertrophy, left atrial enlargement, and atrial fibrillation/flutter suggest a pre-existing condition.

7.2.3 Chronic Heart Failure

ECG findings in patients with inflammatory cardiomyopathy showing a dilated/hypokinetic phenotype are usually indistinguishable from those seen in non-inflammatory dilated cardiomyopathies. In fact, baseline ECG shows signs of chambers' remodeling due to hemodynamic overload, secondary to diastolic and systolic ventricular dysfunction as well as chronic wall inflammation. Specifically, variable degrees of intraventricular delay, left ventricular hypertrophy, left atrial enlargement, and atrial flutter or fibrillation are often detected. Cardiac sarcoidosis and Chagas disease represent two exceptions and are further described in detail.

7.2.4 Life Threatening Conditions

Sudden cardiac death (SCD) occurs in patients with myocarditis and can be the first disease presentation. Ventricular arrhythmias (VA, Fig. 7.5) and bradyarrhythmia (namely, high-degree/complete atrioventricular blocks, Fig. 7.6) can be documented both in acute and chronic myocarditis, with a wide spectrum of clinical presentations, ranging from palpitations to acute heart failure or cardiac arrest. Although they might be present in virtually all forms of myocarditis, the arrhythmogenic burden is generally greater in cases of giant cell myocarditis (GCM) and cardiac sarcoidosis.

The risk of VA is associated with the degree of tissue damage and inflammation. On the other hand, bradyarrhythmias are infrequently encountered, except for some

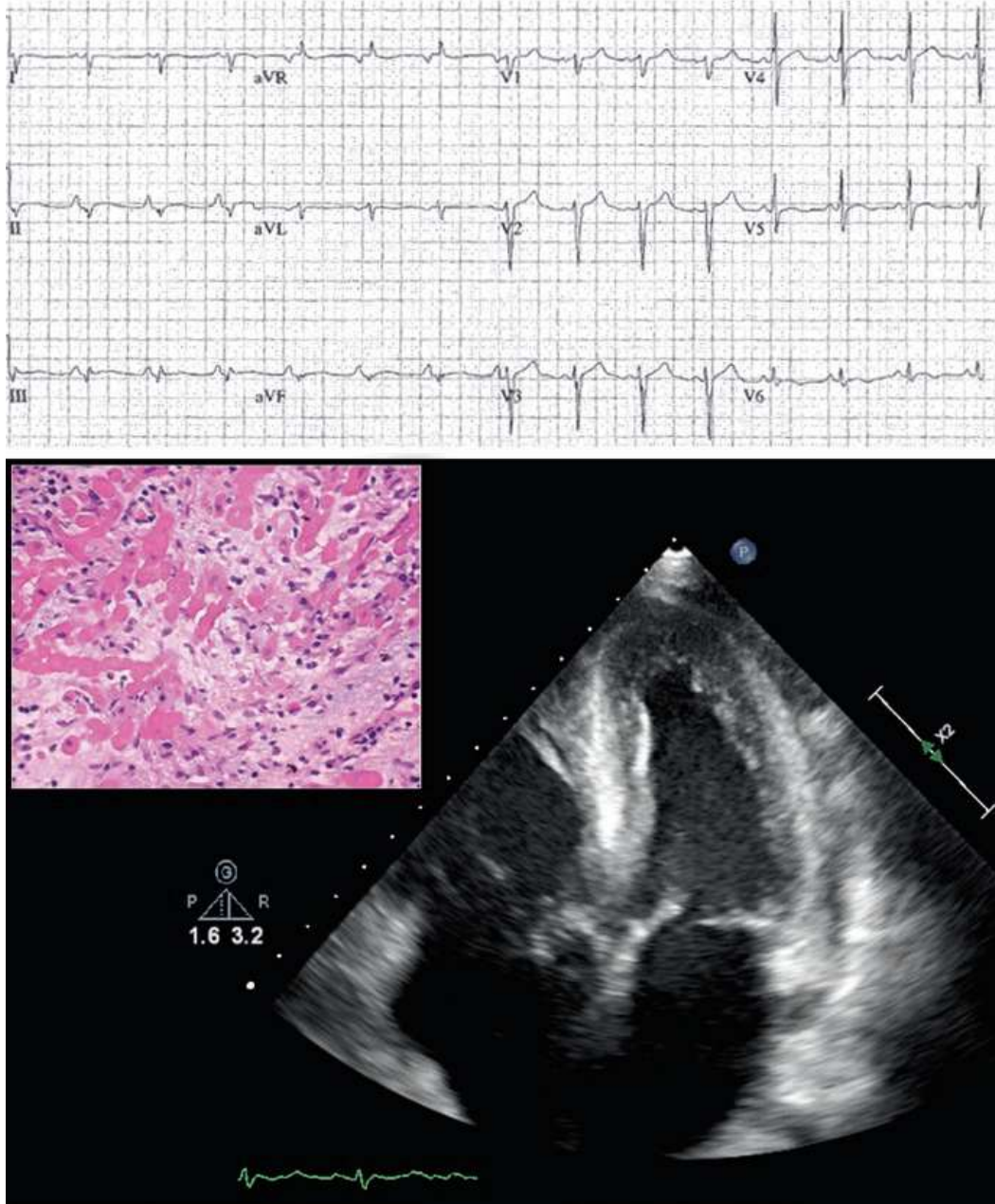


Fig. 7.4 Low QRS voltages in a patient with acute myocarditis admitted for acute heart failure. Echocardiogram showed a thickened and sparkling myocardium. At histology diffuse lymphocytic infiltrates are evident with extensive intramyocardial edema. *Courtesy of Dr. Ornella Leone*

peculiar forms (GCM, Lyme disease, Chagas heart disease, cardiac sarcoidosis). Various pathophysiologic mechanisms have been proposed to explain electrogenesis of VA in the acute setting [18]: electrical instability due to myocyte membrane lysis as a consequence of viral infection or other causes, ischemia from coronary macro/microvascular disease, abnormal calcium handling and ion channel function, and gap junction dysfunction related to abnormal myocardial expression of connexins. In the chronic stage, two kinds of mechanisms can trigger VA: reentry and enhanced

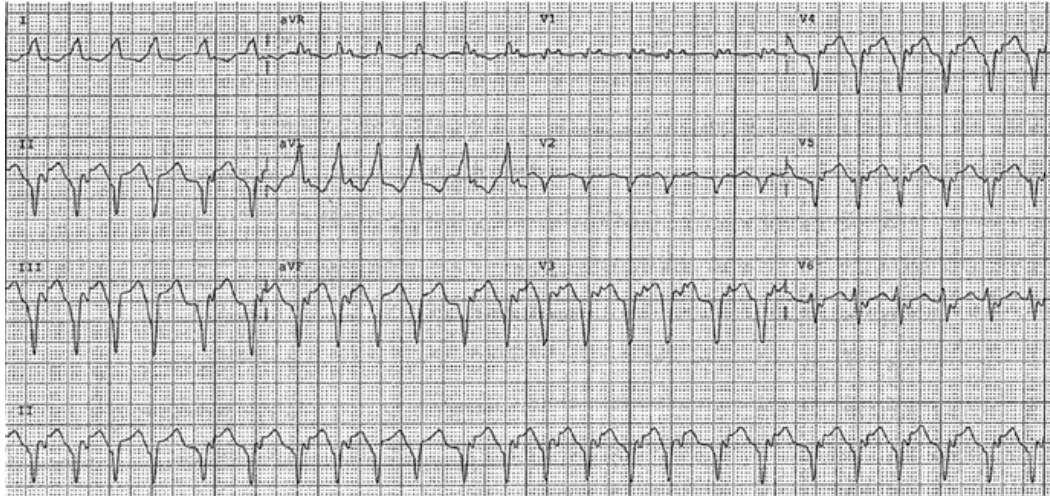


Fig. 7.5 Sustained ventricular tachycardia in a case of acute lymphocytic myocarditis admitted for heart failure

automaticity. Reentry scar-related ventricular tachyarrhythmias, after inflammation resolution, are due to re-entrant circuits secondary to myocardial fibrosis. Indeed, the presence of LGE has been described as a predictor of VA in viral myocarditis. Baseline ECG, in patients with reentry VA, may show signs of the underlying dilated cardiomyopathy, including reduced R wave amplitude, left bundle branch block or intraventricular conduction delay, abnormal Q waves, low voltages and repolarization abnormalities. However, reentry VA can also develop in the setting of normal ECG and/or echocardiogram, especially among young people. Secondly, VA in the chronic setting [18] can be the expression of infection and/or (auto) inflammatory persistence or reactivation: new onset electrical abnormalities may indicate underlying disease activity. Arrhythmic instability with iterative VA, associated with new onset monster ST-T abnormalities, is highly suggestive of acute myocarditis.

7.3 Specific Etiologies

Within the wide spectrum of abnormalities some electrocardiographic patterns may suggest specific etiologies of myocarditis.

Conduction system abnormalities may complicate all forms of myocarditis, as a reflection of inflammatory changes (edema/fibrosis) of the conduction fibers. *Lyme carditis* represents a typical example of intermittent and variable AV block, usually followed by a favorable outcome. A recent review analyzing 45 cases of Lyme carditis showed that 80% of patients presented complete AV block at admission. Atrioventricular blocks may vary in degree and most cases tend to show a benign course with complete regression after adequate antibiotic therapy [19, 20]. However, autaptic cases of sudden cardiac death have been described [21, 22] as well as the possible development of ventricular arrhythmias [23]. Additionally,

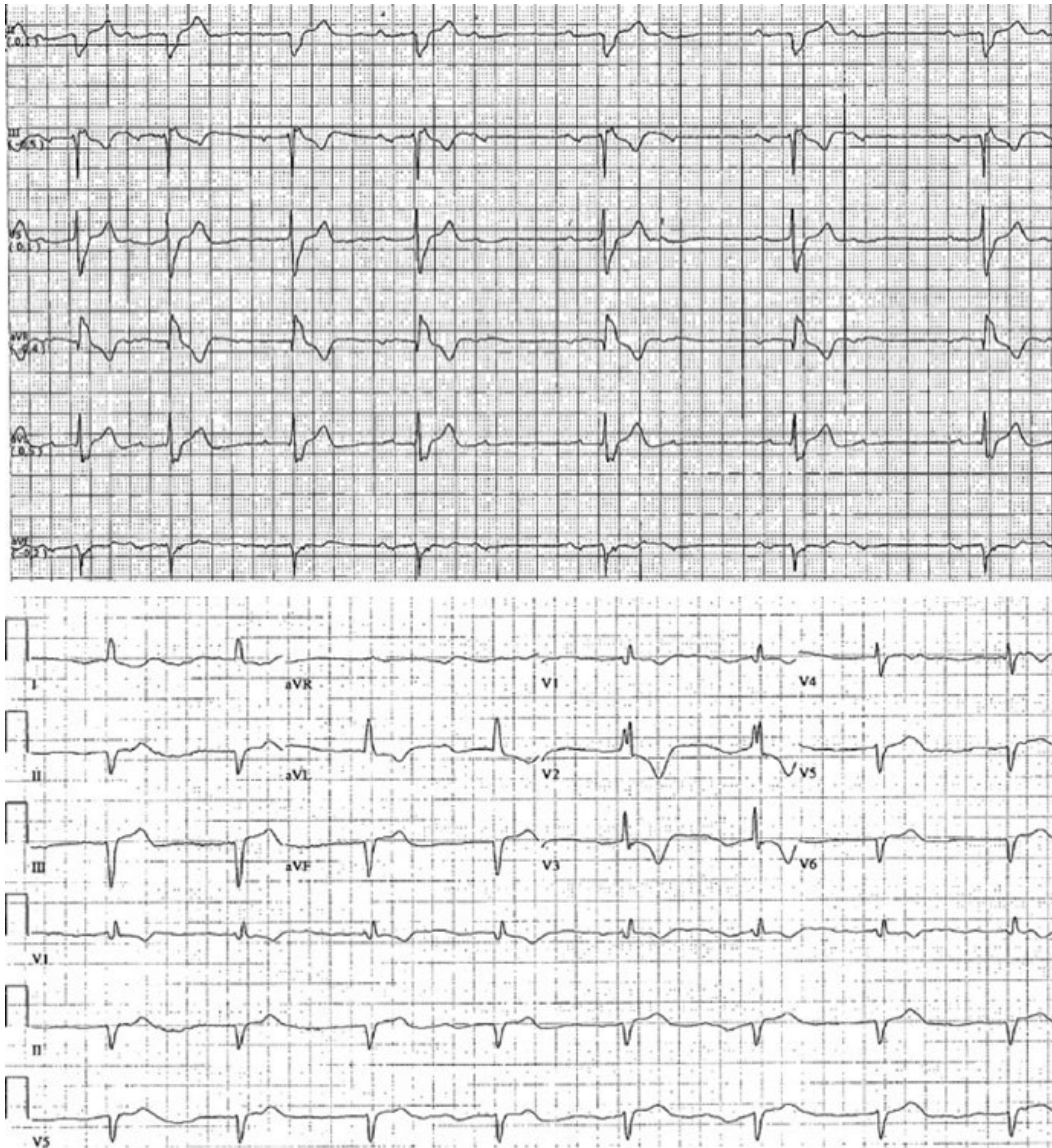


Fig. 7.6 Advanced atrioventricular block in two patients with acute myocarditis. On top a case of 2:1 atrioventricular block; on bottom a case of atrial fibrillation, complete heart block, and escape junctional rhythm

supraventricular arrhythmias may occur; sporadic cases of atrial fibrillation have been described [24, 25].

Although western world countries have established a routine vaccination regimen against diphtheria, this condition is still common in developing countries. Myocardial involvement may be present, often manifesting with conduction disturbances. In fact, a small Indian series of 6 patients with diphtheritic myocarditis revealed the presence of complete heart block, persistent or intermittent, in all cases [26].

ECG is often abnormal in patients with *cardiac sarcoidosis*. In fact, epithelioid granulomas together with the surrounding myocardial fibrosis represent the ideal histopathologic substrate for conduction disturbances. Moreover, the preferential involvement of the basal region of the interventricular septum, spreading to the